

CRANFIELD UNIVERSITY



Lanchang Xing

Passive Slug Mitigation by Applying Wavy Pipes

School of Engineering
Department of Offshore, Process and Energy Engineering

PhD
Academic Year: 2010 - 2011

Supervisor: Prof. Hoi Yeung
August 2011

CRANFIELD UNIVERSITY

School of Engineering
Department of Offshore, Process and Energy Engineering

PhD

Academic Year 2010 - 2011

Lanchang Xing

Passive Slug Mitigation by Applying Wavy Pipes

Supervisor: Prof. Hoi Yeung

August 2011

This thesis is submitted in partial fulfilment of the requirements for the degree of Doctor of Philosophy

© Cranfield University 2011. All rights reserved. No part of this publication may be reproduced without the written permission of the copyright owner.

ABSTRACT

This work is to develop a passive slug mitigation technique based on a novel flow conditioner, wavy pipe, through laboratory experiment and numerical simulation. The wavy pipe has been applied to two types of slug flows: severe slugging in pipeline/riser systems and hydrodynamic slug flow in horizontal pipelines.

The experiment of severe slugging mitigation was conducted on the 2” and 4” pipeline/riser systems in the Three-Phase Test Facility in PSE (Process Systems Engineering) Laboratory. The flow regimes in the pipeline/riser systems have been classified into four categories, i.e. severe slugging, transitional severe slugging, oscillation flow and continuous flow. Experimental results have revealed that: (1) the severe slugging region in the flow regime map can be reduced by applying a wavy pipe; (2) the wavy pipe is more effective when there is a pipe section of an appropriate length between its outlet and the riser base; (3) a smaller severe slugging region can be obtained with a longer wavy pipe (of more bends); (4) even if there is no flow regime transition due to the application of a wavy pipe, the severity of the severe slugging and oscillation flow can be reduced instead. The effects of the wavy pipe have been summarised as reducing the slug length in the pipeline/riser system. For severe slugging the wavy pipe works by accelerating the movement of the gas phase in the pipeline to the riser base to initiate the bubble penetration stage; for the oscillation flow the wavy pipe works by mixing the two phases of gas and liquid.

Two-dimensional CFD models of the 4” pipeline/riser and pipeline/wavy-pipe/riser systems were developed in Fluent (Release 6.3.26) and the effects of the geometrical parameters and location in the pipeline of the wavy pipe on severe slugging mitigation were investigated numerically. The model predictions of the flow regime transition and slug frequency in the pipeline/riser system agree with the experimental data well. It has been concluded from the simulation that: (1) for a given pipeline/riser system experiencing severe slugging, the severe slug length can be reduced further by increasing the amplitude or length of the wavy pipe, respectively; however, the mean, maximum and fluctuation amplitude of the drag and lift forces on the wavy pipe increase with the increase of the wavy pipe amplitude and the mean, maximum and

fluctuation amplitude of the differential pressure across the wavy pipe increase with the increase of the wavy pipe length; (2) the location of the wavy pipe relative to the riser base has significant effects on the performance of wavy pipe; an optimum location of the wavy pipe exists for a pipeline/riser system at given operating conditions.

The wavy pipe in a horizontal pipeline experiencing hydrodynamic slug flow was tested on a two-phase test facility in PSE Laboratory. The wavy pipe has been found to be able to mitigate the adverse impacts of hydrodynamic slug flow on the downstream facilities. It has been concluded that the wavy pipe works as a mixer which is able to agitate the gas/liquid two phases by its upward and downward limbs. More gas entrainment is introduced into the slug body in the wavy pipe. The entrained gas distributes in the slug body extensively due to the agitation effects of the wavy pipe. However, the flow tends to recover after a certain distance downstream of the wavy pipe.

The horizontal wavy-pipe systems under hydrodynamic slug flow were modelled applying STAR-OLGA coupling. The mixing effects of the wavy pipe on gas/liquid two-phase flow identified in the experiment can be presented by the coupling model reasonably well. The effects of the geometrical parameters of the wavy pipe, i.e. amplitude and length, on hydrodynamic slug mitigation were examined. It has been concluded that: (1) a wavy pipe of higher amplitude does not always introduce better mixing effects because the longer upward limbs allow more liquid to accumulate thus the liquid slugs tend to reform; a wavy pipe with amplitude of $1.8d$ is more desirable than those of $1.1d$ and $2.5d$ (d the pipe diameter); (2) a wavy pipe of more bends (7 bends, $L/d = 20.4$, L the length of wavy pipe) is more favourable to mix the gas/liquid two phases than the shorter ones (5 bends, $L/d = 16.5$; 3 bends, $L/d = 11.1$) because more space and time can be provided for the two phases to interact with each other.

The forces acting on a single bend induced by hydrodynamic slug flow were investigated using STAR-OLGA coupling. The predicted peak force on the bend agrees with the experimental data in the literature. The force components on different areas of the bend wall can be presented by the 3-D STAR model. The pressure-induced force contour plots have shown the most vulnerable part on the bend wall prone to mechanical damage.

ACKNOWLEDGEMENT

First of all I would like to express my gratitude to my supervisor Prof. Hoi Yeung for his guidance, encouragement and support throughout the duration of this work. The enthusiastic and fruitful discussions we had always inspired me.

Many thanks go to my colleagues and friends in PSE (Process Systems Engineering) Group. I would also like to thank Dr. Yi Cao, Dr. Liyun Lao and Sarah Jones for their advice on the experiment design and CFD modelling, David Whittington, Clive Wood, Stan Collins and John Knopp for their help with modifications to the test rigs, programming of Labview code and installation of transducers, Sam Skears who was always there whenever I needed any help.

I also benefited from many discussions with participants in TMF4/5 meetings in Imperial College London and Nottingham University. Thanks are due also to Simon Lo, Abderrahmane Fiala and Sreenadh Jonnavithula in CD-adapco for their suggestions on using STAR-CD, STAR-CCM+ and STAR-OLGA coupling.

I am also indebted to my family for their love, understanding and encouragement.

The financial support from the Overseas Research Students Awards Scheme (ORSAS), Cranfield University and Chevron Energy Technology Company is also gratefully acknowledged.

TABLE OF CONTENTS

ABSTRACT	i
ACKNOWLEDGEMENT	iii
LIST OF FIGURES.....	xi
LIST OF TABLES	xvii
1 INTRODUCTION.....	1
1.1 Background	1
1.1.1 Offshore Field Development	1
1.1.2 Flow Assurance	3
1.1.3 Slug Flow and Slug Mitigation.....	5
1.2 Project Objectives	8
1.3 Thesis Outline	9
2 LITERATURE REVIEW	11
2.1 Introduction	11
2.2 Slug Flow Regime.....	11
2.2.1 Flow Regimes of Gas/Liquid Two-Phase Flow	11
2.2.2 Gas/Liquid Slug Flow.....	18
2.3 Slug Flow Modelling.....	24
2.3.1 One-Dimensional Mechanistic Models of Severe Slugging	25
2.3.2 One-Dimensional Mechanistic Models of Hydrodynamic Slug Flow	33
2.3.3 One-Dimensional OLGA Modelling.....	40
2.3.4 Three-Dimensional CFD Modelling.....	43
2.3.5 Coupling of One-Dimensional OLGA and Three-Dimensional CFD	51
2.4 Slug Flow Mitigation	52
2.4.1 Active Slug Mitigation	52
2.4.2 Passive Slug Mitigation.....	57
2.4.3 Comparison between Active and Passive Mitigation Methods.....	63
2.5 Summary	64

3	EXPERIMENTAL STUDY ON SEVERE SLUGGING MITIGATION APPLYING WAVY PIPES IN PIPELINE/RISER SYSTEMS.....	67
3.1	Introduction.....	67
3.2	Wavy Pipe.....	67
3.2.1	Design Parameters of Wavy Pipe.....	67
3.2.2	Wavy Pipes in This Work.....	69
3.3	Experimental Campaign.....	71
3.3.1	Three-Phase Test Facility.....	71
3.3.2	Test Configurations of Pipeline/Wavy-Pipe/Riser Systems.....	72
3.4	Characterisation of the Flow in Pipeline/Riser Systems.....	74
3.4.1	Flow Regimes.....	74
3.4.2	Characteristic Parameters.....	77
3.5	Effects of Wavy Pipes.....	78
3.5.1	Flow Regimes.....	78
3.5.2	M_{MAX} , M_{MIN} and M_{AVE}	82
3.5.3	M_{AMP}	85
3.5.4	T_{PRO}	88
3.5.5	T_{CYC} , T_{BUI} and T_{BFB}	90
3.5.6	Summary.....	92
3.6	Discussions.....	93
3.6.1	Working Principle of Wavy Pipe.....	93
3.6.2	Effects of the Location of Wavy Pipe.....	101
3.6.3	Effects of the Length of Wavy Pipe.....	102
3.7	Summary.....	102
4	CFD MODELLING OF SEVERE SLUGGING IN PIPELINE/WAVY-PIPE/RISER SYSTEMS.....	105
4.1	Introduction.....	105
4.2	CFD Model Development of the Pipeline/Riser System.....	106
4.2.1	Model Geometry.....	106
4.2.2	Boundary Conditions.....	107
4.2.3	Turbulence and Multiphase Models.....	108
4.2.4	Solution Method.....	108
4.2.5	Model Selection.....	109
4.2.6	Hardware of Computers.....	113

4.3	Simulation of the Pipeline/Riser System	113
4.3.1	Flow Regime	114
4.3.2	Slug Frequency	118
4.3.3	Slug Movement	121
4.3.4	Severe Slugging Mitigation Methods	124
4.3.5	Discussions	130
4.4	Simulation of the Pipeline/Wavy-Pipe/Riser System	131
4.4.1	Wavy Pipes of Different Geometries	131
4.4.2	Model Setup and Test Configurations	136
4.4.3	Effects of the Amplitude of Wavy Pipe	138
4.4.4	Effects of the Length of Wavy Pipe	145
4.4.5	Effects of the Location of Wavy Pipe	150
4.4.6	Phase Distribution in the Pipeline/Wavy-Pipe/Riser Systems	158
4.4.7	Discussions	171
4.5	Summary	172
5	EXPERIMENTAL STUDY ON HYDRODYNAMIC SLUG FLOW MITIGATION USING WAVY PIPES IN HORIZONTAL PIPELINES	175
5.1	Introduction	175
5.2	Experimental Campaign	175
5.2.1	Two-Phase Test Facility	175
5.2.2	Test Section with a Wavy Pipe	177
5.3	Flow Behaviour in the Horizontal Wavy-Pipe System	178
5.3.1	Flow Regime Upstream of the Wavy Pipe	178
5.3.2	Flow in the Wavy Pipe	185
5.3.3	Flow Downstream of the Wavy Pipe	187
5.4	Slug Mitigation with Wavy Pipe	190
5.4.1	Gas Entrainment and Flow Recovery Downstream	190
5.4.2	Interaction between Slug Flow and Wavy Pipe	192
5.4.3	Working Principle	195
5.5	Summary	196
6	MODELLING OF HYDRODYNAMIC SLUG FLOW IN HORIZONTAL WAVY-PIPE SYSTEMS APPLYING STAR-OLGA COUPLING	199
6.1	Introduction	199

6.2	STAR-OLGA Coupling	199
6.2.1	Configuration of the Coupling.....	200
6.2.2	Key Issues of the Coupling.....	201
6.3	Development of the Coupling Model.....	203
6.3.1	Geometries and Meshes of Straight-Pipe System	203
6.3.2	Model Setup.....	206
6.3.3	Hardware Configuration	206
6.3.4	Mesh Selection	207
6.3.5	Geometries of Wavy Pipes	211
6.4	Slug Flow in the Horizontal Wavy-Pipe System.....	213
6.4.1	Effects of Wavy Pipe.....	214
6.4.2	Effects of the Amplitude of Wavy Pipe	222
6.4.3	Effects of the Length of Wavy Pipe	225
6.4.4	Discussions	227
6.5	Summary	228
7	INVESTIGATION OF SLUG FLOW INDUCED FORCES ON PIPE BENDS APPLYING STAR-OLGA COUPLING.....	231
7.1	Introduction	231
7.2	Previous Investigations of Slug Forces on Pipe Bends.....	231
7.3	Development of the Coupling Model.....	234
7.3.1	Model Geometry.....	234
7.3.2	Model Setup.....	236
7.3.3	Model Outputs.....	237
7.4	Results and Discussions	239
7.4.1	STAR Model with Single-Phase Flow	239
7.4.2	One-Point Coupling Model with Two-Phase Slug Flow.....	242
7.4.3	Two-Point Coupling Model with Two-Phase Slug Flow	253
7.5	Summary	256
8	CONCLUSIONS AND RECOMMENDATIONS FOR THE FUTURE WORK.....	259
8.1	Conclusions	259
8.1.1	Severe Slugging Mitigation with Wavy Pipes in Pipeline/Riser Systems.....	259

8.1.2	Hydrodynamic Slug Mitigation with Wavy Pipes in Horizontal Pipelines	262
8.2	Recommendations for the Future Work.....	265
8.2.1	Severe Slugging Mitigation with Wavy Pipes in Pipeline/Riser Systems.....	265
8.2.2	Hydrodynamic Slug Mitigation with Wavy Pipes in Horizontal Pipelines	266
REFERENCES	267
APPENDICES	281
Appendix A	Test Facilities.....	281
Appendix B	Phase Distribution in Horizontal Wavy-Pipe Systems...	289
Appendix C	Effects of the Downstream Pipe length on the Forces on the Bend.....	303
Appendix D	Modelling of the Pipeline/Wavy-pipe/Riser System Applying STAR-OLGA Coupling.....	307

LIST OF FIGURES

Figure 1-1 Schematic of an offshore field development system (Lee, 2009).....	2
Figure 1-2 Flexible riser configurations (Bai and Bai, 2005).....	3
Figure 1-3 Schematics of a wavy pipe and a pipeline/wavy-pipe/riser system.....	8
Figure 2-1 Different flow regimes in vertical pipes	12
Figure 2-2 Different flow regimes in horizontal and near horizontal pipes	13
Figure 2-3 Flow regime map for vertical upward flow (Hewitt and Robertson, 1969) .	15
Figure 2-4 Flow regime map for horizontal flow by Mandhane <i>et al.</i> (1974)	16
Figure 2-5 Comparison of the flow regime maps proposed by Taitel and Dukler (1976) and Mandhane <i>et al.</i> (1974).....	17
Figure 2-6 Severe slugging cycle consisting of four stages	19
Figure 2-7 Slug formation process (after Dukler and Hubbard (1975)).....	23
Figure 2-8 Schematic of a slug unit.....	34
Figure 2-9 Schematic of a STAR-OLGA coupling model.....	52
Figure 2-10 Self-gas lifting methods (Sarica and Tengedal, 2000).....	59
Figure 2-11 Venturi-shaped device (Almeida and Gonçalves, 1999 b)	60
Figure 2-12 Pipe device proposed by Makogan and Brook (2007).....	60
Figure 2-13 Helical pipe of low amplitude investigated by Adedigba (2007)	61
Figure 2-14 PST geometries tested by Yeung and Cao (2007).....	63
Figure 3-1 Geometrical parameters of a bend	67
Figure 3-2 Schematics of different geometries formed by connecting bends	68
Figure 3-3 Schematics of a bend and a wavy pipe of 7 bends.....	69
Figure 3-4 Dimensions of a 90° bend and a 45° elbow (Durapipe, 2007)	70
Figure 3-5 Schematics of a 2” ‘bend’ and wavy pipe with 7 ‘bends’	70
Figure 3-6 Schematic of the Three-Phase Test Facility at Cranfield University	72
Figure 3-7 Riser DP time traces of severe slugging (SS), transitional severe slugging (TSS), oscillation flow (OSC) and continuous flow (CON) in plain riser and pipeline/wavy-pipe/riser systems ($U_{SL} = 0.12$ m/s).....	76
Figure 3-8 Definitions of the characteristic parameters based on the riser DP time trace of severe slugging.....	78

Figure 3-9 Test points and stability boundaries for the 2” and 4” plain riser and pipeline/wavy-pipe/riser systems.....	79
Figure 3-10 Test points and stability boundaries for the 2” plain riser and pipeline/wavy-pipe/riser systems.....	81
Figure 3-11 M_{MAX} , M_{MIN} and M_{AVE} of the riser DP for the 2” plain riser and pipeline/wavy-pipe/riser systems of different test configurations.....	85
Figure 3-12 M_{AMP} of the riser DP for the 2” plain riser and pipeline/wavy-pipe/riser systems of different configurations	87
Figure 3-13 Riser DP time traces of SS for the 2” plain riser and pipeline/wavy-pipe/riser systems of different configurations ($U_{SG0} = 0.70$ m/s, $U_{SL} = 0.25$ m/s) .	89
Figure 3-14 T_{PRO} for the 2” plain riser and pipeline/wavy-pipe/riser systems of different configurations ($U_{SG0} = 0.70$ m/s).....	90
Figure 3-15 T_{CYC} , T_{BUI} and T_{BFB} of SS for the 2” plain riser and pipeline/wavy-pipe/riser systems of different configurations ($U_{SG0} = 0.70$ m/s)	92
Figure 3-16 Schematics of the plain riser and pipeline/wavy-pipe/riser systems	95
Figure 3-17 Schematic of the phase distribution upstream of the riser base in the plain riser and pipeline/wavy-pipe/riser systems.....	97
Figure 3-18 Schematic of the phase distribution upstream of the riser base in the pipeline/wavy-pipe/riser system	99
Figure 4-1 Geometry I and II.....	107
Figure 4-2 Riser DP predicted by Model I and II and experimental data for Case 1 and Case 2.....	110
Figure 4-3 Riser DP predicted by Model II with the fine/coarse meshes (grids) for Case 1 ($U_{SG0} = 0.86$ m/s, $U_{SL} = 0.62$ m/s) and experimental data.....	112
Figure 4-4 Comparison of the maximum and minimum riser DP between the model predictions and experimental data	116
Figure 4-5 Comparison of the slug frequency between the model predictions and experimental data.....	120
Figure 4-6 Percentage relative error of slug frequency predicted by the CFD model..	121
Figure 4-7 Time traces of the riser DP and liquid holdup at different locations in the pipeline/riser system	122

Figure 4-8 Riser DP and riser base pressure for Case 1 ($U_{SL} = 0.25$ m/s, $U_{SG0} = 0.51$ m/s)	125
Figure 4-9 Riser DP and riser base pressure for Case 2 ($U_{SL} = 0.49$ m/s, $U_{SG0} = 0.51$ m/s)	126
Figure 4-10 Schematic of a ‘valve’ in the 2-D CFD model	128
Figure 4-11 Model predictions with different valve openings (Case 2: $U_{SL} = 0.49$ m/s, $U_{SG0} = 0.51$ m/s)	130
Figure 4-12 Schematics of pipeline/wavy-pipe/riser systems with the wavy pipes of different amplitudes and lengths in the pipeline	134
Figure 4-13 Schematics of pipeline/wavy-pipe/riser systems with Wavy III at different locations in the pipeline	135
Figure 4-14 Locations for monitoring the pressure at the inlet and outlet of the wavy pipe	136
Figure 4-15 Time traces of the riser DP for the plain riser and pipeline/wavy-pipe/riser systems with Wavy I, Wavy II and Wavy III of 7 bends at Location III	139
Figure 4-16 Time traces of the wavy DP for Wavy I, Wavy II and Wavy III of 7 bends at Location III	140
Figure 4-17 Time traces of the pressure at the inlet of the wavy pipe for Wavy I, Wavy II and Wavy III of 7 bends at Location III	141
Figure 4-18 Time traces of the drag and lift coefficients for Wavy I, Wavy II and Wavy III of 7 bends at Location III	143
Figure 4-19 Statistical parameters of the drag and lift coefficients against the amplitude of the wavy pipe for Wavy I, Wavy II and Wavy III	144
Figure 4-20 Time traces of the riser DP for the plain riser system and pipeline/wavy-pipe/riser systems with Wavy III of 3, 7 and 11 bends at Location II	146
Figure 4-21 Time traces of the wavy DP for Wavy III of 3, 7 and 11 bends at Location II	148
Figure 4-22 Time traces of the pressure at the inlet of Wavy III of 3, 7 and 11 bends at Location II	149
Figure 4-23 Time traces of the riser DP for the plain riser system and pipeline/wavy-pipe/riser systems with Wavy III of 7 bends at Location I to V	152

Figure 4-24 Statistical parameters of the riser DP and the cycle time of the flow process in the pipeline/wavy-pipe/riser systems with Wavy III of 7 bends at Location I to V	153
Figure 4-25 Time traces of the wavy DP for Wavy III of 7 bends at Location I to V .	154
Figure 4-26 Maximum, minimum and mean of the wavy DP with Wavy III of 7 bends at Location I to V	155
Figure 4-27 Time traces of the pressure at the inlet of Wavy III of 7 bends at Location I to V	156
Figure 4-28 Maximum, minimum, mean and standard deviation of the pressure at the inlet of Wavy III of 7 bends at Location I to V	157
Figure 4-29 Phase distribution in the plain riser at the liquid buildup stage, the end of the liquid buildup stage and the gas-blowdown/liquid-fallback stage.....	160
Figure 4-30 Phase distribution at the liquid buildup stage with Wavy I and Wavy III at Location III	163
Figure 4-31 Phase distribution at the end of the liquid buildup stage with Wavy I and Wavy III at Location III.....	164
Figure 4-32 Phase distribution at the end of the gas-blowdown/liquid-fallback stage with Wavy I and Wavy III at Location III.....	165
Figure 4-33 Phase distribution at the end of the liquid buildup stage with Wavy III of 3 bends and 11 bends at Location II	167
Figure 4-34 Phase distribution at the end of the gas-blowdown/liquid-fallback stage with Wavy III of 3 bends and 11 bends at Location II	168
Figure 4-35 Phase distribution at the end of the liquid buildup stage with Wavy III of 7 bends at Location I, III and V	170
Figure 5-1 Schematic of the two-phase test facility	176
Figure 5-2 Schematic of the test section with instruments.....	177
Figure 5-3 Test points and flow regimes in the 2” test rig on Mandhane flow regime map (Mandhane <i>et al.</i> , 1974).....	179
Figure 5-4 Time traces of the liquid holdup for stratified flow with low-frequency and high-amplitude waves	181
Figure 5-5 Time trace of the liquid holdup for stratified flow with high-frequency and low-amplitude waves ($U_{SL} = 0.02$ m/s, $U_{SG} = 9.0$ m/s).....	182

Figure 5-6 Time traces of the liquid holdup for slug flow	184
Figure 5-7 Flow in the wavy pipe for the upstream separate gas and liquid layers	186
Figure 5-8 Flow in the wavy pipe for the upstream high-amplitude waves	186
Figure 5-9 Flow in the wavy pipe for the upstream slug flow	187
Figure 5-10 Liquid holdup upstream and downstream of the wavy pipe for the upstream stratified flow with high-amplitude waves ($U_{SL} = 0.02$ m/s, $U_{SG} = 0.7$ m/s)	188
Figure 5-11 Liquid holdup upstream and downstream of the wavy pipe for stratified flow with low-amplitude waves upstream ($U_{SL} = 0.02$ m/s, $U_{SG} = 9.0$ m/s).....	189
Figure 5-12 Flow downstream of the wavy pipe for the upstream slug flow.....	190
Figure 5-13 Maximum liquid holdup upstream and downstream of the wavy pipe ($U_{SL} = 1.0$ m/s)	191
Figure 5-14 Maximum liquid holdup upstream and downstream of the wavy pipe ($U_{SG} = 1.5$ m/s)	192
Figure 5-15 Average differential pressures across the first 6 limbs of the wavy pipe ($U_{SL} = 1.0$ m/s)	193
Figure 5-16 Average differential pressures across the first 6 limbs of the wavy pipe ($U_{SG} = 1.5$ m/s)	194
Figure 6-1 Schematic of a two-point STAR-OLGA coupling model	200
Figure 6-2 Schematic of the time step synchronisation (Jonnavithula <i>et al.</i> (2009))...	203
Figure 6-3 Profiles of the three pipe sections in the straight-pipe system.....	204
Figure 6-4 Schematic of the hardware configuration for solving the coupling model (after Jonnavithula <i>et al.</i> (2009))	207
Figure 6-5 Liquid holdup time traces and time step series obtained from the OLGA model of different levels of meshes	210
Figure 6-6 Time traces of the liquid holdup in the STAR pipe predicted by the coupling model of different levels of meshes	211
Figure 6-7 Schematics of the wavy pipes of different amplitudes (Wavy I, Wavy II and Wavy III of 7 bends).....	212
Figure 6-8 Schematics of the wavy pipes of different lengths (Wavy I).....	213
Figure 6-9 Comparison of the liquid holdup upstream and downstream of the wavy pipe between the model predictions and experimental data ($U_{SL} = 0.47$ m/s, $U_{SG} = 2.05$ m/s)	215

Figure 6-10 Contour plots of the gas volume fraction upstream of the wavy pipe ($U_{SL} = 0.47$ m/s, $U_{SG} = 2.05$ m/s).....	218
Figure 6-11 Contour plots of the gas volume fraction in the wavy pipe ($U_{SL} = 0.47$ m/s, $U_{SG} = 2.05$ m/s).....	219
Figure 6-12 Contour plots of the gas volume fraction downstream of the wavy pipe ($U_{SL} = 0.47$ m/s, $U_{SG} = 2.05$ m/s).....	220
Figure 6-13 Contour plots of the gas volume fraction in Zone I and Zone II downstream of the wavy pipe ($U_{SL} = 0.47$ m/s, $U_{SG} = 2.05$ m/s).....	220
Figure 6-14 Time traces of the force components on the wavy pipe and liquid holdup upstream of the wavy pipe predicted by the coupling model ($U_{SL} = 0.47$ m/s, $U_{SG} = 2.05$ m/s).....	221
Figure 6-15 Comparison of the liquid holdup time traces downstream of the wavy pipes of different amplitudes ($U_{SL} = 0.95$ m/s, $U_{SG} = 2.14$ m/s).....	223
Figure 6-16 Contour plots of the gas volume fraction downstream of Wavy I, Wavy II and Wavy III ($U_{SL} = 0.95$ m/s, $U_{SG} = 2.14$ m/s).....	224
Figure 6-17 Comparison of the liquid holdup time traces downstream of Wavy I of 7 bends, 5 bends and 3 bends ($U_{SL} = 0.95$ m/s, $U_{SG} = 2.14$ m/s).....	225
Figure 6-18 Contour plots of the gas volume fraction downstream of Wavy I of 7 bends, 5 bends and 3 bends ($U_{SL} = 0.95$ m/s, $U_{SG} = 2.14$ m/s).....	226
Figure 7-1 Schematic of the two-point STAR-OLGA coupling model	235
Figure 7-2 Geometry of the STAR model and mesh on the cross-section	236
Figure 7-3 Division of the bend wall into 4 portions	238
Figure 7-4 Creation of the plane sections in the bend	239
Figure 7-5 Velocity distribution on the transverse section of the bend (Case 2)	241
Figure 7-6 Liquid holdup in the bend and velocities of the slug front and tail predicted by the STAR-OLGA coupling model.....	243
Figure 7-7 Forces on the inner part, outer part and the whole bend with liquid holdup in the bend centre	245
Figure 7-8 Phase distribution in the bend and pressure (gauge pressure) distribution on the outer part of the bend	252
Figure 7-9 Comparison of the forces predicted by the one-point and two-point coupling models.....	256

LIST OF TABLES

Table 4-1 Cell counts of the coarse and fine meshes	107
Table 4-2 Maximum/minimum riser DP and cycle time of SS predicted by Model I and II and experimental data for Case 1 and Case 2	111
Table 4-3 Statistical parameters of the riser base pressure.....	127
Table 4-4 Statistical parameters of the riser DP for Wavy I, Wavy II and Wavy III of 7 bends at Location III.....	139
Table 4-5 Statistical parameters of the pressure at the inlet of the wavy pipe for Wavy I, Wavy II and Wavy III of 7 bends at Location III.....	142
Table 4-6 Statistical parameters of the riser DP for Wavy III at Location II.....	147
Table 4-7 Statistical parameters of the pressure at the inlet of Wavy III of 3, 7 and 11 bends at Location II	149
Table 6-1 Meshes of the OLGA models.....	205
Table 6-2 Meshes of the STAR models	205
Table 7-1 Theoretical and predicted forces	241

1 INTRODUCTION

1.1 Background

1.1.1 Offshore Field Development

The recovery of hydrocarbons (natural gas and oil) from offshore hydrocarbon reservoirs is of crucial economic importance to the world. As more easily accessible fields are depleted, there is an increasing requirement to develop reservoirs in deeper water further offshore.

Since the early 1960s the discovery and exploitation of offshore hydrocarbon reservoirs have been steadily increasing. Of the order of 10,000 offshore facilities had been installed worldwide in the past 50 years before 2000 (Anthony *et al.*, 2000). The first offshore structures were installed in a mere 6 meters of water in the Gulf of Mexico in 1947 (Colligan, 1999). Recently, the exploitation of offshore petroleum reservoirs has moved to ever increasing water depths. The deepest water depth that pipelines had been installed was 2,414 m in the Gulf of Mexico (GOM) by Anadarko for the Independence Hub project in 2007. The record was broken by Petrobras Cascade flowlines installed in 2,689 m of water in GOM in 2009 (Lee, 2009). The record for the maximum deepwater exploration depth has been renewed year by year as new technologies have been introduced.

Offshore field development normally requires four elements as shown in Figure 1-1, namely, subsea systems, pipeline/riser systems, fixed or floating structures and topside processing systems.

The subsea system is used to gather productions from multiple wellheads and send the productions through a smaller number of flowlines. These unprocessed productions, usually taking the form of multiphase fluid, are sent to the topside processing facilities on fixed or floating structures through the pipeline/riser system. The crude product is processed and then the treated product is offloaded to a tanker or exported through pipelines.

If the water depth is relatively shallow, the surface structure can be fixed on the sea floor, called fixed platform. If the water depth is relatively deep, the floating structures like Tension Leg Platforms (TLP), Floating Production Systems (FPS) and Floating Production, Storage and Offloading Systems (FPSO) can be employed (Lee, 2009; DTI, 2001).

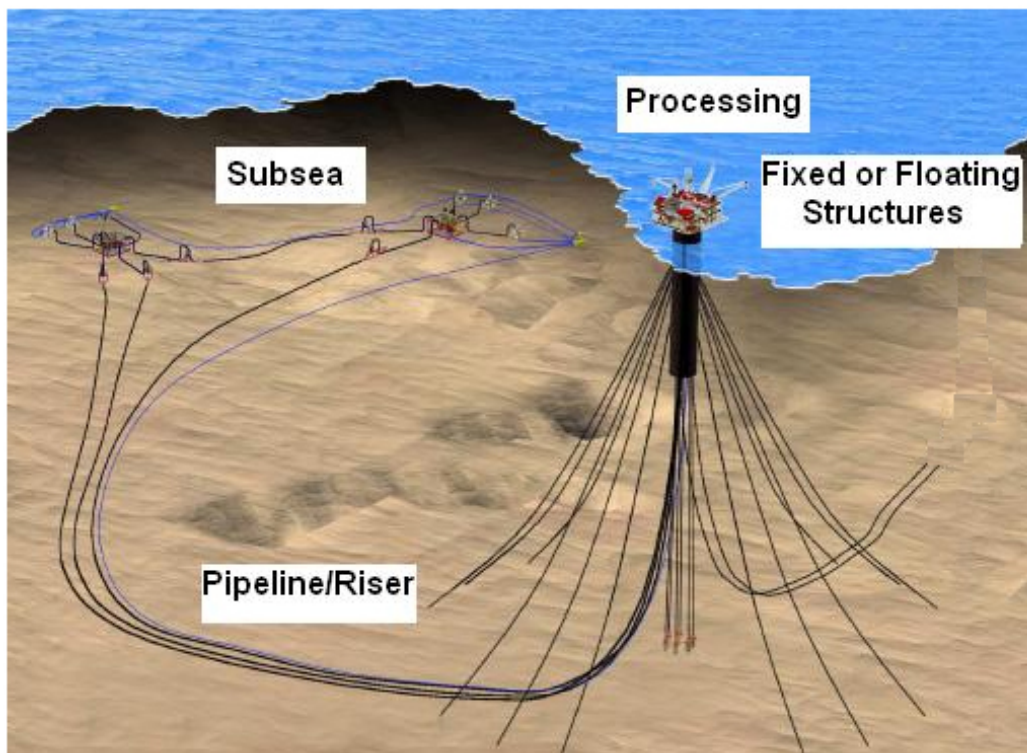


Figure 1-1 Schematic of an offshore field development system (Lee, 2009)

A riser system is essentially conductor pipes connecting the fixed or floating structures on the surface and the wellheads at the seabed. There are essentially two types of risers, namely rigid risers and flexible risers. A hybrid riser is the combination of these two (Bai and Bai, 2005). The riser should be as short as possible in order to reduce the material and installation costs, but it must have sufficient flexibility to allow for large excursions of the surface structures especially for the floating structure. Flexible risers can be installed in a number of different configurations. There are mainly six

configurations for flexible risers, i.e. free hanging catenary, lazy wave, steep wave, lazy-S, steep-S and pliant wave, as shown in Figure 1-2.

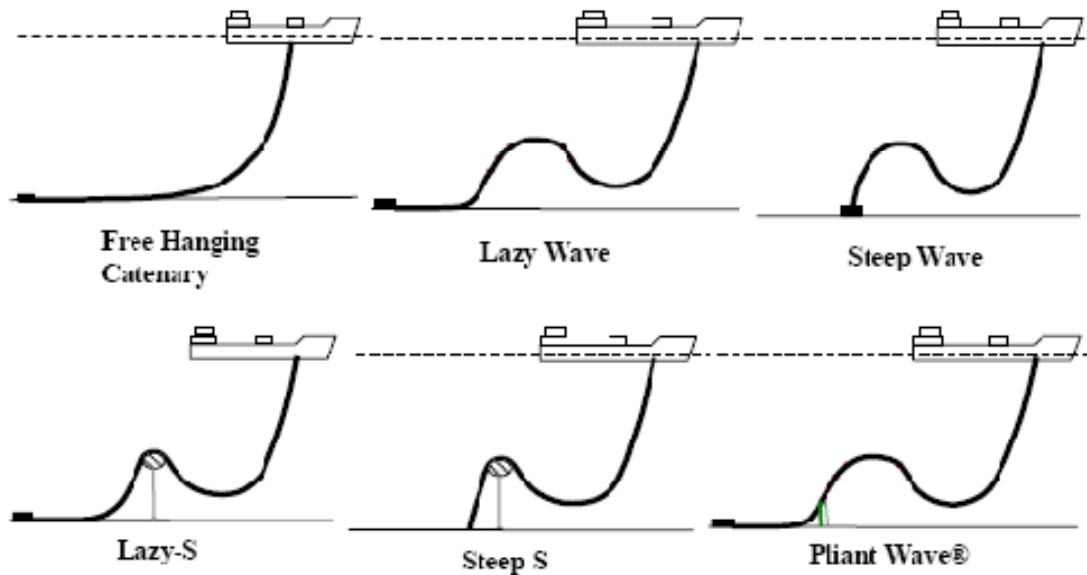


Figure 1-2 Flexible riser configurations (Bai and Bai, 2005)

The selection of an appropriate riser depends on the water depth, environment, station keeping, produced fluids, well system, surface facility and export system. A free hanging catenary riser is the simplest and the least expensive configuration in flexible risers, because it requires the minimal subsea infrastructure and ease of installation. However, a free hanging catenary is exposed to severe loading due to the motion of the floating structures. In water depths less than 300 m the application of a catenary riser is limited, but in larger water depths the benefits of this riser system can be significant (Hatton and Howells, 1996). Hence, the Steel Catenary Riser (SCR) solution has been taken as one of the most important solutions for the oil and gas exploitation in deep waters.

1.1.2 Flow Assurance

The term ‘Flow Assurance’ is thought to be firstly used by Petrobras in the early 1990s as ‘Garantia de Fluxo’, literally translated as ‘Guarantee of Flow’ or Flow Assurance

(Su, 2003). Flow assurance originally covered only the thermal hydraulic and production chemistry issues encountered in the oil and gas production. However, it has become synonymous with a wide range of issues.

Flow assurance analysis is a recognised critical part in the design and operation of offshore oil/gas systems. It becomes more challenging in the offshore field developments involving long distance tie-backs and deepwater in recent years. The most severe operational hazards of offshore pipelines are the risks associated with the transportation of multiphase fluids. When water, oil and gas are flowing simultaneously inside the pipeline, there are quite a few potential problems that can occur (Guo *et al.*, 2005):

- water and hydrocarbon fluids can form hydrate and block the pipeline;
- wax and asphaltene can deposit on the wall and may eventually block the pipeline;
- corrosion may occur with a high enough water cut;
- scales may form and deposit inside the pipeline and restrict the flow with pressure and temperature changes along the pipeline and/or with incompatible water mixing;
- severe slugging may form inside the pipeline and causes operational problems to downstream processing facilities.

Therefore, the challenge that engineers will face is how to design the pipelines and subsea systems to assure that the multiphase fluids are safely and economically transported from the bottom of the wells all the way to the downstream processing plants. Furthermore, as the production systems go deeper and deeper, flow assurance becomes a major issue for the offshore production systems. The traditional approaches are inappropriate for deepwater production systems due to the extreme distances, depths, temperature and economic constraints.

Flow assurance is a production operation that generates a reliable, manageable and profitable flow of fluids from the reservoir to the sales point. Flow assurance requires a simple success strategy defined by component proficiency, integration, implementation,

and improvement, termed as PI3 or π_3 (Brown, 2002). Some flow assurance concerns are listed as follows (Watson *et al.*, 2003; Bai and Bai, 2005):

- **System deliverability:** pressure drop versus production, pipeline size and boosting;
- **Thermal behaviour:** temperature distribution, temperature changes due to start-up and shutdown, insulation options and heating requirements;
- **Production chemistry:** hydrates, waxes, asphaltenes, scaling, sand, corrosivity and rheology;
- **Operability characteristics:** start-up, shutdown, transient behaviour (e.g. slugging) etc;
- **System performance:** mechanical integrity, equipment reliability, system availability etc.

1.1.3 Slug Flow and Slug Mitigation

As mentioned above the slug flow (also called slugging) is one of the most important flow assurance concerns in the oil and gas production with multiphase flowlines. In most of the offshore production systems, there is a significant length of multiphase flowline upstream of the processing facilities. It often happens that significant gas/liquid surges or ‘slugs’ are generated in the flowline from the reservoir to the processing facilities. Slugs generated in oil and gas multiphase flowlines can be classified into three different types based on their initiation mechanisms (Taitel and Barnea, 2000; FEESA, 2004):

- **Terrain-induced slugs:** caused by periodic accumulation and purging of liquid in elevation changes along the flowline, particularly at low flowrates;
- **Hydrodynamic slugs:** formed due to wave instabilities at the gas/liquid interface and grow or shrink depending on the flowline topography;
- **Operation-induced slugs:** formed in the system during operation transfer between steady state and transient state, for example, during start-up or pigging operations.

All of the three types of slugs may be encountered in a multiphase flowline during the life span of a production well. Usually at the early and the late stages of production, terrain-induced slugs may form due to the low gas and liquid flowrates, while hydrodynamic slugs may appear at the middle stage and operation-induced slugs may be induced by the start-up and regular pigging operation throughout the life span.

The terrain-induced slugs mainly include hilly-terrain-induced slugs and riser-induced slugs. The corresponding flow regimes are called ‘hilly-terrain-induced slugging’ and ‘riser-induced slugging’, respectively. Hydrodynamic slugs are also called ‘normal slugs’ and the corresponding flow regime is also called ‘normal slug flow’. It needs to be stressed that, in this study, only these two types of slug flows are investigated, particularly the riser-induced slugging in pipeline/riser systems and hydrodynamic slug flow in horizontal pipelines. In this thesis the terms ‘severe slugging’ and ‘severe slugs’ refer to the riser-induced slugging and slugs, respectively, unless otherwise stated.

Severe slugging can result in various problems to the whole production system including the reservoir, pipeline/riser and downstream processing facilities. The problems exhibit a great challenge to the steady operation of the production, the mechanical integrity of the whole system and the efficient management of the reservoir.

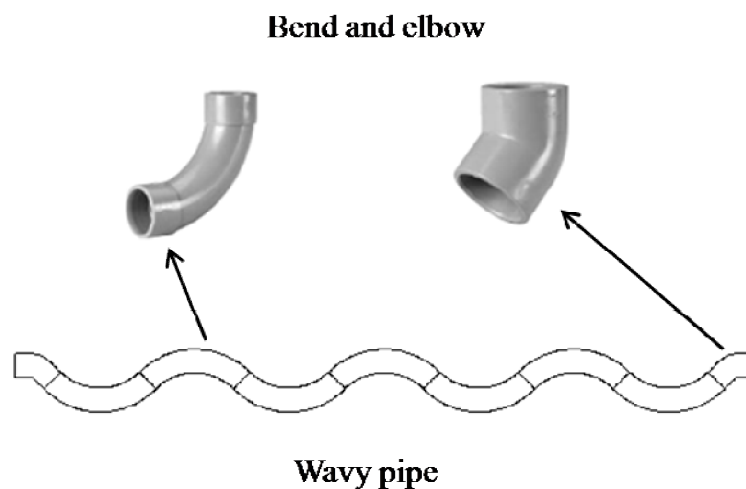
- **Steady operation:** challenged by the cyclic behaviour with a gas blowdown stage of very high liquid and gas delivery and a liquid buildup stage of no or very low flowrate. The highly unsteady operation conditions can lead to failure to meet the production specifications. The high delivery of liquid and gas can cause problems in controlling the downstream separators and compressors, which may result in overflow and shutdown of the separators and unnecessary flaring of gas.
- **Mechanical integrity:** challenged by the long liquid slug and fast moving slug tail. The mechanical loading, corrosion and erosion on pipe bends, joints or valves can be increased significantly.
- **Reservoir management:** challenged by the high riser base pressure and fluctuations. The high riser base pressure can cause high backpressure on the

reservoir and reduce the production; the high pressure fluctuations can result in poor performance of the recoverable reservoir.

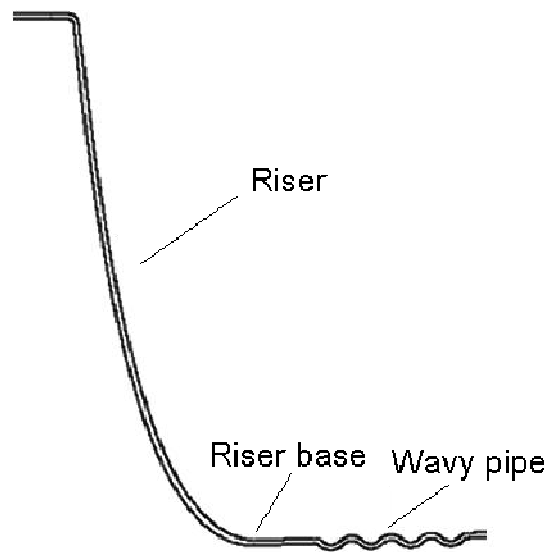
As the production systems go deeper and deeper, the severe slugging induced problems become more and more severe because the risers become longer and longer.

Various slug mitigation methods have been proposed to cope with the undesirable slug flow. They can be classified into different categories based on the working principle. In this work the major slug mitigation methods in the literature are grouped into two categories, i.e. active and passive methods, based on whether the ‘external interference’ is needed or not in operation. The ‘external interference’ is essential to the implementation of the active slug mitigation methods, while the passive slug mitigation methods usually take the form of design changes to the facility.

In this work a new passive method based on a novel flow conditioner, wavy pipe, is developed to mitigate riser-induced severe slugging in pipeline/riser systems and hydrodynamic slug flow in horizontal pipelines. A wavy pipe is a pipe section constructed by connecting the standard piping bends in one plane. The details of the design parameters of wavy pipes are presented in Chapter 3. Figure 1-3 shows the schematics of a wavy pipe of 7 bends and a pipeline/wavy-pipe/riser system.



(a) Wavy pipe of 7 bends



(b) Pipeline/wavy-pipe/riser system

Figure 1-3 Schematics of a wavy pipe and a pipeline/wavy-pipe/riser system

1.2 Project Objectives

The aim of this project is to develop a new passive slug mitigation technique based on a novel flow conditioner, wavy pipe. Firstly the wavy pipe is applied to mitigate severe slugging in pipeline/riser systems, then hydrodynamic slug flow in horizontal pipelines.

The major objectives of this project are presented as follows:

- To characterise the flow behaviour in the pipeline/riser system, pipeline/wavy-pipe/riser systems and horizontal wavy-pipe system through laboratory experiment;
- To understand the effects of the wavy pipe on slug flow in pipeline/riser and horizontal pipeline systems and the effects of the location in the pipeline (in pipeline/riser system) and geometrical parameters of the wavy pipe on its performance of slug mitigation (in both systems) through experiment and modelling;

- To disclose the working principle of wavy pipes on slug mitigation and develop engineering tools for designing pipeline/wavy-pipe/riser systems and horizontal wavy-pipe systems.

1.3 Thesis Outline

The rest of the thesis is organised as follows:

Chapter 2 presents a literature review on the related studies of flow regime classifications, slug flow modelling and slug flow mitigation.

Chapter 3 focuses on an experimental study of severe slugging mitigation applying wavy pipes. The flow behaviour in the pipeline/riser and pipeline/wavy-pipe/riser systems has been characterised. The performance of the wavy pipe on severe slugging mitigation has been presented in terms of the flow regime transition and characteristic parameters of the flow behaviour. The working principle of the wavy pipe has been discussed based on the experimental data.

Chapter 4 is devoted to a numerical study of severe slugging mitigation applying wavy pipes. The pipeline/riser and pipeline/wavy-pipe/riser systems have been modelled with commercial CFD (Computational Fluid Dynamics) code. A set of CFD models has been developed to examine the effects of the location of the wavy pipe in the pipeline and geometrical parameters such as amplitude and length of the wavy pipe on severe slugging mitigation. More understanding of the working principle of wavy pipes of different geometrical parameters located at different positions in the pipeline has been obtained.

Chapter 5 presents an experimental study of hydrodynamic slug mitigation applying wavy pipes. The flow behaviour in the horizontal wavy-pipe system, i.e. upstream of the wavy pipe, in the wavy pipe and downstream of the wavy pipe, has been characterised based on the experimental data. Then the effects of the wavy pipe on hydrodynamic slug flow have been analysed and the working principle of the wavy pipe on hydrodynamic slug flow mitigation has been discussed.

Chapter 6 deals with a numerical study of hydrodynamic slug flow in horizontal wavy-pipe systems applying STAR-OLGA coupling. A set of CFD models of wavy pipes of different amplitudes and lengths has been developed in STAR-CCM+ (Release 5.04.006) then coupled with the OLGA models of the upstream and downstream pipelines. The effects of the geometrical parameters of the wavy pipe on hydrodynamic slug mitigation have been examined based on the model predictions. More understanding of the working principle of wavy pipes of different geometrical parameters has been obtained.

Chapter 7 is dedicated to an extended study to that in Chapter 6. An investigation of the slug flow induced forces on a single bend has been conducted applying STAR-OLGA coupling and the model predictions have been compared with the experimental data in the literature. Detailed information of the transient force and force distribution on the bend wall has been obtained.

Chapter 8 concludes the work presented in this thesis and provides recommendations for the future work.

2 LITERATURE REVIEW

2.1 Introduction

Slug flow is one of the frequently encountered flow regimes during the transportation of oil and gas in pipelines. Numerous investigations have been conducted by many researchers to obtain an understanding of the occurrence, development and physical behaviour of slug flow. Slug flow can result in serious problems to the production system due to its transient behaviour and intermittence nature. Therefore, various slug mitigation methods have been proposed to cope with the undesirable slug flow. The literature reviewed in this Chapter is grouped into three topics as below:

- (1) slug flow regime
- (2) slug flow modelling
- (3) slug flow mitigation

2.2 Slug Flow Regime

2.2.1 Flow Regimes of Gas/Liquid Two-Phase Flow

Two-phase flow usually refers to the simultaneous flow of gas/liquid, gas/solid, liquid/liquid or liquid/solid. The gas/liquid flow has the most complexity due to the deformability and compressibility of the gas phase (Ghajar, 2004). For the gas/liquid two-phase flow the two phases form several flow regimes due to the simultaneous interaction by surface tension and gravity force. In this section the basic flow regimes of the gas/liquid flow in vertical and horizontal pipes are introduced. The flow regime maps that commonly used in the literature are presented.

The flow regime refers to the distribution of each phase relative to the other phase. The important physical parameters in determining the flow regime are (Ghajar, 2004): (a) surface tension which keeps pipe walls always wet and tends to make small liquid drops and small bubbles spherical; (b) gravity which tends to pull the liquid to the bottom of the pipe (in a non-vertical pipe). Generally the classification and description of the flow

regimes are still very subjective. The flow regimes accepted by many researchers were proposed by Mandhane *et al.* (1974), Taitel and Dukler (1976) and Hewitt (1982).

The regimes encountered in vertical flows include bubble flow, slug or plug flow, churn flow, annular flow and wispy annular flow. The schematics of the five flow regimes are shown in Figure 2-1.

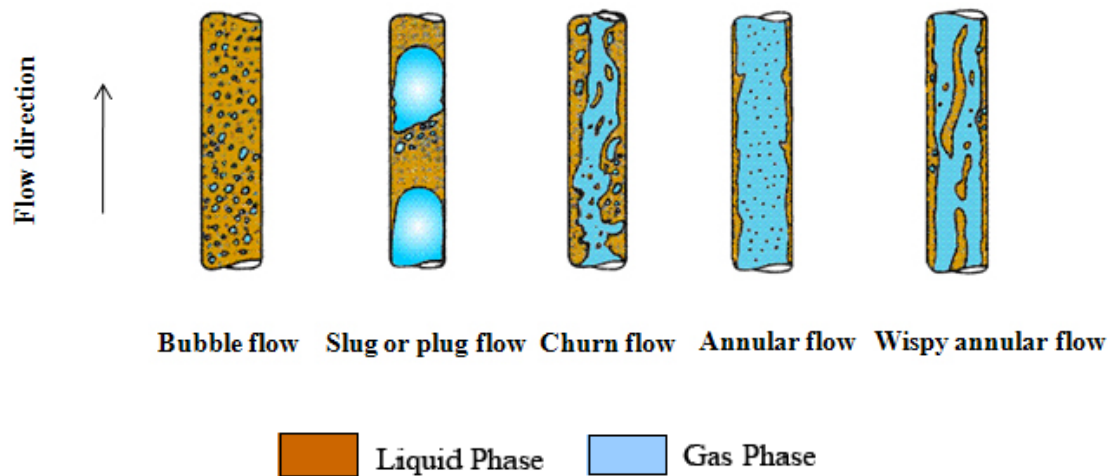


Figure 2-1 Different flow regimes in vertical pipes

The key characteristics of each flow regime are described as below:

- **Bubble flow:** where the liquid is continuous and there is a dispersion of bubbles within the liquid;
- **Slug or plug flow:** where the bubbles have coalesced to form larger bubbles which approach the diameter of the pipe;
- **Churn flow:** where the bubbles in slug flow have broken down to give oscillating churn regime;
- **Annular flow:** where the liquid flows on the pipe wall as a film and the gas flows in the centre with some liquid entrained in the gas core;

- **Wispy annular flow:** where the concentration of droplets increases with the increase of the liquid flowrate, as a result, the large lumps or wisps of liquid form in the gas core.

The flow regimes in horizontal and near horizontal pipes are different from those in vertical pipes due to the large angle between the directions of the flow and gravity. The flow regimes in horizontal and near horizontal pipelines are generally classified into six categories as illustrated in Figure 2-2.

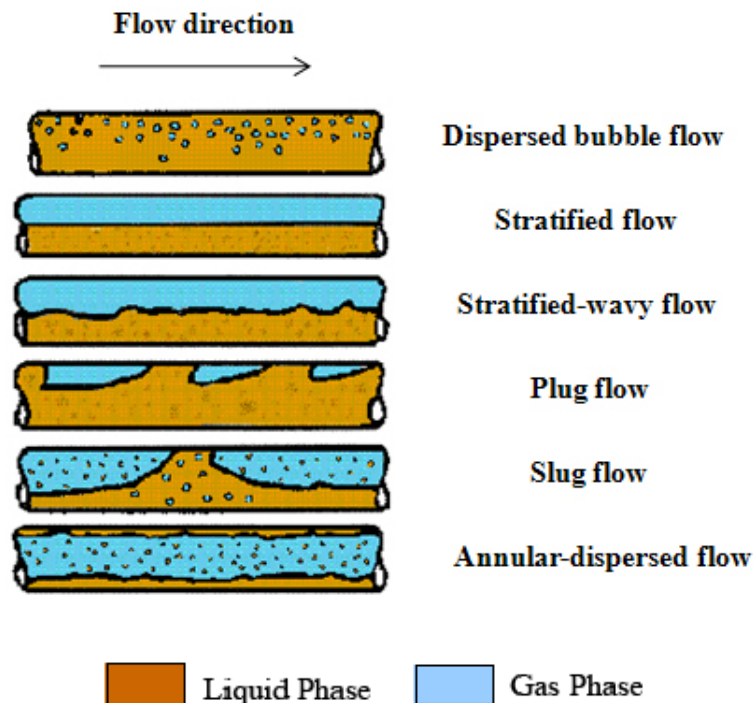


Figure 2-2 Different flow regimes in horizontal and near horizontal pipes

The key characteristics of each flow regime in horizontal and near horizontal pipes are described as below:

- **Dispersed bubble flow:** This flow regime occurs at high superficial liquid velocity and a wide range of superficial gas velocities. The bubbles are dispersed throughout

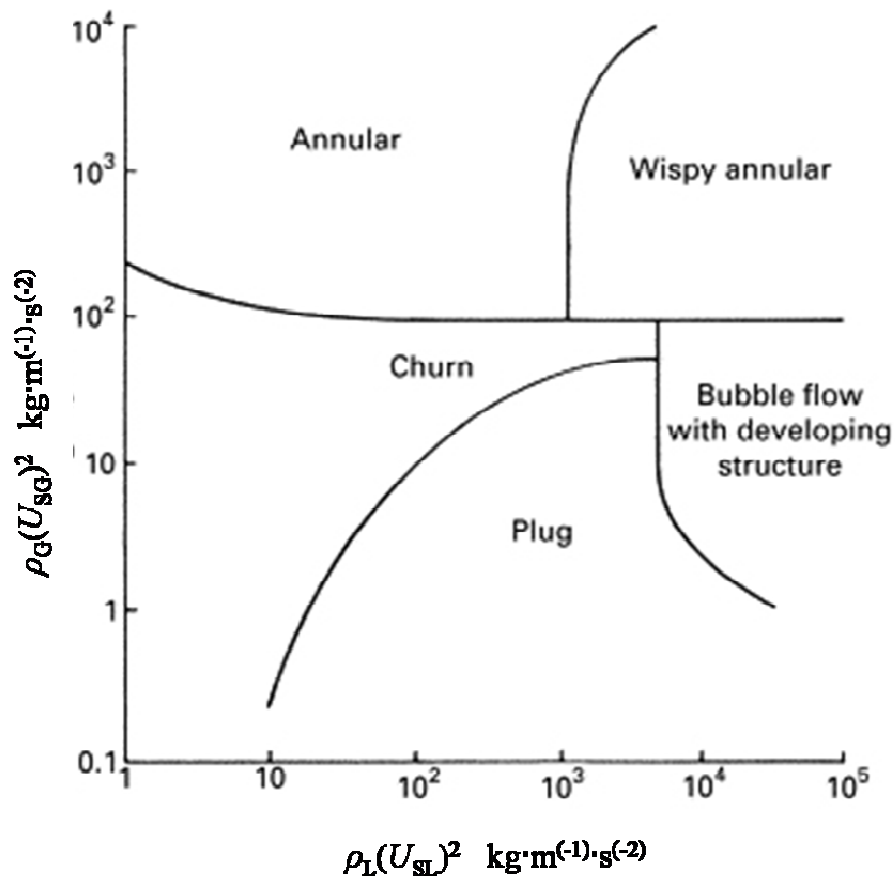
a continuous liquid phase. These bubbles tend to accumulate in the upper part of the pipe due to the effect of buoyancy.

- **Plug flow:** The plug flow occurs at relatively low superficial gas velocity. In the dispersed bubble flow, as the superficial liquid velocity decreases, the smaller bubbles coalesce to form larger bullet-shaped bubbles that move along the top of the pipe.
- **Stratified flow:** At low superficial gas and liquid velocities the gravitational effects result in the total separation of the two phases. The liquid flows along the bottom of the pipe and the gas flows along the top.
- **Stratified wavy flow:** The stratified wavy flow occurs as a result of an increase of the superficial gas velocity in the stratified flow. The increase of the superficial gas velocity results in the increase of the interfacial shear force, rippling the liquid surface and producing a wavy interface.
- **Slug flow:** With the increase of the superficial gas and liquid velocities the stratified liquid level grows and becomes progressively wavier. Eventually the whole cross-section of the pipe is blocked by a wave, i.e. a liquid slug, and then it is accelerated by the elongated gas bubble behind. Hence an intermittent flow regime appear with alternative convey of liquid slugs and elongated gas bubbles.
- **Annular dispersed flow:** At even higher superficial gas velocity the gas pushes through the centre of the pipe leaving an annulus of liquid around the pipe wall. Some liquid may be entrained in the gas core as small and dispersed droplets.

Flow regime maps have been used widely to present the regions of different flow regimes and the transitions among them. The flow regime map is an attempt to separate the space into areas corresponding to the various flow regimes on a two-dimensional graph. Different flow regime maps have been proposed by different researchers for different pipeline orientations.

The flow regime map proposed by Hewitt and Robertson (1969) has been commonly recommended for gas/liquid vertical upward flows. As shown in Figure 2-3 the

coordinates for their map are superficial momentum fluxes for the two phases, respectively. The map works reasonably well for the air/water and steam/water systems. However, the transitions between the neighbour flow regimes appear as lines in their map. Actually the flow regime transitions occur over a range of the given coordinate terms. Therefore, the transitions should be interpreted as broad bands rather than as lines (Ghajar, 2004).

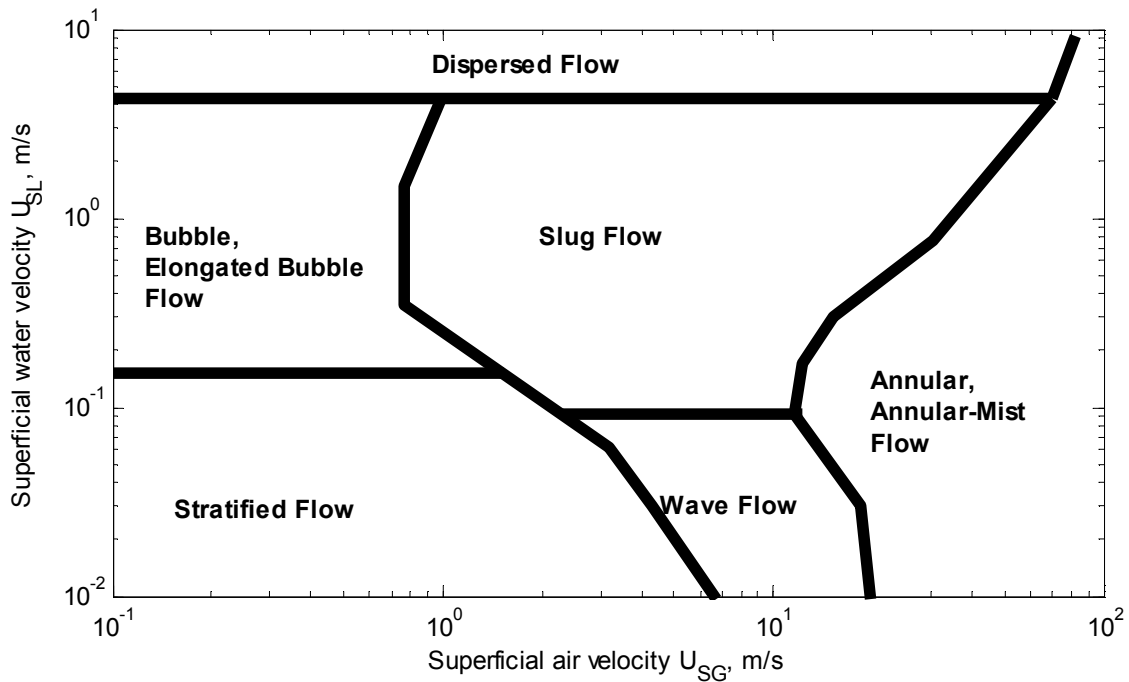


U_{SG} and U_{SL} : Superficial gas and liquid velocities; ρ_G and ρ_L : Gas and liquid densities

Figure 2-3 Flow regime map for vertical upward flow (Hewitt and Robertson, 1969)

A thorough study on the flow regimes in horizontal pipelines was performed by Mandhane *et al.* (1974) based on a large databank of flow regime observations. This study resulted in a map with superficial gas and liquid velocities as coordinates shown

in Figure 2-4. The horizontal flow regimes described by Mandhane *et al.* (1974) were stratified flow, wave flow, bubble/elongated-bubble flow, slug flow, dispersed flow and annular/annular-mist flow.

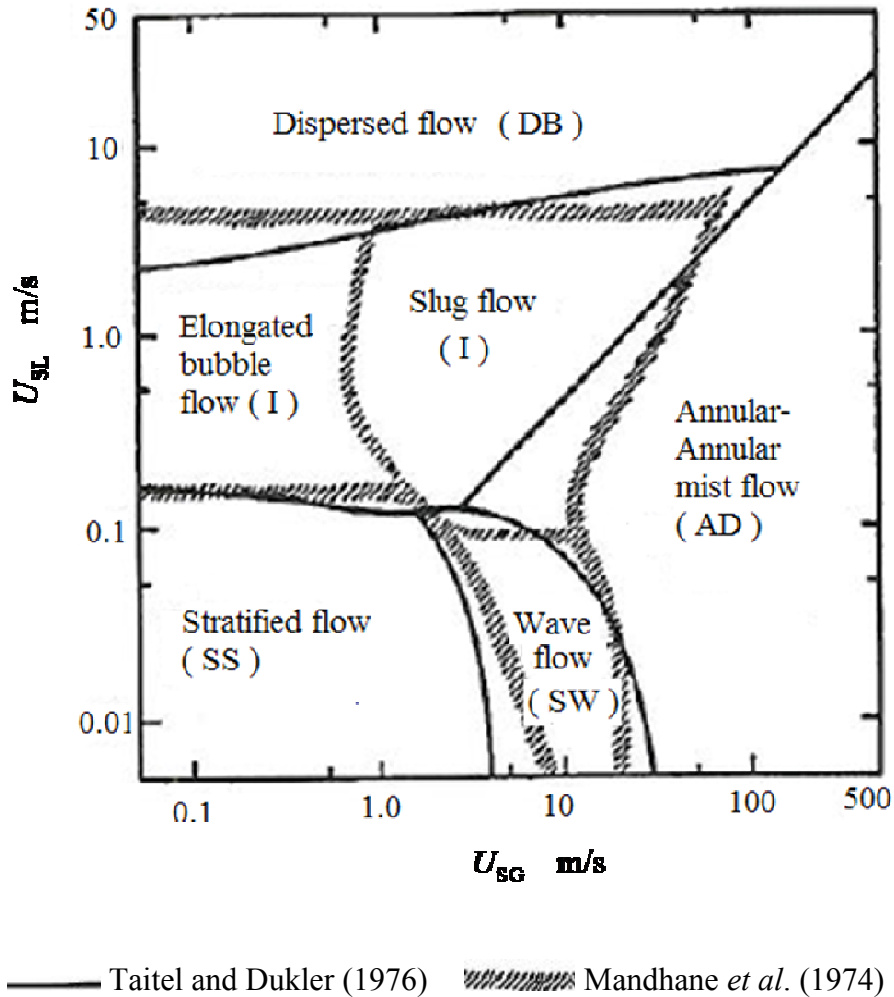


U_{SG} and U_{SL} : Superficial gas and liquid velocities

Figure 2-4 Flow regime map for horizontal flow by Mandhane *et al.* (1974)

Taitel and Dukler (1976) proposed a flow regime map based on a series of semi-theoretical approaches. Five flow regimes were described in their flow regime map, namely, stratified smooth, stratified wavy, intermittent, annular dispersed and dispersed bubble regimes as shown in Figure 2-5. They also presented criteria for each of the flow regime transitions in horizontal and near horizontal flows. The basis of their models was a one-dimensional stratified flow model to give the equilibrium liquid height from which the flow regime transitions were developed. The flow map was plotted in terms of dimensionless parameters. The different physical properties, pipe inclination and pipe diameter can be accommodated. However, it needs to be noted that the empirical correlation factors were largely determined from air/water flows at low pressures in

small diameter pipes. The flow regime map proposed by Taitel and Dukler (1976) is compared with that proposed by Mandhane *et al.* (1974) in Figure 2-5.



DB: dispersed bubble flow; I: intermittent flow; AD: annular-dispersed liquid flow

SS: stratified smooth flow; SW: stratified wavy flow

Figure 2-5 Comparison of the flow regime maps proposed by Taitel and Dukler (1976) and Mandhane *et al.* (1974)

In this work the flow regime map proposed by Mandhane *et al.* (1974) has been used as a reference for the experiment design due to its simplicity and reasonable accuracy.

2.2.2 Gas/Liquid Slug Flow

As mentioned in Section 1.1.3 three types of slugs may appear in the oil and gas transportation flowlines, namely, terrain-induced slugs, hydrodynamic slugs and operation-induced slugs. Riser-induced severe slugging occurs when the liquid blocks the lower point where a down-sloping pipeline is attached to a riser. The blockage initiates the slug, which thereafter grows upward into the riser and back through into the upstream pipeline. In the mean time the upstream gas is compressed until the pressure is sufficiently high to blow the slug out of the riser. Hydrodynamic slug flow usually develops in the horizontal or near horizontal sections of the pipeline where the liquid waves on the gas/liquid interface grow and eventually close the cross-section forming liquid slugs.

Riser-Induced Severe Slugging

Severe slugging can occur in a gas/liquid flow system where a pipeline segment with a downward inclination angle followed by another segment/riser with an upward inclination angle. Severe slugging is believed to be a cyclic process consisting of four stages ((a)-(b)-(c)-(d)) as illustrated in Figure 2-6 (Schmidt *et al.*, 1980; Taitel, 1986).

- (a) **Liquid buildup:** The liquid phase blocks the cross-section of the riser base and forms a slug. But the pressure in the pipeline is not high enough to move the slug forward into the riser and clear the blockage. Then the slug length increases in both of the pipeline and riser due to the continuous liquid inflow and the pressure in the pipeline increases steadily due to the accumulation and compression of the inflowing gas. The slug length can reach one or several riser lengths.
- (b) **Slug production:** The slug production stage starts once the slug front arrives at the riser top. As the gas continues to accumulate at the slug tail the pressure in the pipeline begins to override the riser top pressure slightly. Then the slug tail in the pipeline starts to move forward to the riser base and the slug front moves into the separator. This stage ends once the slug tail (gas/liquid interface) in the pipeline reaches the riser base.

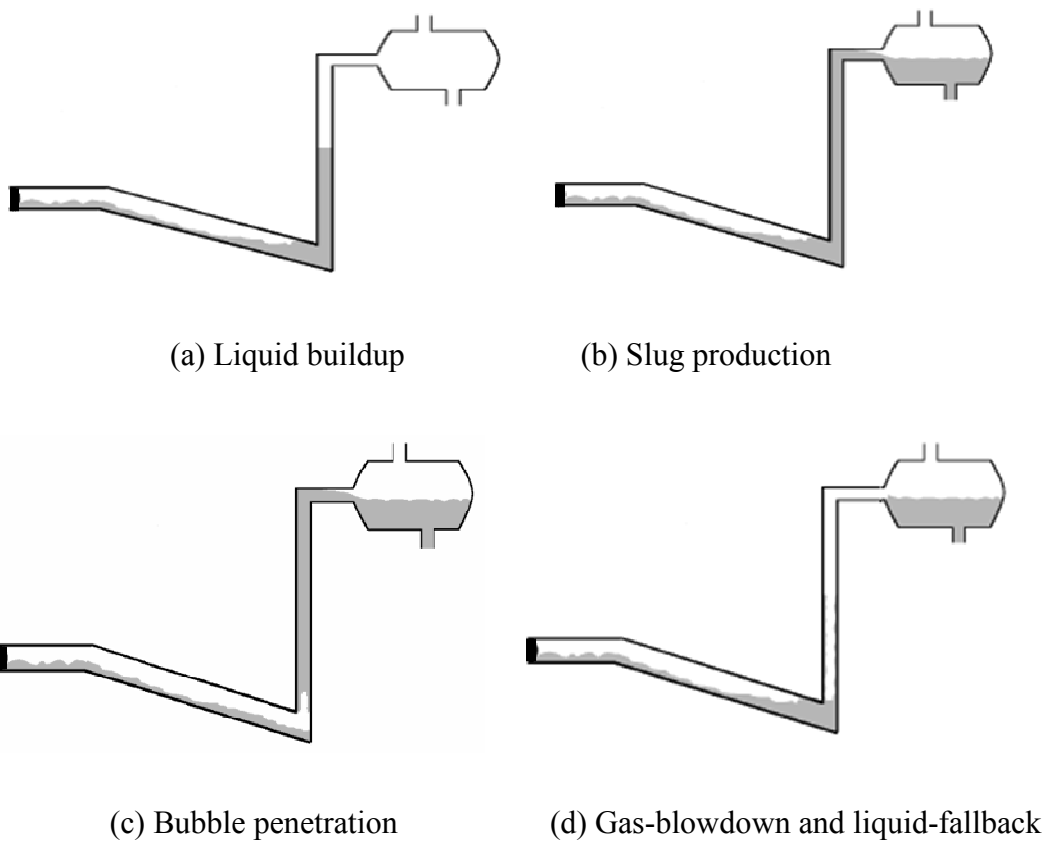


Figure 2-6 Severe slugging cycle consisting of four stages

- (c) **Bubble penetration:** A bubble front forms as the slug tail is approaching the riser base. Then the bubble penetrates into the slug body in the riser, which reduces the hydrostatic pressure of the liquid column. With the motion of the bubble up in the riser the bubble expands due to the reduced pressure on it. The expansion of the bubble in turn reduces the hydrostatic pressure of the liquid column further. At the end of this stage a continuous gas cap forms in the riser.
- (d) **Gas-blowdown and liquid-fallback:** As the gas cap moves up in the riser the drop of hydrostatic pressure accelerates the gas to move into the riser, which in turn results in more drop of the hydrostatic pressure. In this way the gas blowdown is initiated and characterised by a violent swept-out of the remaining liquid in the riser and a fast delivery of the gas subsequently. When the gas flow is not able to support the upward motion of the liquid film on the riser wall, the liquid film begins to fall down to the riser base, namely liquid fallback. Then the liquid from the fallback

and inflow begins to form a new slug, blocking the cross-section of the riser base and initiating the next cycle of severe slugging.

The cyclic process of severe slugging illustrated in Figure 2-6 is a typical example for 'classical' severe slugging. Besides the 'classical' severe slugging, more than one flow regimes resembling to it have been reported. The major classifications of these regimes discussed below are limited to those experienced in vertical and catenary risers only. The flow regimes in other riser configurations such as S-shaped riser are out of the scope of this work.

The phenomenon of severe slugging was first reported by Yocum (1973). The author noticed that the flow capability could be reduced by 50% due to the back pressure fluctuation caused by severe slugging. However, no detailed description of the severe slugging was provided. Schmidt *et al.* (1980) performed a broad range of tests on a 2" vertical riser with air and kerosene as test fluids. They proposed to divide the severe slugging region into three regions, namely, severe slugging in Region I, severe slugging in Region II and transition to severe slugging. Severe slugging in Region I is characterised by the generation of slugs ranging in length from one to several riser lengths, occurring at low gas and liquid flowrates. The characteristic of severe slugging in Region II is that the liquid slugs form only in the riser rather than in both riser and pipeline for the severe slugging in Region I. Thus the length of the liquid slug never exceeds the height of the riser for the severe slugging in Region II. Transition to severe slugging appears when the gas flowrate increases from those for severe slugging in Region II. This flow regime is characterised by the foamed liquid slugs.

The flow regimes in pipeline/riser systems were classified into three main categories by Linga (1987). The three main categories were continuous flow, transitional flow (with occasional severe slugs) and severe slugging. The severe slugging was further classified into two subcategories. The two types of severe slugging were severe slugging Type I and Type II. For severe slugging Type I, the blockage at the riser base is pure liquid; for Type II, the liquid blockage is aerated. Severe slugging Type I was further divided into Type IA and Type IB based on the slug length. For Type IA the liquid slug front reaches the top of the riser before the gas blowdown stage; for Type IB the gas blowdown stage starts before the riser is filled with the liquid slug.

Taitel *et al.* (1990) conducted a series of experiment in a pipeline/riser system. They observed four types of flow characteristics: steady flow, cyclic flow with fallback, cyclic flow without fallback and unstable oscillations. ‘Severe slugging’ is used for either of the cyclic processes with or without fallback when the blowout process is ‘severe’ or occurs as a spontaneous unstable expansion. ‘Severe slugging’ occurs in a pipeline/riser system when the liquid in the riser is unstable and the gas penetrates into the riser. When the liquid column in the riser is stable, there is still a tendency for a cyclic process to occur as reported by Taitel *et al.* (1990). This cyclic process can be damped and become a steady flow or it can continue indefinitely, where the flow can be unstable and lead to a severe slugging type of flow behaviour.

The experiment and analysis carried out by Schmidt *et al.* (1980), Linga (1987) and Taitel *et al.* (1990) were all based on vertical risers. Tin (1991) reported an experimental study on severe slugging in flexible riser systems. The riser was arranged in three configurations, i.e. catenary, Lazy-S and Steep-S. Five types and nine types of severe slugging flow regimes were identified for the catenary and the two S-shaped risers, respectively. As the severe slugging behaviour in S-shaped risers is out of the scope of this work, the details of the nine severe slugging flow regimes are not presented here. The severe slugging flow regimes identified in the catenary riser are described as below:

- **Severe slugging 1 (SS1):** It is similar to the severe slugging in Region I in vertical risers reported by Schmidt *et al.* (1980); however, the bubble penetration at the riser base takes the form of a series of bubbles rather than a single gas cap.
- **Severe slugging 1a (SS1a):** It is similar to SS1 except that the gas blowdown is not initiated by the penetration of the first bubble at the riser base but by a number of bubbles.
- **Severe slugging 2 (SS2):** This is a transitional severe slugging flow regime where the liquid slugs only exist in the riser and bubble penetration occurs before the liquid slug front reaches the riser top.
- **Severe slugging 3 (SS3):** This is also a transitional severe slugging flow regime, characterised by blowdown of the system, periodically reducing the riser base

pressure near to the outlet pressure. The size of the liquid slug is significantly reduced by the high degree of gas penetration.

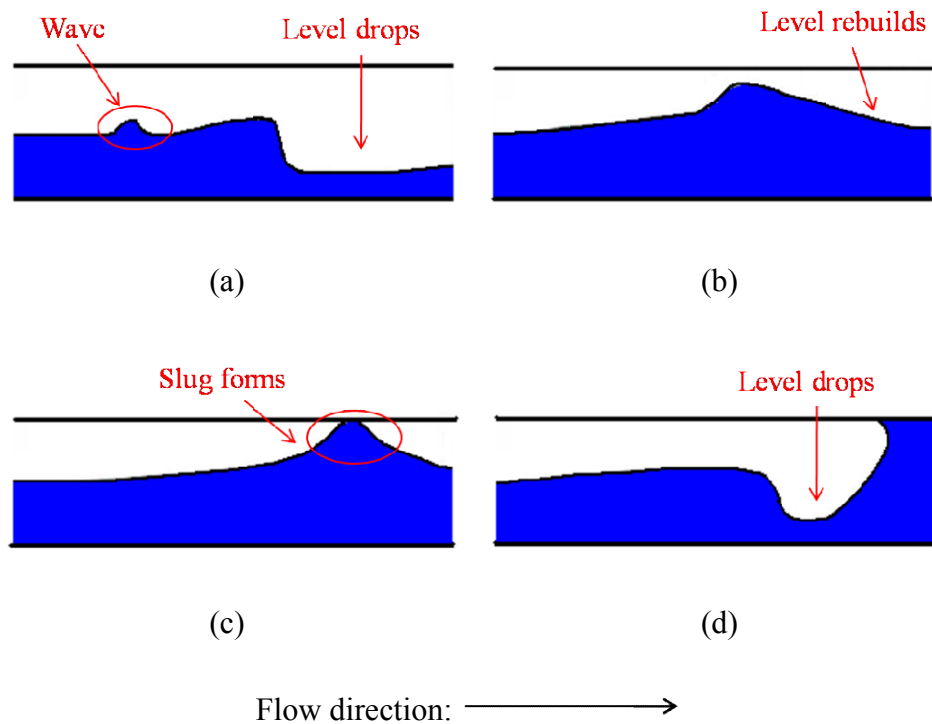
- **Oscillation flow (OSC):** It is a cyclic flow regime with a near-sinusoidal riser base pressure variation against with time.

In this study, a series of experiment have been performed on both vertical and catenary risers. The flow regimes have been classified into four categories, namely, severe slugging, transitional severe slugging, oscillation flow and continuous flow as detailed in Chapter 3.

Hydrodynamic Slug Flow

Hydrodynamic slugs are generally considered to be initiated from the waves at the gas/liquid interface of stratified flow. A commonly accepted mechanism for the growth of these waves is the Kelvin-Helmholtz instability. The process of slug flow is a highly complex unsteady phenomenon. Dukler and Hubbard (1975) explained the flow mechanism of slug flow based on extensive visualisation studies as follows:

- **Slug formation:** Gas and liquid flow concurrently into a pipe. The liquid flows as a stratified layer with the gas phase travelling above near the entrance. At gas and liquid velocities under which the slug flow takes place, the liquid layer decelerates as it moves along the pipe. Consequently the liquid level increases approaching the top of the pipe. In the mean time, waves appear on the liquid surface. Eventually the sum of the rising liquid level plus the wave height is sufficient to bridge the pipe momentarily blocking the gas flow. As soon as the bridging occurs the liquid in the bridge is accelerated to the gas velocity. The liquid acts as a scoop picking up the slow moving liquid in the film ahead of it. By this means the fast moving liquid builds its volume and becomes a slug. Figure 2-7 illustrates the process of slug formation.



(a) Slug just passes out of view to the right inducing level drop; (b) Level rebuilds and wave nearly bridges pipe; (c) Wave bridges pipe forming a slug; (d) Slug sweeps up liquid inducing level drop

Figure 2-7 Slug formation process (after Dukler and Hubbard (1975))

- Slug development:** As the slug travels down the pipe, liquid is shed from its back and forms a film with a free surface. The liquid in the film decelerates rapidly from the slug velocity to a much lower velocity as controlled by the wall and interfacial shear. In the mean time, the slug continues to pick up the liquid ahead which has been shed from the preceding slug. If the picking-up rate at the slug front is greater than the shedding rate at the tail the slug grows in length to form a fully developed slug. For a fully developed slug the picking-up rate is equal to the shedding rate. If the shedding rate is greater the slug will collapse back into a wave.
- Mixing zone in slug:** The slug has a higher kinetic energy than that of the liquid film. Thus the film penetrates a distance into the slug before it finally reaches the same velocity of the slug. A mixing vortex at the slug front is resulted in by the

over-running phenomenon. The gas is trapped in the mixing zone due to the violent mixing operation. With the increase of the gas flowrate and then slug velocity, the degree of aeration of the slug increases.

The hydrodynamic slugs can form in the horizontal pipeline upstream of the riser in pipeline/riser systems. Vázquez and Fairuzov (2009) conducted a theoretical and experimental study to investigate the effects of the riser on the dynamics of the hydrodynamic slugs longer than the riser. A transient mechanistic model was developed and then used to simulate the hydrodynamic slug flow in an offshore production system with a large-diameter pipeline (36 inch). It was found that the long slugs can accelerate in the riser to a velocity of five times greater than the average slug velocity in the pipeline. Therefore, hydrodynamic slugs in pipeline/riser systems can be as problematic as severe slugs due to the great length and high velocity.

2.3 Slug Flow Modelling

In all the engineering problems one has to resort to some approximations to obtain solutions to them. This kind of approximations based on which the physics of the problem is formulated in a format tractable by analytical or numerical means is termed 'modelling' (Taitel, 1994). Slug flow is a highly complex flow with an unsteady nature. Mechanistic modelling of slug flow is to simplify the flow configuration so that an analysis of the flow and prediction of the flow parameters are possible. In this section various modelling methodologies of slug flows have been reviewed. Special emphasis has been placed on the modelling of the riser-induced severe slugging and hydrodynamic slug flow. The methodologies are organised as follows:

- (1) One-dimensional (1-D) mechanistic models of severe slugging
- (2) One-dimensional (1-D) mechanistic models of hydrodynamic slug flow
- (3) One-dimensional (1-D) OLGA modelling
- (4) Three-dimensional (3-D) CFD (Computational Fluid Dynamics) modelling
- (5) Coupling of 3-D CFD and 1-D OLGA models

As stated by Taitel (1994) the ‘mechanistic modelling’ has been adopted where the physical phenomenon is approximated by taking into consideration of the most important processes, neglecting other less important effects that can complicate the problem but do not add considerably to the accuracy of the solution. The mechanistic model needs to be sufficiently simple so that the solution can be obtained with reasonable analytical or numerical efforts. The ‘one-dimensional’ (1-D) model is also a kind of simplification to the long pipeline. In the 1-D approach for a pipeline the model parameters are only a function of the axial distance and time. The 3-D CFD modelling and coupling of 3-D CFD and 1-D OLGA are discussed in Section 2.3.4 and Section 2.3.5, respectively.

2.3.1 One-Dimensional Mechanistic Models of Severe Slugging

The mechanistic models of severe slugging can be classified into three categories as follows (Taitel, 1994): (1) predicting the occurrence of severe slugging, i.e. conditions that lead to severe slugging; (2) predicting the characteristics of severe slugging such as slug length, slug frequency and slug velocity; (3) predicting the characteristics of the flow with a severe slugging mitigation method applied. Three subsections have been organised to deal with the three kinds of models, respectively.

Models for Severe Slugging Occurrence

Schmidt *et al.* (1980) realised that the slug flow reported by Yocum (1973) was significantly different from the hydrodynamic slug flow. They characterised the phenomenon as ‘severe slugging’. Three separate transition criteria for severe slugging to occur in a pipeline/riser system were provided by Schmidt *et al.* (1980, 1985):

- (1) The flow regime in the pipeline upstream of the riser base is stratified flow.
- (2) For a given liquid flowrate there is a critical gas flowrate as the boundary between severe slugging and non severe slugging. A higher gas flowrate is sufficient to overcome the rate of the hydrostatic gain in the riser caused by the liquid flow.

- (3) The pressure drop in the riser decreases as the gas flowrate increases for a given liquid flowrate, then the flow is regarded to be unstable and susceptible to severe slugging.

The first criterion above is the boundary between the stratified flow and non stratified flow. Taitel and Dukler (1976) proposed a criterion for the flow regime transition from stratified flow to non stratified flow. Based on the inviscid Kelvin-Helmholtz theory (Milne-Thompson, 1960), the condition for a small wave growth between a pair of parallel plates is:

$$U_{SG} > \left[\frac{g(\rho_L - \rho_G)h_G}{\rho_G} \right]^{\frac{1}{2}} \quad (2-1)$$

where U_{SG} is the superficial gas velocity, g is the acceleration due to gravity, ρ_L and ρ_G are the liquid and gas densities, respectively, and h_G is the height occupied by the gas phase. The stratified flow occurs when the actual U_{SG} is lower than that calculated by the right hand side term of (2-1). For the flow in a pipe with a circular cross-section the critical U_{SG} is expressed by (2-2) and (2-3) as follows (Goldzberg and McKee, 1985):

$$U_{SG} < C_2 \left[\frac{g(\rho_L - \rho_G)\cos(\beta)A_G}{\rho_G(dA_L/dh_L)} \right]^{\frac{1}{2}} \quad (2-2)$$

where $C_2 \approx A_G/A_L$, β is the inclination angle of the pipe to the horizontal, A and h are the area and the corresponding height occupied by a given phase, respectively; moreover,

$$\frac{dA_L}{dh_L} = d \sqrt{1 - \left(2 \frac{h_L}{d} - 1 \right)^2} \quad (2-3)$$

where d is the pipe diameter. It needs to be noted that the phase fractions in the pipe have to be obtained first, then h is calculated based on the area occupied by each phase.

There are two typical methods proposed by Bøe (1981) and Pots *et al.* (1987), respectively, to account for the second criterion above. The rate of the increase of the hydrostatic pressure in the riser greater than that of the gas pressure in the pipeline is expressed in (2-4) (Bøe, 1981):

$$\frac{\partial(P_{\text{HYD}})}{\partial t} > \frac{\partial(P_{\text{P}})}{\partial t} \quad (2-4)$$

where t is time, P_{HYD} and P_{P} are the hydrostatic pressure induced by the liquid column in the riser and pressure in the pipeline upstream of the riser, respectively. Based on the constant inlet flowrates, gas mass balance in the pipeline and pressure balance over the riser, the terms in (2-4) can be expressed as:

$$\frac{\partial(P_{\text{HYD}})}{\partial t} = \rho_{\text{L}} g U_{\text{SL}} \sin\beta \quad (2-5)$$

and

$$\frac{\partial(P_{\text{P}})}{\partial t} = \frac{P_{\text{P}}}{(1 - \varepsilon_{\text{LP}})L_{\text{P}}} U_{\text{SG}} \quad (2-6)$$

where β is the inclination angle of the riser to the horizontal, L_{P} is the length of the pipeline and ε_{LP} is the liquid volume fraction in the pipeline. The liquid volume fraction, ε_{LP} , was calculated with (2-7) assuming that there is no slip between the two phases (Bøe,1981).

$$\varepsilon_{\text{LP}} = \frac{U_{\text{SL}}}{U_{\text{SG}} + U_{\text{SL}}} \quad (2-7)$$

Hence (2-4) was resolved to give (2-8) for severe slugging to occur:

$$U_{\text{SL}} > \frac{P_{\text{P}}}{\rho_{\text{L}} g (1 - \varepsilon_{\text{LP}}) L_{\text{P}} \sin\beta} U_{\text{SG}} \quad (2-8)$$

Pots *et al.* (1987) proposed a similar criterion, Pi criterion, to predict the operating region for severe slugging to occur as follows:

$$\Pi_{\text{SS}} = \frac{ZRT/M_{\text{W}}}{g(1 - \varepsilon_{\text{LP}})L_{\text{P}}} \frac{W_{\text{G}}}{W_{\text{L}}} \quad (2-9)$$

where Z is the compressibility factor of the gas phase, R is the gas constant, T is the temperature, M_{W} is the molecular weight of the gas, W_{G} and W_{L} are the gas and liquid mass flowrates, respectively. The severe slugging occurs when Π_{SS} is less than 1. For a

vertical riser the Pi criterion reduces to the Bøe (1981) criterion when it is expressed in terms of superficial velocities and pressure and the effect of Z is neglected.

Taitel (1986) proposed a stability criterion for a steady-state operation to be achieved in pipeline/riser systems. The condition under which severe slugging is impossible to occur, is

$$\frac{\partial(\Delta F)}{\partial y} < 0 \quad (2-10)$$

at $y = 0$, where y is the height of the gas cap front in the riser and ΔF is the pressure difference acting on the liquid column in the riser expressed in (2-11).

$$\Delta F = \left[(P_S + \rho_L g L_R) \frac{\varepsilon_{GP} L_P}{\varepsilon_{GP} L_P + \varepsilon'_G y} \right] - [P_S + \rho_L g (L_R - y)] \quad (2-11)$$

where P_S is the separator pressure, ε_{GP} is the gas volume fraction in the pipeline, ε'_G is the gas volume fraction in the gas cap penetrating into the liquid column in the riser, L_R and L_P are the lengths of the riser and pipeline upstream of the riser base, respectively. The resultant criterion for severe slugging to occur was expressed as follows:

$$\frac{P_S}{P_0} > \frac{(\varepsilon_{GP}/\varepsilon'_G)L_P - L_R}{P_0/\rho_L g} \rho_L \quad (2-12)$$

where P_0 is the atmospheric pressure. It can be observed that the criterion is determined by the system geometry, liquid volume fractions in the pipeline and the gas cap penetrating into the liquid column. A constant value of $\varepsilon'_G = 0.89$ was assumed and ε_{GP} was expressed as a function of U_{SL} by Taitel (1986). For a specific pipeline/riser system the criterion provided an upper limiting liquid flowrate for severe slugging to occur.

Various assumptions and simplifications, such as straight pipeline, straight riser (or straight vertical riser) and no liquid fallback, were made in the models presented above, which restrict the application of them. For an undulating pipeline it is challenging to estimate the liquid or gas volume fractions in the pipeline and apply the stratified flow criterion; for a catenary or S-shaped riser the expressions of the hydrostatic pressure in

the riser and the assumptions of the shape of the penetrated gas cap and gas volume fraction in the gas cap (Taitel, 1986) were not taken into account by the above models.

Models for Severe Slugging Characteristics

The first mechanistic model of severe slugging was proposed by Schmidt *et al.* (1980) to predict the dynamic slug characteristics such as slug length and slug buildup time. Constant inlet gas and liquid mass flowrates, constant separator pressure and liquid slugs free of entrained bubbles were assumed in the model. The model was developed based on mass flow and pressure balance for the pipeline and riser at the liquid buildup stage. To close the model equations empirical correlations for the liquid holdup in the pipeline and the liquid fallback in the riser were required to account for the preceding severe slugging cycle. A good agreement with the experimental data was obtained; however, the generality of this model is limited due to the use of the empirical correlations. Schmidt *et al.* (1985) developed a model of the entire severe slugging cycle using different mass and pressure balance equations for each stage of the cycle. The transition between each stage in the severe slugging cycle was defined in terms of the position of the gas/liquid interface. Similarly to the previous model by Schmidt *et al.* (1980), empirical correlations for the liquid holdup in the pipeline and the liquid fallback in the riser were required to close the model. The simulation results compared favourably against the experimental data of Schmidt *et al.* (1980). Pots *et al.* (1987) extended this model to account for the pipeline inclination and showed how the increasing pipeline inclination increased the slug length and liquid buildup time.

Fabre *et al.* (1987) recognised that severe slugging was essentially the propagation of large scale instabilities and void fraction waves through a vertical column of liquid. To model these phenomena they developed a model based on the considerations of the unstable flow in the riser. A simplified stratified flow model for the pipeline and a partial differential equation (PDE) based model for the riser were employed. In contrast to the previous attempts at modelling severe slugging, the same general formulation of equations was employed for each stage of the severe slugging cycle in the riser. The drift flux model (Zuber and Findlay, 1965) was used to close the model equations. The void fraction, velocity and pressure profiles in the severe slugging cycle could be provided by the model. The model predictions were in good agreement with the

experimental results for the liquid buildup and gas blowdown stages of severe slugging. However, the slug production stage was not well predicted due to the simplicity of the pipeline model. The study of Fabre *et al.* (1987) was extended by Sarica and Shoham (1991). They included a model for the interaction of the gas/liquid two phases in the pipeline. A stratified gas/liquid flow with the liquid accumulating at a distance upstream of the riser base was assumed in the pipeline.

As mentioned in Section 2.2.2 Taitel *et al.* (1990) observed four flow regimes: steady flow, cyclic flow with fallback, cyclic flow without fallback and unstable oscillations in a pipeline/riser system (a vertical riser). A model was developed to predict the flow regime and flow parameters such as local liquid holdup in the riser, pressure fluctuations, liquid penetration into the pipeline, cycle time and blowout time. The initial condition of the model was the beginning of bubble penetration stage when the gas bubbles penetrate into the riser full of liquid. These bubbles corresponded to a void fraction wave propagating through the riser. The propagation of the bubble front through the riser was calculated based on the mixture velocity entering the riser base. It was assumed that the bubbles penetrating into the riser were Taylor bubbles. The interaction between the flow in the pipeline and riser was taken into account to allow for the liquid fallback. The flow regimes in the pipeline/riser system observed in the experiment could be differentiated through the model predictions. However, the predictions for severe slugging characteristics suffered from inaccuracies because the model equations became ill-posed below the Taitel stability line (Montgomery, 2002).

Most of the aforementioned models were developed for vertical risers. Most recently, Baliño *et al.* (2010) proposed a model of severe slugging for risers with variable inclinations. The model considered one-dimensional and isothermal flow in both pipeline and riser subsystems. The liquid phase was assumed incompressible and the gas phase was considered as an ideal gas. The flow regime in the pipeline was assumed as stratified and the inertia in the riser was neglected. In this way, severe slugging was controlled mainly by gravity in the riser and compressibility in the pipeline. It was claimed that the model was able to handle discontinuities in the flow, such as liquid accumulation in the pipeline, liquid level in the riser and void fraction waves. They applied their model to simulate the experimental data for vertical risers and obtained

better results than those developed by Taitel *et al.* (1990) and Sarica and Shoham (1991). The model was also successfully used to simulate the experimental data from a catenary riser. It was claimed that their model did not suffer from the problem, ‘infinite gas penetration’ at the bottom of the riser, experienced by the models proposed by Taitel *et al.* (1990) and Sarica and Shoham (1991).

Models for Severe Slugging Mitigation

The models presented in the above subsections are developed for pipeline/riser systems without any slug mitigation methods applied. In this subsection some typical models accounting for the changes in operational conditions when applying slug mitigation methods have been introduced.

As recognised by Schmidt *et al.* (1979) choking can eliminate severe slugging by increasing the back pressure proportionally to the velocity increase at the choke. Gas lift was also considered to be effective for severe slugging mitigation (Schmidt *et al.*, 1979; Pot *et al.*, 1987; Hill, 1989). The injected gas can reduce the hydrostatic head in the riser and keep the liquid moving up the riser. A theoretical and experimental study on these two severe slugging mitigation methods was conducted by Jansen *et al.* (1996). They applied two approaches to analyse the pipeline/riser system with severe slugging mitigation methods. The first approach was a stability analysis of the system based on the stability concept proposed by Taitel (1986). They performed an overall force balance including the effects of the choke and gas lift. The second approach was an extension of the quasi-equilibrium model developed by Taitel *et al.* (1990) to include the performance of the choke and gas lift. The stability model was a time independent force balance assuming severe slugging to occur at unstable riser flow conditions, while the quasi-equilibrium model was a transient model. The transient model can be used to estimate the characteristics of the flow such as slug length and cycle time with the choking and gas lift methods applied. It was claimed that both models gave good agreement with the experimental data.

A novel approach called self-gas lifting was proposed by Sarica and Tengedal (2000) to mitigate or eliminate severe slugging in pipeline/riser systems. The principle of the proposed technique was to connect the riser to the downward inclined segment of the

pipeline with a small diameter conduit. The details of this slug mitigation technique can be found in Section 2.4.2. A prediction model for the bypass gas-lifting configuration was developed through modifying the model proposed by Sarica and Shoham (1991) to investigate the feasibility of this novel approach. The development of the model was based on one-dimensional gravity-dominant flow in both the pipeline and riser. The system variables in the riser were functions of both time and space, while in the pipeline they were only functions of time. A drift-flux formulation was used for the flow in the riser. The void fraction in the pipeline under stratified flow was calculated based on the inlet conditions using a local equilibrium concept. No mass transfer between the phases was considered. The model equations and the procedure for solving them are referred to Sarica and Tengedal (2000) and Sarica and Shoham (1991).

As stated by Sarica and Tengedal (2000) the pressure losses in the bypass system may have an effect on the rate of the gas transfer with obvious impact on the holdup in the riser and total pressure behaviour of the system. However, the pressure losses were ignored for simplicity by Sarica and Tengedal (2000). This disadvantage was overcome by a steady model presented by Tengedal *et al.* (2003). Tengedal *et al.* (2003) claimed that: (1) the model could be used as a design tool for the self-gas lifting concept by determining the operation envelope for a successful self-lifting operation; (2) the model could predict the acceptable range of pressure losses in the gas bypass for the continuous steady-state operation of the self-gas lifting system. The model was found to perform well compared with the experimental data.

Storkaas (2005) conducted an investigation of severe slugging mitigation using active control methods. In the study of Storkaas (2005) the severe slugging in a pipeline/riser system was suppressed by manipulating the topside choke valve through PID (Proportional, Integral and Derivative) controllers. To design an effective control system it is essential to have an accurate model of the process. However, they found that the available models were mostly based on two approaches, i.e. two-fluid modelling and drift-flux modelling. From a control point of view those models are poorly suitable for controller design because they are based on partial differential equations (PDE) and thus infinite-dimensional. The PDE-based two-fluid model can result in too many state variables for the design of controllers. Furthermore, they found that a lot of the spatial

variations and fast dynamics included in the PDE-based models were unnecessary. Hence they proposed a simplified dynamic model that could describe the dominant behaviour of a pipeline/riser system with severe slugging. The model had only three dynamic states, i.e. the holdup of gas and liquid in the riser and the holdup of gas in the upstream pipeline. The most important adjustable parameters are the ‘valve constant’ for the flow of gas into the riser and two parameters describing the fluid distribution in the riser. The model predictions agreed with the data from an OLGA test case and experiments. Furthermore, the model was verified by showing that its controllability predictions were almost identical to those of a more detailed two-fluid model based on PDEs. The simplified model was then used as a tool for designing control systems, such as evaluating different measurement candidates for control and testing various control configurations.

Most recently, Ogazi (2011) recognised the limitations of the simplified model proposed by Storakaas (2005): (1) the riser outlet pressure (similar to the separator pressure) was assumed to be constant; (2) the model did not account for the slug production stage in the severe slugging cycle; (3) the gas volume in the pipeline was assumed to be constant, which limited the simultaneously accurate prediction of the pressure amplitude and slug frequency; (4) the inlet gas/liquid flowrates were assumed to be constant, otherwise the model parameters needed to be re-tuned. Accordingly the original model proposed by Storakaas (2005) was improved by Ogazi (2011): (1) a topside separator model was added; (2) the accumulated liquid upstream of the riser was modelled to enhance the prediction of the slug production stage; (3) the upstream gas volume was modelled as a function of the dynamic pipeline pressure and inlet flowrates; (4) a linear well model was added to account for the variation of the inlet flowrates. Based on the validation by the experimental data it was claimed that the improved model could provide better predictions of the severe slug characteristics such as pressure amplitude and slug frequency.

2.3.2 One-Dimensional Mechanistic Models of Hydrodynamic Slug Flow

The discussions in this section are divided into two subsections dealing with steady-state models and transient models, respectively. The steady-state models are developed based on the ‘unit-cell’ assumption and the transient models mainly include slug

tracking and slug capturing models. The discussions below only highlight the modelling methodologies, differences from others and comments on its advantages and shortcomings.

Steady-State Models of Slug Flow (Unit-Cell based Models)

Steady-state models are developed based on the ‘unit-cell’ assumption. In these models a sequence of slugs is treated as a series of identical slug units. A ‘slug unit’ includes a slug region and a film region as illustrated in Figure 2-8. In the film region a liquid film is located below an elongated gas bubble.

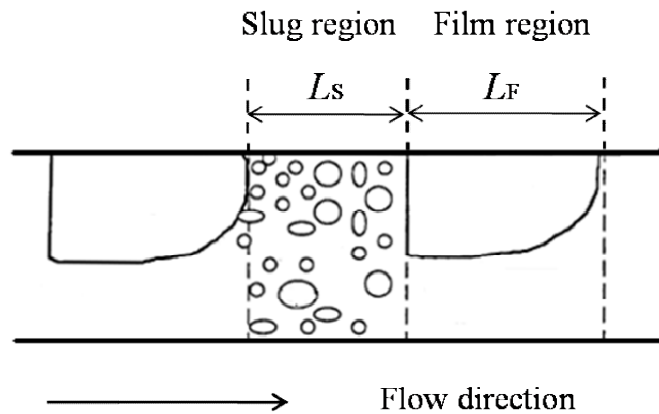


Figure 2-8 Schematic of a slug unit

Based on the ‘slug unit’ concept an ‘average slug’ and its associated Taylor bubble are modelled. Then the flow is assumed to consist of a number of identical slug units. The growth, shrinkage, generation and disappearance of slugs as they propagate along the pipe are not taken into consideration. The ‘slug unit’ based modelling of slug flow has been reviewed by many researchers (Taitel and Barnea, 1990; Fabre and Liné, 1992; Bendiksen *et al.*, 1996; King, 1998; Manfield, 2000; Hale, 2000; Ujang, 2003).

An early model of slug flow in horizontal pipes was proposed by Kordyban (1961). The following assumptions were made: (1) part of the liquid flows in the lower section of the tube obeying the laws of the open channel flow; (2) the rest flows in disk-shaped

slugs that alternate with gas bubbles in the upper part of the tube; (3) the liquid slugs move at the same velocity as the gas bubble and skate over the top of the slower moving liquid below. A pressure drop expression containing frictional and acceleration terms was developed based on the above assumptions. The acceleration terms were then eliminated by assuming that the thickness of the liquid layer was constant and that the ratio of gas mass flowrate to total mass flowrate was constant. However, the resultant predictions were worse than those obtained from the empirical correlation of Lockhart and Martinelli (1949). Hence Kordyban (1961) concluded that the model was inadequate to predict the flow regime properly.

The model developed by Singh and Griffith (1970) provided better pressure drop predictions. To describe the slug unit they assumed that the nose and tail of the bubble region were perfectly flat and perpendicular to the axis and the liquid film was flat. The pressure drop over the slug unit was calculated by considering the wall shear forces in the slug region and gravitational forces on the whole slug unit. However, the pressure drop due to the wall shear forces on the liquid film and the gas phase were neglected. It needs to be mentioned that the liquid holdup in the slug body was assumed to be unity. For a horizontal pipe the pressure gradient was due only to the frictional contribution in the slug region in their model.

Bonnecaze *et al.* (1971) proposed a similar model to that by Singh and Griffith (1970) to calculate the pressure gradient over a slug unit. They proposed that the total pressure drop across a slug comprised three components: (1) the frictional pressure drop in the 'essentially all liquid' slug core; (2) the pressure drop in the mixing zone at the front of the slug body; (3) the pressure drop in the film region. However, the pressure drop in the mixing zone and film region was considered to be comparatively small and then neglected in the later analysis. Consequently only the frictional force in the slug region and gravitational force were taken into consideration. Bonnecaze *et al.* (1971) introduced an independent friction factor correlation based on the experimental data from a 6 inch field line instead of using the Fanning-type friction factor as Singh and Griffith (1970).

In the model of Vermeulen and Ryan (1971) the pressure drop consists of two components induced by the wall shear stress in the slug region and the acceleration of

the liquid film at the front of the slug, respectively. The pressure drop induced by the gas phase was neglected. To calculate the frictional component the single phase shear relations for turbulent flow in a smooth pipe were used and the slug was assumed to have the same density as the liquid phase and travel at the mixture velocity. When calculating the acceleration component of the pressure drop, it was assumed that the film velocity was zero relative to the wall before being accelerated to that of the slug. It was claimed that this model was a great improvement on the earlier one proposed by Kordyban (1961) because the contribution of the liquid film to the overall pressure drop of the slug unit was taken into consideration.

Dukler and Hubbard (1975) proposed a more complete model than those discussed above. Their model could predict the detailed structure of slug flow with given flowrates, fluid properties, pipe geometries/inclinations, slug frequency and liquid holdup in the slug. They described the slug unit in their model as follows. The slug unit is made up of two regions: a film region in which the liquid flows as a film beneath a large elongated bubble; a liquid slug region in which the two phases flow as a homogeneous mixture. The front of the liquid slug contains a mixing region. In the film region, the film height rapidly decreases with the increasing distance from the tail of the slug until it reaches an equilibrium level. It needs to be mentioned that the pressure drop in the film region was also neglected in their model.

Taitel and Barnea (1990) proposed a comprehensive model for predicting the details of slug flow based on the 'slug unit' concept. They argued that the pressure drop in the film region could not be neglected for a long gas bubble. Three distinct cases with various degrees of simplicity for the hydrodynamics of the liquid film were presented.

- Case 1: describing the liquid film using the one-dimensional channel flow approximation with both phases taken into consideration;
- Case 2: treating the liquid film as a free surface channel flow;
- Case 3: assuming the liquid film to be uniform along the bubble region.

These three cases differed with regard to the accuracy of the solution and ease of the calculations. The authors concluded that: (1) Case 2 and Case 3 were primarily used for

horizontal and vertical flows, respectively; (2) Case 2 could be inaccurate for long liquid film regions; (3) Case 1 was recommended as it was not more difficult to be solved but gave a better description of the film profile than Case 2. There are some deficiencies to be investigated further such as the treatment of bubble shape, estimation of the friction factors and the theories to determine the liquid holdup in liquid slug, slug lengths and slug frequency. However, it needs to be noted that the proposed models are still useful for the practical applications due to their simplicity.

The steady-state models are not able to predict the transition from one flow regime to another, the formation, growth, decay and dissipation of slugs as they travel along the pipe. To address the above issues the transient models are required.

Transient Models of Slug Flow (Slug Tracking and Slug Capturing Models)

Different from the steady-state models that assume the unit cells of slug flow, the transient models treat each slug to be unique. The transient models of slug flow are mainly classified into two categories, i.e. slug tracking and slug capturing models. In slug tracking models the movement, growth and disappearance of slugs are effected by tracking individual slugs. Firstly the slugs are usually generated based on flow regime maps, then the position of each slug tail and front is monitored along the pipe in Lagrangian coordinates with time. Then the position information is fed into the mass/momentum flux calculations at slug fronts and tails (Bendiksen *et al.*, 1990; Straume *et al.*, 1992; Issa and Kempf, 2003). In slug capturing models the slug flow regime is predicted as a mechanistic and automatic outcome of the growth of hydrodynamic instabilities (Issa and Woodburn, 1998).

One of the earliest studies on slug tracking modelling of slug flow was conducted by Scott *et al.* (1987). Two types of slug growth in long pipelines were found in their investigations, i.e. developing slug growth and long term slug growth. The developing slug growth was induced by the pickup process at the slug front when the pickup rate was greater than the shedding rate at the slug tail. The long term slug growth took place due to the expansion of gas and merging of slugs. To describe the slug growth the liquid holdup in slug body was obtained by the correlation proposed by Gregory *et al.* (1978). A uniform film profile was assumed and determined by a momentum balance between

the wall shear stress of the liquid phase and the interfacial shear stress (the shear stress of the gas phase was neglected). The ‘no slip’ assumption was made in the slug body.

Bendiksen and Espedal (1992) proposed a similar model to that of Scott *et al.* (1987) in the study of the flow regime transition from stratified flow to slug flow. In their model the translational velocity was obtained by the correlation of Bendiksen (1984) and the film region was considered to be equilibrium stratified flow. Their model was developed further by Woods and Hanratty (1996). In the study of Woods and Hanratty (1996) the phase slip in the slug body was considered with the mixture velocity higher than 7 m/s. The slip ratio, defined as the superficial gas velocity over superficial liquid velocity, was established as 1.5 based on their experiment. In their study the film height and liquid holdup in slug body came from the experimental data. The gas velocity was assumed to be equal to that of Taylor bubble and the liquid film velocity was calculated based on a momentum balance using the correlation of Andritsos and Hanratty (1987) for the interfacial shear term.

Barnea and Taitel (1993) applied the slug tracking approach to calculate the slug length distribution at any desired position along the pipe. A random distribution of slug length at the inlet of the pipe was assumed and the increase or decrease in each individual slug length and the disappearance of the short slugs were predicted by the model. Two types of slug length distribution were used, namely, uniform distribution and normal distribution. It was found that the slug length distribution in the developed region followed approximately the log-normal distribution as observed by Brill *et al.* (1981), which was not sensitive to the inlet slug length distribution. It needs to be noted that, in their model, the film region between slugs was not considered; hence the velocity of the slug front was equal to the velocity of the slug tail ahead. The slug tail velocity was calculated by the correlation of Bendiksen (1984).

In the slug tracking model developed by Nydal and Banerjee (1995, 1996), the effects of pressure were taken into consideration before incorporating some kinematic effects. It was assumed that: (1) no gas was entrained in slugs; (2) the thickness of the liquid film between slugs was constant; (3) the pressure drop in the film region was negligible. They used an object-oriented algorithm and treated each slug and bubble discretely and in sequence. A wake effect of the same form used by Barnea and Taitel (1993) was

introduced when calculating the bubble translational velocity. It needs to be noted that the gas phase was treated as incompressible and a constant bubble length was assumed when calculating the slug length distribution.

The effects of the gas compressibility were included in the slug tracking model reported by Larsen *et al.* (1997). Similar to the model of Nydal and Banerjee (1995, 1996) no gas entrainment in the slug body and uniform film height in the film region were assumed. Taitel and Barnea (1998) also investigated the effects of the gas compressibility on a slug tracking model. The liquid holdup in the slug body was obtained by the correlation of Gregory *et al.* (1978). The liquid film between slugs had a uniform thickness, calculated based on a quasi-equilibrium force balance. The model predictions showed that an increase in the slug unit length was induced with the inclusion of the gas compressibility, but the growth of the slug body was not affected significantly.

Issa and co-workers (Issa and Kempf, 2003; Issa *et al.*, 2011) developed a slug capturing method based on the numerical solution of the two-fluid model equations using fine meshes. In their slug capturing model the slug flow regime was predicted as mechanistic and automatic outcome of the growth of hydrodynamic instabilities (Issa and Woodburn, 1998). The same set of governing equations, i.e. the one-dimensional transient two-fluid model and closure laws, were used for the stratified, slug and transition regimes. The increase of the liquid volume fraction and formation of the slugs happened naturally as a numerical solution of the two-fluid model equations. The development, growth, merging and collapse of the slugs only depended on the solution of the transport equations for mass and momentum for each phase. The only empirical information used in their model was the closure relations for the liquid/wall, gas/wall and interfacial shear forces. Issa and Kempf (2003) claimed that they were the first to demonstrate that the two-fluid model was able to capture the development of slug flow from the growth of instabilities in stratified flow in a natural way. The model predictions of the growth rate of instabilities, transition from stratified to slug flow and slug characteristics such as slug length and frequency were compared well with the analytic solutions and/or experimental measurements. However, the accuracy of the model predictions were sensitive to some of the closure models for shear forces in the momentum equations, especially the wall shear force on the liquid phase. To increase

the numerical accuracy of the model it was recommended to use fine enough meshes, but the huge computation amount is an issue for engineering applications.

2.3.3 One-Dimensional OLGA Modelling

OLGA is one of the multiphase flow simulation codes widely used in the oil and gas industry. OLGA was originally developed for two-phase hydrocarbon flow in pipelines and pipeline networks, with processing equipment included (SPT Group, 2006). Later, a water option was included which treats the water as a separate liquid phase.

Essentially OLGA is a transient one-dimensional (1-D) modified two-fluid model, i.e. separate continuity equations for the gas, liquid bulk and liquid droplets are applied; these may be coupled through interfacial mass transfer. Only two momentum equations are used; one for the continuous liquid phase and one for the combination of gas and possible liquid droplets. The velocity of any entrained liquid droplets in the gas phase is given by a slip relation. One mixture energy equation is applied; both phases are at the same temperature. This yields six conservation equations to be solved: three for mass, two for momentum and one for energy. The continuity equations for bulk water and water droplets are added with the water option on. The bulk water velocity is obtained from a correlation for water velocity relative to the average liquid bulk velocity. The closure laws are based on two main flow regime classifications, namely, separated flow and distributed flow. In the case of separated flows such as stratified flow and annular mist flow, the closure laws are in the form of correlations for each flow-regime dependent parameter. For distributed flows such as bubble flow and slug flow, the closure laws take the form of a ‘slip relations’, relating the phase velocities to one another.

Applications to Severe Slugging

The first attempt at predicting severe slugging was that carried out as part of the OLGA code development. The code predictions were compared against the data of Schmidt *et al.* (1980) and from the SINTEF Two-Phase Flow Laboratory (Linga and Østvang, 1985). It was shown how the employed numerical scheme smoothed out the liquid

holdup discontinuities in severe slugging. The pressure cycling characteristics were not predicted by the code reasonably well.

Mazzoni *et al.* (1993) described the predictions of severe slugging in an offshore field using OLGA. The pressure cycling and liquid accumulation process in the riser was clearly shown. Courbot (1996) reported the use of OLGA to predict the region of potential severe slugging in an offshore pipeline/riser application. Unfortunately there was little recorded data to be compared with the model predictions in both of the above cases.

Kashou (1996) verified OLGA by comparing the simulation results with the experimental data from two riser configurations (an S-shaped riser and a catenary riser). Generally the simulations showed a degree of success in predicting the overall flow regimes, cycle times and slug lengths in the pipeline/riser systems; however, details of the severe slugging characteristics such as peak production rate were not correctly predicted by the code. OLGA experienced difficulty in predicting the slug production period, particularly at high gas velocities.

Yeung *et al.* (2003) reported a series of simulation results from an S-shaped riser. The results showed that the variations of boundary conditions affected the flow behaviour in the riser significantly and the liquid holdup in the down comer of the riser was over predicted due to the assumption of a horizontal gas/liquid interface (curved interface in reality). The effects of the downstream equipment conditions on the flow behaviour in a catenary riser were demonstrated through OLGA by Yeung *et al.* (2006). The model predictions agreed with the experimental data reasonably well although there were some differences in detail. It was found that imposing a pressure boundary at the riser outlet to represent the downstream equipment resulted in quite different flow behaviour in the riser. Therefore, they recommended that, in any simulation study on pipeline/riser systems, the downstream equipment and controls need to be included in the model.

Applications to Hydrodynamic Slug Flow

OLGA is the first commercial code to incorporate a non-diffusive slug tracking scheme (Bendiksen *et al.*, 1990; Straume *et al.*, 1992). Two numerical schemes are employed to

solve the model equations. One is an implicit scheme used for separated and bubbly flows and a Lagrangian tracking scheme for slug flows (Straume *et al.*, 1992). The implicit scheme is used for most normal transient calculations. Bendiksen *et al.* (1991) stated that the implicit numerical schemes were more efficient and stable for pipeline simulations of slow transients and were favoured over explicit schemes in these cases due to the improved computational efficiency. However, for slug flow regime the purely implicit schemes were highly undesirable (Straume *et al.*, 1992). Numerical diffusion inherent in the implicit schemes causes a ‘smoothing out’ of void fraction discontinuities, such as the slug front and tail. To track the propagation of the slugs a Lagrangian slug tracking scheme is adopted by OLGA. The slug tracking scheme traces the movement of a discontinuity. The cell that contains the discontinuity is divided into two regions with separate flow regimes. Then the flow parameters are calculated based on each flow regime.

As summarised by King (1998) the slug tracking model in OLGA had received a lot of attentions. Hustvedt (1993) used OLGA to predict the slug distribution in a Tunisian oil pipeline and compared with experimental data. The experimental results exhibited the typical Log-Normal (Brill *et al.*, 1981) or Inverse Gaussian (Dhulesia *et al.*, 1993) shapes of slug length distributions. OLGA predicted the correct distribution shape, maximum and mean slug length. However, it predicted twice the number of slugs observed in practice. Burke and Kashou (1993) highlighted one of the shortcomings of the OLGA model that the slug frequency within the pipe needed to be specified. Because the slug frequency has not been modelled adequately, a significant limitation is imposed on the application of the slug tracking model within OLGA. This is most limiting in the design of new pipelines where there is no experimental data available to ‘tune’ the simulation model.

Most recently, Nordsveen *et al.* (2009) reported an investigation on slug flow development in high risers. Based on the analysis of the field data and previous experimental data from SINTEF Two-Phase Flow Laboratory, they found that: (1) the slugs generated in a near horizontal pipeline could develop a long high void (low liquid holdup) zone in front of a low void zone (high liquid holdup) as the slugs moved upwards in a high riser; (2) the two zones were separated by a relatively sharp void front.

The high void zone was confirmed to be liquid continuous and thus a part of the slug observed in their new experiment conducted in the Well Flow Loop at IFE. Different versions of OLGA were applied to predict the high void zone. A new numerical scheme, 2nd order explicit TVD (Total Variation Diminishing) scheme, for the mass equations and the convective transport volume in the volume equation was implemented in OLGA 6.0. The 2nd order explicit TVD is less diffusive than the 1st order upwind implicit (Backward Euler) scheme in the previous versions. It was found that the prediction of the void front with the previous OLGA code failed mainly because the mass gradients were smeared out due to numerical diffusion, while the new numerical scheme was shown to be able to improve the predictions of the sharp void gradient. It was pointed out that OLGA did not predict the slug length distribution properly and the correlations for the gas entrainment and slip in slugs needed to be improved.

2.3.4 Three-Dimensional CFD Modelling

The modelling of slug flow with 1-D mechanistic approaches (including OLGA) has been discussed in Section 2.3.1, 2.3.2 and 2.3.3. The actual 3-D slug flow is reduced to 1-D flow by employing simplified physical models and empirical closure relationships. Consequently, the flow characteristics in the radial direction have been disregarded with the 1-D models. The 3-D CFD (Computational Fluid Dynamics) models are able to predict the whole flow field and provide more detailed information of the slug flow characteristics. This section is divided into two subsections: (1) basics of CFD modelling and related physical models; (2) a review on the related studies of slug flow modelling applying CFD.

Basics of CFD Modelling and Related Physical Models

CFD is concerned with the appropriate numerical solution of the equations governing the transport of mass and momentum in a fluid. For an incompressible Newtonian fluid, these are posed as the continuity and Navier-Stokes equations. In a Cartesian system of coordinates the equations are expressed as follows (ANSYS, 2006):

Continuity equation:

$$\frac{\partial u}{\partial x} + \frac{\partial v}{\partial y} + \frac{\partial w}{\partial z} = 0 \quad (2-13)$$

Navier-Stokes equations:

$$\rho \left(\frac{\partial u}{\partial t} + u \frac{\partial u}{\partial x} + v \frac{\partial u}{\partial y} + w \frac{\partial u}{\partial z} \right) = - \frac{\partial p}{\partial x} + \mu \left(\frac{\partial^2 u}{\partial x^2} + \frac{\partial^2 u}{\partial y^2} + \frac{\partial^2 u}{\partial z^2} \right) + F_x \quad (2-14)$$

$$\rho \left(\frac{\partial v}{\partial t} + u \frac{\partial v}{\partial x} + v \frac{\partial v}{\partial y} + w \frac{\partial v}{\partial z} \right) = - \frac{\partial p}{\partial y} + \mu \left(\frac{\partial^2 v}{\partial x^2} + \frac{\partial^2 v}{\partial y^2} + \frac{\partial^2 v}{\partial z^2} \right) + F_y \quad (2-15)$$

$$\rho \left(\frac{\partial w}{\partial t} + u \frac{\partial w}{\partial x} + v \frac{\partial w}{\partial y} + w \frac{\partial w}{\partial z} \right) = - \frac{\partial p}{\partial z} + \mu \left(\frac{\partial^2 w}{\partial x^2} + \frac{\partial^2 w}{\partial y^2} + \frac{\partial^2 w}{\partial z^2} \right) + F_z \quad (2-16)$$

where F_x , F_y and F_z are the components of body forces induced by the gravitational or electrical or magnetic fields in the x , y and z directions, respectively. The analytical solutions of the pressure and velocity throughout a system can be obtained by solving the above equations only for extremely simple systems. The new branch of fluid dynamics, CFD, is capable of solving the discretised Navier-Stokes equations numerically over a mesh of nodes/cells representing the flow region.

There are several commercial CFD packages available such as Fluent, STAR-CCM+, STAR-CD and CFX. In this study only Fluent (Release 6.3.26) and STAR-CCM+ (Release 5.04.006) were employed and the latter was used for STAR-OLGA coupling.

The first step for CFD modelling is to specify the geometry of the region where the flow is to be simulated. Then the region (computation domain) is divided into a mesh of small and adjacent cells. The Navier-Stokes equations are discretised and solved over the mesh of cells. The number, shape, size and distribution of the cells may affect the solution of the model equations. Generally a higher accuracy of the solution can be obtained from a finer mesh with a larger number of cells (smaller size) in a given region. However, it needs to be noted that a finer mesh involves more intensive computation efforts. Therefore, a tradeoff between the cost such as time and computers and the accuracy of the solution needs to be considered in CFD modelling.

The solver makes approximations to the partial differential equations for mass and momentum using discretised forms of the derivatives. The resulting equations are no longer continuous and then applied to the discrete mesh of cells in the computation domain. The discretised Navier-Stokes equations form a large system of non-linear equations, which are then solved by iterative matrix techniques. To simulate any practical flow system some physical models must be used in conjunction with the basic mass and momentum conservation equations, such as turbulence models and multiphase models.

Turbulent flows are characterised by fluctuating velocity fields. These fluctuations mix transported quantities such as momentum, energy and species concentration, then result in the fluctuations of the transported quantities. These fluctuations are too computationally expensive to simulate directly in practical engineering calculations because they can be of high frequency and small scale. Instead, the exact governing equations can be time-averaged, ensemble-averaged or otherwise manipulated to remove the small scales to obtain a modified set of equations. These equations are computationally less expensive to solve, however, some unknown variables are required. To determine these variables the turbulent models are needed.

In Reynolds averaging, the solution variables in the instantaneous (exact) Navier-Stokes equations are decomposed into the mean (ensemble-averaged or time-averaged) and fluctuating components (ANSYS, 2006). For the velocity components:

$$u_i = \bar{u}_i + u_i \quad (2-17)$$

where \bar{u}_i and u_i are the mean and fluctuating velocity components ($i = 1, 2$ and 3).

Likewise, for the pressure and other scalar quantities:

$$\phi = \bar{\phi} + \phi' \quad (2-18)$$

where ϕ denotes a scalar such as pressure, energy or species concentration.

The Reynolds-averaged Navier-Stokes (RANS) equations can be obtained by substituting the above expressions for the flow variables into the instantaneous

continuity and momentum equations and taking a time (or ensemble) average as follows (ANSYS, 2006): (It needs to be noted that the over bar on the mean velocities have been dropped for brevity.)

$$\frac{\partial \rho}{\partial t} + \frac{\partial(\rho u_i)}{\partial x_i} = 0 \quad (2-19)$$

$$\frac{\partial(\rho u_i)}{\partial t} + \frac{\partial(\rho u_i u_j)}{\partial x_j} = -\frac{\partial p}{\partial x_i} + \frac{\partial}{\partial x_j} \left[\mu \left(\frac{\partial u_i}{\partial x_j} + \frac{\partial u_j}{\partial x_i} - \frac{2}{3} \delta_{ij} \frac{\partial u_l}{\partial x_l} \right) \right] + \frac{\partial(-\overline{\rho u_i u_j})}{\partial x_j} \quad (2-20)$$

The RANS equations have the same general form as the instantaneous Navier-Stokes equations with the velocities and other solution variables representing ensemble-averaged (or time-averaged) values. Additional terms like Reynolds stress $-\overline{\rho u_i u_j}$ representing the effects of turbulence needs to be modelled.

The simplest ‘complete models’ of turbulence are two-equation models. The turbulent velocity and length scales can be determined independently by solving the two separate transport equations. The standard k - ϵ model has been extensively used due to its robustness, economy and reasonable accuracy for a wide range of turbulent flows. The standard k - ϵ model is a semi-empirical model based on model transport equations for the turbulence kinetic energy (k) and its dissipation (ϵ). The model transport equation for k was derived from the exact equation, while the model transport equation for ϵ was obtained using physical reasoning and bears little resemblance to its mathematically exact counterpart. The assumption made during the derivation of the standard k - ϵ model is that the flow is fully turbulent and the effects of molecular viscosity are negligible. Therefore, the standard k - ϵ model is valid only for fully turbulent flows.

The turbulence kinetic energy, k , and its rate of dissipation, ϵ , are obtained from the following transport equations (ANSYS, 2006):

$$\frac{\partial(\rho k)}{\partial t} + \frac{\partial(\rho k u_i)}{\partial x_i} = \frac{\partial}{\partial x_j} \left[\left(\mu + \frac{\mu_t}{\sigma_k} \right) \frac{\partial k}{\partial x_j} \right] + G_k + G_b - \rho \epsilon - Y_M + S_k \quad (2-21)$$

$$\frac{\partial(\rho \epsilon)}{\partial t} + \frac{\partial(\rho \epsilon u_i)}{\partial x_i} = \frac{\partial}{\partial x_j} \left[\left(\mu + \frac{\mu_t}{\sigma_\epsilon} \right) \frac{\partial \epsilon}{\partial x_j} \right] + C_{1\epsilon} \frac{\epsilon}{k} (G_k + C_{3\epsilon} G_b) - C_{2\epsilon} \rho \frac{\epsilon^2}{k} + S_\epsilon \quad (2-22)$$

where G_k and G_b represent the generation of turbulence kinetic energy due to the mean velocity gradients and buoyancy, respectively; Y_M is the contribution of the fluctuating dilatation in compressible turbulence to the overall dissipation rate; $C_{1\epsilon}$, $C_{2\epsilon}$ and $C_{3\epsilon}$ are constants; σ_k and σ_ϵ are the turbulent Prandtl numbers for k and ϵ , respectively; S_k and S_ϵ are user-defined source terms.

The turbulent viscosity, μ_t , is calculated by combining k and ϵ as follows:

$$\mu_t = \rho C_\mu \frac{k^2}{\epsilon} \quad (2-23)$$

where C_μ is a constant.

The model constants $C_{1\epsilon}$, $C_{2\epsilon}$, C_μ , σ_k and σ_ϵ have the following default values in Fluent (ANSYS, 2006):

$$C_{1\epsilon} = 1.44, C_{2\epsilon} = 1.92, C_\mu = 0.09, \sigma_k = 1.0, \sigma_\epsilon = 1.3$$

The default values were determined from experiments with air and water. They have been found to work fairly well for a wide range of wall bounded and free shear flows.

Turbulent flows are significantly affected by the walls. Very close to the wall, the viscous damping reduces the tangential velocity fluctuations, while the kinematic blocking reduces the normal fluctuations. Towards the outer part of the near-wall region, the turbulence is rapidly augmented by the production of turbulence kinetic energy due to the large gradients in the mean velocity. However, the standard k - ϵ model is valid only for fully developed turbulent flows located in the regions somewhat far from the walls. There are two approaches for modelling the near-wall region in Fluent (ANSYS, 2006). One of them is using ‘wall functions’ to bridge the viscosity-affected region between the wall and the fully turbulent region. Wall functions are a collection of semi-empirical formulas and functions that in effect link the solution variables at the near-wall cells and the corresponding quantities on the wall. The wall functions include: (1) laws-of-the-wall for the mean velocity and temperature (or other scalars); (2) formulas for the near-wall turbulent quantities. With the wall functions adopted there is no need to modify the turbulent models to account for the presence of the wall and resolve the

flow field in the viscosity-affected near-wall region. In most high-Reynolds-number flows the wall function approach is popular because it is economical, robust and reasonably accurate.

Currently there are two approaches for the numerical calculation of multiphase flow: Euler-Lagrange approach and Euler-Euler approach. In the Euler-Euler approach, the different phases are treated mathematically as interpenetrating continua. The volume fractions of the phases are assumed as continuous functions of time and space. The sum of all the phase volume fractions is one. There are three Euler-Euler multiphase models in Fluent (ANSYS, 2006): (1) VOF (volume of fluid) model; (2) mixture model; (3) Eulerian model. The VOF model is usually used for modelling gas/liquid slug flow and thus adopted throughout this study. Therefore, only the VOF model is introduced below.

The VOF modelling is a surface-tracking technique applied to a fixed Eulerian mesh. It is designed for two or more immiscible fluids where the position of the interface between them is of concern. In the VOF model a single set of momentum equations is shared by the fluids. The volume fraction of each fluid in each computational cell is tracked throughout the domain. The VOF formula relies on the fact that two or more fluids are not interpenetrating. In each cell (control volume) the volume fractions of all phases sum to unity. Three conditions are possible in one cell within the computational domain: (α_q is the volume fraction of the q^{th} fluid in the cell)

- $\alpha_q = 0$: the cell is empty of the q^{th} fluid;
- $\alpha_q = 1$: the cell is full of the q^{th} fluid;
- $0 < \alpha_q < 1$: the cell contains the interface between the q^{th} fluid and other fluids.

The appropriate fluid properties and flow variables are assigned to each cell based on the value of α_q . The flow fields for all variables and properties are shared by the phases and represent volume-averaged values. Hence the variables and properties in any given cell are either representative of one of the phases or a mixture.

In order to obtain a reasonable representation of the interface between the phases, a special interpolation treatment is usually applied to the cells that lie near the interface.

In Fluent the geometric reconstruction scheme is recommended as it is considered to be the most accurate and applicable for general unstructured meshes. This scheme represents the interface using a piecewise-linear approach. It is assumed that the interface between two fluids is linear within each cell.

The effects of surface tension along the interface between each pair of phases can be included in the VOF model. The surface tension coefficient can be specified as a constant, as a function of temperature or through a UDF (User Defined Function). In this work a constant surface tension coefficient for water was used in the air/water two-phase flow simulations.

Slug Flow Modelling Applying CFD

As one of the early studies Hope (1990) used CFD codes, PHOENICS and HARWELL-FLOW3D, to model horizontal stratified wavy and slug flow. The horizontal slug flow was modelled in two and three dimensions by splitting the unit into two sections, i.e. front and tail. The two sections were considered separately. The slug front was treated as a steady flow with the observed 3-D interface between the gas and liquid described through body-fitted coordinates. The tail behaviour was calculated by a transient technique using an adapted scalar equation method in cylindrical-polar coordinates to track the actual evolution of the gas/liquid interface, allowing the growth or decay of the slug unit to be estimated. The author concluded that it was possible to study the detailed mechanisms associated with slug flow numerically using their methods.

Moe (1993) wrote a CFD programme to simulate the motion of Taylor bubbles in stagnant and moving liquid with emphasis on the effect of the interfacial friction factor on the bubble propagation velocity in stagnant liquid. However, the feasibility of simulating the Taylor bubbles in moving liquid was demonstrated qualitatively only. Realising that Hope (1990) had not produced any quantitative results of simulating a single slug tail in horizontal flow, Pan (1996) extended the method proposed by Hope (1990) and used CFDS-FLOW3D (later CFX) code to quantitatively study the motion of Taylor bubbles in moving liquid at different pipe inclinations. The numerical results for the horizontal and vertical upward flows agreed with the experimental data and some correlations well, showing the reliability of the CFD models. Manfield (2000)

developed a new method to study the motion of Taylor bubbles in the horizontal flow and performed simulations using CFX. In the CFD model of Manfield (2000) a solid boundary was employed to represent the front of a liquid slug, which allowed for the simulation of the ‘recirculation zone’ at the front of the slug. The model predictions showed good agreement with the experimental observations of the ‘wake effect’ by Fagundes Netto *et al.* (1998) and Cook and Behnia (2000). The ‘dam break’ method used to simulate the development of the gas/liquid interface in the slug tail region was extended to the slug front. It was shown that the shape of the slug front interface and the liquid recirculation zone could be correctly simulated, however, the prediction of the slug front interface in the region where it intersected the pipe wall was poor.

Recently Taha and Cui (2006) conducted a numerical study on the motion of single Taylor bubbles in both stagnant and flowing liquids in vertical tubes. The shape and velocity of the slug, the velocity distribution and the distribution of the local wall shear stress were computed and compared favourably with the published experimental data. The CFD model they developed using Fluent is described as follows:

- Two-dimensional (2-D) coordinate system assuming axial symmetry about the centerline of the pipe; domain length: $11 d$ (d the tube diameter); uniform mesh containing quadrilateral cells with extra refinement near the walls;
- Initial bubble shape consisting of one hemisphere connected to a cylinder of the same radius; initial film thickness calculated using simple mass balance; initial bubble rise velocity using the correlation of Nicklin *et al.* (1962);
- No-slip wall condition applied on the walls; the fluid mass flux at the inlet specified using a profile for a fully developed flow through a pipe; a moving frame of reference with the wall moving at the velocity of the bubble rise velocity employed to save computation time; the geometric reconstruction scheme based on piece-linear interface calculation method applied to reconstruct the bubble free surface; the RNG k - ε model adopted to model the turbulence;

Based on the predictions of their CFD model they claimed that a complete description of the bubble propagation in vertical flows was obtained.

To investigate the hydrodynamic characteristics of slug flow and the mechanism of slug flow induced CO₂ corrosion Zheng *et al.* (2007) performed a set of CFD simulations. The hydrodynamic characteristics of slug flow under investigation were the shape of the Taylor bubble, the terminal velocity and thickness of falling liquid film, the shape and length of the wake vortexes, the near wall mass transfer and wall shear stress. Similarly to Taha and Cui (2006) they also adopted a 2-D coordinate system assuming axial symmetry about the centerline of the pipe, a moving frame of reference with the wall moving at the velocity of the bubble rise velocity, the VOF model with geometric reconstruction scheme based on piece-linear interface calculation method and no-slip assumption on the wall. But differently they applied standard $k-\varepsilon$ model rather than RNG $k-\varepsilon$ model by Taha and Cui (2006) to model the turbulence. It was claimed that the CFD simulation results matched with the previous experimental observations reasonably well.

2.3.5 Coupling of One-Dimensional OLGA and Three-Dimensional CFD

The 1-D and 3-D models of slug flow have been discussed in the above sections from Section 2.3.1 to Section 2.3.4. Compared with the 3-D models the 1-D models involve much less computation effort, but the detailed information of the flow field cannot be obtained; while the 3-D models are able to present the whole flow field but expensive computational resources such as time and computers are usually required. It is an interesting idea to make the most of the advantages of the 1-D and 3-D models and achieve a tradeoff between the speed and details of the models.

OLGA is a transient 1-D model widely used in the oil and gas industry. The slug tracking module in OLGA can give predictions of the characteristic parameters of slug flow. Recently, a novel co-simulation tool called STAR-OLGA coupling has been proposed by CD-adapco. During the development of the STAR-OLGA coupling tool the code of the coupling between OLGA and STAR-CD/STAR-CCM+ has been validated in this work. The STAR-OLGA coupling tool in STAR-CCM+ is responsible for the data transfer between the 3-D STAR-CCM+ and 1-D OLGA codes. Compared with a pure OLGA model the coupling model is able to provide increased details of a specific part by replacing that part with a 3-D element. Compared with a pure 3-D STAR-CCM+ model the calculation time can be significantly reduced by applying the

high-speed 1-D code OLGA to long pipelines. The coupling provides a good compromise between the speed of the 1-D code and the details of the 3-D code (CD-adapco, 2010).

In this study the hydrodynamic slug flow is investigated applying STAR-OLGA coupling. The schematic of a coupling model is shown in Figure 2-9. The local pipe component of interest, i.e. wavy pipe or a single bend in this study, is modelled in STAR-CCM+ (Release 5.04.006); while the upstream and downstream pipelines are modelled in OLGA (Release 5.3.2).

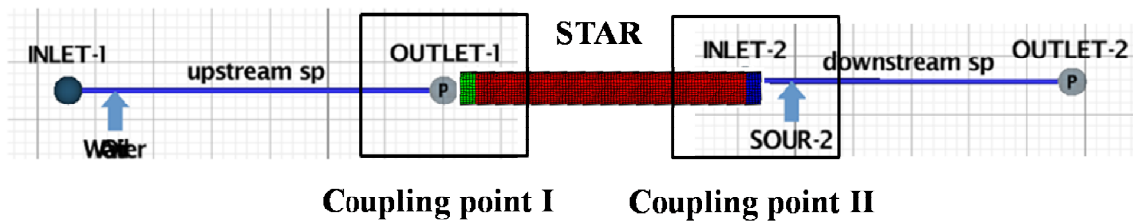


Figure 2-9 Schematic of a STAR-OLGA coupling model

2.4 Slug Flow Mitigation

Various slug flow mitigation or elimination methods are introduced in this section. Most of these methods are originally designed for severe slugging mitigation in pipeline/riser systems, because severe slugging is more problematic than hydrodynamic slug flow. In this work the major methods in the literature are grouped into two categories, i.e. active and passive slug mitigation, based on whether the ‘external interference’ is needed or not in operation. The ‘external interference’ is essential to the implementation of the active slug mitigation methods, while the passive slug mitigation methods usually take the form of design changes to the facility.

2.4.1 Active Slug Mitigation

The active methods mainly include three types: topside choking at the riser top, external-gas lifting and control-based methods.

Topside Choking

Topside choking was one of the first methods for severe slugging mitigation/elimination, where a valve located at the riser top was operated manually. Yocum (1973) claimed that choking could cause severe reductions in the flow capacity in the system, however, Schmidt *et al.* (1979) found that severe slugging in a pipeline/riser system could be eliminated or minimized by careful choking, resulting in little or no change in the flowrates and system pressure.

The working mechanism of the topside choking for mitigating severe slugging was explained by Schmidt *et al.* (1985). The pressure drop in a riser induced by the gas/liquid two-phase flow decreases, reaches a minimum, and then increases with the increase of the gas flowrate at a constant liquid flowrate. The regions to the left and right of the minimum pressure drop are referred to as unstable and stable regions, respectively. Severe slugging region is a sub-region of the unstable region. The unstable flow in the riser can be transformed into stable flow by choking at the riser outlet. Choking introduces an additional pressure drop which increases with the increasing gas flowrate. The total pressure drop of the choke and riser reaches its minimum at a lower gas flowrate than that without choking. As a result, the boundary between the unstable region and stable region is shifted to the lower gas flowrate and the severe slugging region can be reduced.

Fargalhy (1987) presented field applications of choking showing that severe slugging could be eliminated at no reduction of the production rate.

It needs to be mentioned that the choking method discussed above involves a manual operation of a valve at the riser top. The manual choking often results in sudden operation changes, as a result, the system may become unstable due to the non-linear nature of multiphase flow (Ogazi, 2011). To achieve stable operating conditions the dynamic choking based on active control is recommended and discussed in the subsection *Control-Based Methods* below.

External-Gas Lifting

Gas lifting in the pipeline/riser systems can be used to mitigate or eliminate slug flow by the following interrelated mechanisms (FEESA, 2004):

- Increasing the flowrate in the system can help to avoid liquid slugs;
- Decreasing the pressure drop in the riser can reduce the propensity for liquids to accumulate at the riser base;
- Decreasing the pressure in the flowline can reduce the compression of the gas, then the flowline gas expands and the velocities increase; increasing the velocities in the flowline can help to prevent terrain slugs from being formed in dips upstream of the riser base.

The riser-base gas lifting method was first used to control hydrodynamic slug flow in vertical risers. However, Schmidt *et al.* (1985) dismissed it because this technique was considered not to be economically feasible due to the cost of a compressor for pressurising the gas for injection and pipelines for transporting the gas to the riser base.

Pots *et al.* (1987) investigated the application of the gas lifting method to eliminate severe slugging. They concluded that the severity of the severe slugging was considerably lower with the riser injection of about 50% inlet gas flow. It was observed that the severe slugging did not completely disappear even with 300 % injection.

Hill (1989) described the riser-base gas injection tests performed in the S. E. Forties field to eliminate severe slugging. The gas injection was shown to be able to reduce the extent of severe slugging. Since the objective was to bring the flow regime in the riser to annular flow, a large amount of injection gas was required to completely stabilise the flow.

Johal *et al.* (1997) pointed out that the riser-base gas injection method might cause additional problems due to Joule-Thomson cooling of the injected gas. The expansion of the injected gas could cause cooling and make the flow conditions more susceptible to wax precipitation and hydrate formation. Hence, they proposed an alternative technique 'Multiphase Riser Base Lift'. This method required nearby high capacity multiphase

lines diverted to the pipeline/riser system experiencing severe slugging. The diverted flows of high flowrates could alleviate severe slugging without exposing the system to other potential problems. This method needs other multiphase flowlines nearby, which may not be available in the fields.

The external-gas lifting method provides artificial lift for the liquids, moving them steadily through the riser. This technique can alleviate the problem of severe slugging by changing the flow regime from slug flow to annular or dispersed flow. However, in deepwater systems, the injection gas of high flowrate may result in increased frictional pressure loss and Joule-Thomson cooling (Sarica and Tengedal, 2000).

Control-Based Methods

Control-based methods for handling slugs are characterised by using the process information to adjust available degrees of freedom (such as pipeline chokes, pressure and levels) to reduce or eliminate the effects of slugs on the downstream separation and compression units (Havre and Dalsmo, 2002). A dynamic choke is usually manipulated by controllers based on real-time changes of system variables (process information). The riser base pressure, riser top pressure and flowrate are commonly used as controlled variables. Typical studies applying these three parameters as controlled variables are discussed below. A more detailed review on the control-based methods has been reported in Ogazi (2011).

The suitability of the riser base pressure as a controlled variable to suppress severe slugging was reported by Henriot *et al.* (1999), Molyneux and Kinvig (2000), Drengstig and Magndal (2001) and Storkaas and Skogestad (2004). In the study of Drengstig and Magndal (2001), a PI (Proportional and Integral) controller was implemented with the pressure difference between the riser base and riser top as controlled variable and the top valve opening as manipulated variable. The pressure difference between the riser base and riser top was obtained by measuring both of the riser base and top pressure. They concluded that the riser base pressure was the optimum controlled variable for slug control. Storkaas and Skogestad (2004) conducted a systematic analysis of the pipeline/riser system based on control theory. The stability characteristics of the system with the riser top valve opening as the manipulated variable was analysed. Based on the

analysis they identified the riser base pressure as the best controlled variable for stabilising the pipeline/riser system.

Different views on the use of the riser topside measurements as controlled variables were reported. The controllability analysis conducted by Storkaas and Skogestad (2004) showed that the riser top pressure alone was not a good variable for stabilising the pipeline/riser system. That was based on the results that the zeros of the corresponding transfer function were in the right-half-plane of the complex plane. However, Cao *et al.* (2009) developed a slug control system using only topside variables such as the riser top pressure, total volumetric flowrate and total fluid density. The slug control system was demonstrated to work successfully on the pipeline/riser system in PSE (Process Systems Engineering) Laboratory at Cranfield University.

The riser outlet flowrate has also been used as a controlled variable for suppressing severe slugging. Storkaas (2005) found that using the volumetric flowrate at the riser outlet resulted in poor performance at low frequency, but the performance could be improved by using it in the inner loop of a cascade control system. Kovalev *et al.* (2003, 2004) reported a slug control system, called S^3 , and showed success when applying to both severe slugging and hydrodynamic slug flow on several field applications. They added a mini-separator or a large diameter pipe section between the riser outlet and downstream separator to allow for a separation of the gas/liquid two phases. Then the liquid level in the mini-separator and total volumetric flowrate were controlled by throttling the liquid stream and the gas stream, respectively. The control scheme of S^3 was based on controlling the total volumetric flowrate and liquid flowrate. The measured variables included the liquid and gas volumetric flowrates, the separator pressure and liquid level.

As introduced in Section 2.3.1 Ogazi (2011) improved the model of a pipeline/riser system developed by Storkaas (2005). Based on the improved model the controllability analysis of the unstable pipeline/riser system for stability and production was performed. Then different types of slug controllers were designed. It was shown that both of the topside and subsea variables could be used for stabilising control of the pipeline/riser system by implementing appropriate strategies. Three types of controllers including the relay auto-tuned controller, the robust PID (Proportional, Integral and Derivative)

controller and the H_∞ robust controller were designed and their performance was compared. It was concluded that the H_∞ robust controller could achieve the largest valve opening at the riser outlet, and thus impose lower pressure increase in the system. Simulation results from an industrial system in OLGA confirmed that the maximum production of the fluids from the well could be achieved by utilising the H_∞ robust controller.

Various slug control systems have been proposed and applied to the fields. However, how flexible/robust such a control system is, i.e. how far it allows a system to deviate from the unstable region, whether it can work throughout the field life on a number of different scenarios, has not yet been investigated sufficiently (FEESA, 2004).

2.4.2 Passive Slug Mitigation

The discussions below focus on the passive slug mitigation methods with emphasis on the one applying a flow conditioner to modify the flow regime in the pipeline so as to mitigate severe slugging i.e. flow conditioning. Three typical passive methods including slug catcher, self-gas lifting and flow conditioning are discussed.

Slug Catcher

The most commonly used method to suppress the effects of liquid slugs on the downstream facilities is slug catcher. It is a vessel located downstream of the riser outlet with sufficient volume to buffer the liquid slugs acting as a first stage gas/liquid separator. A slug catcher actually is designed to temporarily store the liquid slugs which will be treated afterwards.

A vessel type slug catcher is essentially a conventional vessel, which is simple in design and maintenance. A ‘finger type’ slug catcher consists of several long pieces of pipes (fingers) of large diameters, which form the buffer volume through the common manifolds. The advantage of the ‘finger type’ slug catcher is that it is much simpler to design the pipe segments for high pressure than a large vessel. A disadvantage is that its footprint can become excessively large.

Generally a slug catcher is not able to deal with all slug sizes due to its limited buffer volume. It is usually sized for hydrodynamic slugs, thus the problems induced by the long liquid slugs under severe slugging can only be mitigated rather than eliminated. In order to eliminate the impacts of severe slugging a much larger slug catcher has to be designed but it may not be achievable due to the limited space on the offshore surface structures. Furthermore, slugs might be larger than expected and consequently the pressure and flow fluctuations could still lead to unfavorable impacts on the downstream processing facilities. Therefore, the issues with slug catchers for slug mitigation are how to predict the slug sizes and how to size the required buffer volume.

Self-gas Lifting

The external-gas lifting needs compressors to compress the large amount of external gas and separate pipelines to transport the compressed gas to the designed injection places (Jansen *et al.*, 1996). In contrast to the external-gas lifting method, the self-gas lifting does not need compressors, extra pipelines and external gas. The gas needed for lifting comes from the gas flow in the pipeline upstream of the riser base.

Sarica and Tengedal (2000) proposed two types of self-gas lifting methods as illustrated in Figure 2-10. The principle of this technique is to connect the riser to the downwardly inclined segment of the pipeline with a small diameter conduit. The conduit can transfer the gas from the downwardly inclined segment to the riser at points above the riser base. The transfer process can reduce both of the hydrostatic head in the riser and the pressure in the pipeline; consequently the severe slugging can be mitigated or eliminated. It needs to be noted that there are some practical difficulties when applying these methods to the fields. The liquid dropping out from the transferred gas flow may accumulate in the dip of the bypass or inserted pipe; the insertion of the smaller diameter pipe causes inherent intrusion to the flow path, resulting in problems to pigging operations.

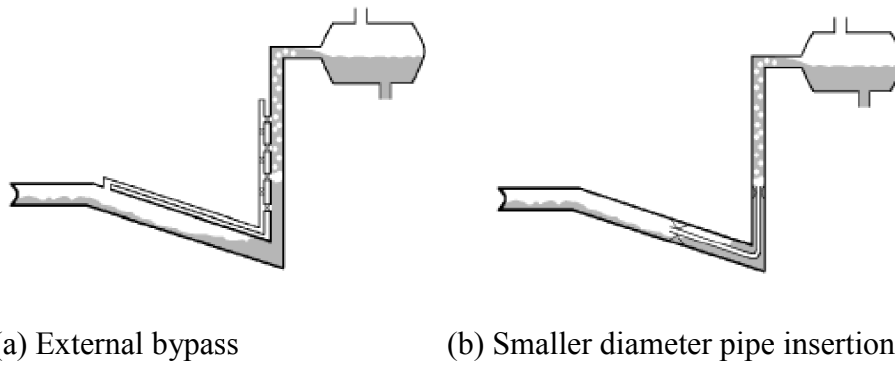


Figure 2-10 Self-gas lifting methods (Sarica and Tengedal, 2000)

Flow Conditioning

A flow conditioner for severe slugging mitigation refers to a pipe device installed in the pipeline upstream of the riser base. As proposed by Schmidt *et al.* (1980, 1985) one of the necessary conditions for severe slugging to occur is that the flow regime in the pipeline upstream of the riser base is stratified flow. The flow conditioner is used to alter the stratified flow to a non stratified flow in the pipeline, i.e. flow conditioning.

Almeida and Gonçalves (1999 a) proposed a venturi-shaped device comprising a convergent nozzle section followed by a divergent diffuser section as shown in Figure 2-11. This device was proposed to be located near to the riser base in the pipeline. It was claimed that the venturi-shaped device could introduce a pressure drop causing a mixing effect and converting the stratified flow to a non-stratified flow temporarily. They performed experimental study of the venturi-shaped device on a small-scale test rig and verified their claims (Almeida and Gonçalves, 1999 b). However, the existence of the contraction section may pose problems to the pigging operations for the pipeline.

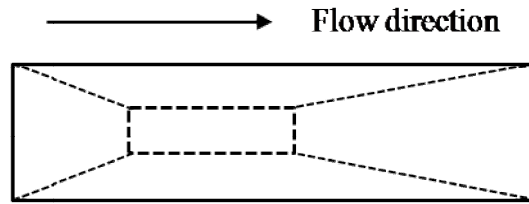
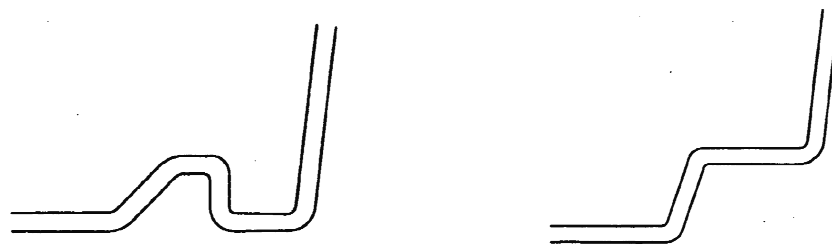


Figure 2-11 Venturi-shaped device (Almeida and Gonçalves, 1999 b)

Another type of flow conditioner for mitigating severe slugging in a pipeline/riser system was patented by Makogan and Brook (2007). The pipe device they proposed can be positioned immediately upstream of the riser and comprises at least one unit of an upwardly inclined pipe section upstream of a downwardly inclined pipe section or a horizontal pipe section as illustrated in Figure 2-12 (a) and (b), respectively. The inclination angle of the upwardly inclined pipe section to the horizontal ranges from 5° to 90° and the length of the upwardly inclined pipe section ranges from 0.3 m to 9.1 m. The lengths of the horizontal sections in Figure 2-12 (a) and (b) and the downwardly inclined section in Figure 2-12 (a) were recommended to be less than 6.1 m by Makogan and Brook (2007).



(a) Upward/downward pipe section (b) Upward/horizontal pipe sections

Figure 2-12 Pipe device proposed by Makogan and Brook (2007)

It was claimed that this device could eliminate severe slugging by establishing short liquid slugs in the pipeline. The volume of each liquid slug could be sufficiently small

to be transported by the gas pressure building up behind it. Consequently severe slugging could be changed into plug flow or intermittent flow. Most recently, Makogan *et al.* (2011) reported an experimental and simulation study on the proposed pipe device. It was shown that their device could reduce or eliminate the severe slugging in risers; however, there was no detailed presentation of the flow behaviour in their device and explanations to the working principle of it.

Adedigba (2007) examined the flow characteristics of the single phase and gas/liquid two-phase flows in helical pipes. The work performed by Adedigba (2007) focused on helical pipes with the internal diameter of 50 mm and low amplitude. In the experiment a helical pipe was made by ‘wrapping’ a reinforced flexible pipe with an internal diameter of 50 mm round a straight steel pipe with a smaller diameter of 19 mm as shown in Figure 2-13.

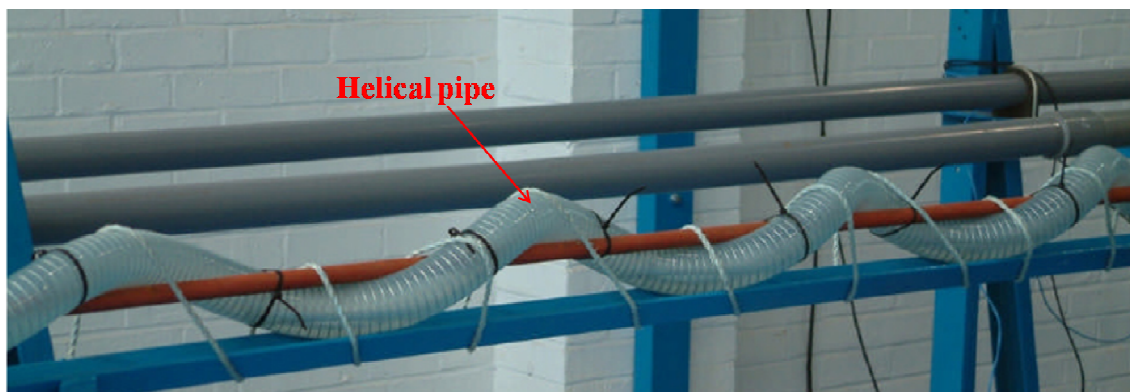


Figure 2-13 Helical pipe of low amplitude investigated by Adedigba (2007)

The helical pipe positioned horizontally was tested with air/water two-phase flow by Adedigba (2007). It was found that, at certain superficial air and water velocities, the stratified flow or slug flow prevailed in a straight pipe while the bubbly flow occurred in the tested helical pipe instead. Those findings showed that the helical pipe had a potential for severe slugging mitigation because the stratified flow regime could be converted into bubbly flow if installed in the pipeline upstream of the riser base. Then the performance of the helical pipe on severe slugging mitigation was justified

experimentally. It was demonstrated that the severe slugging region could be reduced by installing a helical pipe upstream of the riser base and even in severe slugging region the severity of the flow regime in terms of liquid/gas surges and pressure oscillations could also be reduced. The helical pipe investigated by Adedigba (2007) had a patented spiral geometry, SMAHT (Small Amplitude Helical Technology). The SMAHT tube is proposed to be made by intertwining a larger diameter pipe against a smaller diameter pipe. The ratio of the helix amplitude to the tube diameter is less than 0.5.

Encouraged by the effectiveness of the SMAHT tube on mitigating severe slugging (Adedigba, 2007), a new pipe device called PST (Pseudo Spiral Tube) was proposed (Yeung and Cao, 2007; Shen and Yeung, 2008). PST is constructed by connecting a series of standard piping elbows (or bends) together. The geometry of PST depends on the internal angle of elbow, the ratio of the elbow radius to the pipe diameter and the angle of twist between two adjacent elbows. The differences between PST and SMAHT tube are highlighted as below (Yeung and Cao, 2007):

- PST is made of standard piping elbows while SMAHT tube is made by intertwining a large diameter pipe against a smaller diameter pipe;
- PST always has a circular cross-sectional area while SMAHT tube may not have a circular cross-sectional area at certain parts;
- PST can have any amplitude to diameter ratios while SMAHT tube is defined as having an amplitude to diameter ratio less than 0.5;
- PST can be of non-helical shape when the twist angle between two adjacent elbows is 180°.

Two PST geometries as shown in Figure 2-14 were tested by Yeung and Cao (2007). PST1 was made of 26 elbows with the internal angle of 45° and with the radius/diameter ratio of 1.5 twisted by 90°; PST2 was made of 7 elbows of 90° internal angle and 2.2 radius/diameter ratio twisted by 180°. A series of tests to examine the effectiveness of PST1 and PST2 on severe slugging mitigation in pipeline riser systems was carried out. The experimental results showed that PST2 of a wave shape was more effective than PST1 of a helical shape when located in the pipeline upstream of the riser.



(a) PST1: 26 elbows



(b) PST2: 7 elbows

Figure 2-14 PST geometries tested by Yeung and Cao (2007)

This work focuses on the investigation of the wave-shaped PST and the terminology ‘wavy pipe’ is adopted in the rest of the thesis instead of ‘PST’. The details of designing a wavy pipe can be found in Chapter 3.

2.4.3 Comparison between Active and Passive Mitigation Methods

The external interference is essential to the implementation of the active slug mitigation methods. The active methods mainly include three types: topside choking at the riser top, external-gas lifting and control-based methods. The riser top choking method needs operators to adjust the opening of the choking valve manually (Schmidt *et al.*, 1985; Taitel, 1986); the external-gas lifting needs compressors to compress the external gas and separate pipelines to transport the compressed gas to the designed injection places (Jansen *et al.*, 1996); the control-based methods need controllers to adjust an actuator such as a valve to deal with different flow and operating conditions (Havre and Dalsmo, 2002; Storakaas, 2005). The passive slug mitigation methods usually take the form of design changes to the facility itself such as sizing of slug catcher, gas lifting by re-routing the gas in the pipeline to the riser and flow regime modification by a flow

conditioner in the pipeline. The function of the passive methods can be achieved without any external interference.

The advantages of the active methods are that they can be adjusted or tuned by operators according to the real situations encountered and severe slugging can be totally eliminated. However, these methods often need extra resources such as expensive compressors, long pipelines for gas injection and sensors for the parameter measurement as inputs to the controllers. Furthermore, although the severe slugging can be eliminated, the backpressure induced by the choking and control methods is often very high, which may reduce the production of the oil and gas from the wells.

Compared with the active methods the passive methods are less flexible because they can hardly be adjusted once the designed system is commissioned. However, there are remarkable advantages of these methods. They do not need extra investment on operators, compressors, measurement instruments and actuators. Furthermore, they can work in collaboration with the active methods, which could ease the challenge of severe slugging induced problems to the active methods and save the external resources required.

2.5 Summary

The gas/liquid two-phase flow has the most complexity due to the deformability and compressibility of the gas phase. Slug flow is one of the frequently encountered flow regimes during the transportation of oil and gas in pipelines. Three types of slugs may appear in the oil and gas transportation flowlines, namely, terrain-induced slugs, hydrodynamic slugs and operation-induced slugs. Riser-induced severe slugging occurs when the liquid blocks the lower point where a down-sloping pipeline is attached to a riser. The blockage initiates the slug, which thereafter grows upward into the riser and back through into the upstream pipeline. In the mean time the upstream gas is compressed until the pressure is sufficiently high to blow it out of the riser. Hydrodynamic slug flow usually develops in the horizontal and near horizontal sections of the pipeline where the liquid waves on the gas/liquid interface grow and eventually close the cross-section forming liquid slugs.

The modelling methodologies of slug flows have been reviewed with emphasis on the riser-induced severe slugging and hydrodynamic slug flow. The methodologies are grouped into two categories: one-dimensional modelling (mechanistic modelling) and three-dimensional modelling (CFD modelling). The mechanistic models of severe slugging can be classified into three categories as follows: (1) predicting the occurrence of severe slugging; (2) predicting the characteristics of severe slugging; (3) predicting the characteristics of the flow with a severe slugging mitigation method applied. For hydrodynamic slug flow there are mainly two types of mechanistic models: steady-state models and transient models. The steady-state models are developed based on the ‘slug unit’ and the transient models mainly include slug tracking and slug capturing models which treat each of the slugs as unique. OLGA is a transient modified two-fluid model for two-phase/three-phase hydrocarbon flow in pipelines and pipeline networks, with processing equipment included. Both severe slugging and hydrodynamic slug flow can be modelled with OLGA. When modelling slug flow applying 1-D mechanistic models (including OLGA), the actual 3-D slug flow is reduced to 1-D flow by employing simplified physical models and empirical closure relationships. Consequently, the flow characteristics in the radial directions have been disregarded with the 1-D models. The 3-D CFD modelling is able to predict the whole flow field and provide more detailed information of the slug flow characteristics.

The STAR-OLGA coupling tool in STAR-CCM+ is responsible for the data transfer between the 3-D STAR-CCM+ and 1-D OLGA codes. Compared with a pure OLGA model the coupling model is able to provide increased details of a specific part by replacing that part with a 3-D element. Compared with a pure 3-D STAR-CCM+ model the calculation time can be significantly reduced by applying the high-speed 1-D code OLGA to long pipelines. In this study the hydrodynamic slug flow has been investigated applying STAR-OLGA coupling. The local pipe component of interest, i.e. wavy pipe or a single bend in this study, is modelled in STAR-CCM+; while the upstream and downstream pipelines are modelled in OLGA.

The major slug mitigation methods in the literature are grouped into two categories, i.e. active and passive methods, based on whether the ‘external interference’ is needed or not in operation. The external interference is essential to the implementation of the

active slug mitigation methods. The passive slug mitigation methods usually take the form of design changes to the facility. The advantages of the active methods are that they can be adjusted or tuned by operators according to the real situations encountered and the severe slugging can be totally eliminated. However, these methods usually need expensive external resources. Compared with the active methods the passive methods are less flexible as they can hardly be adjusted once the designed system is commissioned. However, they do not need extra investment on the external resources and can work in collaboration with the active methods. In this work a new passive method based on a novel flow conditioner, wavy pipe, is developed to mitigate severe slugging in pipeline/riser systems and hydrodynamic slug flow in horizontal pipelines.

3 EXPERIMENTAL STUDY ON SEVERE SLUGGING MITIGATION APPLYING WAVY PIPES IN PIPELINE/RISER SYSTEMS

3.1 Introduction

The wavy pipe is a pipe section constructed by connecting piping bends in series in one plane. The wavy pipe installed in the pipeline upstream of the riser is expected to be able to modify the way of the interaction between gas and liquid and further affect the flow behaviour in the whole pipeline/riser system.

A series of experiments were conducted on a group of test configurations: 2" and 4" pipeline/riser systems, pipeline/wavy-pipe/riser systems with the wavy pipe at different locations in the pipeline, pipeline/wavy-pipe/riser systems with the wavy pipe of different lengths. The performance of the wavy pipe on severe slugging mitigation has been presented in terms of the flow regime transition and characteristic parameters of the flow behaviour. The working principle and the effects of the geometrical parameters and location in the pipeline of the wavy pipe have been disclosed.

3.2 Wavy Pipe

3.2.1 Design Parameters of Wavy Pipe

The minimum unit of a wavy pipe is a piping bend, which can be described by three geometrical parameters. Figure 3-1 shows the geometrical parameters of a bend, i.e. the internal diameter of the tube (d), bend radius (R) and bend angle (α).

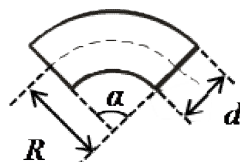
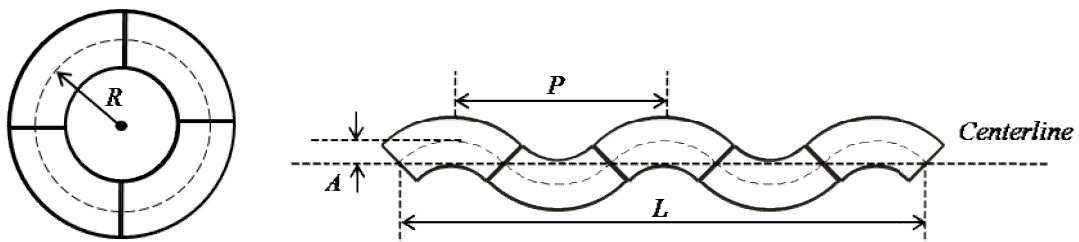


Figure 3-1 Geometrical parameters of a bend

Different geometries can be created by joining several bends together in different manners. Four 90° bends connecting together without any twist forms a doughnut shape, which has a circle central line with a radius of R . A wave-shaped pipe, wavy pipe, can be formed by twisting each connection between two adjacent bends by 180° . Thus the wavy pipe can be made by connecting the piping bends in series in one plane. The schematics of a doughnut-shaped device and a wavy pipe of five bends are shown in Figure 3-2.



(a) Doughnut shape

(b) Wavy pipe

Figure 3-2 Schematics of different geometries formed by connecting bends

The wavy pipe is described by the following geometrical parameters as indicated in Figure 3-2 (b):

- **Amplitude (A):** the maximum distance between the bend centreline and the centreline of wavy pipe
- **Pitch (P):** the distance between the adjacent two peaks or dips
- **Length (L):** the distance between the central points of the two ends of wavy pipe

The geometrical parameters of the wavy pipe are dependent on the bend angle (α), the ratio of the bend radius to pipe diameter (R/d) and the number of bends (N). The geometrical features of the wavy pipe are highlighted as follows:

- The wavy pipe can be made of ‘standard’ piping bends, thus it is easy to be constructed. There is no need for a further and special treatment on the existing components, i.e. standard bends.
- The wavy pipe has a circular cross-sectional area, thus no additional obstacle is induced to the flow path.
- The wavy pipe can have various ratios of the amplitude to pipe diameter (A/d), which is dependent on the bend angle (α) and the ratio of the bend radius to pipe diameter (R/d).

3.2.2 Wavy Pipes in This Work

A series of wavy pipes of different pipe diameters, i.e. 2” and 4”, were constructed and tested in the experimental campaign.

Figure 3-3 shows the schematics of a 4” bend ($\alpha = 90^\circ$) and a wavy pipe composed of 7 such bends and 2 elbows at the two ends. It needs to be noted that the elbows at the two ends are required to ensure that the wavy pipe matches the upstream and downstream pipelines.

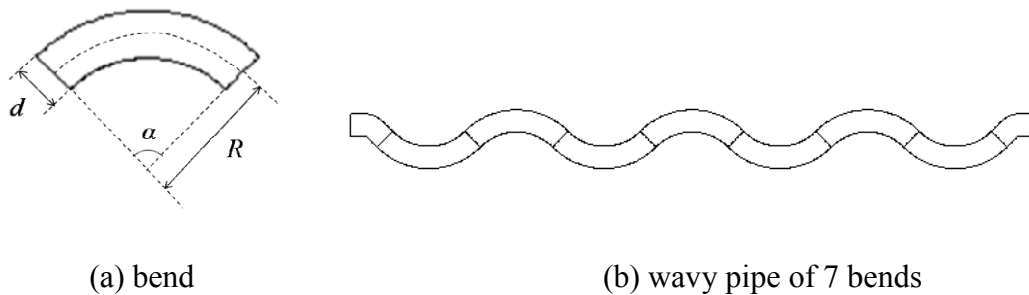


Figure 3-3 Schematics of a bend and a wavy pipe of 7 bends

The 4” bends and elbows used in this work were made from ABS (a copolymer of Acrylonitrile Butadiene Styrene). Figure 3-4 shows the photographs and schematics of the bends and elbows. It needs to be noted that there are two sockets at the two ends of

the bend and each of them has a length $C - Z_1 = 0.056$ m (Figure 3-4 (a)). The sockets allow the bends to be connected together conveniently. The geometrical parameters of the 4" bends are: $d = 0.101$ m, $R = 0.216$ m and $\alpha = 90^\circ$. The 45° elbows were selected to ensure that the wavy pipe could match the upstream and downstream pipelines. The geometrical parameters of the wavy pipe shown in Figure 3-3 (b) are: $A = 0.082$ m, $P = 0.792$ m and $L = 2.772$ m (7 bends).

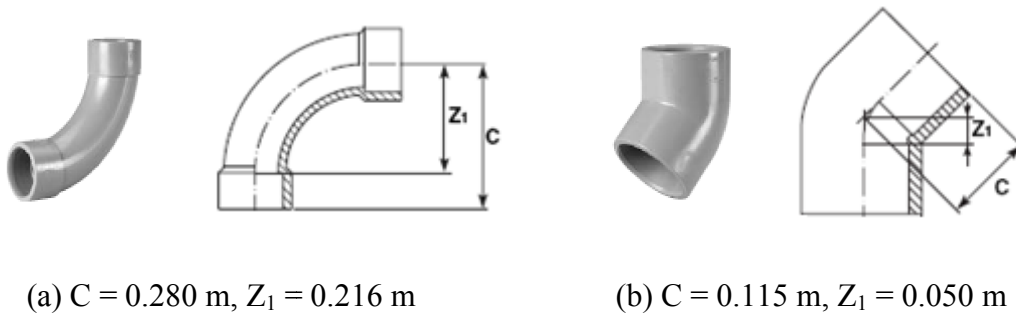


Figure 3-4 Dimensions of a 90° bend and a 45° elbow (Durapipe, 2007)

In order to visualise the flow development in the wavy pipe the 2" wavy pipes were made of clear PVC (PolyVinyl Chloride) components. As the 2" bends made from clear PVC were not available, the 2" 90° 'bend' was made by connecting one 90° elbow and two straight pipe sections at the two ends as shown in Figure 3-5 (a). The geometrical parameters of such a 'bend' are: $d = 0.052$ m, $R = 0.096$ m and $\alpha = 90^\circ$. Figure 3-5 (b) shows the schematic of a 2" wavy pipe composed of 7 such 'bends'. The geometrical parameters of the wavy pipe are: $A = 0.057$ m, $P = 0.281$ m and $L = 1.061$ m.

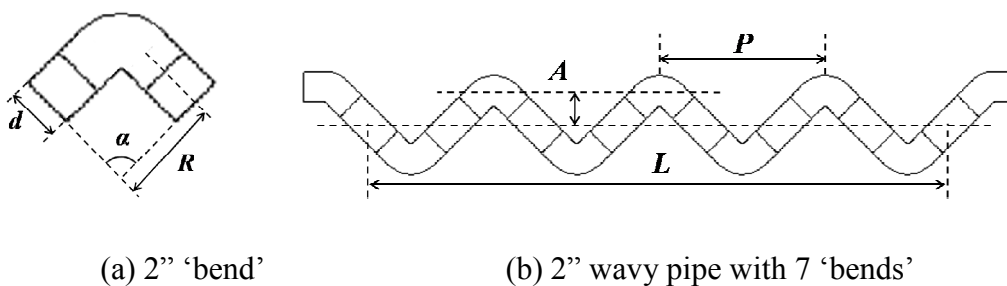


Figure 3-5 Schematics of a 2" 'bend' and wavy pipe with 7 'bends'

3.3 Experimental Campaign

3.3.1 Three-Phase Test Facility

The experiments were conducted on the Three-Phase (air, oil and water) Test Facility (Figure 3-6) in PSE (Process Systems Engineering) Laboratory at Cranfield University. The test facility comprises four areas: the fluid supply and metering area, valve manifold area, test area and separation area. This facility is controlled by the DeltaV[®] plant management system, which is a Fieldbus based Supervisory, Control And Data Acquisition (SCADA) system to ensure that the system is monitored, the desired operation conditions are achieved and the required data are recorded. The facility is capable of supplying controlled and measured flowrates of the air, oil and water from the fluid supply and metering area into the test area and finally into the separation area where the air, oil and water are separated.

A maximum air flowrate of 1410 m³/h at 7 barg can be supplied by the compressors. Then the air accumulates in a large air receiver (maintained at 7 barg) to reduce the pressure fluctuations from the compressor. The water is supplied from a 12.5 m³ capacity water tank and the oil is supplied from an oil tank of similar capacity. The water and oil are supplied by two identical multistage Grundfos CR90-5 pumps respectively. A maximum flowrate of 100 m³/h at 10 barg can be supplied by each of them. The startup, speed control and shutdown of the two pumps are operated remotely through the DeltaV[®].

There are two pipeline/riser systems (2" vertical riser and 4" catenary riser systems) in the test area. The two riser systems can be run alternatively by setting appropriate valves in the valve manifold area. The 4" pipeline/riser system consists of a 55 m long pipeline with 2° downwardly inclined and a catenary riser with a vertical height of 10.5 m. The 2" pipeline is 40 m long and the vertical riser is 11 m high. Each of the risers discharges the fluids into a vertical two-phase separator (1.2 m high and 0.5 m in diameter) where the fluids are separated into liquid and gas for metering individually. The outlet air and liquid flowrates are measured by a vortex flow meter and a Coriolis meter, respectively. A Coriolis meter is installed at the near vertical section at the top of

the 4" riser. This meter gives an indication of the fluid mass flowrate and density at the riser top.

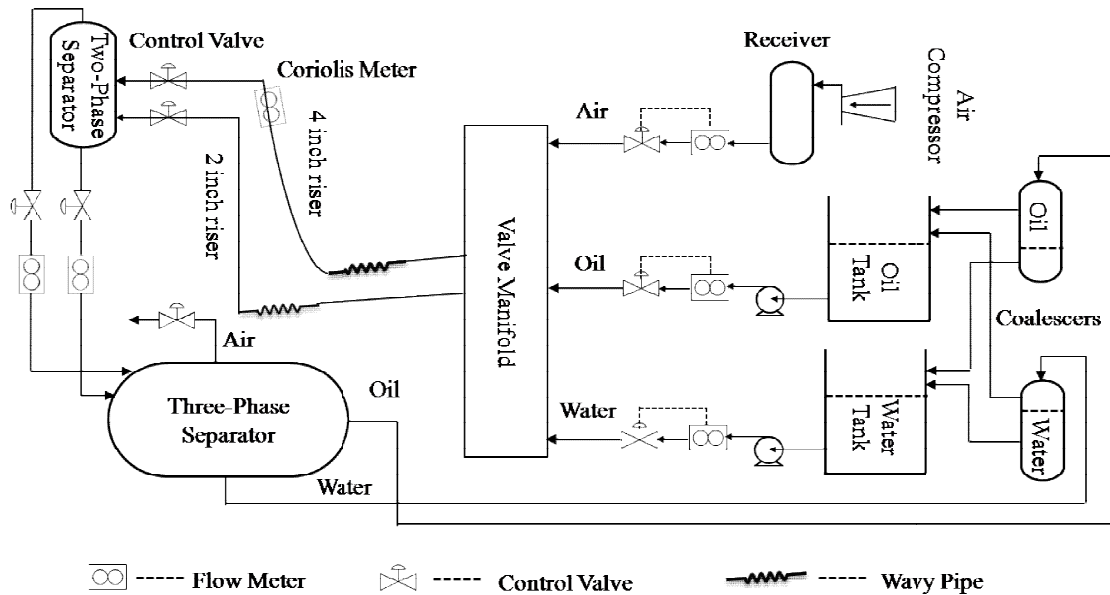


Figure 3-6 Schematic of the Three-Phase Test Facility at Cranfield University

The air and liquid return to the horizontally positioned three-phase separator. The air, water and oil are gravitationally separated in the three-phase separator. The pressure, oil/water interface level and gas/liquid interface level are controlled by a pressure controller and two level controllers, respectively. The pressure in the three-phase separator is controlled through the gas outlet valve. After separation in the three-phase separator the air is exhausted into the atmosphere and the water and oil enter their respective coalescers, where the liquids are cleaned before returning to their respective storage tanks.

3.3.2 Test Configurations of Pipeline/Wavy-Pipe/Riser Systems

The experiments were carried out on the 2" and 4" pipeline/riser systems with air and water as test fluids. The superficial liquid velocity (U_{SL}) ranged from 0.1 m/s to 1.0 m/s and superficial air velocity (U_{SG0}) at standard conditions (101325 Pa, 20 °C) was from

0.3 m/s to 3.0 m/s. The pressure in the three-phase separator was controlled by a PID controller with the set value of 1 barg in each test run. It needs to be noted that fluctuations of the separator pressure could not be avoided due to the variations of the flow regimes in the pipeline/riser system and the imperfection of control. The pressure in the three-phase separator fluctuated between 0.95 barg and 1.05 barg (Xing, 2009). The test configurations of the pipeline/wavy-pipe/riser systems were as follows:

- **Configuration I (CI):** the outlet of the wavy pipe located at the riser base (2" and 4" wavy pipes of 7 bends); the CI is used to test the performance of the wavy pipes of different diameters.
- **Configuration II (CII):** the outlet of the wavy pipe located at a distance (1.5 m and 3 m for the 2" and 4" 7-bend wavy pipes, respectively) from the riser base; the CII is used to test the effects of the location in the pipeline of the wavy pipe on its performance.
- **Configuration III (CIII):** the outlet of the wavy pipe located at the riser base (2" wavy pipe of 7 and 11 bends); the CIII is used to test the effects of the length of the wavy pipe on its performance.
- **Configuration IV (CIV):** the outlet of the wavy pipe located at a distance (1.5 m) from the riser base (2" wavy pipe of 7 and 11 bends); the CIV is used to test the effects of both the location and length of the wavy pipe on its performance and compare with the results from the CIII.

It needs to be mentioned that the same test runs have been performed on the pipeline/riser system without a wavy pipe installed. The pipeline/riser system without a wavy pipe is also called 'plain riser system' in this thesis. The flow behaviour in the plain riser system serves as the baseline for comparison with that in the pipeline/wavy-pipe/riser systems to examine the effects of the wavy pipe.

3.4 Characterisation of the Flow in Pipeline/Riser Systems

3.4.1 Flow Regimes

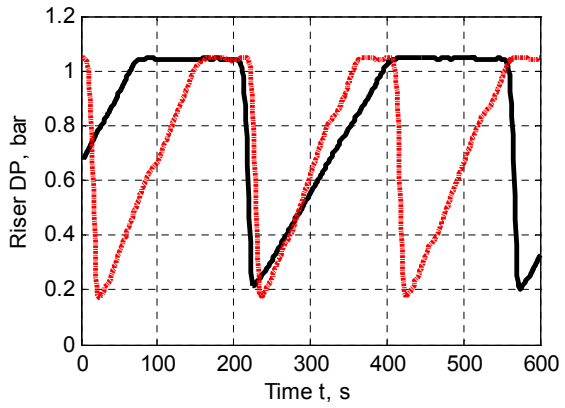
The flow regimes in a pipeline riser system have been classified into different categories by different researchers (Linga, 1987; Schmidt *et al.*, 1980; Taitel *et al.*, 1990; Tin, 1991) as discussed in Chapter 2. In this work the flow regimes observed in the 2” vertical and 4” catenary riser are classified into four categories, i.e. severe slugging (SS), transitional severe slugging (TSS), oscillation flow (OSC) and continuous flow (CON). The flow regimes can be identified based on both visual observations and analysis of the differential pressure between the riser base and riser top (riser DP). The flow regimes are described below and typical riser DP time traces of the four flow regimes in the plain riser system and pipeline/wavy-pipe/riser system are compared in Figure 3-7.

Severe slugging (SS): There are four stages in one SS cycle: liquid buildup stage, slug production stage, bubble penetration stage and gas-blowdown/liquid-fallback stage. At the liquid buildup stage the slug length increases in both of the riser and pipeline and the riser DP increases gradually. Once the slug front arrives at the riser top the riser DP reaches its maximum and then remains roughly constant for a period (slug production stage). At this stage the slug tail in the pipeline moves towards the riser base and the slug front at the riser top moves to the topside separator. The liquid slug is hence longer than the riser. The gas-blowdown/liquid-fallback stage starts when the gas bubbles behind the slug tail continuously come into the riser. At this stage the liquid slug is swept out of the riser violently and then the gas rushes into the topside separator at a high velocity and the riser DP decreases sharply to its minimum.

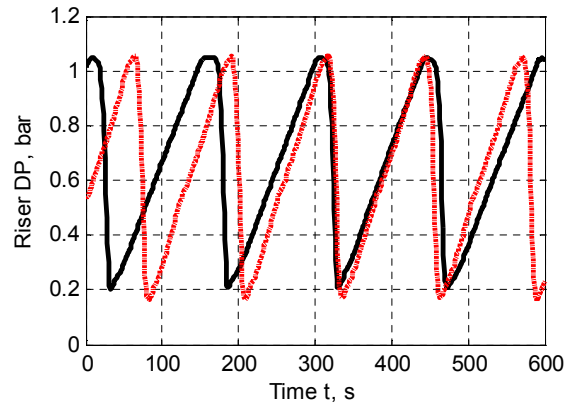
Transitional severe slugging (TSS): At the liquid buildup stage the slug length increases only in the riser but no liquid backup in the pipeline can be found. The gas in the pipeline penetrates into the slug in the riser just as the slug front arrives at the riser top. Hence the slug length is approximately equal to the length of the riser. The maximum riser DP is almost the same with that of severe slugging, but it does not remain constant for a period of time for slug production. The TSS is characterised by the absence of the slug production stage compared with SS.

Oscillation flow (OSC): At the liquid buildup stage the gas and liquid move into the riser alternatively, thus more than one aerated slugs coexist in the riser separated by gas packets. (In the discussions below a slug of the same length with the sum of the slugs is considered as an equivalent of them.) This stage ends when the front of the first slug arrives at the riser top and a gas blowdown stage follows immediately. The riser DP still exhibits cyclic behaviour, although the maximum is lower than those of SS and TSS.

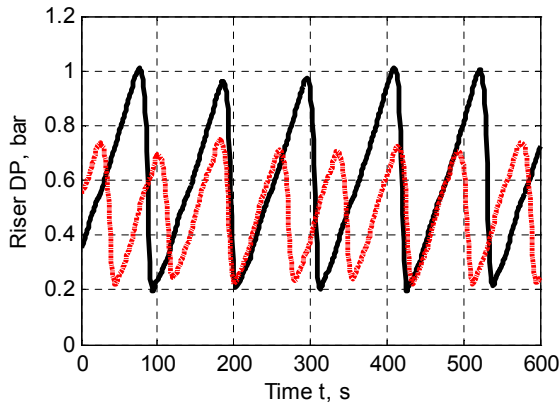
Continuous flow (CON): The gas and liquid come into the riser continuously. No obvious 'liquid buildup' stages can be observed. The flow regimes in the riser are mainly slug flow with Taylor bubbles or churn flow. The riser DP remains roughly constant with irregular fluctuations of small amplitudes.



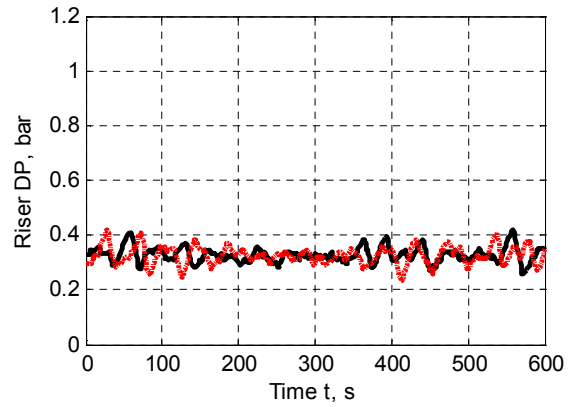
(a) SS and SS: $U_{SG0} = 0.70$ m/s



(b) SS and TSS: $U_{SG0} = 1.06$ m/s



(c) OSC and OSC: $U_{SG0} = 1.41$ m/s



(d) CON and CON: $U_{SG0} = 2.82$ m/s

— Plain riser system - - - Pipeline/wavy-pipe/riser system

Figure 3-7 Riser DP time traces of severe slugging (SS), transitional severe slugging (TSS), oscillation flow (OSC) and continuous flow (CON) in plain riser and pipeline/wavy-pipe/riser systems ($U_{SL} = 0.12$ m/s)

3.4.2 Characteristic Parameters

The long liquid slugs in SS and TSS are most problematic to the downstream facilities of the pipeline/riser production system. In OSC the liquid slug is shorter than the riser; however, the induced pressure fluctuations in the pipeline still challenge the stability of the whole production system.

In order to characterise the flow behaviour of the SS, TSS and OSC flow regimes and evaluate the performance of different wavy pipes qualitatively, a series of characteristic parameters (CPs) are defined. The CPs include two groups of parameters based on the analysis of the riser DP time traces, i.e. magnitude parameters (M_{MAX} , M_{MIN} , M_{AMP} , M_{AVE}) and time parameters (T_{BUI} , T_{PRO} , T_{BFB} , T_{CYC}). The M_{MAX} , M_{MIN} , M_{AMP} and M_{AVE} refer to the maximum, minimum, fluctuation amplitude and time average of the riser DP, respectively; while the T_{BUI} , T_{PRO} , T_{BFB} and T_{CYC} are the time periods of the liquid buildup stage, slug production stage, bubble-penetration/gas-blowdown/liquid-fallback stages and total cycle time, respectively. Figure 3-8 illustrates the definitions of the CPs based on the riser DP time trace of a severe slugging test case.

The CPs can be used to assess the severity of the flow regimes qualitatively. For SS and TSS the M_{MAX} is generally equal to the hydrostatic pressure of the liquid column filling the riser. For OSC the M_{MAX} can be treated as the consequence of the maximum equivalent slug length in the riser. The M_{MIN} indicates how much liquid has been left in the riser after the gas-blowdown/liquid-fallback stage. The M_{AMP} is an indicator of the slug length produced into the separator during the gas blowdown stage. The M_{AVE} is used to calculate the average pressure at the riser base. The riser base pressure should be as low as possible to obtain as much production from the supply source as possible. The T_{BUI} is an indicator of the slug front velocity at the liquid buildup stage. The average velocity can be estimated in conjunction with the M_{MAX} and M_{MIN} . The T_{PRO} is only valid for SS, which indicates how long it takes for the severe slug to be produced at the slug production stage. At the same flowrates of the gas and liquid, the longer the T_{PRO} is the longer the severe slug is produced and the more severe the flow regime is. Similar to the T_{PRO} the T_{BFB} can be used to estimate the average slug velocity at the gas blowdown stage. The inverse of the T_{CYC} can be regarded as the slug frequency of the severe slugs for SS/TSS and the equivalent slugs for OSC.

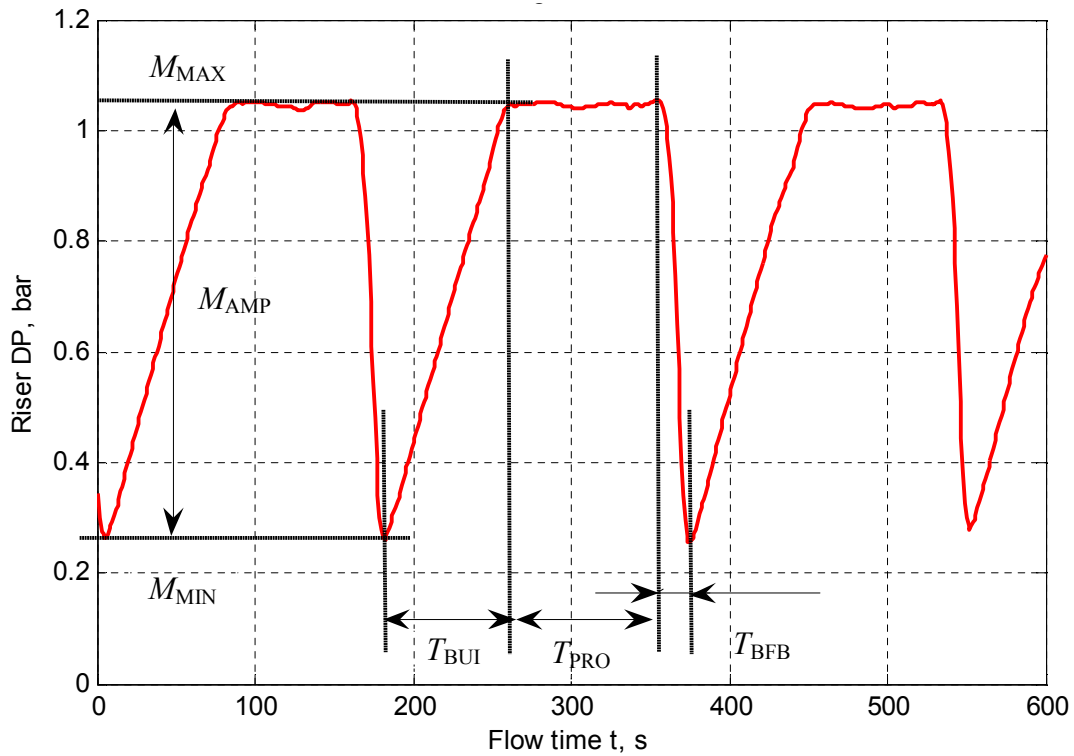


Figure 3-8 Definitions of the characteristic parameters based on the riser DP time trace of severe slugging

3.5 Effects of Wavy Pipes

Different test configurations were designed as stated in Section 3.3.2. The effects of the wavy pipes on the flow behaviour in the pipeline/riser systems are discussed below in terms of the flow regime transition and characteristic parameters defined in Section 3.4.

3.5.1 Flow Regimes

The basic flow regime map with the superficial gas and liquid velocities as coordinates can be divided into two regions: Region I and II. Region I includes SS, whereas Region II includes OSC and CON. In the flow regime map discussed below, a boundary (also called stability boundary) is placed between Region I and Region II, where TSS is expected to occur. It needs to be noted that at some superficial liquid velocities TSS did

not appear explicitly in the designed test matrix. To obtain a stability boundary TSS was assumed to occur at a U_{SG0} located in the middle of the last SS case and the first OSC case with the increase of U_{SG0} at the same U_{SL} .

Figure 3-9 shows the stability boundaries for the 2" and 4" plain riser and pipeline/wavy-pipe/riser systems of the test configuration CI. Region I and Region II are located on the left and right side of the stability boundary, respectively. It can be seen clearly that Region I is reduced with the application of the wavy pipe. The stability boundary is shifted towards the lower superficial gas velocity, U_{SG0} , by up to 0.4 m/s and 0.5 m/s for the 2" and 4" systems, respectively. The flow regimes for the test cases located between the two boundaries (with and without a wavy pipe) used to be SS in the plain riser system, but have become into OSC in the pipeline/wavy-pipe/riser system. This indicates that the slug lengths for those cases have been reduced.

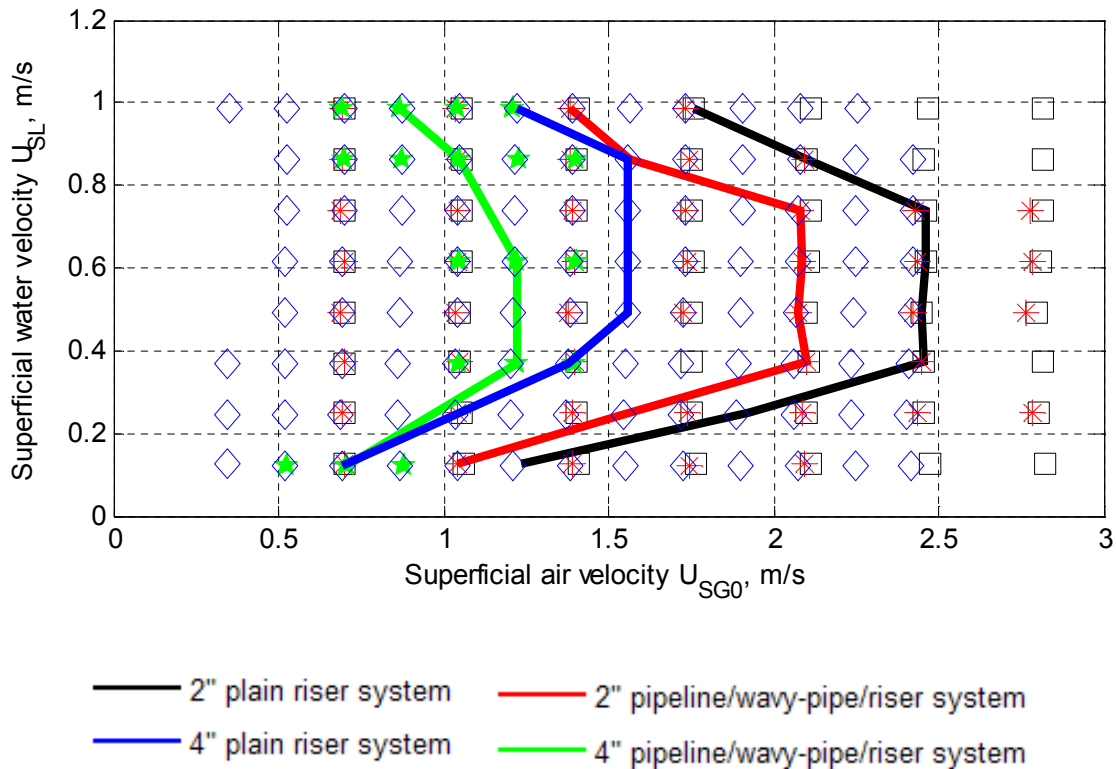
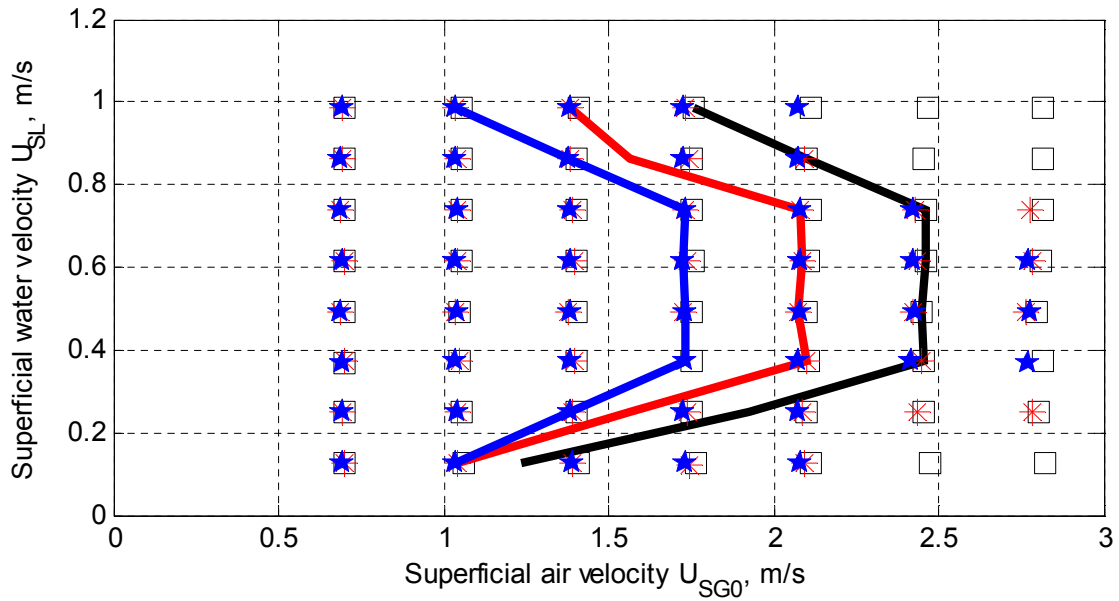
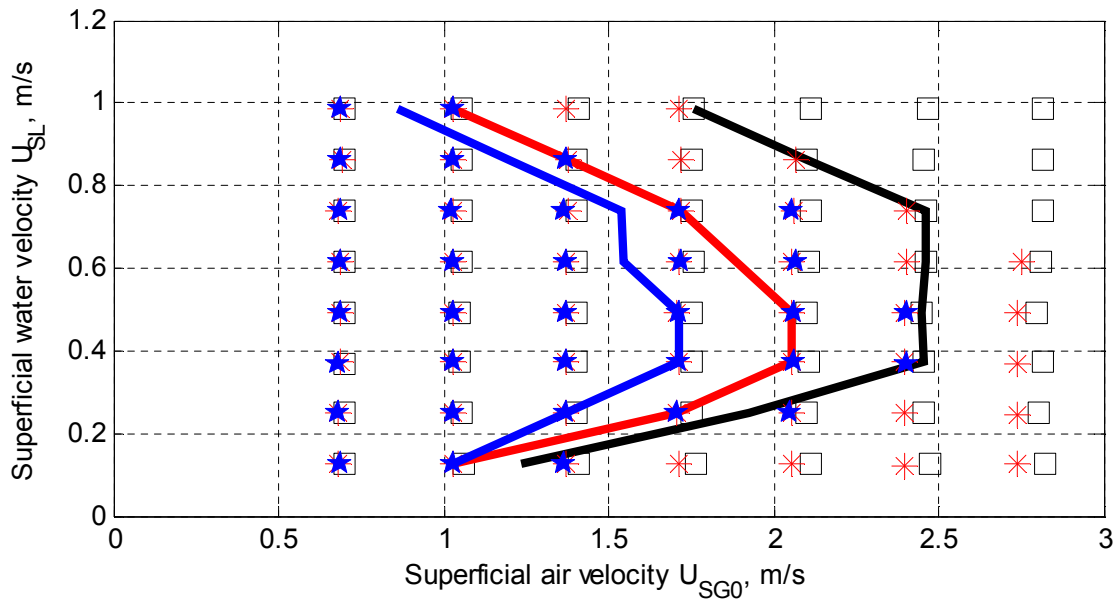


Figure 3-9 Test points and stability boundaries for the 2" and 4" plain riser and pipeline/wavy-pipe/riser systems

Figure 3-10 shows the stability boundaries for the 2" plain riser and pipeline/wavy-pipe/riser systems with the wavy pipe outlet located at the riser base and upstream of the riser base. Figure 3-10 (a) and (b) illustrate the stability boundaries for the wavy pipes of 7 and 11 bends, respectively. It can be seen that Region I (severe slugging region) can be further reduced when there is a pipe section between the outlet of the wavy pipe and riser base. For the cases of U_{SL} between 0.6 m/s and 0.8 m/s, the stability boundary with the 11-bend wavy pipe is located at lower U_{SG} comparing Figure 3-10 (a) and (b). Therefore, a smaller Region I (SS region) tends to be obtained with a wavy pipe of more bends.



(a) Wavy pipes of 7 bends



(b) Wavy pipes of 11 bends

- Plain riser system
- Pipeline/wavy-pipe/riser system of CIII
- Pipeline/wavy-pipe/riser system of CIV

Figure 3-10 Test points and stability boundaries for the 2" plain riser and pipeline/wavy-pipe/riser systems

3.5.2 M_{MAX} , M_{MIN} and M_{AVE}

The maximum, minimum and time average of the riser DP have been plotted against the superficial gas velocity (U_{SG0}) at fixed superficial liquid velocities (U_{SL}) for different test configurations.

Figure 3-11 (a) and (b) shows the plots for $U_{SL} = 0.25$ m/s and 0.86 m/s respectively. The riser base pressure is of concern because the production from the supply source is highly dependent on it in the field production system. The riser base pressure is the sum of the riser top pressure and the riser DP. Thus the M_{AVE} of the riser DP is expected to be as low as possible to obtain the lowest average pressure at the riser base. Based on the analysis of Figure 3-11 (a) and (b) it can be concluded that the severity of the flow regimes (SS and OSC) can be reduced by applying wavy pipes. The effects of the wavy pipes on the flow behaviour in the pipeline/riser systems are discussed below in detail.

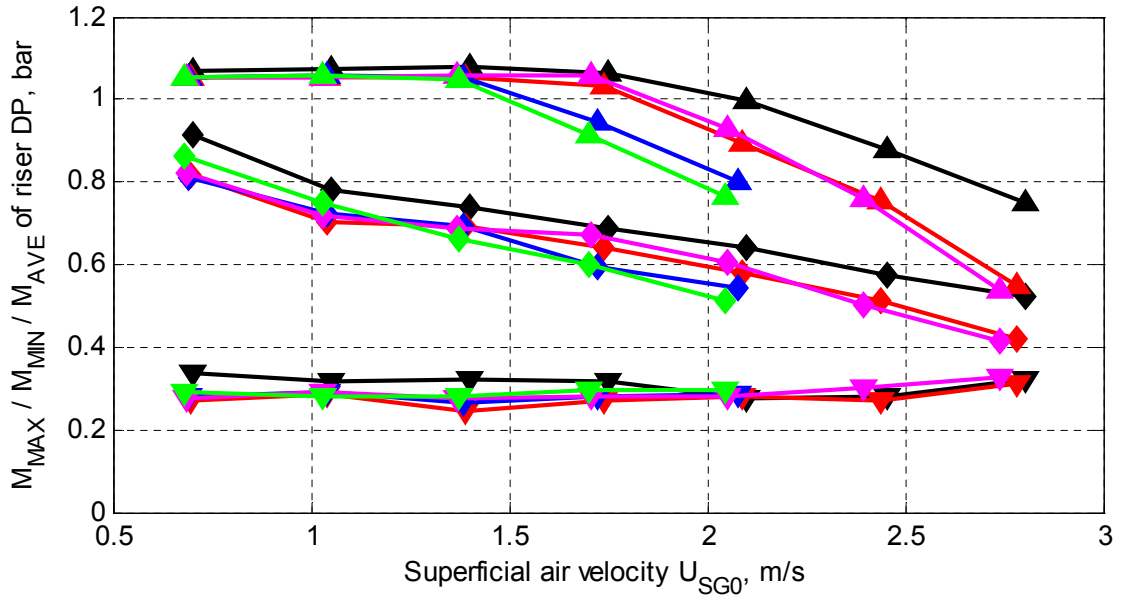
The M_{MAX} of the riser DP are almost the same for the SS cases because the riser can be filled with water. For the OSC cases the M_{MAX} is the highest in the plain riser system consistently and it is the lowest in the pipeline/wavy-pipe/riser system of the configuration CIV (11-bend). It is indicated that the maximum equivalent slug length in the riser is the shortest when the outlet of the 11-bend wavy pipe located upstream of the riser base (1.5 m in the experiment).

With the increase of U_{SG0} the M_{MIN} of the riser DP decreases for the SS cases then increases for the OSC cases. For the SS cases the liquid left in the riser after the gas-blowdown/liquid-fallback stage at lower U_{SG0} is more than that at higher U_{SG0} as indicated by the M_{MIN} . It is postulated that there is less energy from the expansion of the trapped gas at the liquid buildup stage at lower U_{SG0} . The effects of the wavy pipe on the M_{MIN} of the riser DP are not significant for SS and OSC. However, the critical U_{SG0} for CON to occur is much lower in the pipeline/wavy-pipe/riser systems than that in the plain riser system as indicated in Figure 3-11 (b).

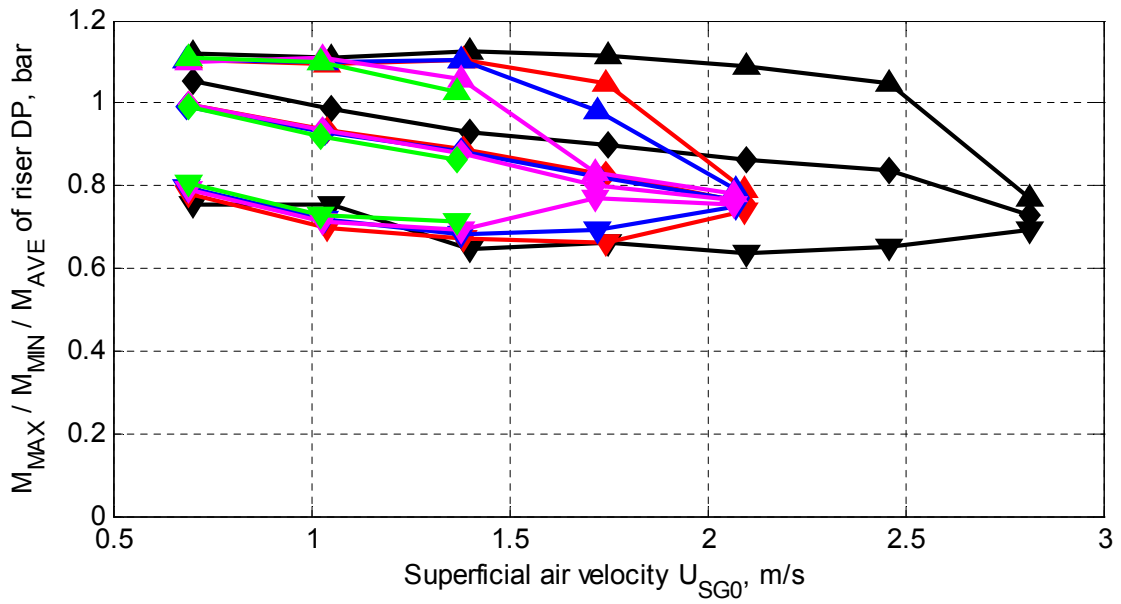
The M_{AVE} of the riser DP decreases with the increase of U_{SG0} monotonously. For SS the decrease of the M_{AVE} is induced by the reduction of the slug length and slug production time in one cycle. For OSC the decrease of the M_{AVE} is induced by the decrease of the

M_{MAX} of riser DP, which can also be regarded as the reduction of the maximum equivalent slug length. Compared with that in the plain riser system a lower M_{AVE} can be obtained in the pipeline/wavy-pipe/riser systems.

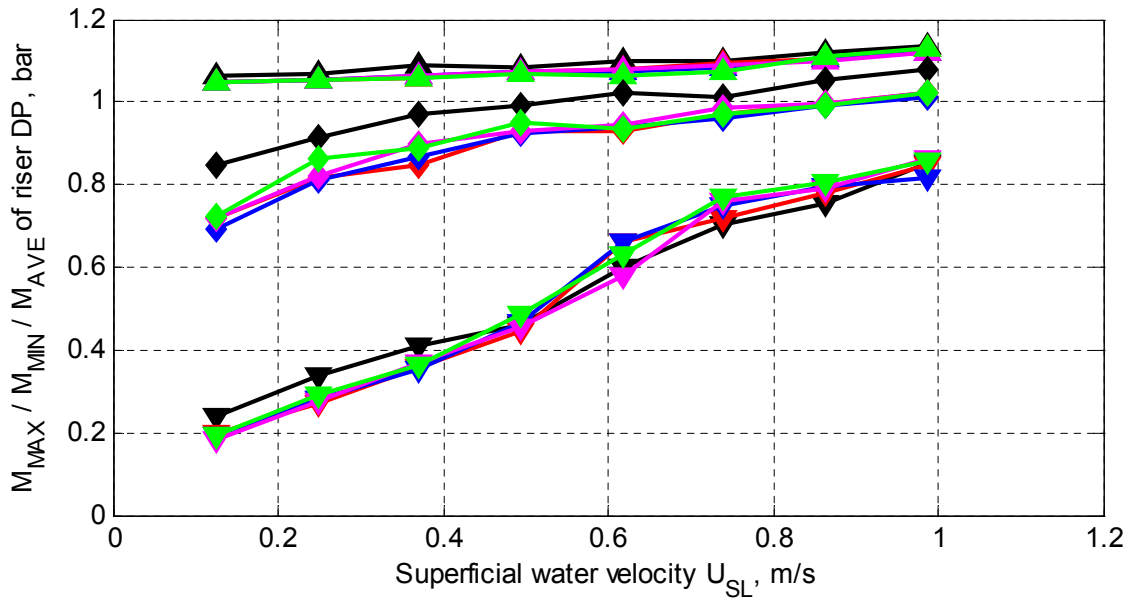
The variation of the M_{MAX} , M_{MIN} and M_{AVE} of the riser DP for SS with the increase of U_{SL} is shown in Figure 3-11 (c) at $U_{SG0} = 0.70$ m/s. Both of the M_{MIN} and M_{AVE} increase with the increase of U_{SL} . At the same U_{SG0} more liquid tends to be left in the riser after the gas-blowdown/liquid-fallback stage at higher U_{SL} . The M_{AVE} in pipeline/wavy-pipe/riser systems is consistently lower than that in the plain riser system.



(a) $U_{SL} = 0.25$ m/s



(b) $U_{SL} = 0.86$ m/s



(c) $U_{SG0} = 0.70$ m/s

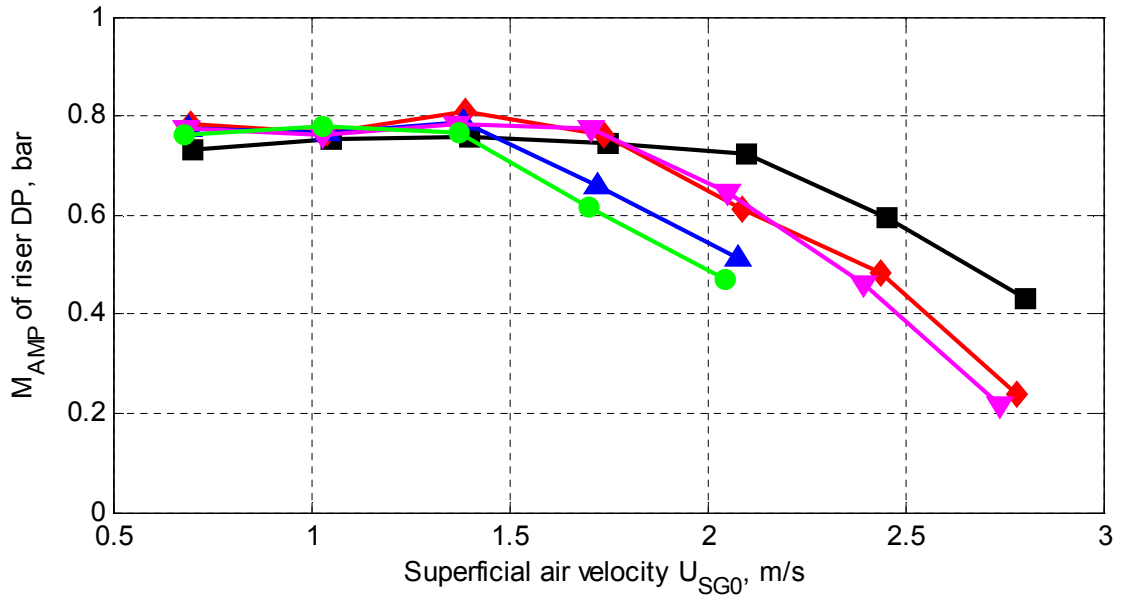
▲ M_{MAX} ; ◆ M_{AVE} ; ▼ M_{MIN}

— Plain riser system — 7-bend wavy pipe of CI — 7-bend wavy pipe of CII
 — 11-bend wavy pipe of CIII — 11-bend wavy pipe of CIV

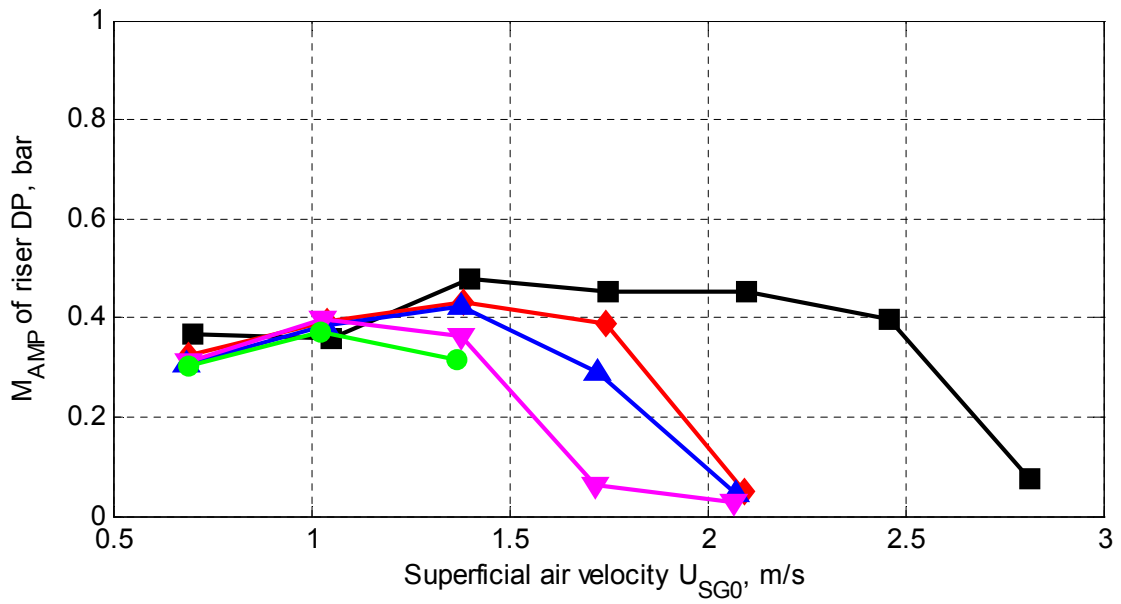
Figure 3-11 M_{MAX} , M_{MIN} and M_{AVE} of the riser DP for the 2” plain riser and pipeline/wavy-pipe/riser systems of different test configurations

3.5.3 M_{AMP}

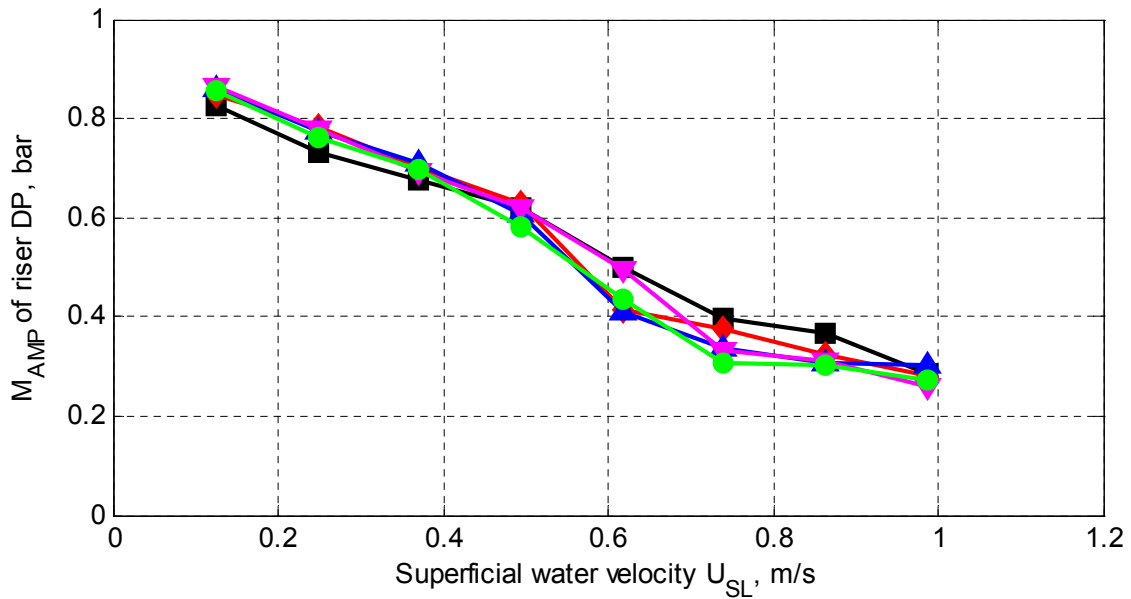
The M_{AMP} is an indicator of the length of the severe slug for SS and the equivalent slug for OSC produced out of the riser at the gas blowdown stage. The variations of the M_{AMP} of the riser DP for different test configurations are illustrated in Figure 3-12 at constant U_{SL} (Figure 3-12 (a) and (b)) and U_{SG0} (Figure 3-12 (c)), respectively.



(a) $U_{SL} = 0.25$ m/s



(b) $U_{SL} = 0.86$ m/s



(c) $U_{SG0} = 0.70$ m/s

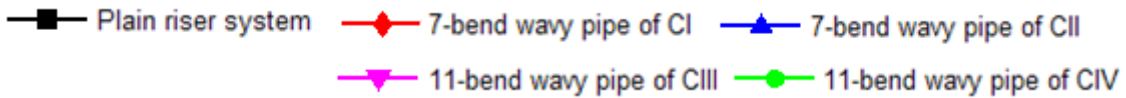


Figure 3-12 M_{AMP} of the riser DP for the 2” plain riser and pipeline/wavy-pipe/riser systems of different configurations

It can be observed in Figure 3-12 (a) and (b) that the variations of the M_{AMP} with the increase of U_{SG0} are different at the lower and higher U_{SL} . At the lower U_{SL} ($U_{SL} = 0.25$ m/s) the M_{AMP} fluctuates slightly for SS and decreases significantly for OSC; at the higher U_{SL} ($U_{SL} = 0.86$ m/s) the M_{AMP} increases for SS and decreases for OSC. Referring to the discussions in Section 3.5.2 it can be concluded that the increase of M_{AMP} for SS is mainly induced by the decrease of the M_{MIN} at the higher U_{SL} ($U_{SL} = 0.86$ m/s). It needs to be noted that the M_{AMP} for OSC in the pipeline/wavy-pipe/riser systems are consistently lower than that in the plain riser system. The lowest M_{AMP} has been obtained with the outlet of the 11-bend wavy pipe located upstream of the riser base. It can be concluded that the maximum equivalent slug length for OSC can be reduced by applying the wavy pipe. The shortest equivalent slug has been obtained with the outlet of the 11-bend wavy pipe located upstream of the riser base.

As can be seen in Figure 3-12 (c) the M_{AMP} decreases approximately linearly with the increase of U_{SL} for the SS cases. The reduction of the M_{AMP} indicates that the slug produced out of the riser at the gas blowdown stage becomes shorter and shorter with the increase of U_{SL} . No obvious effects of the test configurations of the wavy pipes on the relationship between the M_{AMP} and U_{SL} can be found for SS.

3.5.4 T_{PRO}

As discussed in Section 3.5.1 the SS region in the flow regime map can be reduced by installing a wavy pipe in the pipeline, however, there is still a smaller region for SS to occur. In this smaller region the severity of the flow has been reduced in terms of slug length although SS remains. The T_{PRO} is an indicator of the length of the severe slug produced out of the riser at the slug production stage.

The riser DP time traces of a sample SS case for different test configurations (2" system) are compared in Figure 3-13. The average T_{PRO} are 181.5 s, 66 s, 58 s, 88 s, and 79.5 s for the plain riser, 7-bend wavy pipe of CI and CII, 11-bend wavy pipe of CIII and CIV, respectively. The longer the T_{PRO} is the longer the produced severe slug is, because the inlet mass flowrates of gas and liquid are the same for the five configurations. Furthermore, it can be observed that the severe slug in the plain riser system has been split into more than one shorter slugs in the test configurations with wavy pipes. The smallest T_{PRO} has been obtained with a 7-bend wavy pipe located 1.5 m away from the riser base.

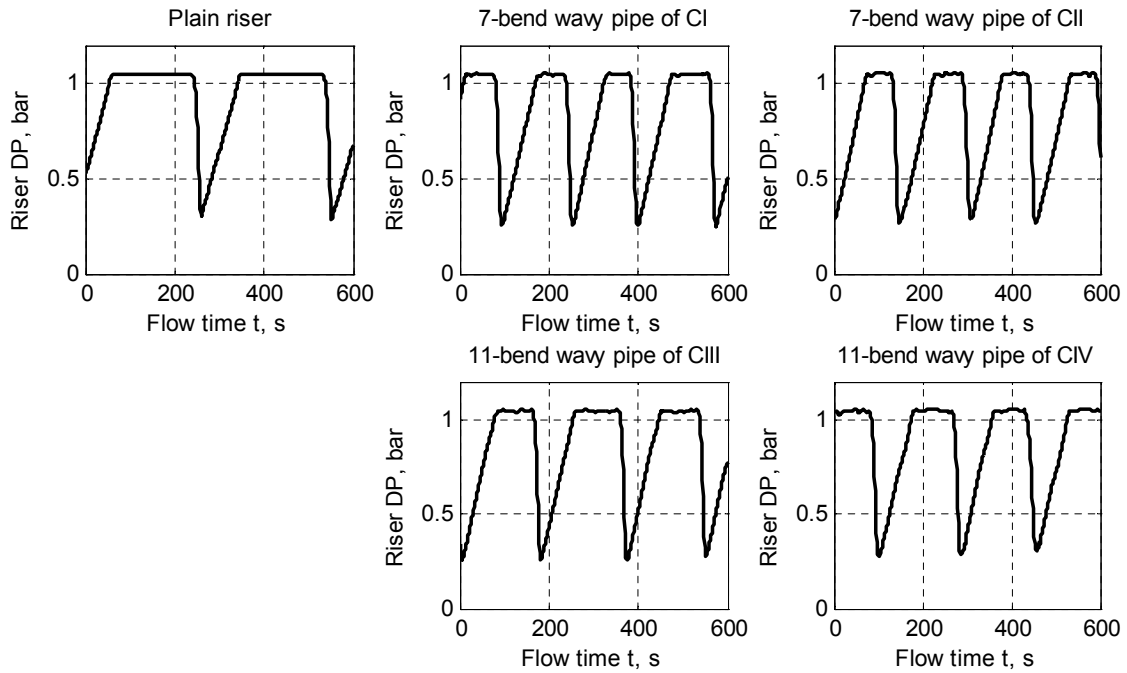


Figure 3-13 Riser DP time traces of SS for the 2'' plain riser and pipeline/wavy-pipe/riser systems of different configurations ($U_{SG0} = 0.70$ m/s, $U_{SL} = 0.25$ m/s)

Figure 3-14 shows the variation of the T_{PRO} with the increase of U_{SL} at the same superficial gas velocity $U_{SG0} = 0.70$ m/s. It can be observed that: (1) the T_{PRO} for the plain riser system is much larger than those for the pipeline/wavy-pipe/riser systems; (2) the T_{PRO} for the pipeline/11-bend-wavy-pipe/riser systems are larger than those for the pipeline/7-bend-wavy-pipe/riser systems; (3) the T_{PRO} for the pipeline/wavy-pipe/riser systems with the outlet of the wavy pipe at the riser base are larger than those with the outlet located upstream of the riser base. To summarise, the shortest severe slug produced out of the riser at the slug production stage has been obtained by employing a 7-bend wavy pipe with the outlet located upstream of the riser base (1.5 m away from the riser base in the 2'' pipeline/riser system in the experiment).

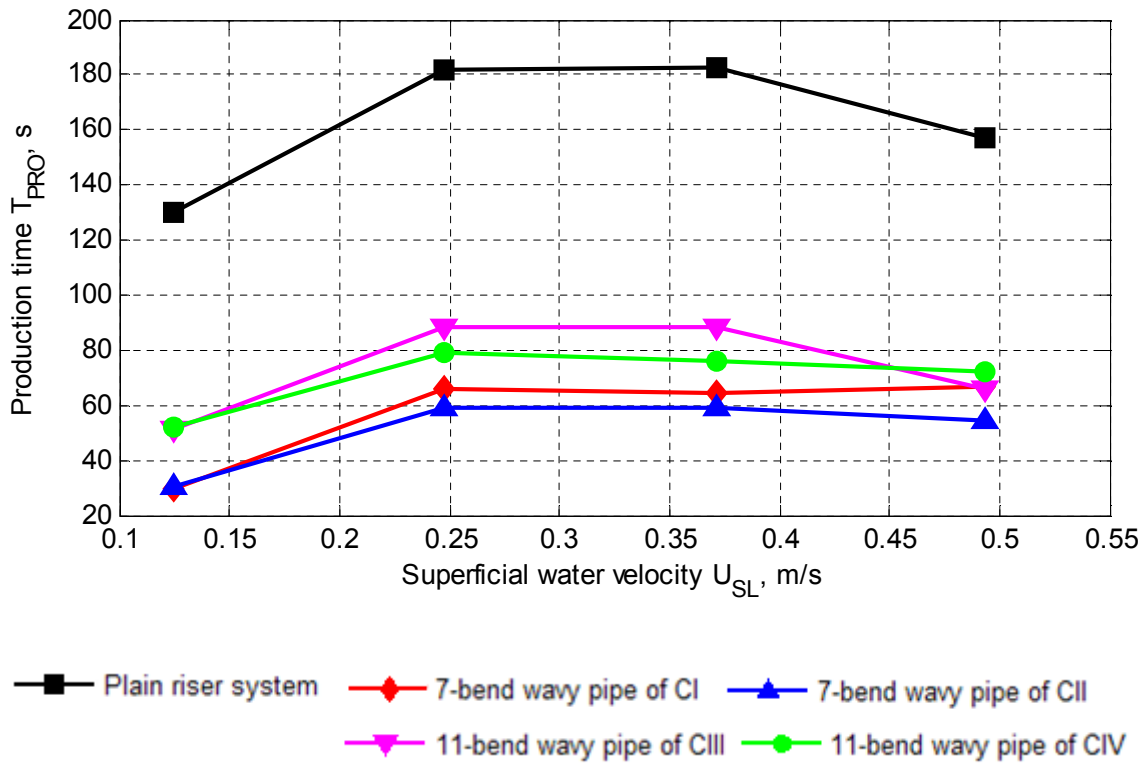


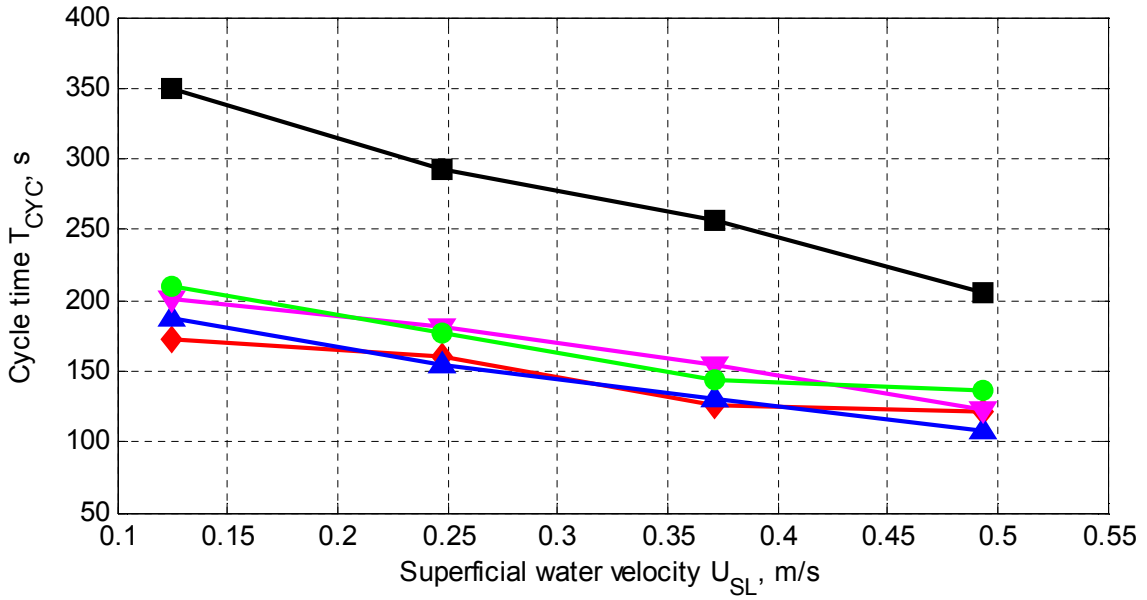
Figure 3-14 T_{PRO} for the 2” plain riser and pipeline/wavy-pipe/riser systems of different configurations ($U_{SG0} = 0.70$ m/s)

3.5.5 T_{CYC} , T_{BUI} and T_{BFB}

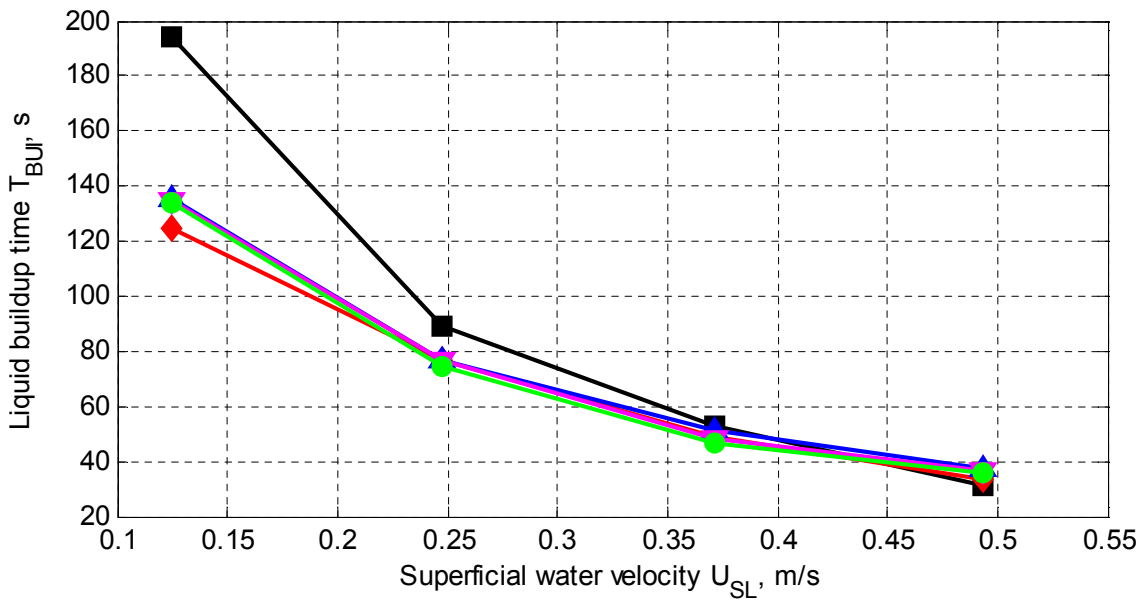
The SS flow regime is a cyclic process. The cycle time of SS can be obtained by examining the average cycle time (T_{CYC}) of the riser DP. The same SS cases with those discussed in Section 3.5.4 have been analysed and the T_{CYC} , T_{BUI} and T_{BFB} are plotted against U_{SL} in Figure 3-15 (a) (b) and (c), respectively.

The T_{CYC} decreases with the increase of U_{SL} at the same U_{SG0} and the relationship between them is approximately linear. With a wavy pipe applied the T_{CYC} has been reduced by more than 40 % of that for the plain riser system. A smaller T_{CYC} means a higher slug frequency. A higher slug frequency results in shorter slugs in the system because the inlet mass flowrates of air and water are the same for the plain riser and

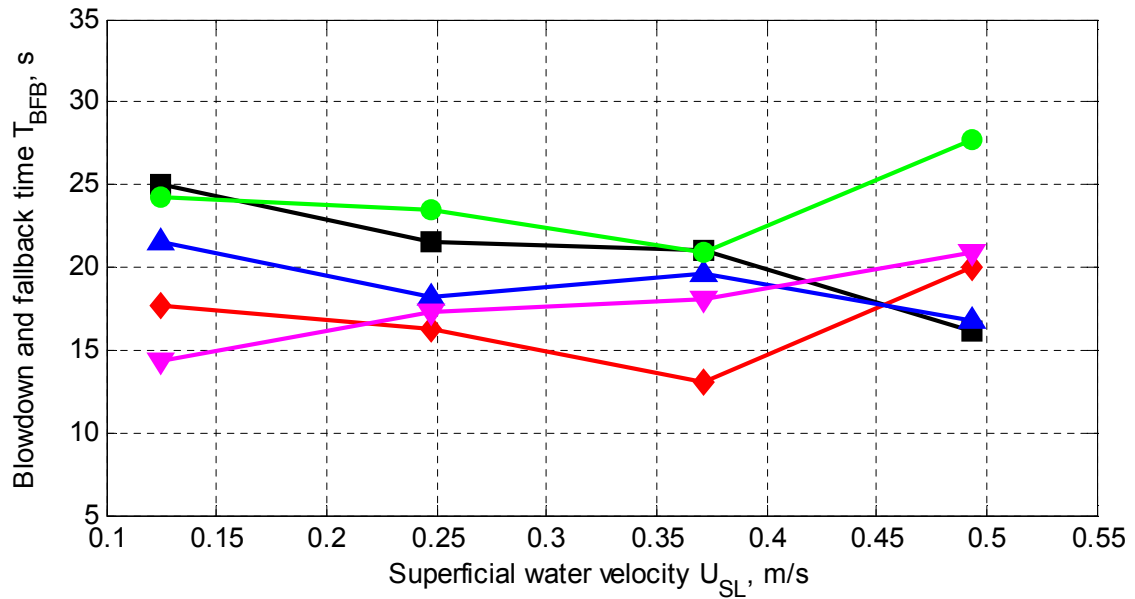
pipeline/wavy-pipe/riser systems. Therefore, the slug length in the pipeline/riser system has been reduced by applying a wavy pipe.



(a) T_{CYC}



(b) T_{BUI}



(c) T_{BFB}

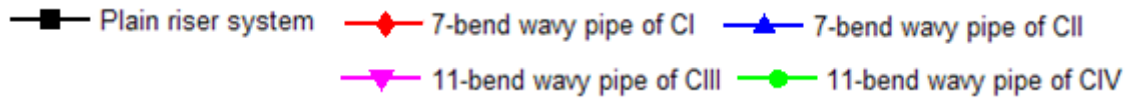


Figure 3-15 T_{CYC} , T_{BUI} and T_{BFB} of SS for the 2” plain riser and pipeline/wavy-pipe/riser systems of different configurations ($U_{SG0} = 0.70$ m/s)

The T_{BUI} decreases with the increase of U_{SL} at the same U_{SG0} . At the lower U_{SL} ($U_{SL} < 0.4$ m/s) the T_{BUI} for the plain riser is larger than those for the pipeline/wavy-pipe/riser systems. At the higher U_{SL} ($U_{SL} > 0.4$ m/s) no significant effects of the test configurations of the wavy pipe on the T_{BUI} can be observed. The T_{BFB} for the SS cases varies between 10 s and 30 s. It can be observed that neither the U_{SL} nor the wavy pipe has consistent effects on the T_{BFB} .

3.5.6 Summary

The effects of the wavy pipe on the flow behaviour in the pipeline/riser system have been discussed in term of flow regime transition and characteristic parameters of the riser DP. It has been demonstrated that: (1) the SS region in the flow regime map can be reduced by installing a wavy pipe in the pipeline and the region can be reduced further

when the outlet of the wavy pipe is located at a distance away from the riser base; (2) the M_{AVE} in the pipeline/wavy-pipe/riser system is lower than that in the plain riser system and the lowest M_{MAX} and M_{AMP} for the OSC cases can be obtained in the pipeline/11-bend-wavy-pipe/riser system with the outlet of the wavy pipe located at a distance away from the riser base; (3) The T_{PRO} and T_{CYC} in the pipeline/wavy-pipe/riser systems are smaller than those in the plain riser system.

Essentially all the effects of the wavy pipe discussed above can be regarded as reducing the slug length in the pipeline/riser system. When the SS flow regime is transformed into the OSC flow by applying a wavy pipe, the long severe slug (longer than the riser) has been split into more than one short slugs (shorter than the riser). A lower M_{MAX} and M_{AMP} of OSC means a shorter maximum equivalent slug and shorter slugs produced out of the riser at the gas blowdown stage, respectively. A smaller T_{PRO} means a shorter slug produced out of the riser at the slug production stage and a smaller T_{CYC} indicates a higher slug frequency. It needs to be mentioned that a higher slug frequency indicates shorter slugs in the pipeline/riser system because the inlet gas/liquid flowrates are the same for different test configurations.

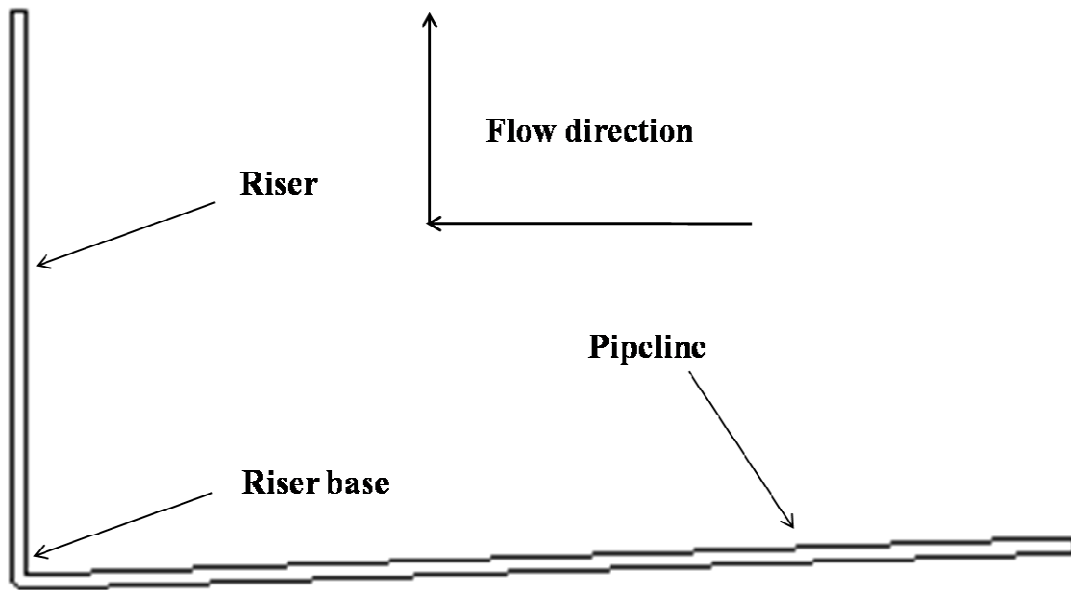
3.6 Discussions

3.6.1 Working Principle of Wavy Pipe

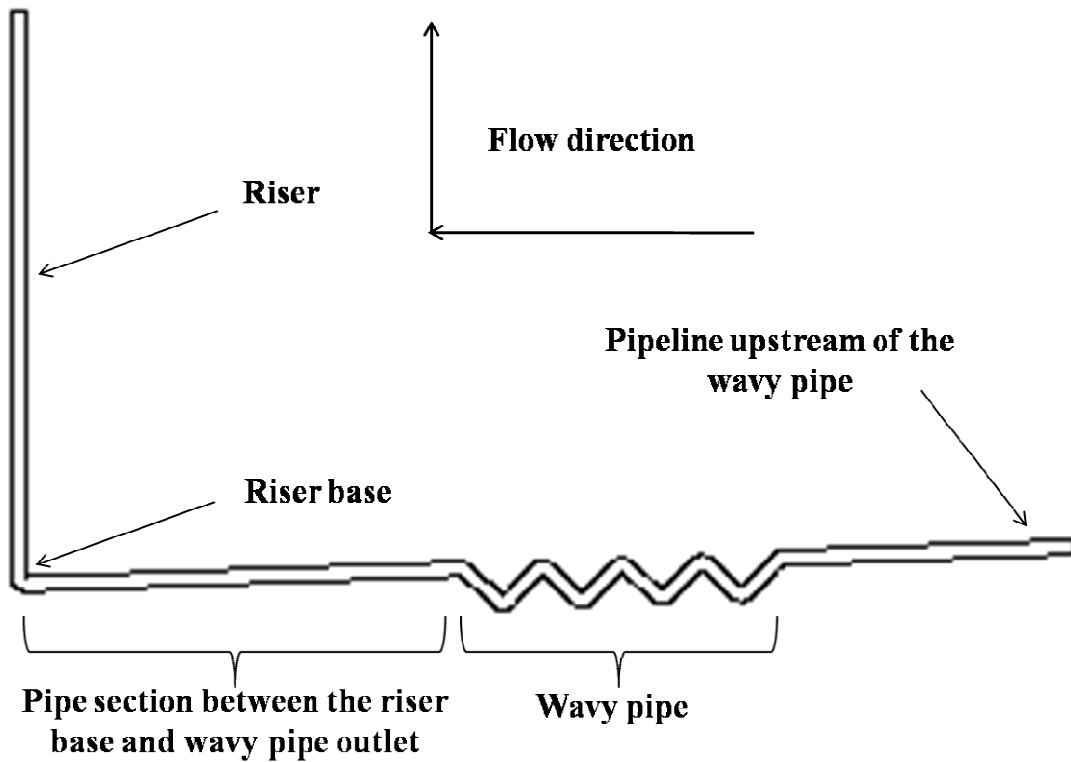
It has been concluded in Section 3.5 that the slug length in the pipeline/riser system can be reduced with a wavy pipe applied. Three scenarios of slug length reduction are discussed below to disclose the working principle of the wavy pipe.

- **Scenario I:** SS in both of the plain riser and pipeline/wavy-pipe/riser systems
- **Scenario II:** SS in the plain riser system but OSC flow in the pipeline/wavy-pipe/riser system
- **Scenario III:** OSC flow in both of the plain riser and pipeline/wavy-pipe/riser systems

As stated in Section 3.4.1 there are four stages in one SS cycle, i.e. liquid buildup stage, slug production stage, bubble penetration stage and gas-blowdown/liquid-fallback stage, but only two stages, i.e. liquid buildup and gas blowdown stages, for OSC. The flow behaviour in the pipeline/wavy-pipe/riser system is described for different stages individually. Figure 3-16 (a) and (b) shows the schematics of the plain riser system and pipeline/wavy-pipe/riser system, respectively.



(a) Plain riser system (pipeline/riser system)



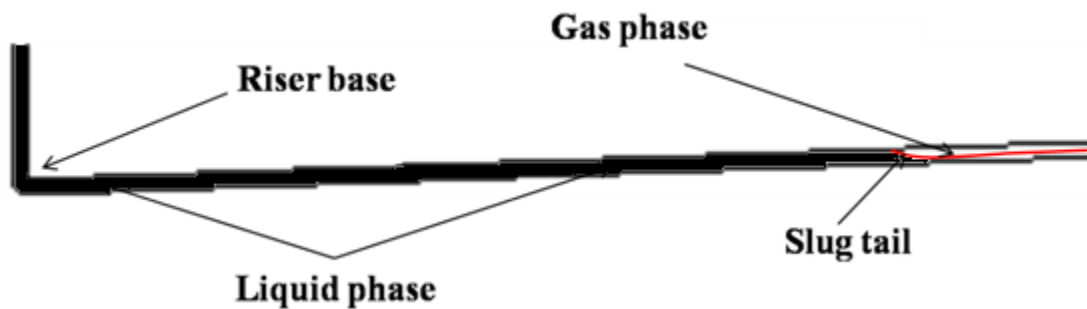
(b) Pipeline/wavy-pipe/riser system

Figure 3-16 Schematics of the plain riser and pipeline/wavy-pipe/riser systems

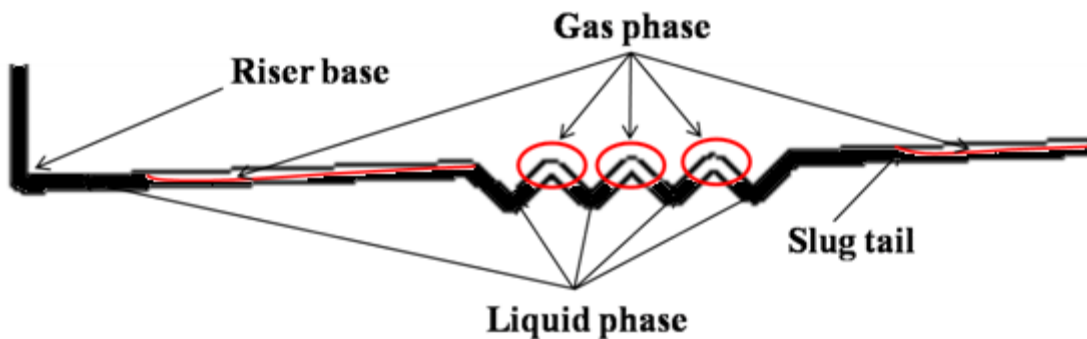
Scenario I:

The SS flow regime in the plain riser system has not been changed into OSC with a wavy pipe applied at a range of lower superficial gas and liquid velocities as presented in Section 3.5.1. However, the length of the severe slug has been reduced. Thus the severity of the SS flow regime has been mitigated by applying the wavy pipe. In ***Scenario I*** a typical SS case with a long severe slug is discussed. The slug tail can arrive at the upstream of the wavy pipe at the end of the liquid buildup stage.

At the liquid buildup stage of SS the liquid slug grows in both of the riser and pipeline starting from the riser base. In the plain riser system the gas is trapped and compressed behind the slug tail in the pipeline and there is no gas entrainment in the severe slug body in the pipeline. However, in the pipeline/wavy-pipe/riser system there are a series of locations where the gas is trapped in the slug body in the pipeline. A certain amount of gas is usually trapped in the wavy pipe and the pipe section between the riser base and wavy pipe outlet. It has been observed in the experiment that the gas is usually trapped in the humps of the Λ sections separated by the liquid packets in the dips of the V sections in the wavy pipe. As a result, the severe slug in the pipeline is separated into several portions by the trapped gas in the wavy pipe and the pipe section between the riser base and wavy pipe outlet. Figure 3-17 shows the phase distribution upstream of the riser base in the plain riser and pipeline/wavy-pipe/riser systems.



(a) Plain riser system



(b) Pipeline/wavy-pipe/riser system

Figure 3-17 Schematic of the phase distribution upstream of the riser base in the plain riser and pipeline/wavy-pipe/riser systems

At the slug production stage the slug tail in the pipeline moves towards the riser base. In the plain riser system all the gas coming from the pipeline inlet is trapped behind the slug tail (Figure 3-17 (a)) and moves with the whole slug body slowly. However, in the pipeline/wavy-pipe/riser system the trapped gas is distributed at three locations mentioned above, i.e. the pipe section between the riser base and wavy pipe outlet, the humps of the wavy pipe and the pipeline upstream of the wavy pipe (Figure 3-17 (b)). While the slug body is moving upwards along the riser, the trapped gas in the pipe section between the riser base and the wavy pipe outlet arrives at the riser base first, then that in the wavy pipe and finally that in the pipeline upstream of the wavy pipe. The gas pressure at the riser base then increases due to the accumulation of the trapped

gas. Once the pressure of the gas is high enough several gas bubbles penetrate into the liquid column in the riser. The hydrostatic pressure induced by the liquid column in the riser decreases due to the bubble penetration into it. The reduction of the pressure at the riser base allows for the upstream gas trapped in the wavy pipe and behind the slug tail to move to the riser base more quickly. As more and more gas accumulates at the riser base the bubble penetration stage is initiated and the slug production stage ends.

It needs to be noted that the bubble penetration stage in the pipeline/wavy-pipe/riser system starts earlier than that in the plain riser system. In the plain riser system the bubble penetration stage is initiated by the gas behind the slug tail, while in the pipeline/wavy-pipe/riser system it is initiated by the trapped gas in the pipe section between the riser base and wavy pipe outlet and in the wavy pipe in the pipeline/wavy-pipe/riser system. Because it takes less time for the gas in the pipe section between the riser base and wavy pipe outlet to move into the riser, the slug production stage ends before the arrival of the slug tail at the riser base in the pipeline/wavy-pipe/riser system. Consequently, part of ‘slug body’ located between the riser base and slug tail (Figure 3-17 (b)) is cut out from the main severe slug body in the pipeline/wavy-pipe/riser system.

To summarise, the slug body in the pipeline is split into several portions by the trapped gas at the liquid buildup stage with a wavy pipe applied; the trapped gas in the slug body in the pipeline initiates the bubble penetration stage earlier than that in the plain riser system. As a result, a smaller slug production stage time, T_{PRO} , and shorter liquid slug have been obtained in the pipeline/wavy-pipe/riser system than those in the plain riser system.

Scenario II:

The SS in the plain riser system has been changed into OSC with the application of the wavy pipe at a certain range of superficial gas and liquid velocities in the flow regime map. This scenario takes place when the severe slug in the pipeline is short enough and the slug tail is located between the riser base and the wavy pipe inlet as shown in Figure 3-18.

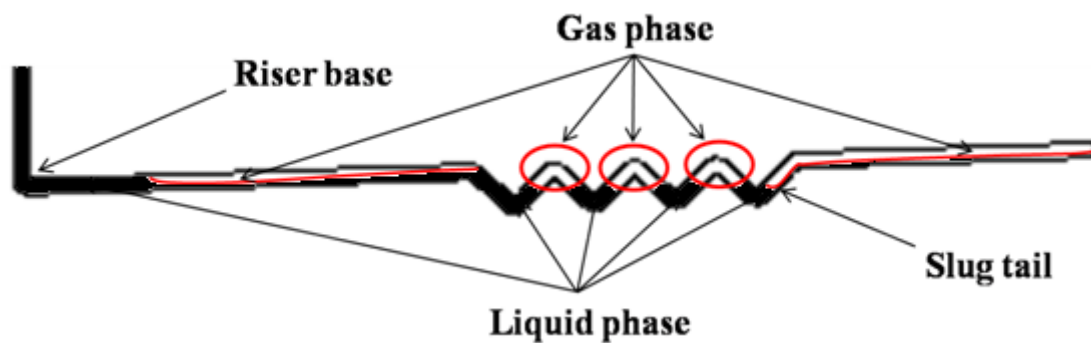


Figure 3-18 Schematic of the phase distribution upstream of the riser base in the pipeline/wavy-pipe/riser system

Similar to the SS in the pipeline/wavy-pipe/riser system described in *Scenario I*, there is also some gas trapped in the pipe section between the riser base and wavy pipe outlet and in the humps of the Λ sections at the liquid buildup stage in *Scenario II*. The difference is that the slug tail is located downstream of the wavy pipe inlet as shown in Figure 3-18. Because there is no continuous distribution of the liquid phase in the wavy pipe, the actual slug tail can be regarded to be located between the riser base and wavy pipe outlet rather than the location indicated in Figure 3-18. Hence the slug length in the pipeline/wavy-pipe/riser system has been reduced compared with that in the plain riser system at the same operating conditions. A shorter liquid slug in the pipeline allows the upstream gas to be more close to the riser base. As a result, the compressed gas in the pipeline penetrates into the liquid column in the riser before the arrival of the slug front at the riser top. Therefore, there is no chance for a slug longer than the riser, i.e. severe slug, to form. Hence the SS in the plain riser system has been changed into OSC in the pipeline/wavy-pipe/riser system.

Scenario III:

The OSC flow regime prevails in the plain riser system at a range of higher superficial gas and liquid velocities. It has been found that the equivalent slug of OSC in the

pipeline/wavy-pipe/riser system is shorter than that in the plain riser system. Thus the severity of the OSC flow regime can be reduced with a wavy pipe applied.

In the plain riser system the flow regime in the downwardly inclined pipeline is always stratified flow at different stages of OSC. At the liquid buildup stage the liquid tends to accumulate at the riser base and then the liquid is pushed into the riser by the upstream gas. By this way several short slugs form at the riser base and then coexist in the riser at the liquid buildup stage. However, when there is a wavy pipe upstream of the riser base, the stratified flow no longer persists in the pipeline. The gas/liquid two phases are churned up by the Λ and V sections of the wavy pipe. As a result, the flow at the outlet of the wavy pipe becomes into highly aerated slug flow or even homogenous flow. Hence a mixture of the gas/liquid two phases instead of two separated phases in the plain riser system arrives at the riser base in the pipeline/wavy-pipe/riser system. Therefore, the possibility for the liquid slugs as long as those in the plain riser system to form at the riser base is reduced significantly. Consequently the maximum equivalent length of the slugs coexisting in the riser is reduced for the OSC flow with a wavy pipe in place.

Summary:

Three scenarios of slug length reduction have been discussed above individually to disclose the working principle of the wavy pipe. To conclude, the wavy pipe works by reducing the length of the severe slug and equivalent slug for SS and OSC, respectively. In ***Scenario I*** the bubble penetration stage is initiated before the arrival of the slug tail at the riser base, thus the remaining portion of the slug body in the pipeline is removed from the main body of the severe slug; in ***Scenario II*** the slug tail is shifted to the pipe section between the riser base and wavy pipe outlet from a location in the wavy pipe, thus the slug length in the pipeline is reduced; in ***Scenario III*** the gas/liquid two phases are churned up by the wavy pipe and the flow regime upstream of the riser base is changed into highly aerated slug flow or even homogenous flow from the stratified flow without a wavy pipe, thus even shorter slugs than those without a wavy pipe tend to form at the riser base.

In the SS flow regime the wavy pipe acts as an ‘accelerator’ which can accelerate the movement of the gas in the pipeline to the riser, as a result, both of the slug production time and the length of the severe slug can be reduced. The SS is changed into OSC when the slug production time is zero and the severe slug is shorter than the riser. In the OSC flow regime the wavy pipe acts as a ‘mixer’ which mixes the gas/liquid two phases and turns the stratified flow into highly aerated slug flow or even homogenous flow moving towards the riser base in the pipeline. Thus even shorter slugs tend to form at the riser base and in the riser.

3.6.2 Effects of the Location of Wavy Pipe

It has been demonstrated in Section 3.5 that a smaller SS region and shorter T_{PRO} than those in the plain riser system can be obtained with a wavy pipe applied. The wavy pipe is more effective on reducing the slug length when there is a pipe section between the riser base and wavy pipe outlet.

As discovered in *Scenario I* and *II* in Section 3.6.1, a certain amount of gas is trapped in the slug body in the pipeline at the liquid buildup stage. When the outlet of the wavy pipe is located at the riser base the gas is only trapped in the humps of the wavy pipe; when there is a pipe section between the riser base and wavy pipe outlet, some gas is also trapped in that pipe section. Hence more gas can be trapped in the slug body in the pipeline when the wavy pipe outlet is located at a distance away from the riser base than at the riser base. To initiate the bubble penetration stage it is required that there is enough amount of gas at the riser base and the pressure of the gas is high enough. Therefore, with more trapped gas in the pipe section between the riser base and wavy pipe outlet, it takes less time for the required gas to be collected and compressed at the riser base to initiate the bubble penetration stage. As a result, the slug production time, T_{PRO} , can be reduced further compared with that with the outlet of the wavy pipe located at the riser base. When the T_{PRO} is reduced to zero, the flow regime SS has been transformed into TSS or even OSC. However, it needs to be noted that the pipe section between the riser base and wavy pipe outlet cannot be too long to ensure that the slug tail is located in the wavy pipe or upstream of the wavy pipe. The appropriate length of the pipe section has been investigated through CFD models presented in Chapter 4.

3.6.3 Effects of the Length of Wavy Pipe

Two wavy pipes of different lengths, i.e. 7 and 11 bends, have been tested on the 2” pipeline/riser system. The experimental data presented in Section 3.5 have shown that lower M_{MAX} and M_{AMP} for the OSC flow, indicating a shorter equivalent slug length in the riser, are obtained with a longer wavy pipe applied.

The wavy pipe acts as a ‘mixture’ in the OSC flow regime as concluded in Section 3.6.1. A longer wavy pipe with more Λ and V sections is able to agitate the gas/liquid two phases more effectively. The mixture of the gas/liquid two phases tend to be more ‘homogeneous’ and the slugs forming at the riser base are even shorter. Hence the equivalent slug length in the riser is reduced further for OSC with a longer wavy pipe of more bends. As a result, the M_{MAX} and M_{AMP} are lower in the pipeline/11-bend-wavy-pipe/riser system than those in the pipeline/7-bend-wavy-pipe/riser system.

3.7 Summary

Wavy pipes have been employed for mitigating severe slugging in pipeline/riser systems. A series of experiments were conducted on a group of test configurations: 2” and 4” plain riser systems without wavy pipes, pipeline/wavy-pipe/riser systems with the wavy pipe at different locations in the pipeline, pipeline/wavy-pipe/riser systems with the wavy pipe of different lengths (different number of bends). The performance of the wavy pipe on severe slugging mitigation has been presented in terms of the flow regime transition and characteristic parameters of the flow behaviour. The working principle and the effects of the geometrical parameters and location in the pipeline of the wavy pipe have been disclosed.

To characterise the flow behaviour in the pipeline/riser systems four flow regimes and two groups of characteristic parameters were defined based on the analysis of the riser DP. The four flow regimes are severe slugging (SS), transitional severe slugging (TSS), oscillation flow (OSC) and continuous flow (CON). The four flow regimes, i.e. SS, TSS, OSC and CON, appear in sequence with the increasing gas flowrate at a fixed liquid flowrate. The TSS is characterised by the absence of the slug production stage compared with SS. In the flow regime map with superficial gas and liquid velocities as

the coordinates a flow regime transition boundary is placed where the TSS is expected to occur. The characteristic parameters include magnitude parameters (M_{MAX} , M_{MIN} , M_{AMP} , M_{AVE}) and time parameters (T_{BUL} , T_{PRO} , T_{BFB} , T_{CYC}). The M_{MAX} , M_{MIN} , M_{AMP} and M_{AVE} refer to the maximum, minimum, fluctuation amplitude and time average of the riser DP, respectively; while the T_{BUL} , T_{PRO} , T_{BFB} and T_{CYC} are the time period of the liquid buildup stage, slug production stage, bubble-penetration/gas-blowdown/liquid-fallback stages and total cycle time, respectively. The performance of the wavy pipe on severe slugging mitigation can be assessed in terms of the flow regime transition boundary and characteristic parameters.

The flow regime transition boundary between SS and OSC can be shifted towards the SS region when a wavy pipe is installed in the pipeline upstream of the riser; consequently the region in the flow regime map for SS to occur is reduced. The location of the wavy pipe relative to the riser base has significant effects on its performance. The wavy pipe is more effective when there is a pipe section of an appropriate length between its outlet and the riser base. A smaller SS region can be obtained with a longer wavy pipe (of more bends). In the regions where the flow regimes, SS and OSC, have not been changed by employing a wavy pipe, the severity of the flow can be reduced instead. The average riser DP (M_{AVE}) is consistently lower in the pipeline/wavy-pipe/riser systems than that in the plain riser system without a wavy pipe. For the SS cases the reduction of M_{AVE} is attributed to the reduction of the slug production time (T_{PRO}), while for the OSC cases it is due to the reduction of the maximum riser DP (M_{MAX}). The fluctuation amplitude of the riser DP (M_{AMP}) is reduced due to the reduction of M_{MAX} for OSC.

The effects of the wavy pipe discussed above can be regarded as reducing the slug length in the pipeline/riser system. When the SS flow regime is transformed into the OSC flow with a wavy pipe applied, the long severe slug (longer than the riser) is split into more than one short slugs (shorter than the riser). When there is no flow regime change with a wavy pipe employed: (1) the lower M_{MAX} and M_{AMP} of OSC indicate shorter maximum equivalent slugs and shorter slugs produced out of the riser at the gas blowdown stage, respectively; (2) a smaller T_{PRO} means a shorter slug produced out of the riser at the slug production stage and a smaller T_{CYC} indicates a higher slug

frequency thus shorter slugs (because the inlet gas/liquid flowrates are the same for different test configurations).

The wavy pipe essentially reduces the severe slug length of SS by acting as an ‘accelerator’ and the equivalent slug length of OSC by acting as a ‘mixer’. In the SS flow regime the wavy pipe can accelerate the movement of the gas in the pipeline to the riser, as a result, the production time thus length of the severe slug can be reduced. The SS is transformed into OSC when the slug production time is zero and the original severe slug becomes shorter than the riser. In the OSC flow regime the wavy pipe mixes the gas/liquid two phases and turns the original stratified flow into highly aerated slug flow or even homogenous flow moving towards the riser base in the pipeline. Thus even shorter slugs tend to form at the riser base and in the riser.

4 CFD MODELLING OF SEVERE SLUGGING IN PIPELINE/WAVY-PIPE/RISER SYSTEMS

4.1 Introduction

As reviewed in Chapter 2 a series of mechanistic models has been proposed for predicting the occurrence of severe slugging, the characteristics of severe slugging and the characteristics of the flow with a severe slugging mitigation method applied. Various assumptions and simplifications have been made to simplify the problem and ensure the existence of the solution in the mechanistic models. The main simplifications include: simplified geometry with a straight pipeline followed by a straight (vertical) riser; estimated liquid holdup in the pipeline and void fraction in the riser with empirical correlations; neglected pressure loss along the pipeline and riser. Consequently, the models are not applicable to a system of complex geometry such as a pipeline with a number of undulate sections and catenary or S-shape riser, where the liquid holdup in the pipeline and void fraction in the riser cannot be estimated accurately by the correlations and the pressure loss cannot be neglected. Furthermore, the mechanistic models cannot provide information of the phase distribution in the system.

Computational Fluid Dynamics (CFD) modelling plays an important role in the study of multiphase flow. The details of the flow field in two-dimensional (2-D) and three-dimensional (3-D) spaces can be presented by CFD models. A 3-D CFD model of a pipeline/riser system involves unacceptable amount of numerical computation due to the large scale of the system. It is demonstrated in this chapter that a 2-D model is able to predict the flow behaviour in a pipeline/riser system with reasonable accuracy.

The gas/liquid two-phase flow in the pipeline/riser and pipeline/wavy-pipe/riser systems has been simulated by 2-D CFD models developed in Fluent (Release 6.3.26). Firstly, the CFD model of the pipeline/riser system was developed and the model predictions were compared with the experimental data. Secondly, the CFD model was employed to assess the performance of two classical severe slugging mitigation techniques. Thirdly, the CFD model was extended to include the wavy pipe and used to examine the effects

of the geometrical parameters and location of the wavy pipe in the pipeline on its performance of severe slugging mitigation.

4.2 CFD Model Development of the Pipeline/Riser System

4.2.1 Model Geometry

The geometries and meshes of the CFD models were created in Gambit. The 4” pipeline/catenary-riser system in the Three-Phase Test Facility presented in Chapter 3 was modelled. Two kinds of simplifications to the real pipeline/riser system were made in the CFD models. Firstly 2-D rather than 3-D models were created to reduce the computation efforts; secondly a majority of the long pipeline was simplified into a buffer vessel of the same volume with the represented pipeline. The meshing of the buffer vessel is more flexible than the long pipeline with a smaller cross-section. Because the resultant mesh of the buffer vessel is independent of the cell count of the cross-section of the pipeline. It becomes possible that a coarser mesh of lower aspect ratio is created in the buffer vessel.

The boundary conditions downstream of the pipeline/riser system have significant effects on the flow behaviour in the riser as demonstrated by Yeung *et al.* (2006). There are two separators, i.e. topside two-phase separator and three-phase separator on the ground, downstream of the pipeline/riser in the Three-Phase Test Facility. It is required to determine how to model the facilities downstream of the pipeline/riser. Two geometries as shown in Figure 4-1 were tested. Geometry I has no separator, while Geometry II has a two-phase separator of the same size with the topside separator in the experiment.

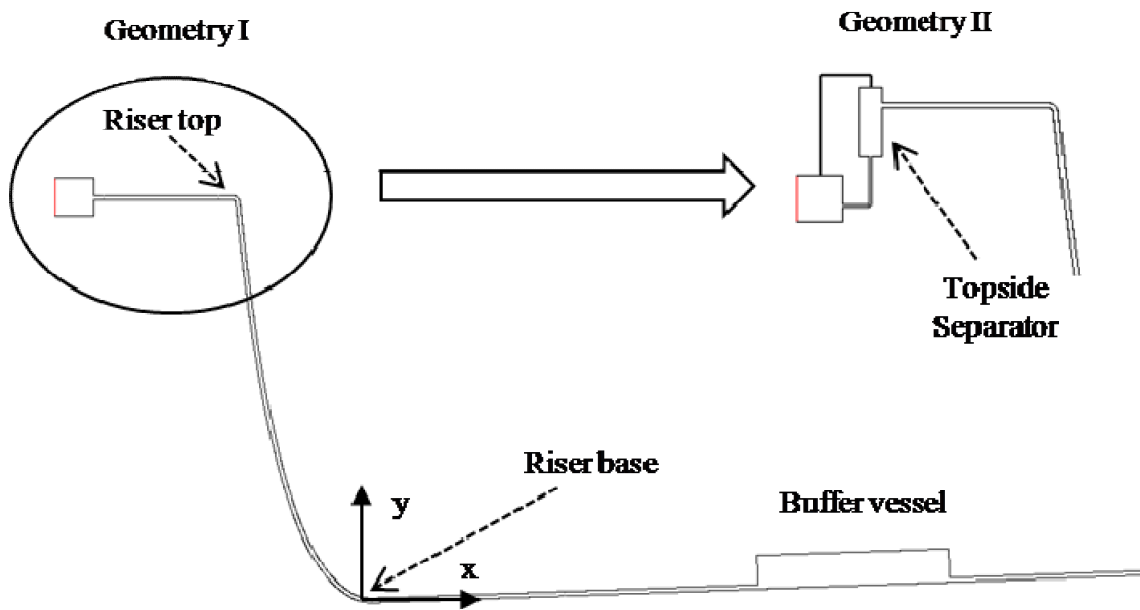


Figure 4-1 Geometry I and II

The uniform mesh containing quadrilateral control volumes was employed to discretise the computation domain. To check the mesh dependency of the model solutions the computation domain was meshed with coarse and fine meshes. The cell counts of the coarse and fine meshes are listed in Table 4-1.

Table 4-1 Cell counts of the coarse and fine meshes

	Cell count (coarse)	Cell count (fine)
Geometry I	10, 826	40, 906
Geometry II	15, 813	48, 205

4.2.2 Boundary Conditions

In the experiment the air and water mass flowrates at the pipeline inlet and the pressure in the three-phase separator were controlled by a series of PID (Proportional, Integral

and Derivative) controllers. The set values of the controllers for the inlet flowrates and pressure in the separator were constant; however, fluctuations of the actual flowrates and pressure could not be avoided due to the pressure variations in the pipeline and imperfect control. In this work constant mass flowrates and pressure were specified as the inlet and outlet boundary conditions of the CFD models, respectively, for simplicity.

The difference of the fluid temperature at the pipeline inlet and in the topside separator was at most 1 °C in each test run of the experiment. Therefore, the effects of the temperature change were neglected in the CFD models. The fluid temperatures at the inlet and outlet were set to be the same.

4.2.3 Turbulence and Multiphase Models

The standard k - ϵ model has been frequently used in practical engineering flow applications due to its robustness, economy and reasonable accuracy for a wide range of turbulent flows (ANSYS, 2006). As discussed in Chapter 3 the two-phase flow behaves in four different ways (four kinds of flow regimes, i.e. SS, TSS, OSC and CON) under different operation conditions in the pipeline/riser system. Even at the same conditions the flow behaviour in the riser is totally different from that in the pipeline. Considering the wide scope of the flow characteristics in the pipeline/riser system to be modelled the standard k - ϵ model was selected to model the turbulence.

The gas phase (air) was assumed as compressible ideal gas. The compressibility of the gas phase has to be taken into account because the compression and expansion of the gas phase are the key processes in the SS, TSS and OSC flow regimes. The liquid phase (water) is incompressible and has constant physical properties. The VOF (Volume of Fluid) model was selected to model the air/water two-phase flow and track the volume fraction of each phase. The geometrical reconstruction scheme was adopted to represent the interface between the air and water applying a piecewise-linear approach.

4.2.4 Solution Method

The flow regimes such as SS, TSS and OSC in the pipeline/riser system are cyclic processes, thus the unsteady solver was employed to simulate the transient flow behaviour. Several cycles of the flow processes had to be simulated to obtain a

statistically steady-state cycle of the flow behaviour. Hence the computation amount for the SS flow regime with a long cycle time was very large.

The variable time stepping method was adopted to reduce the computation time of CPU. The time step was adjusted automatically based on the Courant number. The Courant number is a dimensionless number that compares the time step (Δt) in a calculation to the characteristic time ($\Delta t_{\text{Transit}}$) of transit for a fluid element across a control volume (ANSYS, 2006).

$$\Delta t_{\text{Transit}} = \text{Min} \left(\frac{\text{volume}}{\sum \text{outgoing fluxes}} \right) \quad (4-1)$$

The volume of each cell is divided by the sum of the outgoing fluxes. The smallest of the resulting time represents the time it would take for the fluid to empty out of the cell. The global time step Δt_{Global} is calculated as follows:

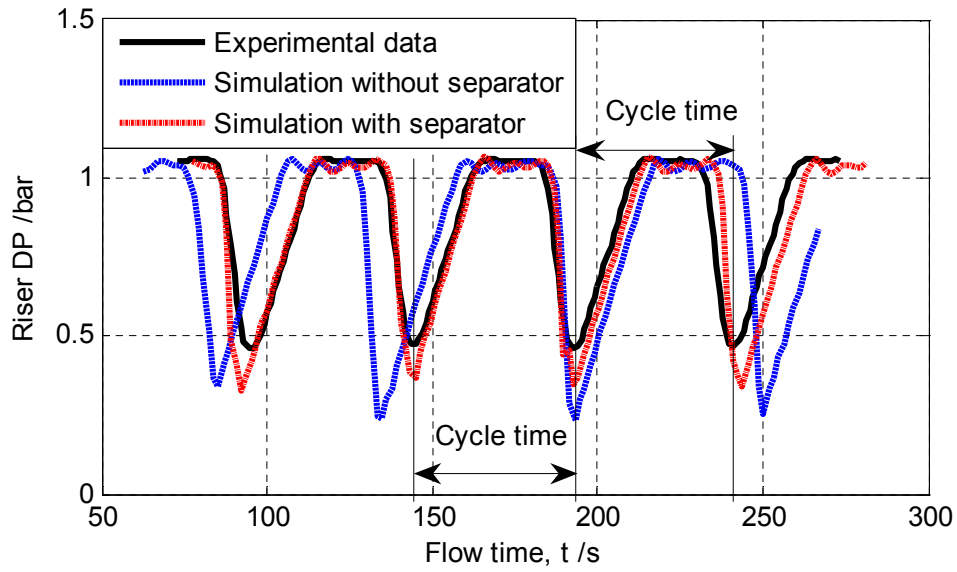
$$\Delta t_{\text{Global}} = CFL_{\text{Global}} \times \Delta t_{\text{Transit}} \quad (4-2)$$

where CFL_{global} is the global Courant number. The global Courant number applied in this work was 5~10 for different flow conditions. The resulting time step varied from 0.001 s to 0.01 s.

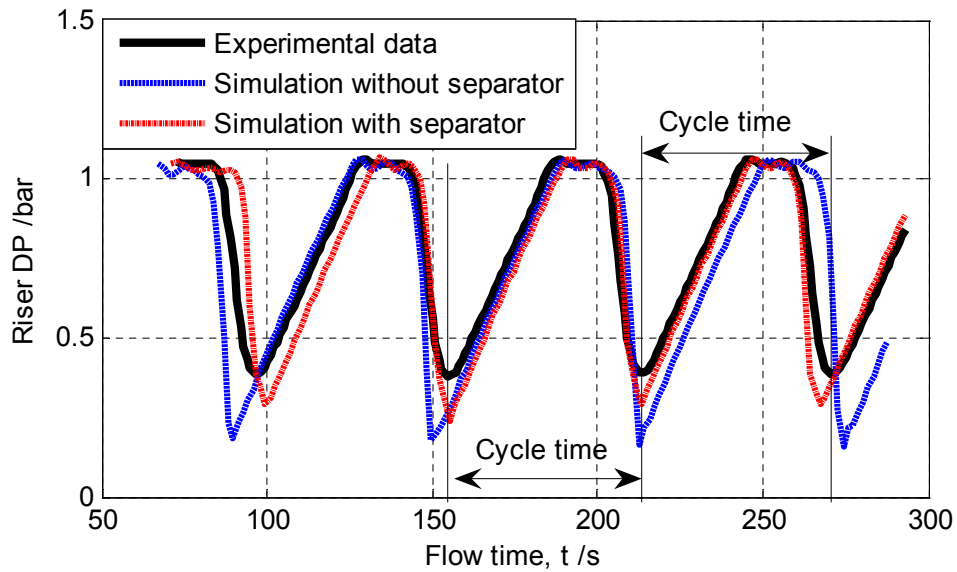
4.2.5 Model Selection

Two typical severe slugging cases were simulated to examine the performance of the two geometries and mesh dependency of the solution. The model with an appropriate geometry and mesh density was selected based on the comparison between the model predictions and experimental data.

The outlet pressure of the CFD models was set to 1 barg. The inlet superficial air velocity (U_{SG0}) was 0.86 m/s, while the superficial water velocities (U_{SL}) were 0.62 m/s and 0.37 m/s for Case 1 and Case 2, respectively. Figure 4-2 (a) and (b) illustrate the comparison of the riser DP between the model predictions and experimental data for Case 1 and Case 2, respectively. The maximum/minimum riser DP and cycle time are summarised in Table 4-2.



(a) Case 1: $U_{SG0} = 0.86$ m/s $U_{SL} = 0.62$ m/s



(b) Case 2: $U_{SG0} = 0.86$ m/s $U_{SL} = 0.37$ m/s

Figure 4-2 Riser DP predicted by Model I and II and experimental data for Case 1 and Case 2

Table 4-2 Maximum/minimum riser DP and cycle time of SS predicted by Model I and II and experimental data for Case 1 and Case 2

	Case 1			Case 2		
	Max (bar)	Min (bar)	Cycle time (s)	Max (bar)	Min (bar)	Cycle time (s)
Experiment	1.05	0.46	48.5	1.05	0.38	58.0
Model I	1.04	0.23	57.8	1.04	0.16	62.2
Model II	1.04	0.35	49.5	1.04	0.29	56.5

It can be seen in Table 4-2 that the maximum riser DP predicted by the models agrees with the experimental data well. Thus the flow regime, i.e. severe slugging, has been identified correctly for both cases. Compared with experimental data the cycle time is over predicted by about 19 % (Model I) and 2 % (Model II) for Case 1; for Case 2 Model I over predicts it by 7 % and Model II under predicts it by 2.5 %. Hence Model II gives more accurate predictions of the cycle time for both cases.

However, the deviation of the minimum riser DP predicted by the two models from the experimental data are significant. Model I under predicts the minimum riser DP by 50 % and 58 % for Case 1 and Case 2, respectively; while Model II under predicts it by 24 % for both cases. It can be seen that the minimum riser DP predicted by Model II with a topside separator is higher than that by Model I and is closer to the experimental data. Thus Model II provides better predictions of the minimum riser DP than Model I.

At the gas blowdown stage of severe slugging the compressed gas behind the severe slug expands and pushes the slug tail along the riser violently. A pressure surge at the riser top is then induced due to the impact of the slug tail and accumulation of the gas. In Model I the liquid and gas can flow out of the system quickly, however, they are trapped in the topside separator serving as a buffer vessel for a period of time in Model II. Therefore, the pressure surge at the riser top maintains at a high level for a longer time in Model II than that in Model I. The high pressure at the riser top resists the

movement of the slug tail and the expansion of the gas in the riser. Consequently less liquid is pushed out by the gas and more liquid is left in the riser then falls back to the riser base in Model II. As a result, a higher minimum riser DP is obtained in Model II than that in Model I, because the minimum riser DP is mainly induced by the remaining liquid at the end of the gas blowdown stage.

To summarise, more reasonable predictions of the riser DP can be obtained by Model II with a topside separator than Model I compared with the experimental data. Therefore, Model II was selected for the discussions below.

It needs to be mentioned that the simulation results shown in Figure 4-2 were obtained with the fine mesh as listed in Table 4-1. Figure 4-3 compares the riser DP predicted by Model II with the fine/coarse meshes and experimental data. As the same conclusion can be drawn from the two cases, only Case 1 is shown in Figure 4-3 and discussed below.

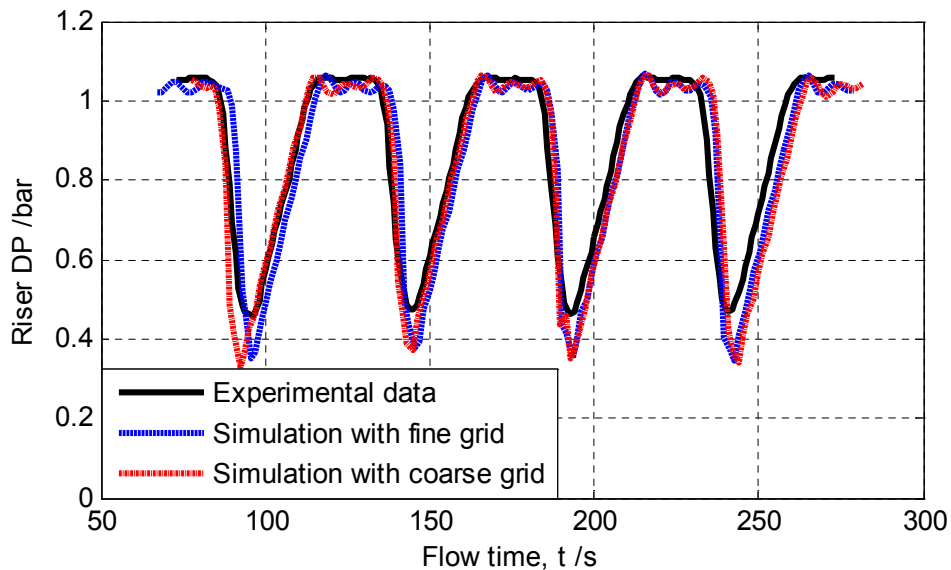


Figure 4-3 Riser DP predicted by Model II with the fine/coarse meshes (grids) for Case 1 ($U_{SG0} = 0.86$ m/s, $U_{SL} = 0.62$ m/s) and experimental data

It can be seen in Figure 4-3 that the predicted riser DP by Model II with the coarse and fine meshes agrees with each other well. This indicates that the solution does not deviate significantly even with the average cell size increased to 4 times in area. The computation time can be significantly reduced by using the coarse mesh; however, the fine mesh has been employed throughout the rest of this work. Because more reliable solutions are expected to be obtained for a wide range of flow conditions with the finer mesh and the computation time is still acceptable.

4.2.6 Hardware of Computers

All the simulations were performed on the computational "Grid" at Cranfield University. Grid compute nodes are HP DL160G5 servers, each of which has 2 Intel Xeon 5272 "Wolfdale" dual-core processors (clock speed 3.4 GHz) with 16 GB of RAM & 80 GB local SATA disk. Each simulation case is run on one compute node with 4 cores in parallel. It took about 48 hours of CPU time to simulate 300 s of flow time for the models selected above.

4.3 Simulation of the Pipeline/Riser System

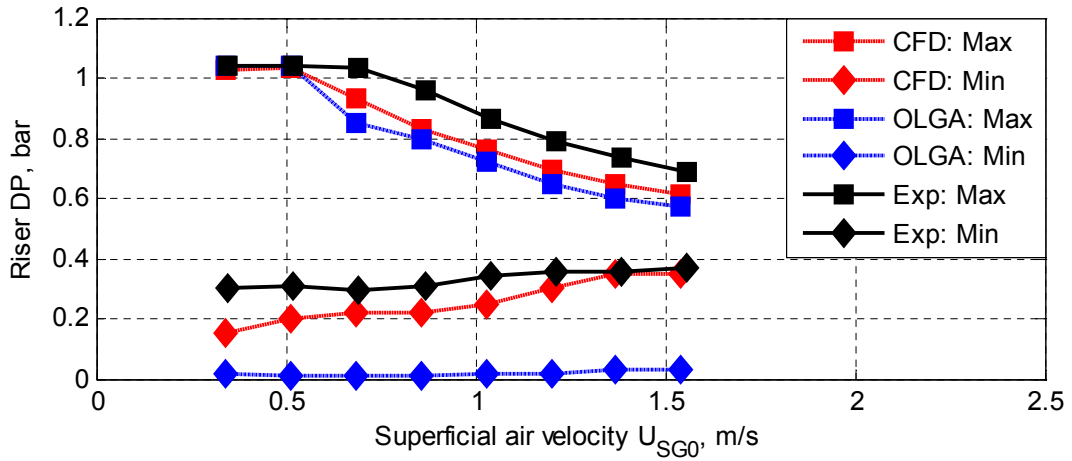
The CFD model with a topside separator downstream (Model II) and finer mesh was solved at a wide range of inlet flowrates, i.e. $Q_L = 1$ kg/s to 4 kg/s and $Q_G = 10$ Sm³/h to 70 Sm³/h ($U_{SL} = 0.1$ m/s to 0.5 m/s and $U_{SG0} = 0.3$ m/s to 2.5 m/s). The flow regime and slug frequency predicted by the CFD model have been compared with the experimental data and predictions of the OLGA model. More understanding of the slug movement in severe slugging has been obtained by inspecting the liquid holdup time traces predicted by the CFD model.

Two typical slug mitigation methods, i.e. increasing back pressure and choking riser outlet valve, have been studied experimentally in the previous work by Yeung *et al.* (2008). This section presents the simulation results of the two slug mitigation methods with the proposed CFD model.

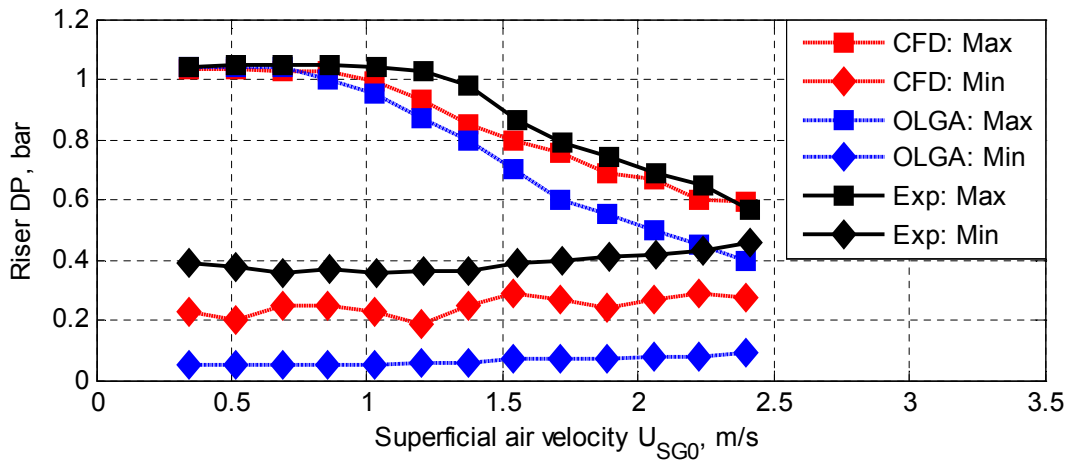
4.3.1 Flow Regime

The flow regimes in the pipeline/riser system can be identified through inspecting the time traces of the riser DP. As discussed in Section 3.4.1 severe slugging is characterised by a slug production stage, where the riser DP remains roughly constant at its maximum. The maximum riser DP is no less than 1.03 bar because the riser height is 10.5 m. As observed in the experiment the flow regime changes from severe slugging to the oscillation flow with the increase of U_{SG0} at the same U_{SL} .

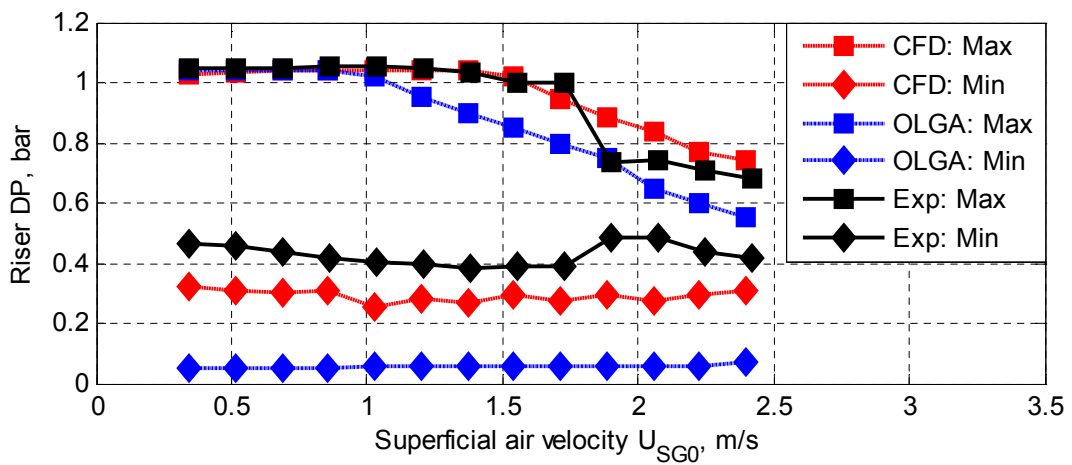
Figure 4-4 shows the variation of the maximum and minimum riser DP with the increase of the superficial air velocity at fixed superficial water velocities. The flow regime transition can be identified clearly from the significant drop of the maximum riser DP. Compared with the experimental data the critical U_{SG0} , at which the transitional severe slugging (TSS) is expected to occur, can be predicted well by the CFD model. The mismatch of the critical U_{SG0} between the CFD model prediction and experimental data is less than 0.17 m/s (5 Sm³/h for the 4" riser). At a lower superficial water velocity ($U_{SL} = 0.12$ m/s) the predicted critical U_{SG0} is lower, while at a higher superficial water velocity ($U_{SL} = 0.49$ m/s) the predicted value is higher than those obtained from the experiment. At the medium superficial water velocities ($U_{SL} = 0.25$ m/s and 0.37 m/s) the critical U_{SG0} are the same with those in the experiment. The OLGA model gives the same predictions of flow regime with the CFD model at $U_{SL} = 0.12$ m/s and $U_{SL} = 0.25$ m/s, but at $U_{SL} = 0.37$ m/s and $U_{SL} = 0.49$ m/s the transition from SS to OSC takes place at a much lower U_{SG0} .



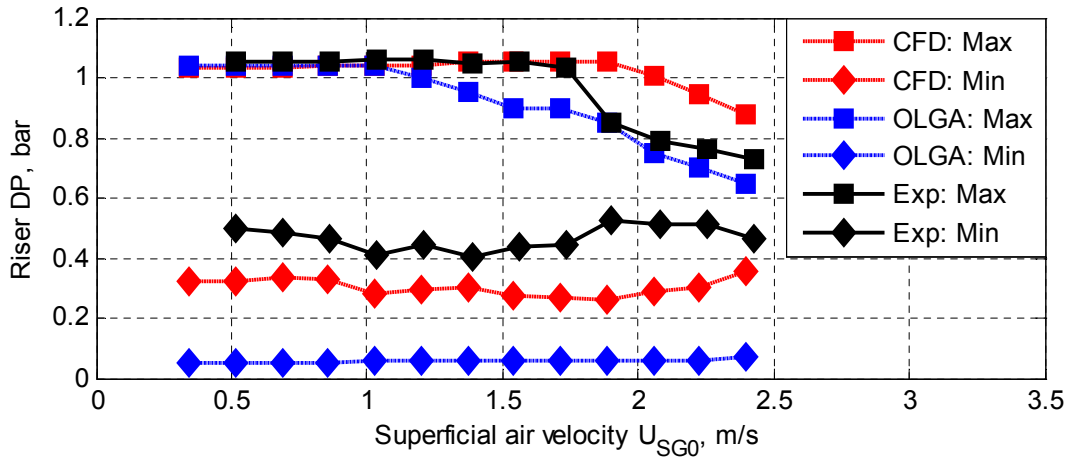
(a) $Q_L = 1 \text{ kg/s}$ $U_{SL} = 0.12 \text{ m/s}$



(b) $Q_L = 2 \text{ kg/s}$ $U_{SL} = 0.25 \text{ m/s}$



(c) $Q_L = 3 \text{ kg/s}$ $U_{SL} = 0.37 \text{ m/s}$



(d) $Q_L = 4 \text{ kg/s}$ $U_{SL} = 0.49 \text{ m/s}$

Figure 4-4 Comparison of the maximum and minimum riser DP between the model predictions and experimental data

Examining the maximum and minimum riser DP, it can be found that the discrepancies between the model predictions and experimental data vary with U_{SL} and flow regime.

(a) **Maximum of riser DP:** The maximum riser DP predicted by the CFD and OLGA models changes smoothly with the increase of U_{SG0} . The same trend can be found in the experimental data at the lower superficial water velocities ($U_{SL} = 0.12 \text{ m/s}$ and 0.25 m/s), however, at the higher superficial water velocities ($U_{SL} = 0.37 \text{ m/s}$ and 0.49 m/s) an abrupt decrease of the maximum riser DP takes place on the flow regime transition point from SS/TSS to OSC. For OSC the maximum riser DP is under and over predicted by the CFD model at the lower and higher superficial water velocities, respectively; while the OLGA model consistently under predicts the maximum riser DP compared with the experimental data.

(b) **Minimum of riser DP:** The minimum riser DP is consistently under predicted by both models for all the simulation cases. Similarly to the predicted maximum riser DP discussed above the minimum riser DP also changes smoothly with the increase of U_{SG0} . At the lowest superficial water velocity ($U_{SL} = 0.12 \text{ m/s}$) the minimum riser DP predicted by the CFD model increases with the increase of U_{SG0} , which agrees

with the experimental data well. However, at the higher superficial water velocity ($U_{SL} = 0.37$ m/s and 0.49 m/s) abrupt increases of the minimum riser DP cannot be observed on the flow regime transition points from SS/TSS to OSC. It needs to be noted that the minimum riser DP predicted by the OLGA model is very low (lower than 0.1 bar for all the cases).

The possible reasons to account for the mismatch of the model predictions (CFD and OLGA models) with the experimental data are discussed as follows:

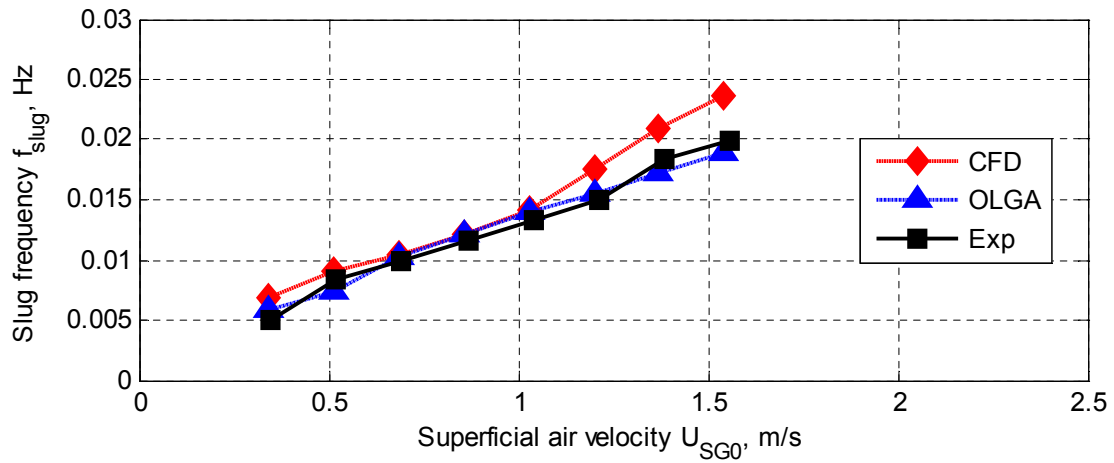
- (a) **Under/over prediction of the maximum riser DP for OSC:** The maximum riser DP for OSC mainly depends on the equivalent slug length at the liquid buildup stage. In the experiment more than one aerated slugs separated by gas packets coexist in the riser at the liquid buildup stage and many gas bubbles with different sizes and shapes are distributed in the aerated slugs. It is postulated that the volume fractions of the widely distributed gas bubbles in the aerated slugs are not modelled appropriately. Consequently the equivalent slug length is not predicted accurately.
- (b) **Under prediction of the minimum riser DP:** The minimum riser DP mainly depends on the amount of liquid left in the riser at the end of the gas blowdown stage. The under prediction of the minimum riser DP indicates that less liquid is left in the riser in the simulation. Firstly, the resistance of the system is not represented by the model adequately. The extra resistance induced by the Coriolis flow meter upstream of the riser top (as shown in Figure 3-6) has not been taken into consideration in the simulation models. The under representation of the resistance significantly reduces the resist to the fast movement of the fluids especially at the gas blowdown stage. As a result, more liquid tends to be blown out of the riser. Secondly, the phase slip between the gas/liquid two phases in the riser has not been modelled properly. At the gas blowdown stage more liquid tends to be taken out of the riser by the gas with a very high velocity. At the end of this stage the liquid velocity drops with the decrease of the pressure in the pipeline but no obvious liquid fallback can be observed in the model predictions.

4.3.2 Slug Frequency

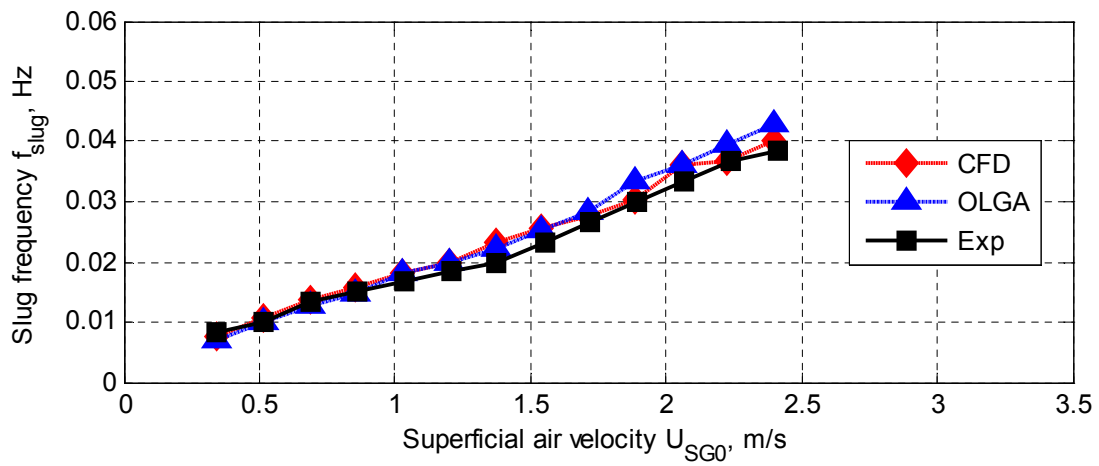
The SS, TSS and OSC are all cyclic processes. The cycle time of the riser DP can be regarded as the cycle time of these flow processes. The slug frequency, f_{slug} , is the reciprocal of the average cycle time. For SS and TSS the f_{slug} is the frequency of the severe slugs; while for OSC the f_{slug} is a description of the equivalent slug in the riser.

The slug frequency predicted by the CFD and OLGA models is compared with the experimental data in Figure 4-5. It can be observed from both of the experimental and simulation data that the slug frequency increases monotonously with the increase of U_{SG0} at the same U_{SL} . A reasonably good agreement of the slug frequency between the model predictions and experimental data has been obtained although there are slight differences in detail at the higher superficial water velocities ($U_{\text{SL}} = 0.37$ m/s and 0.49 m/s). It needs to be noted that the predictions of the CFD and OLGA models agree with each other very well.

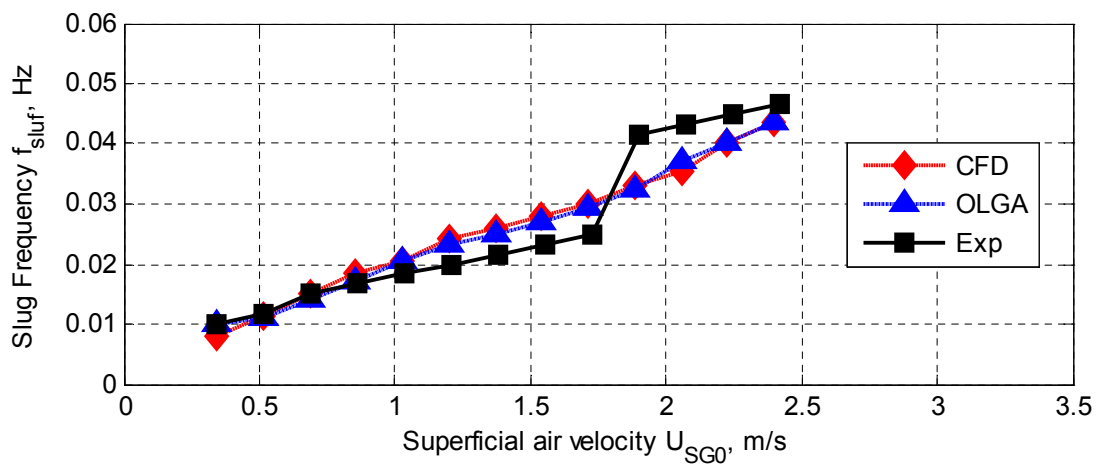
The relationship between the predicted f_{slug} and U_{SG0} are almost linear at the same U_{SL} . However, this is not always the case in the experiment. The experimental data have shown the flow regime dependency of the relationship between the f_{slug} and U_{SG0} at higher U_{SL} . As can be seen in Figure 3-5 (c) and (d) there is a ‘jump’ of the slug frequency at the critical U_{SG0} for flow regime transition with the increase of U_{SG0} . Similarly the abrupt change of the maximum/minimum riser DP can also be observed in Figure 3-4 (c) and (d).



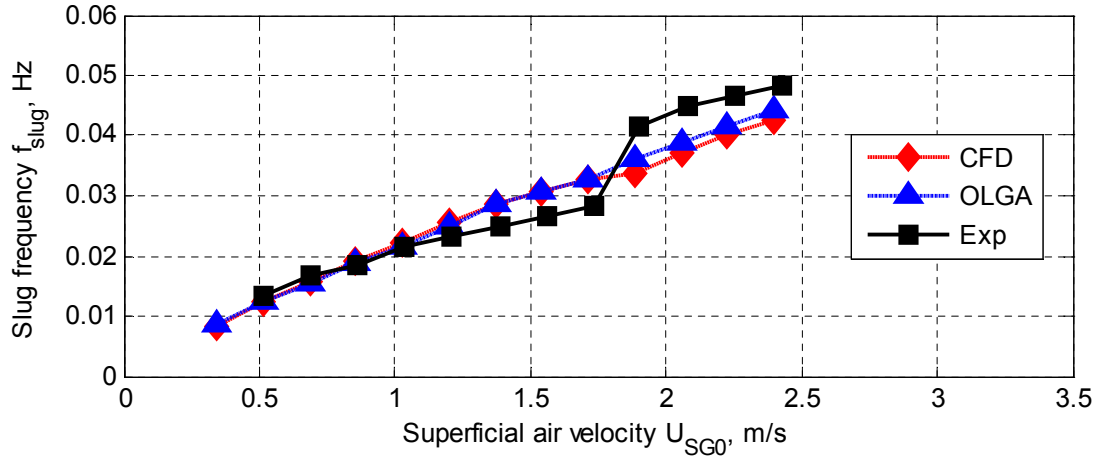
(a) $Q_L = 1 \text{ kg/s}$ $U_{SL} = 0.12 \text{ m/s}$



(b) $Q_L = 2 \text{ kg/s}$ $U_{SL} = 0.25 \text{ m/s}$



(c) $Q_L = 3 \text{ kg/s}$ $U_{SL} = 0.37 \text{ m/s}$



(d) $Q_L = 4 \text{ kg/s}$ $U_{SL} = 0.49 \text{ m/s}$

Figure 4-5 Comparison of the slug frequency between the model predictions and experimental data

Figure 4-6 shows the percentage relative error of the slug frequency predicted by the CFD model compared with the experimental data. The percentage relative error, E_R , is calculated as follows:

$$E_R = \frac{f_{slug}^P - f_{slug}^E}{f_{slug}^E} \times 100 \% \quad (4-3)$$

where f_{slug}^P and f_{slug}^E are the slug frequency predicted by the CFD model and obtained from the experiment, respectively. The relative error is within +/- 20 % for most of the simulated cases.

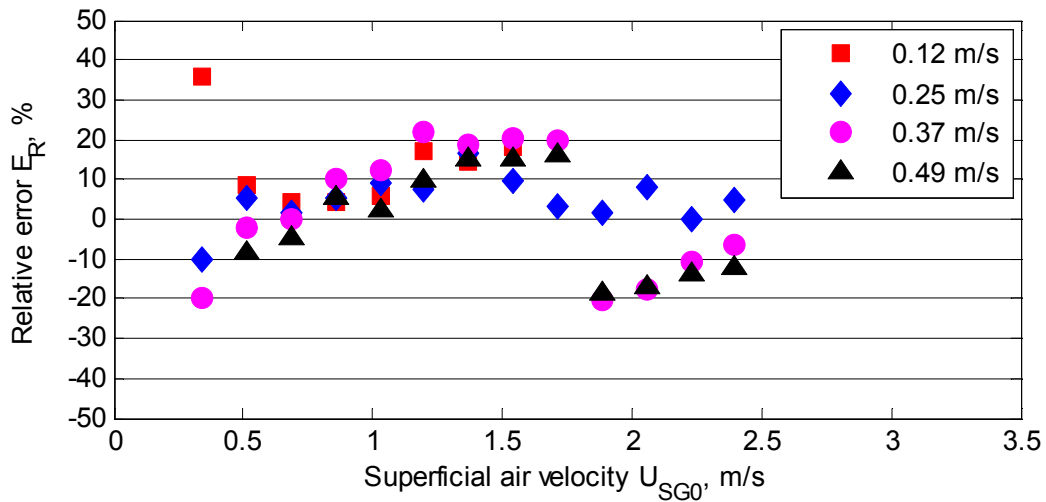
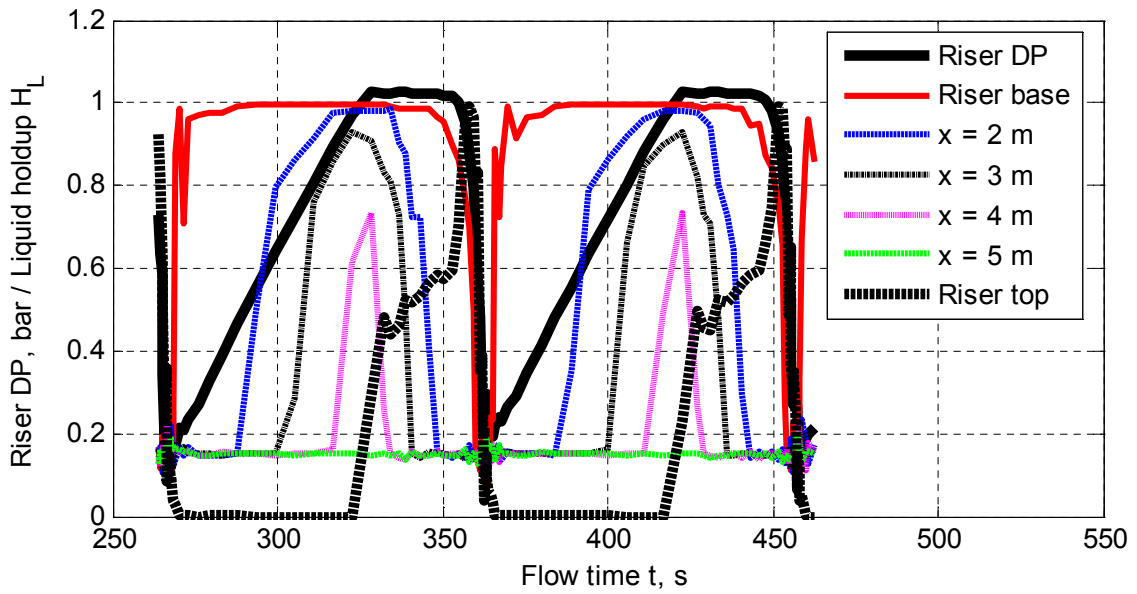


Figure 4-6 Percentage relative error of slug frequency predicted by the CFD model

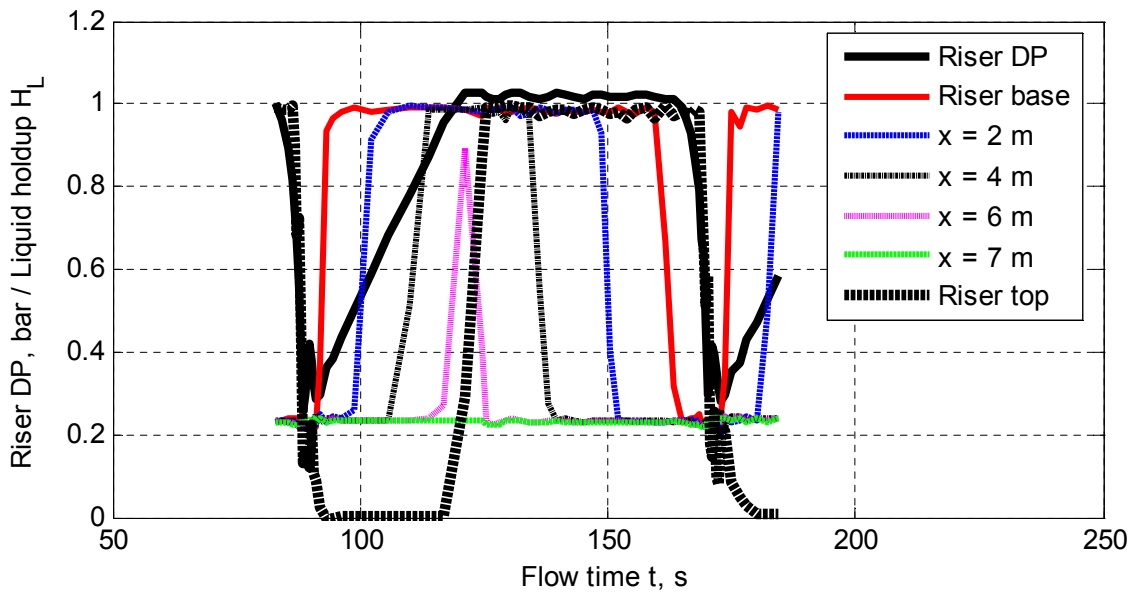
4.3.3 Slug Movement

The slug movement can be tracked by inspecting the time traces of the liquid holdup in the pipeline/riser system. The liquid holdup has been monitored at the riser top, riser base and different locations in the pipeline. The monitored locations in the pipeline are specified by the distance from the riser base, i.e. x in the discussions below.

Figure 4-7 illustrates the liquid holdup time traces at different locations for two sample severe slugging cases. The riser DP is also plotted to indicate the different stages of a severe slugging cycle. The two cases have the same superficial air velocity, $U_{SG0} = 0.51$ m/s, while the U_{SL} are 0.25 m/s and 0.49 m/s, respectively.



(a) Case 1: $U_{SL} = 0.25$ m/s $U_{SG0} = 0.51$ m/s



(b) Case 2: $U_{SL} = 0.49$ m/s $U_{SG0} = 0.51$ m/s

x : Distance between the riser base and the monitored locations in the pipeline

Figure 4-7 Time traces of the riser DP and liquid holdup at different locations in the pipeline/riser system

At the beginning of the liquid buildup stage, the riser base is blocked immediately by the liquid phase (the liquid holdup at the riser base rises to 1 quickly). Then the slug tail moves backwards to the upstream pipeline from the riser base. This can be evidenced by the sharp increase of the liquid holdup at $x = 2$ m then 3 m for Case 1, $x = 2$ m then 4 m for Case 2. The liquid holdup at the locations $x = 2$ m, 3 m for Case 1 and $x = 2$ m, 4 m for Case 2 arrives at its maximum before the liquid buildup stage ends; while at the locations $x = 4$ m for Case 1 and $x = 6$ m for Case 2 it arrives at its maximum just at the end of the liquid buildup stage. The holdup at $x = 5$ m for Case 1 and $x = 7$ m for Case 2 is around 0.15 and 0.23 respectively, and no obvious fluctuation can be found. This indicates that the slug tail is located between $x = 4$ m and 5 m for Case 1 and between $x = 6$ m and 7 m for Case 2. The severe slug in Case 2 with a higher superficial water velocity ($U_{SL} = 0.49$ m/s) is longer than that in Case 1 with $U_{SL} = 0.25$ m/s at the same superficial air velocity, $U_{SG0} = 0.51$ m/s. The liquid holdup at the riser top remains zero as the front of the severe slug has not arrived at the riser top at the liquid buildup stage.

Once the slug front arrives at the riser top the slug production stage begins. Then the liquid holdup at the riser top starts to increase and the riser DP arrives at its maximum at the same time. The decrease of the liquid holdup at the monitored locations in the pipeline indicates that the slug is moving towards the riser base at the slug production stage. At this stage the time traces of the liquid holdup at the riser top for the two cases behave in different manners. For Case 1 the liquid holdup at the riser top increases to around 0.5 quickly at the beginning then increases slowly to around 0.6 by the end of this stage; while for Case 2 the holdup increases to 1 quickly at the beginning then remains around 1 until the end of this stage. The difference is caused by the different U_{SL} in the two cases. A higher U_{SL} allows the slug to move faster and occupy the whole pipe cross-section.

The liquid holdup at the riser top rises to 1 quickly at the beginning of the gas blowdown stage then drops to 0 sharply at the end of this stage for Case 1. However, for Case 2 the liquid holdup remains around 1 until the gas blowdown stage begins then it decreases to 0 sharply. The liquid holdup in the pipeline drops back to its minimum after the gas blowdown stage.

4.3.4 Severe Slugging Mitigation Methods

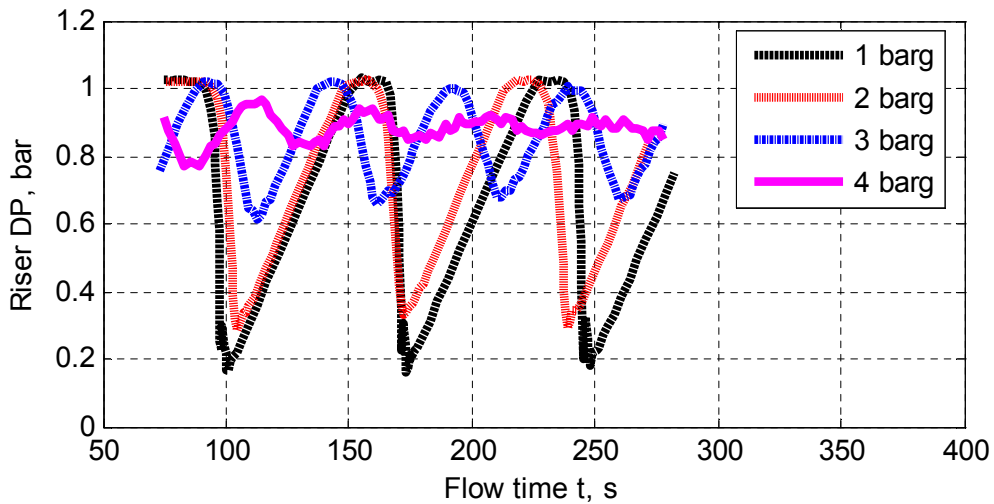
Two slug mitigation methods, i.e. increasing back pressure and choking riser outlet valve, have been applied to the CFD model discussed above. The two cases presented here are the same with those in Section 4.3.3.

When applying the method ‘increasing back pressure’, the pressure at the outlet of the model increases from 1 barg to 4 barg for Case 1 and to 5 barg for Case 2. The model predictions of the riser DP and riser base pressure are illustrated in Figure 4-8 and Figure 4-9 for Case 1 and Case 2, respectively. The main statistical parameters of concern such as the average cycle time of the flow, the fluctuation amplitude and mean of the riser base pressure are listed in Table 4-3 for comparison.

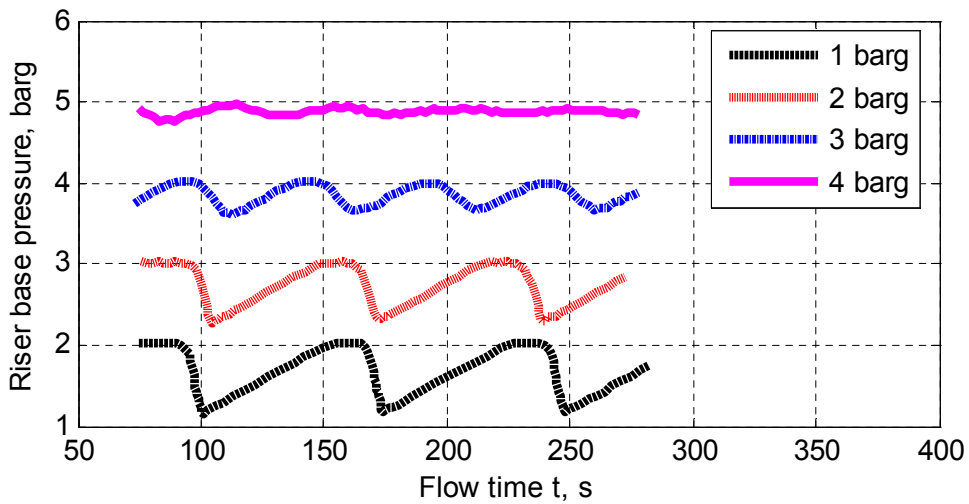
It can be seen in Figure 4-8 and Figure 4-9 that the increase of the back pressure has favorable effects on mitigating or even eliminating severe slugging in the pipeline/riser system. However, the average riser base pressure increases significantly with the increase of the back pressure. The effects of increasing back pressure on the flow behaviour in the pipeline/riser system are discussed as follows:

- (a) The transition of the flow regime from severe slugging to continuous flow can be achieved by increasing the back pressure. For Case 1 with a lower superficial water velocity ($U_{SL} = 0.25$ m/s) the back pressure has to be increased to 4 barg; while for Case 2 with a higher superficial water velocity ($U_{SL} = 0.49$ m/s), a back pressure as high as 5 barg is needed for the continuous flow to form in the pipeline/riser system.
- (b) The fluctuation amplitude and cycle time of the riser base pressure decrease with the increase of the back pressure. This indicates that the long severe slugs have been split into more slugs with shorter lengths. Thus the flow regime, severe slugging, has been transformed into the oscillation flow. Eventually the flow becomes into the continuous flow with the riser base pressure of small fluctuations.
- (c) The significant increase of the riser base pressure is one of the most undesirable effects of increasing back pressure on the system. The severe slugging prevails with the back pressure 1 barg and the average riser base pressures are 1.61 barg and 1.78 barg for Case 1 and Case 2, respectively. When the severe slugging transforms into

the continuous flow with increased back pressure, the average riser base pressures increase to as high as 4.88 barg and 5.94 barg for Case 1 and Case 2, respectively. In the field production system a higher riser base pressure results in a higher pressure on the wellhead. The production and recovery capacity of hydrocarbons from the reservoir can be reduced due to the high pressure on the wellhead.

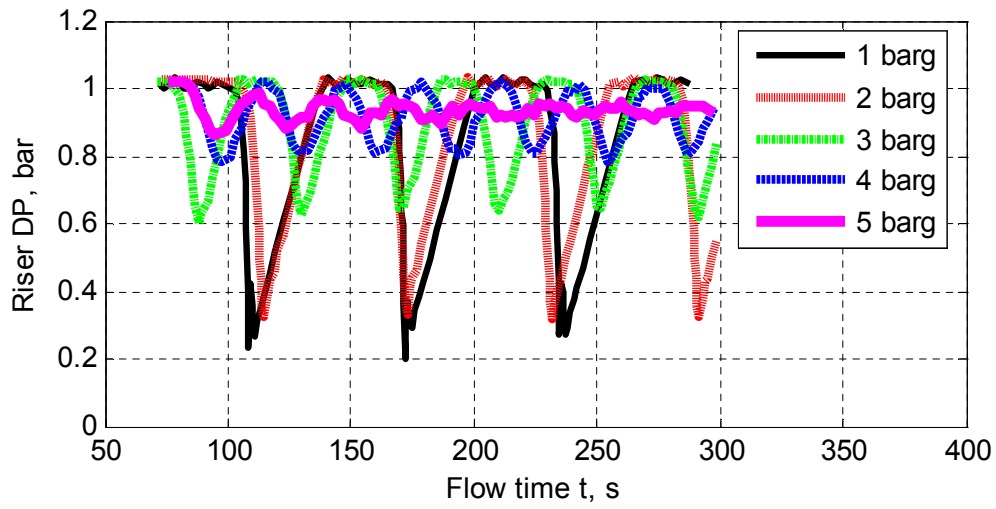


(a) Riser DP

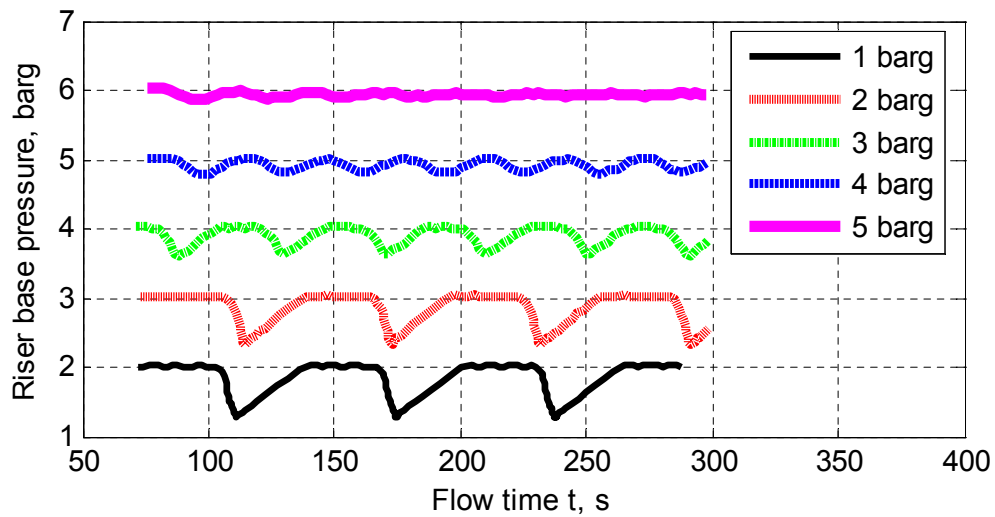


(b) Riser base pressure

Figure 4-8 Riser DP and riser base pressure for Case 1 ($U_{SL} = 0.25$ m/s, $U_{SG0} = 0.51$ m/s)



(a) Riser DP



(b) Riser base pressure

Figure 4-9 Riser DP and riser base pressure for Case 2 ($U_{SL} = 0.49$ m/s, $U_{SG0} = 0.51$ m/s)

Table 4-3 Statistical parameters of the riser base pressure

Back pressure (barg)	Case 1			Case 2		
	Cycle time (s)	Fluctuation (bar)	Mean (bar)	Cycle time (s)	Fluctuation (bar)	Mean (bar)
1	73.8	0.85	1.61	62.6	0.76	1.78
2	67.1	0.74	2.69	59.8	0.72	2.81
3	49.0	0.32	3.84	40.0	0.39	3.88
4	-----	-----	4.88	32.6	0.20	4.92
5	-----	-----	-----	-----	-----	5.94

----- : not applicable

The above observations from the CFD model predictions qualitatively agree with the experimental results presented by Yeung *et al.* (2008). It needs to be noted that the previous experiment was conducted with fixed valve openings for both of the gas and liquid lines rather than fixed inlet flowrates. The expected inlet air/water flowrates were achieved when the back pressure was 1 barg. It was observed that the water flow supplied by the centrifugal pump reduced significantly with the increase of the riser base pressure. However, the inlet air/water mass flowrates are constant without taking into account of the effects on the inlet flowrates of the pressure in the system in the above simulations. This ensured that the model predictions were comparable with each other at the same inlet flowrates.

When applying the method ‘choking’ to the CFD model, the valve simulated in the 2-D model takes the form of two rectangular restrictions attached to the pipe wall with a desired opening in between. The schematic of a ‘valve’ used in the CFD model is shown in Figure 4-10. The opening (Z) of this ‘valve’ is defined by $Z = L2 / (L1+L2+L3) \times 100 \%$.

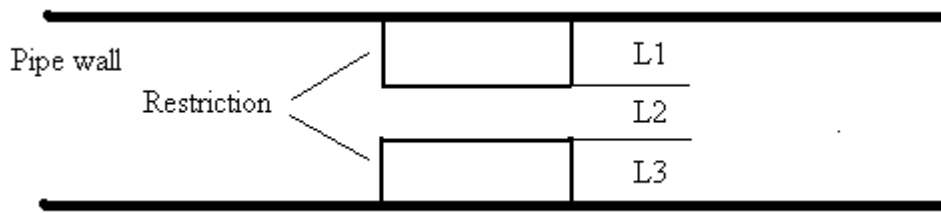
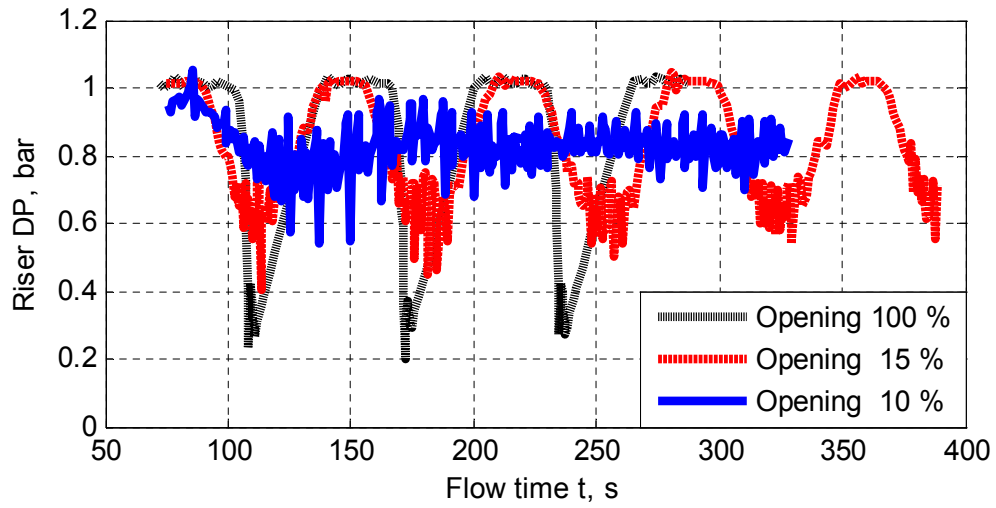


Figure 4-10 Schematic of a ‘valve’ in the 2-D CFD model

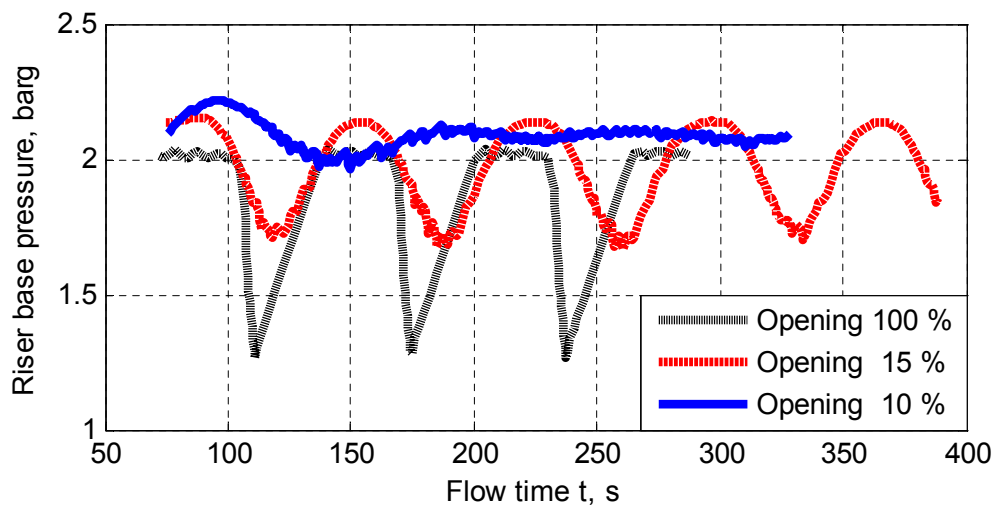
The valve is located in the horizontal pipe section between the riser top and topside separator. Case 2 has been simulated under different valve openings, i.e. 100 %, 15 % and 10 %, to demonstrate the effects of choking riser outlet valve on the flow behaviour in the pipeline/riser system. The model predictions of the riser DP, riser base pressure and pressure difference across the valve (valve DP) are shown in Figure 4-11 at different valve openings.

It can be observed in Figure 4-11 that the severe slugging prevails when the riser top valve is fully open while it can be eliminated entirely by choking the valve to 10 %. Qualitative agreement with the experimental results presented by Yeung *et al.* (2008) has been obtained.

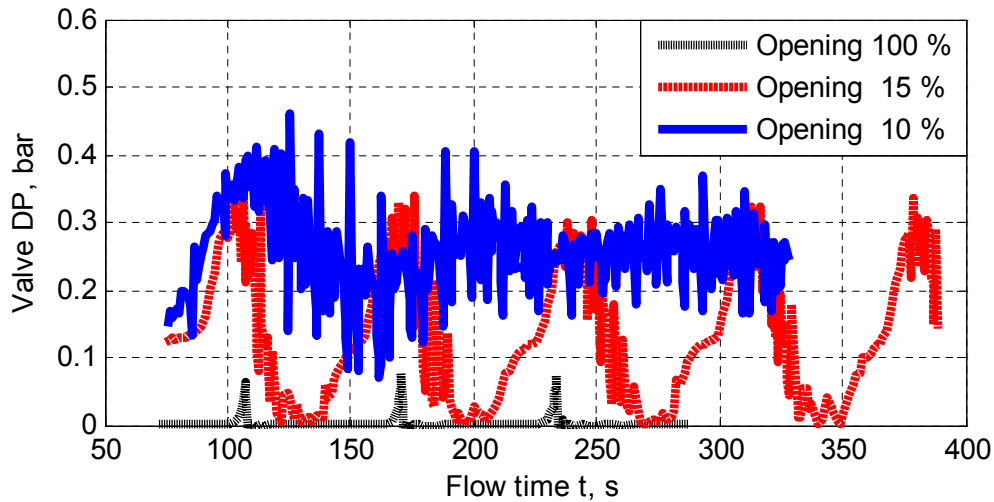
- (a) With the valve choked to 15 % the fluctuation amplitude of the riser base pressure decreases to 0.45 bar from 0.75 bar with the valve fully open (100 %, i.e. without a valve) and the cycle time increases slightly. The average riser base pressure increases from 1.78 barg to 1.94 barg and 2.09 barg at the valve openings 15 % and 10 %, respectively. The increase of the riser base pressure is mainly induced by increase of the valve DP as the back pressure is constant, i.e. 1 barg.
- (b) The riser DP time traces become much more ‘noisy’ with the riser outlet valve choked compared with that with a fully open valve. This is mainly induced by the fluctuation of the riser top pressure due to the intensive interactions between the two-phase flow and restrictions of the ‘valve’.



(a) Riser DP



(b) Riser base pressure



(c) Valve DP

Figure 4-11 Model predictions with different valve openings (Case 2: $U_{SL} = 0.49$ m/s, $U_{SG0} = 0.51$ m/s)

Experimental studies on the comparison of the two slug mitigation methods, i.e. increasing back pressure and choking riser outlet valve, have been conducted by Schmidt *et al.* (1985) and Yeung *et al.* (2008). It was concluded that, in order to eliminate severe slugging, a much smaller pressure increase in the system can be obtained by applying the choking method than increasing the back pressure. Thus choking has been claimed to be a more effective slug elimination method. The same conclusion can be drawn from the CFD modelling discussed above. To eliminate severe slugging for Case 2 the back pressure has to be increased to 5 barg and the resulting average riser base pressure is 5.94 barg. For the same case the severe slugging disappears when the riser outlet valve is choked to 10 % and the resulting average riser base pressure is only 2.09 barg.

4.3.5 Discussions

A 2-D CFD model of the pipeline/catenary-riser system in the laboratory was developed. The model predictions of the flow regime transition and slug frequency were compared with the experimental data. Furthermore, two classical severe slugging mitigation

methods, i.e. increasing the back pressure and choking the riser outlet valve, were simulated with the proposed CFD model.

The proposed CFD model is able to predict the flow regime transition and slug frequency reasonably well. It has been found that the discrepancy between model predictions and experimental data are flow conditions dependent such as water flowrate and flow regime. The minimum riser DP is under predicted by the CFD model consistently. One of the reasons is the inadequate representation of the resistance in the system, such as the Coriolis flow meter at the riser top, by the 2-D model.

Qualitative agreement with the experimental results has been obtained when applying the slug mitigation methods to the CFD model. This shows the potential of the proposed CFD model for evaluating the performance of severe slugging mitigation methods. The passive slug mitigation method based on wavy pipe has been investigated employing the proposed CFD model as discussed in Section 4.4.

4.4 Simulation of the Pipeline/Wavy-Pipe/Riser System

The wavy pipe was installed in the pipeline/riser system to mitigate severe slugging in the experimental campaign discussed in Chapter 3. The experimental data have revealed that the wavy pipe is effective to mitigate severe slugging and oscillation flow and the performance is affected by its length and location in the pipeline. A 2-D CFD model of the 4" pipeline/riser system has been developed and validated by the experimental data in Section 4.3. In this section the wavy pipe is added into the CFD model. Hence the CFD model can be used to simulate a pipeline/wavy-pipe/riser system and examine the effects of the geometrical parameters and locations of the wavy pipe on its performance.

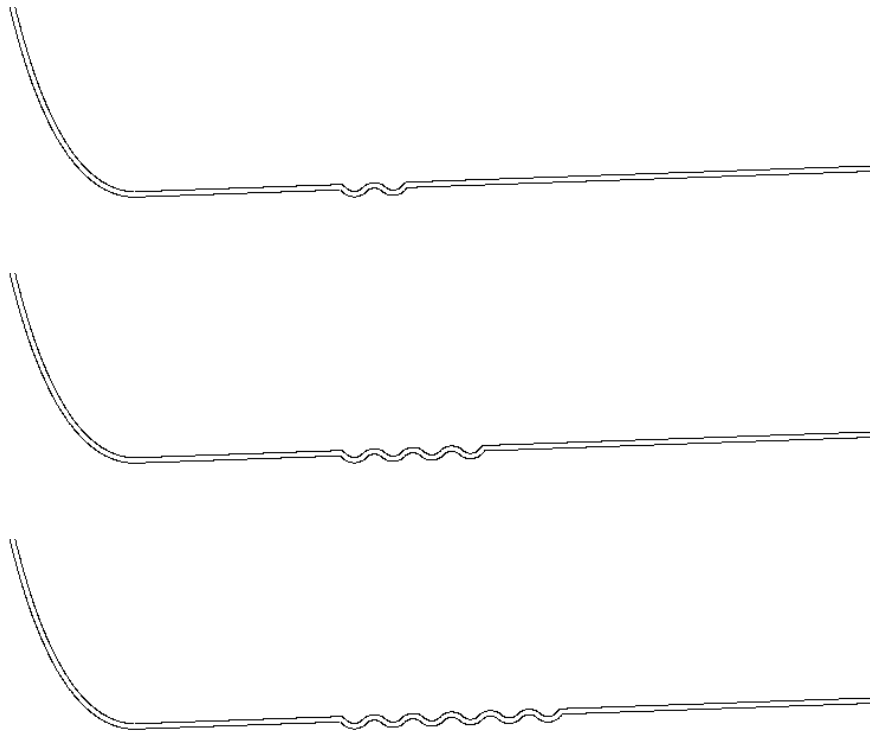
4.4.1 Wavy Pipes of Different Geometries

A series of wavy pipes of different amplitudes and lengths were created. The wavy pipes were placed at different locations to examine the location effects on their performance of severe slugging mitigation.

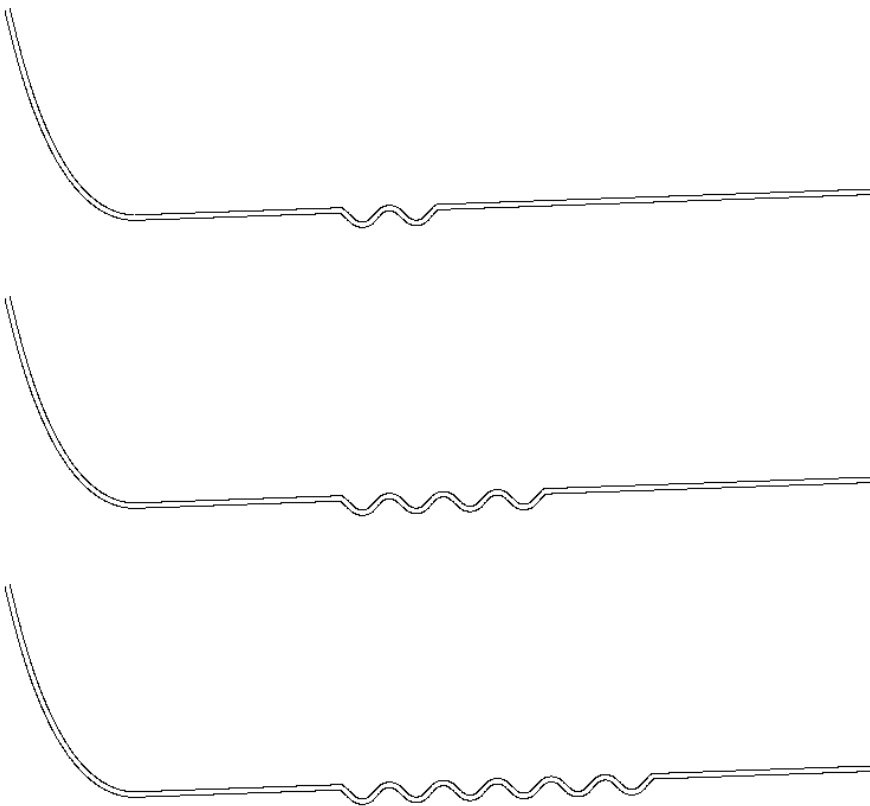
Three wavy pipes of different amplitudes were created. Geometry I has the same amplitude with the tested wavy pipe in the experiment. Geometry II and III are variants

of Geometry I. Geometry II and III are obtained by extending each end of the bend in Geometry I by a straight pipe section with a length of $1d$ and $2d$, respectively ($d = 0.101$ m, the pipe diameter). The wavy pipes of Geometry I, II and III are denoted as Wavy I, Wavy II and Wavy III, respectively. The amplitudes of Wavy I, Wavy II and Wavy III are 0.082 m, 0.160 m, and 0.238 m, with the ratio of amplitude to diameter (A/d) of 0.8, 1.6 and 2.4, respectively. Three wavy pipes of different lengths with 3, 7 and 11 bends were employed. The lengths of the three wavy pipes for Wavy III are 2.628 m, 5.456 and 8.285 m, with the ratio of length to diameter (L/d) of 26.0, 54.0 and 82.0, respectively.

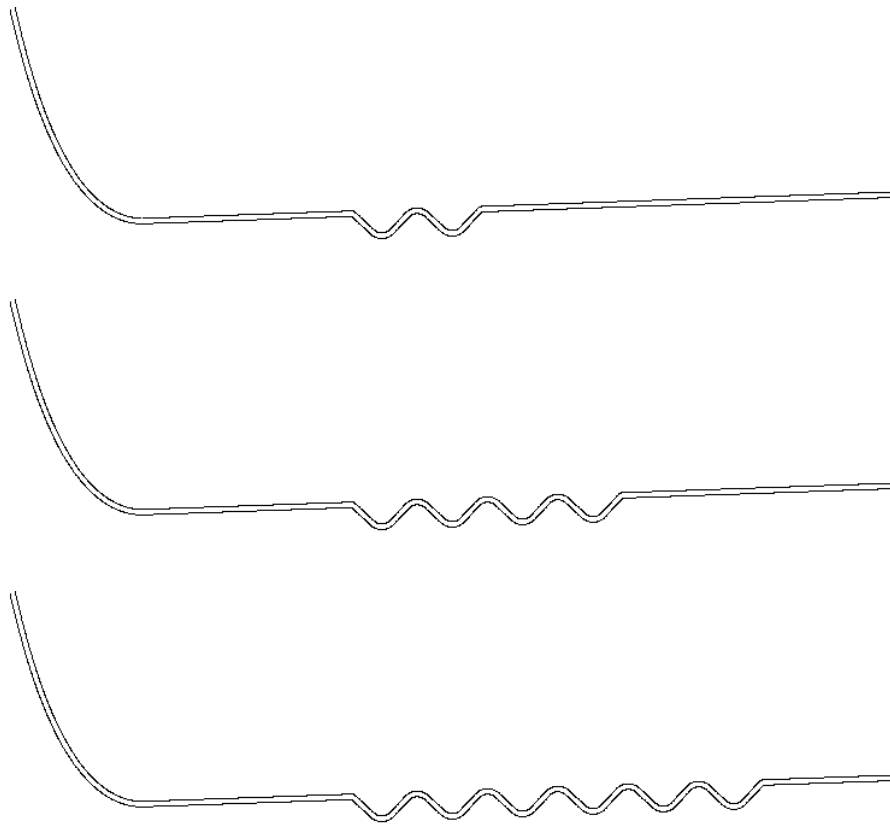
Figure 4-12 shows the schematics of the pipeline/riser systems with the wavy pipes of different amplitudes and lengths in the pipeline. Firstly the wavy pipes were placed at the riser base with the outlet located 1.2 m ($11.9d$) from the riser base as in the experiment, then moved upstream to examine the effects of the location. Figure 4-13 shows the pipeline/wavy-pipe/riser system with Wavy III of 7 bends at different locations in the pipeline. Five locations were tested with the outlet of the wavy pipe at 1.2 m ($11.9d$), 4.2 m ($41.6d$), 7.2 m ($71.3d$), 10.2 m ($101.0d$), and 16.2 m ($160.4d$) from the riser base.



(a) Wavy I: 3 bends, 7 bends and 11 bends



(b) Wavy II: 3 bends, 7 bends and 11 bends

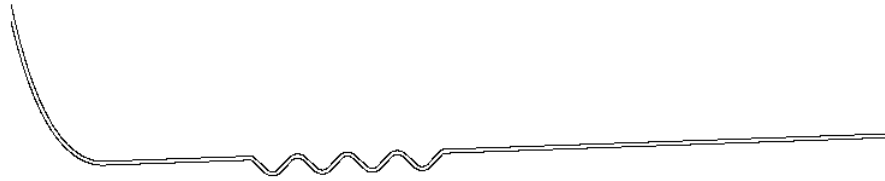


(c) Wavy III: 3 bends, 7 bends and 11 bends

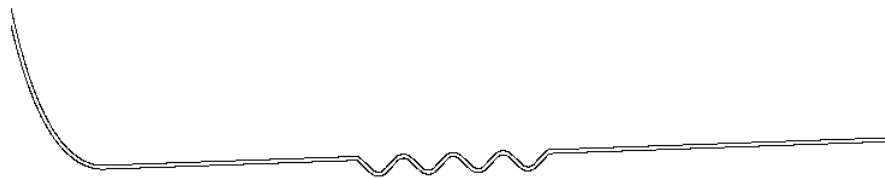
Figure 4-12 Schematics of pipeline/wavy-pipe/riser systems with the wavy pipes of different amplitudes and lengths in the pipeline



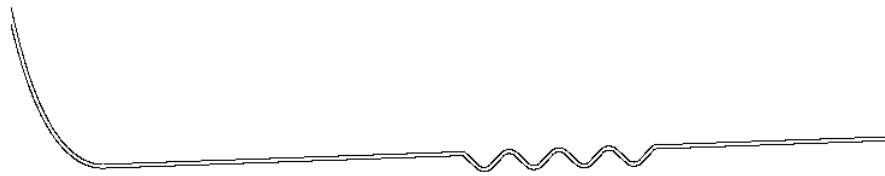
(a) Location I: 1.2 m upstream ($11.9d$)



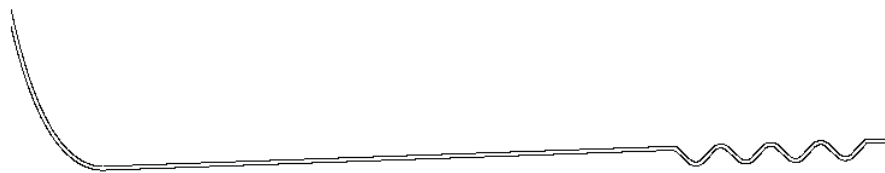
(b) Location II: 4.2 m upstream ($41.6d$)



(c) Location III: 7.2 m upstream ($71.3d$)



(d) Location IV: 10.2 m upstream ($101.0d$)



(e) Location V: 16.2 m upstream ($160.4d$)

Figure 4-13 Schematics of pipeline/wavy-pipe/riser systems with Wavy III at different locations in the pipeline

4.4.2 Model Setup and Test Configurations

The setup of the models for the pipeline/wavy-pipe/riser systems is similar to that for the plain riser system presented in Section 4.2. The only difference is that more parameters have been monitored for the wavy pipe. The pressure at the inlet and outlet of the wavy pipe is recorded as shown in Figure 4-14.

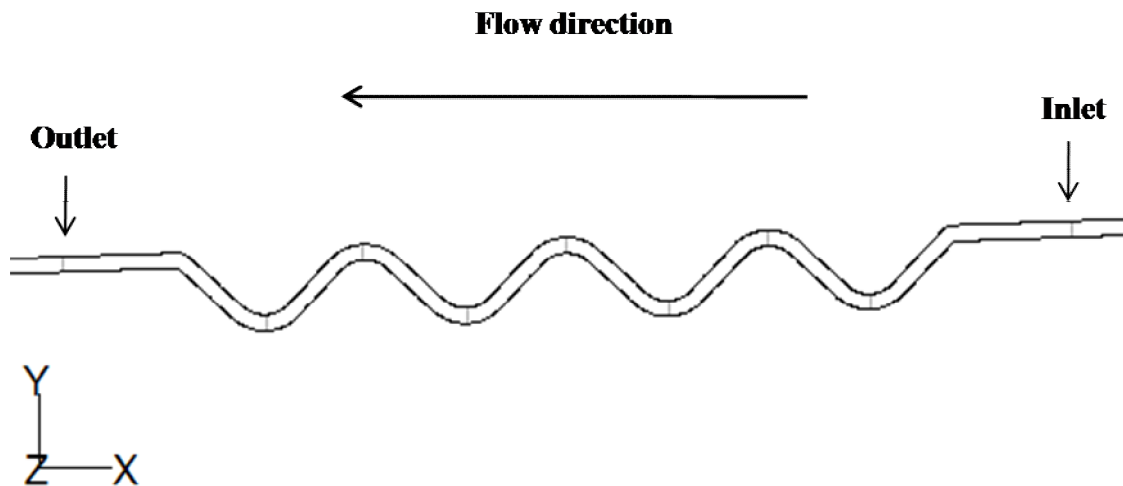


Figure 4-14 Locations for monitoring the pressure at the inlet and outlet of the wavy pipe

The contour plots of gas volume fraction in the pipeline/wavy-pipe/riser system have been saved during the calculation of the model. Then the distribution and interactions between the gas/liquid two phases can be observed ‘visually’.

It has been observed in the experiment that there are mechanical oscillations of the wavy pipe when the gas/liquid two-phase flow passing through it. Therefore, the forces exerting on the wavy pipe by the two-phase flow are monitored in terms of drag and lift force coefficients. The drag and lift coefficients of the force acting on the wavy pipe calculated in the CFD model are defined as follows (ANSYS, 2006):

$$C_D = \frac{\vec{F} \cdot \vec{n}_D}{\frac{1}{2}(\rho_{\text{ref}}v_{\text{ref}}^2A_{\text{ref}})} \quad (4-4)$$

$$C_L = \frac{\vec{F} \cdot \vec{n}_L}{\frac{1}{2}(\rho_{\text{ref}}v_{\text{ref}}^2A_{\text{ref}})} \quad (4-5)$$

where C_D and C_L are the drag and lift coefficients, respectively; \vec{F} is the force vector on the walls of the wavy pipe; \vec{n}_D and \vec{n}_L are the user-specified direction vector and they are in the negative x and negative y directions as indicated in Figure 4-14, respectively; ρ_{ref} , v_{ref} , and A_{ref} are the reference density, velocity and area and they are 1.225 kg/m³, 1 m/s and 1 m², respectively.

A typical severe slugging case with $U_{\text{SL}} = 0.37$ m/s and $U_{\text{SG0}} = 1.37$ m/s at the inlet of the plain riser system has been tested. The effects of the amplitude, length and location of the wavy pipe on the flow have been examined through a series of numerical tests using the above CFD models. The configurations of the numerical tests are listed as below:

- the wavy pipes of different amplitudes, i.e. Wavy I, Wavy II and Wavy III, are tested at different locations;
- the wavy pipes of different lengths, i.e. 3 bends, 7 bends and 11 bends, are tested for Wavy I, Wavy II and Wavy III;
- the wavy pipes of 7 bends placed at different locations in the pipeline are tested for Wavy I, Wavy II and Wavy III.

The differential pressure across the wavy pipe is denoted as wavy DP, calculated by subtracting the inlet pressure by the outlet pressure. The model predictions of the riser DP, wavy DP, pressure at the inlet of the wavy pipe and force coefficients are discussed below. Based on the discussions the effects of the amplitude, length and location of the wavy pipe on the flow behaviour in the pipeline/wavy-pipe/riser system are examined.

4.4.3 Effects of the Amplitude of Wavy Pipe

The amplitudes of Wavy I, Wavy II and Wavy III are 0.082 m, 0.160 m, and 0.238 m, with the ratio of amplitude to diameter (A/d) of 0.8, 1.6 and 2.4, respectively. The effects of the amplitude have been examined by comparing the riser DP, wavy DP, pressure at the inlet of the wavy pipe and force coefficients of the wavy pipes. Figure 4-15 shows the time traces of the riser DP for the plain riser and pipeline/wavy-pipe/riser systems with Wavy I, Wavy II and Wavy III of 7 bends at Location III (with the wavy pipe outlet 7.2 m upstream of the riser base). The mean, maximum, minimum and standard deviation of the riser DP time series between $t = 250$ s and $t = 450$ s are listed in Table 4-4. *It needs to be mentioned that the 'maximum' and 'minimum' in Table 4-4 are calculated by averaging those of all the cycles between $t = 250$ s and $t = 450$ s. The same calculation of the 'maximum' and 'minimum' has been performed for the other variables in Section 4.4.*

It can be seen in Figure 4-15 and Table 4-4 that the maximum riser DP in the pipeline/wavy-pipe/riser systems is lower than that in the plain riser system. The maximum riser DP is consistently lower than 1.03 bar with a wavy pipe applied, therefore, it can be concluded that the riser is never filled with the liquid. The flow regime, severe slugging, in the plain riser system has been changed into oscillation flow in the pipeline/wavy-pipe/riser systems. With the increase of the amplitude of the wavy pipe from $0.8d$ to $2.4d$ the average maximum riser DP decreases and the minimum increases consistently. The maximum riser DP has decreased by 8 %, 13 % and 29 %, with Wavy I, Wavy II and Wavy III respectively, of that without a wavy pipe. The fluctuation amplitude decreases consistently with the increase of the amplitude of the wavy pipe. The standard deviation of the riser DP dropped by 23 %, 38 % and 65 %, with Wavy I, Wavy II and Wavy III respectively, of that without a wavy pipe. To summarise, the slug length is reduced thus the severity of the flow is mitigated with a wavy pipe applied; the performance is better with a higher-amplitude wavy pipe ($A = 2.4d$). However, an increase of the mean riser DP, about 25 %, has been induced by applying the wavy pipe. It decreases slightly with the increase of the wavy pipe amplitude.

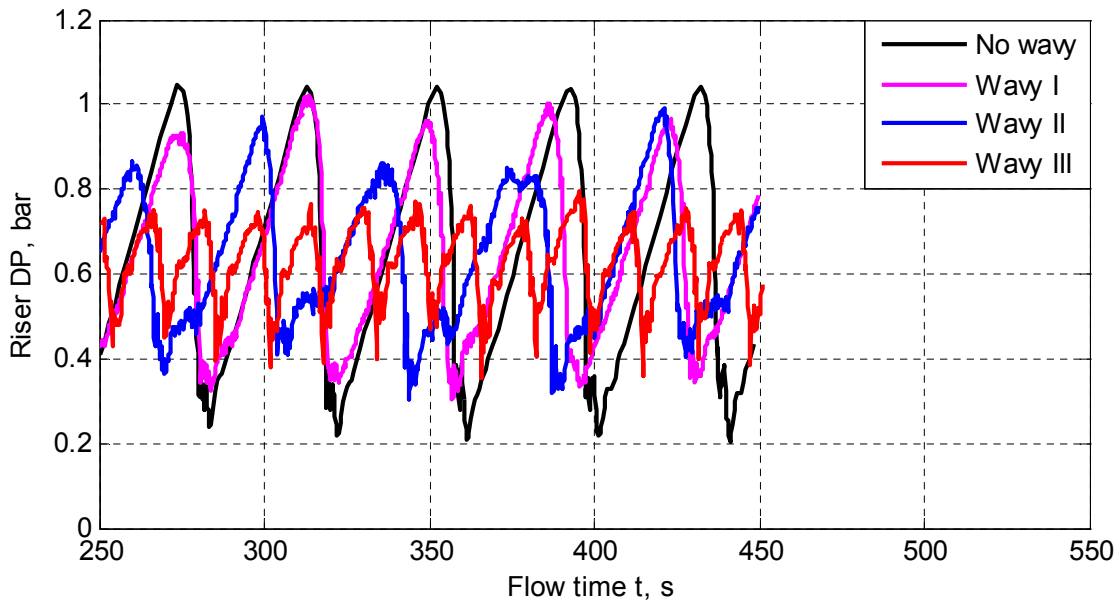


Figure 4-15 Time traces of the riser DP for the plain riser and pipeline/wavy-pipe/riser systems with Wavy I, Wavy II and Wavy III of 7 bends at Location III

Table 4-4 Statistical parameters of the riser DP for Wavy I, Wavy II and Wavy III of 7 bends at Location III

	No wavy	Wavy I	Wavy II	Wavy III
Mean (bar)	0.51	0.65	0.64	0.63
Maximum (bar)	1.05	0.97	0.91	0.75
Minimum (bar)	0.22	0.33	0.36	0.40
Standard deviation (bar)	0.26	0.20	0.16	0.09

The time traces of the wavy DP for Wavy I, Wavy II and Wavy III are compared in Figure 4-16. The mean, maximum and fluctuation amplitude of the wavy DP increases significantly with the increase of the amplitude of the wavy pipe. The mean of the wavy DP is 15 mbar, 48 mbar and 67 mbar for Wavy I, Wavy II and Wavy III, respectively. The mean wavy DP of Wavy III is more than 4 times of that of Wavy I, although the

amplitude of Wavy III ($A = 2.4d$) is only 3 times of that of Wavy I ($A = 0.8d$). The maximum and standard deviation of the wavy DP of Wavy III are more than 3 times of those of Wavy I. Therefore, it can be concluded that the wavy pipe of higher amplitude results in a higher pressure drop of more intensive fluctuations in the pipeline upstream of the riser base.

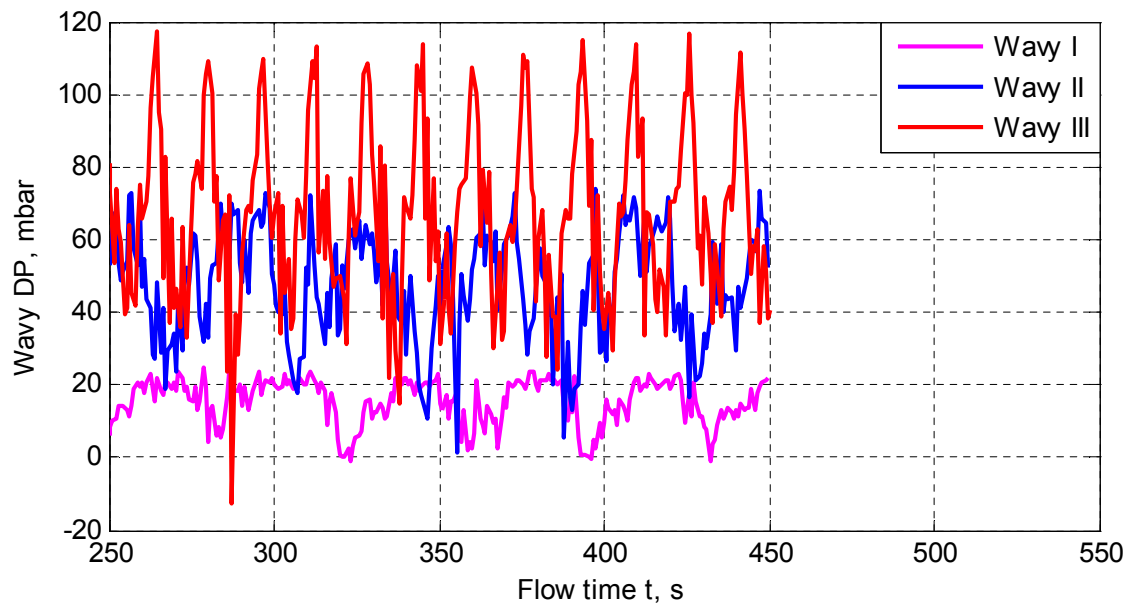


Figure 4-16 Time traces of the wavy DP for Wavy I, Wavy II and Wavy III of 7 bends at Location III

As discussed above the maximum and fluctuation amplitude of the riser DP can be reduced further by applying a higher-amplitude wavy pipe. However, a higher pressure drop of more intensive fluctuations over the wavy pipe is induced. The pressure at the inlet of the wavy pipe is the sum of the riser base pressure and the pressure drop over the wavy pipe. The pressure upstream of the wavy pipe in the pipeline is of concern because the incoming flowrates from the sources (wells in field production systems) is highly dependent on it.

Figure 4-17 compares the time traces of the pressure at the inlet of Wavy I, Wavy II and Wavy III and the statistical parameters of the time series are listed in Table 4-5. The

mean pressure increases slightly with the increase of the amplitude of the wavy pipe, 1.66 barg, 1.68 barg and 1.68 barg for Wavy I, Wavy II and Wavy III, respectively. The maximum pressure drops and the minimum rises consistently with the increase of the wavy pipe amplitude. Consequently the fluctuation amplitude of the pressure decreases consistently and the standard deviation for Wavy III has been reduced by 50 % of that for Wavy I. To conclude, with the increase of the wavy pipe amplitude: (1) the pressure in the pipeline upstream of the wavy pipe becomes more and more stable (lower fluctuations); (2) the mean of the pressure increases slightly due to the increases of the wavy DP.

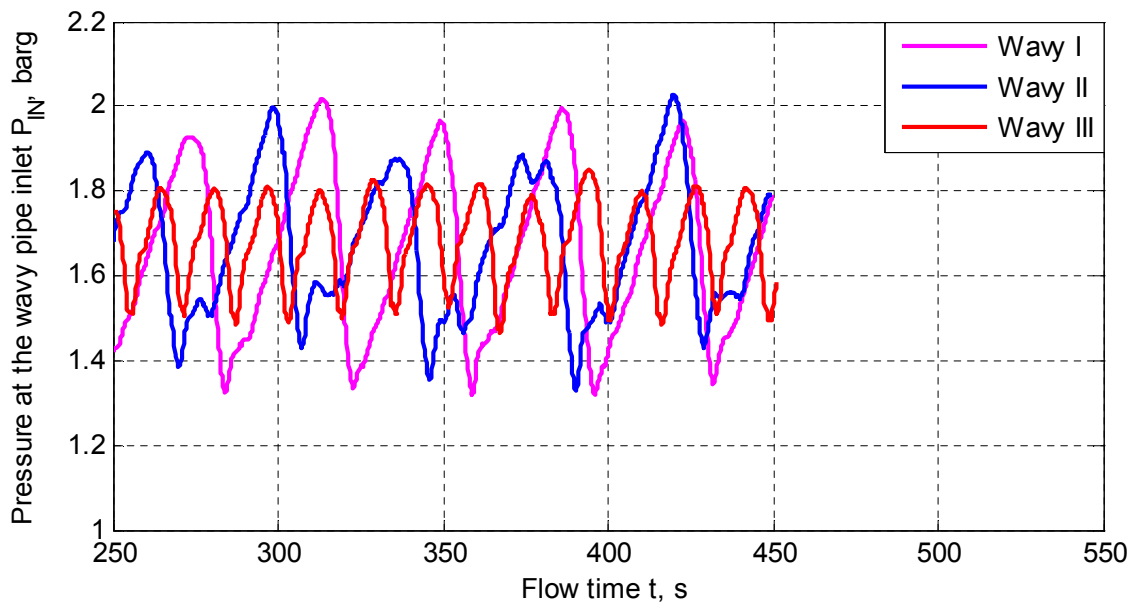


Figure 4-17 Time traces of the pressure at the inlet of the wavy pipe for Wavy I, Wavy II and Wavy III of 7 bends at Location III

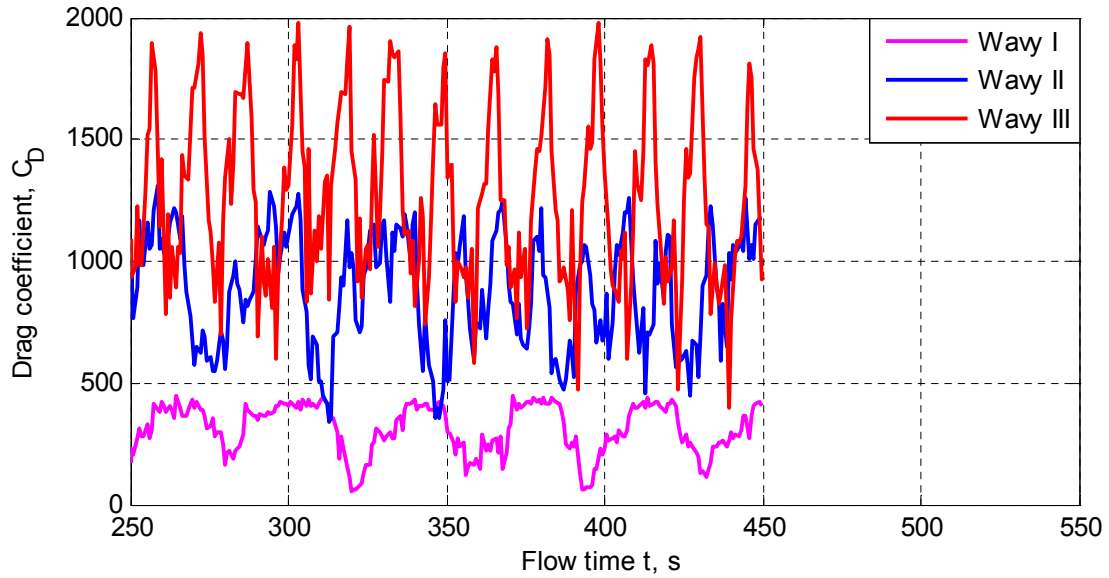
Table 4-5 Statistical parameters of the pressure at the inlet of the wavy pipe for Wavy I, Wavy II and Wavy III of 7 bends at Location III

	Wavy I	Wavy II	Wavy III
Mean (barg)	1.66	1.68	1.68
Maximum (barg)	1.98	1.94	1.81
Minimum (barg)	1.33	1.39	1.51
Standard deviation (barg)	0.20	0.17	0.10

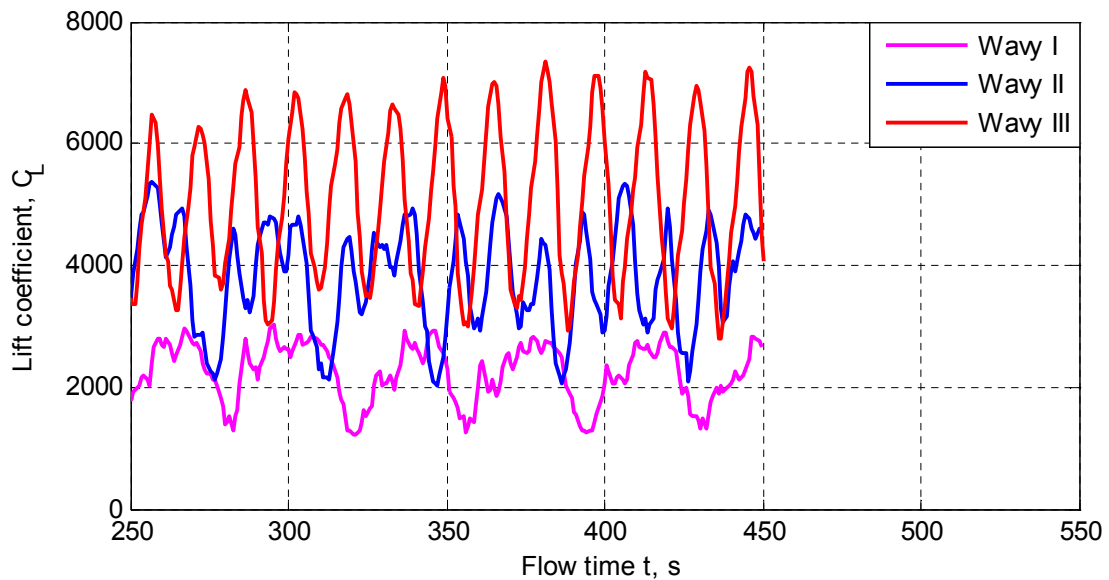
It has been observed that the wavy pipe experiences mechanical oscillations on the vertical plane especially at the gas blowdown stage. At this stage the mini liquid slugs and trapped gas pass through the Λ and V sections alternatively at a high velocity. Significant forces can be imposed on the wall of the wavy pipe. The forces on the wavy pipe have been monitored in terms of the drag and lift coefficients. The drag and lift forces presented in this section are in the negative x and negative y directions as shown in Figure 4-14, respectively. The direction of the presented lift force below is the same with that of the gravity.

The time traces of the drag and lift coefficients are compared in Figure 4-18 for Wavy I, Wavy II and Wavy III of 7 bends at Location III. The statistical parameters of the time series between $t = 250$ s and $t = 450$ s are plotted against the amplitude of the wavy pipe in Figure 4-19. The force coefficients oscillate with the same cycle time of the wavy DP. The lift force is larger in amplitude than the drag force. The statistical parameters of concern, i.e. mean, maximum, minimum and standard deviation, for both the drag and lift coefficients increase significantly with the increase of the amplitude of the wavy pipe. The mean and maximum drag coefficient for Wavy III are more than 4 times of that for Wavy I, and the mean and maximum lift coefficient for Wavy III are more than twice of that for Wavy I. The minimum of the drag and lift coefficient for Wavy III is more than 6 times and about 3 times of those for Wavy I, respectively. The standard deviation of the drag and lift coefficients for Wavy III is about 3 times and twice of those for Wavy I, respectively. Based on the comparison above it can be concluded that

the magnitude and fluctuation amplitude of the drag and lift forces on the wavy pipe increase almost proportionally with the increase of the amplitude of the wavy pipe. The larger forces acting on the wavy pipe of higher amplitude result in higher mechanical instability of the pipeline.

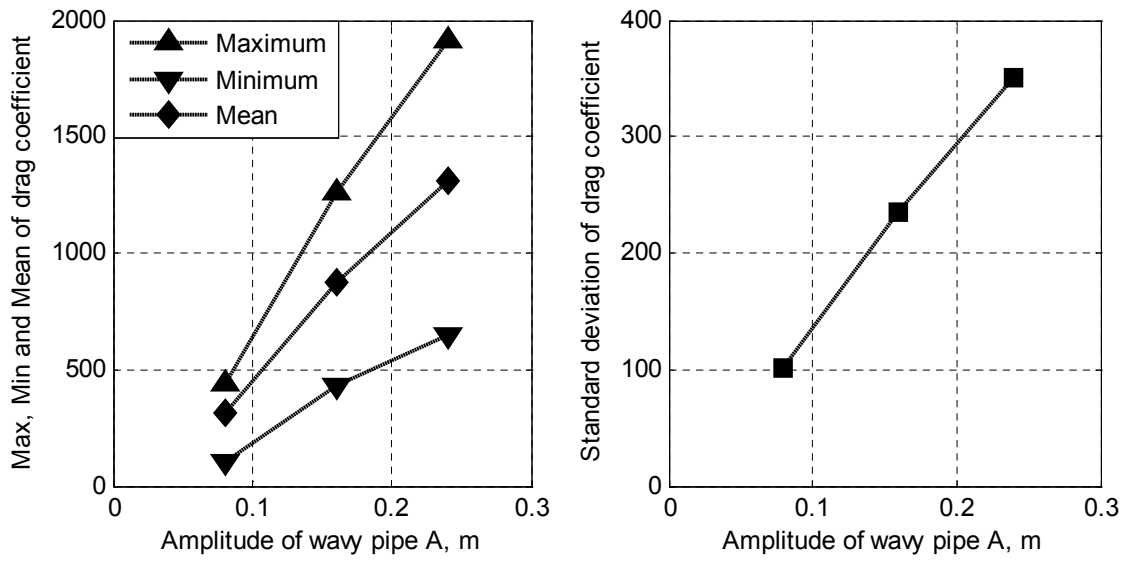


(a) Drag coefficient

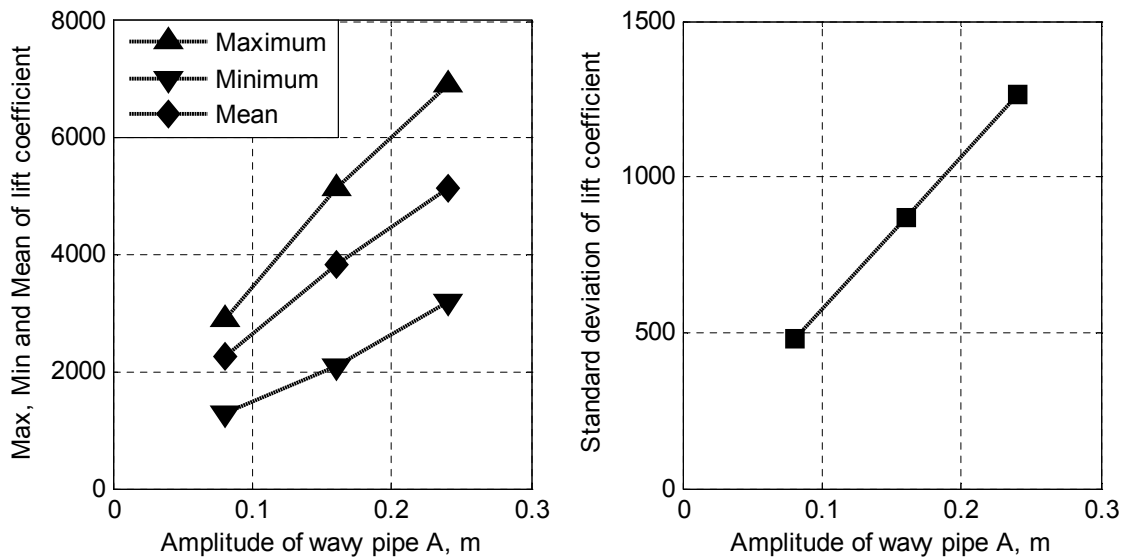


(b) Lift coefficient

Figure 4-18 Time traces of the drag and lift coefficients for Wavy I, Wavy II and Wavy III of 7 bends at Location III



(a) Drag coefficient



(b) Lift coefficient

Wavy I: $A = 0.082$ m; Wavy II: $A = 0.160$ m; Wavy III: $A = 0.238$ m

Figure 4-19 Statistical parameters of the drag and lift coefficients against the amplitude of the wavy pipe for Wavy I, Wavy II and Wavy III

To summarise, the effects of the amplitude of the wavy pipe have been examined by comparing the riser DP, wavy DP, pressure at the inlet of the wavy pipe and the force coefficients of the wavy pipes. Three wavy pipes of different amplitudes, i.e. Wavy I ($A = 0.8d$), Wavy II ($A = 1.6d$) and Wavy III ($A = 2.4d$), have been tested. It has been found that:

- (1) the maximum and fluctuation amplitude of the riser DP decrease with the increase of the amplitude of the wavy pipe; this indicates that the slug length and severity of the flow can be reduced further by applying a wavy pipe of a higher amplitude; the mean riser DP decreases slightly with the increase of the amplitude of the wavy pipe;
- (2) the mean, maximum and fluctuation amplitude of the wavy DP increases sharply with the increase of the amplitude of the wavy pipe; the maximum and fluctuation amplitude of the pressure at the inlet of the wavy pipe can be reduced further with a higher-amplitude wavy pipe; this indicates that a more stable pressure upstream of a higher-amplitude wavy pipe in the pipeline can be obtained; the mean of the pressure increases slightly due to the increases of the wavy DP;
- (3) the mean, maximum and fluctuation amplitude of the drag and lift forces on the wavy pipe increase sharply (almost proportionally) with the increase of the amplitude of the wavy pipe; this indicates that the wavy pipe of a higher amplitude increases the mechanical instability of the pipeline significantly.

4.4.4 Effects of the Length of Wavy Pipe

The effects of the wavy pipe length, in terms of the number of the bends, have been examined through the CFD model. The wavy pipes of 3, 7 and 11 bends located at Location II have been tested. *As similar conclusions have been drawn from the three wavy pipes of different amplitudes, i.e. Wavy I, Wavy II and Wavy III, the discussions below will focus on the analysis of the results from Wavy III for brevity.*

Figure 4-20 compares the riser DP from the plain riser system and pipeline/wavy-pipe/riser systems with Wavy III of different lengths at Location II (with the wavy pipe outlet 4.2 m upstream of the riser base). The mean, maximum, minimum and standard deviation of the riser DP time series between $t = 250$ s and $t = 450$ s are listed in Table

4-6. It can be seen that the maximum riser DP decreases and the minimum increases consistently with the increase of the length of the wavy pipe. Thus the fluctuation amplitude of the riser DP drops and the lowest fluctuation amplitude can be obtained with the longest wavy pipe (of 11 bends). With the 3-bend, 7-bend and 11-bend wavy pipe applied, the maximum riser DP has dropped by about 5 %, 10 % and 30 % of that for the plain riser system, respectively; while the minimum has increased by about 40 %, 70 % and 90 %, respectively. With the decrease of the maximum and increase of the minimum, the standard deviation of the riser DP has been reduced significantly. The standard deviation has been reduced by about 12 %, 35 % and 70 % of that for the plain riser system, respectively. With Wavy III applied the mean riser DP increases by about 20 % of that for the plain riser system. The length of the wavy pipe does not affect the mean riser DP significantly. It has been shown that a longer wavy pipe of 11 bends is more effective on reducing the slug length and mitigating the severity of the flow in the pipeline/riser system than the shorter ones of 3 and 7 bends.

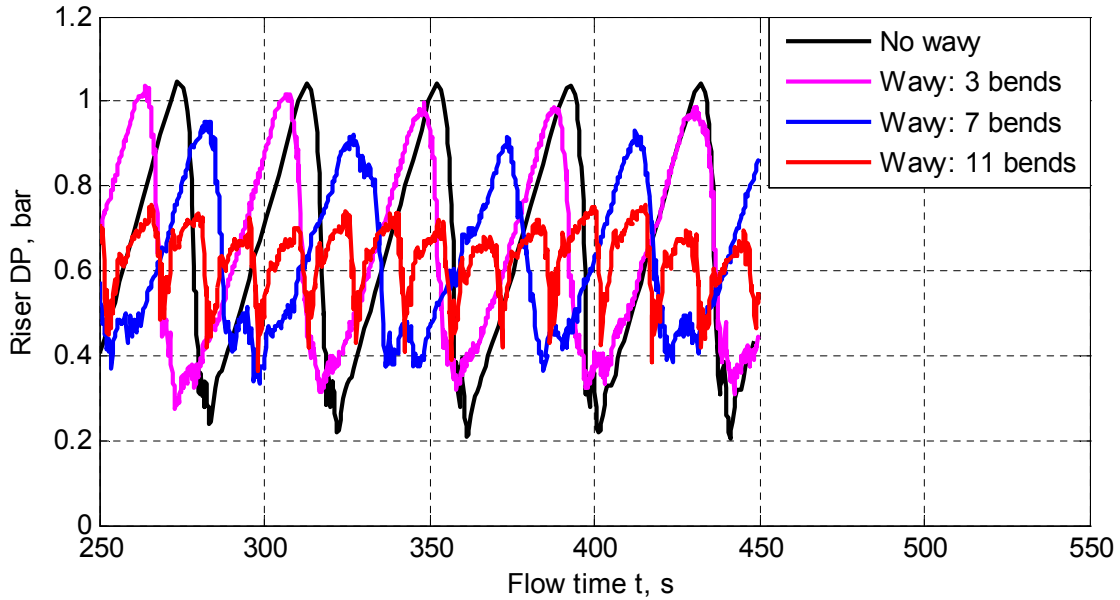


Figure 4-20 Time traces of the riser DP for the plain riser system and pipeline/wavy-pipe/riser systems with Wavy III of 3, 7 and 11 bends at Location II

Table 4-6 Statistical parameters of the riser DP for Wavy III at Location II

	No wavy	3 bends	7 bends	11 bends
Mean (bar)	0.51	0.64	0.63	0.63
Maximum (bar)	1.05	1.00	0.93	0.72
Minimum (bar)	0.22	0.31	0.37	0.42
Standard deviation (bar)	0.26	0.23	0.17	0.08

The time traces of the wavy DP for Wavy III of 3, 7 and 11 bends at Location II are compared in Figure 4-21. The lengths of Wavy III of 3, 7 and 11 bends are 2.628 m, 5.456 and 8.285 m, with the ratio of length to diameter (L/d) of 26.0, 54.0 and 82.0, respectively. We can see that the mean, maximum and fluctuation amplitude of the wavy DP increase significantly with the increase of the length of the wavy pipe. The mean of the wavy DP is 38 mbar, 75 mbar and 99 mbar for Wavy III of 3, 7 and 11 bends, respectively. The average differential pressure per bend becomes smaller and smaller with the increase of the length of the wavy pipe, 13, 11 and 9 mbar/bend for Wavy III of 3, 7 and 11 bends, respectively. With the length of the wavy pipe increasing from 2.628 m (3 bends) to 8.285 m (11 bends) the maximum and standard deviation have increased from 54 mbar to 151 mbar and 11 mbar to 35 mbar, respectively. The maximum and standard deviation have increased by 1.8 and 2.2 times while the length increases by 2.2 times. To conclude, the mean, maximum and fluctuation amplitude of the wavy DP increases with the increase of the length of the wavy pipe, however, the average differential pressure per bend decreases.

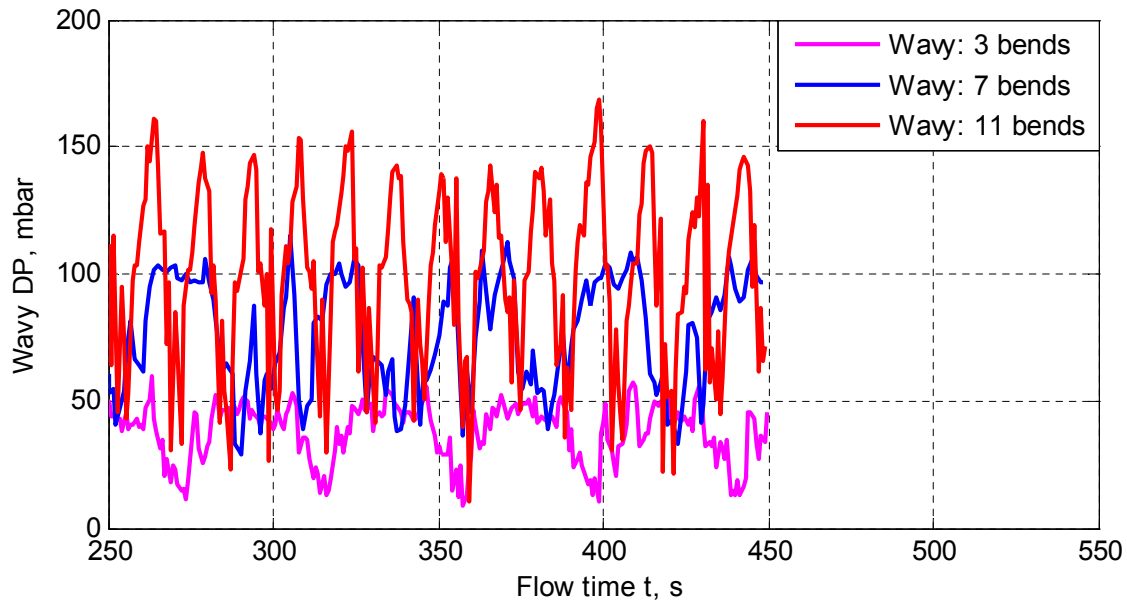


Figure 4-21 Time traces of the wavy DP for Wavy III of 3, 7 and 11 bends at Location II

As stated in Section 4.4.3 it is of interest to examine the pressure at the inlet of the wavy pipe. Figure 4-22 compares the time traces of the pressure at the inlet of Wavy III of 3, 7 and 11 bends at Location II and the statistical parameters of the time series are listed in Table 4-7. The mean pressure increases slightly with the increase of the length of the wavy pipe, 1.68 barg, 1.68 barg and 1.72 barg for the 3-, 7- and 11-bend wavy pipes, respectively. The maximum pressure decreases and the minimum increases consistently with the increase of the length of the wavy pipe. The maximum inlet pressure for the 11-bend wavy pipe has dropped and the minimum rises by about 10 % and 15 % of that for the 3-bend wavy pipe, respectively. As a result, the standard deviation of the pressure for the 11-bend wavy pipe has dropped by 57 % of that for the 3-bend wavy pipe. This indicates that a more stable pressure in the pipeline can be obtained with a longer wavy pipe (of 11 bends) applied.

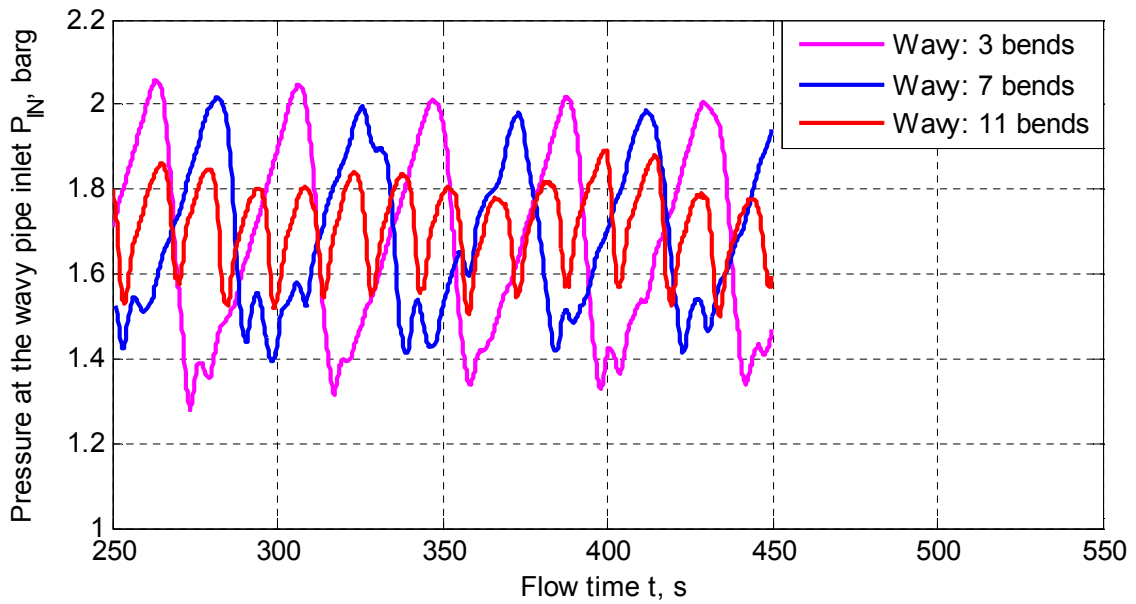


Figure 4-22 Time traces of the pressure at the inlet of Wavy III of 3, 7 and 11 bends at Location II

Table 4-7 Statistical parameters of the pressure at the inlet of Wavy III of 3, 7 and 11 bends at Location II

	3 bends	7 bends	11 bends
Mean (barg)	1.68	1.68	1.72
Maximum (barg)	2.03	2.00	1.83
Minimum (barg)	1.33	1.42	1.54
Standard deviation (barg)	0.23	0.18	0.10

In summary, the effects of the length of the wavy pipe have been discussed by comparing the riser DP, wavy DP and pressure at the inlet of the wavy pipe. The wavy pipes of different lengths, i.e. 3, 7 and 11 bends, have been tested. It has been found that:

- (1) the maximum and fluctuation amplitude of the riser DP decrease with the increase of the length of the wavy pipe; this indicates that the slug length and severity of the

flow can be reduced further by applying a wavy pipe of more bends; the mean riser DP increases slightly with the increase of the length of the wavy pipe;

- (2) the mean, maximum and fluctuation amplitude of the wavy DP increases sharply but the average differential pressure per bend decreases with the increase of the length of the wavy pipe;
- (3) the maximum and fluctuation amplitude of the pressure at the inlet of the wavy pipe can be reduced further with a wavy pipe of more bends; this indicates that a more stable pressure in the pipeline can be obtained with a longer wavy pipe.

4.4.5 Effects of the Location of Wavy Pipe

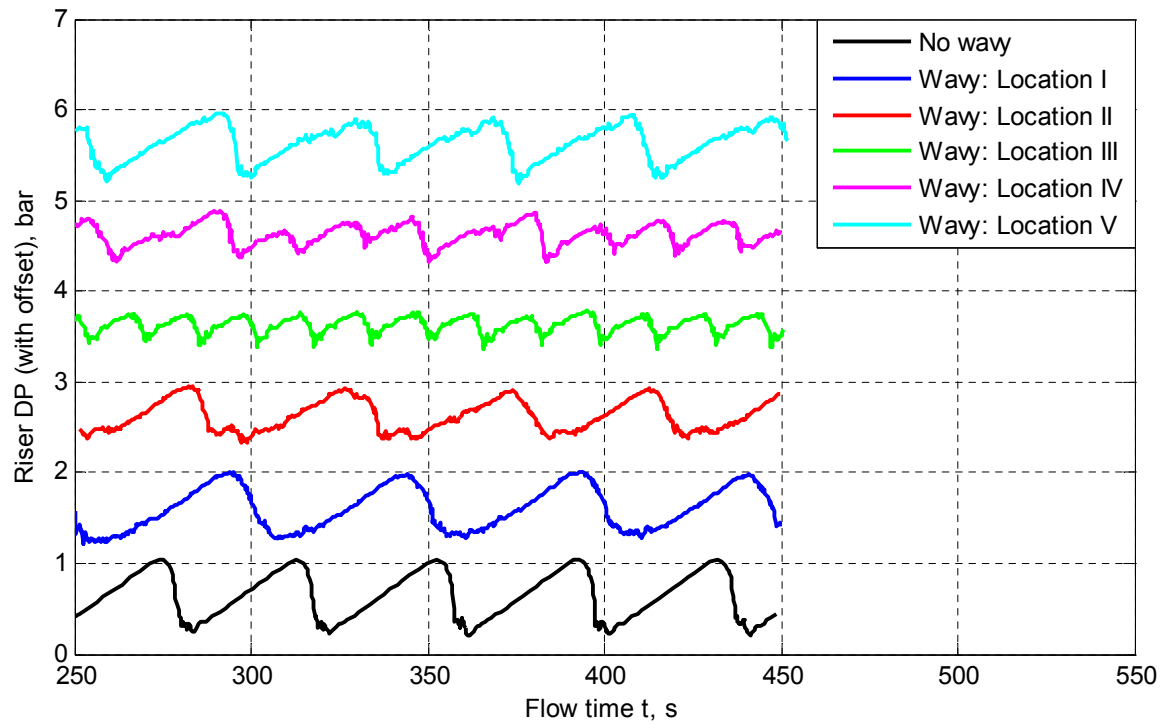
It has been evidenced by the experimental data presented in Chapter 3 that the location of the wavy pipe in the pipeline affects its performance on slug mitigation. However, only two locations have been tested in the experiment due to the restriction of the test rigs. Alternatively the effects of the location of the wavy pipe are examined through the CFD model, which is more flexible than the experimental rigs. The wavy pipe, Wavy III of 7 bends, has been placed at Location I (1.2 m upstream of the riser base), II (4.2 m), III (7.2 m), IV (10.2 m) and V (15.2 m) in the pipeline in the CFD model as shown in Figure 4-13. The riser DP, wavy DP and pressure at the inlet of the wavy pipe have been inspected and compared for the different test configurations.

Figure 4-23 shows the time traces of the riser DP for the plain riser system and pipeline/wavy-pipe/riser systems with Wavy III of 7 bends at different locations. It needs to be noted that the riser DP for the pipeline/wavy-pipe/riser systems have been plotted with offsets 1 bar, 2 bar, 3 bar, 4 bar and 5 bar for Location I, II, III, IV and V, respectively, for clarity. The statistical parameters of the riser DP time series, i.e. mean, maximum, minimum and standard deviation, have been plotted against the distance to the riser base from the wavy pipe outlet in Figure 4-24 (a) and (b). The cycle time of the flow process in the pipeline/riser systems shown in Figure 4-24 (c) is computed based on the riser DP shown in Figure 4-23.

It can be observed in Figure 4-24 that: with the increase of the distance between the riser base and wavy pipe outlet, i.e. from Location I to Location V, (1) the maximum

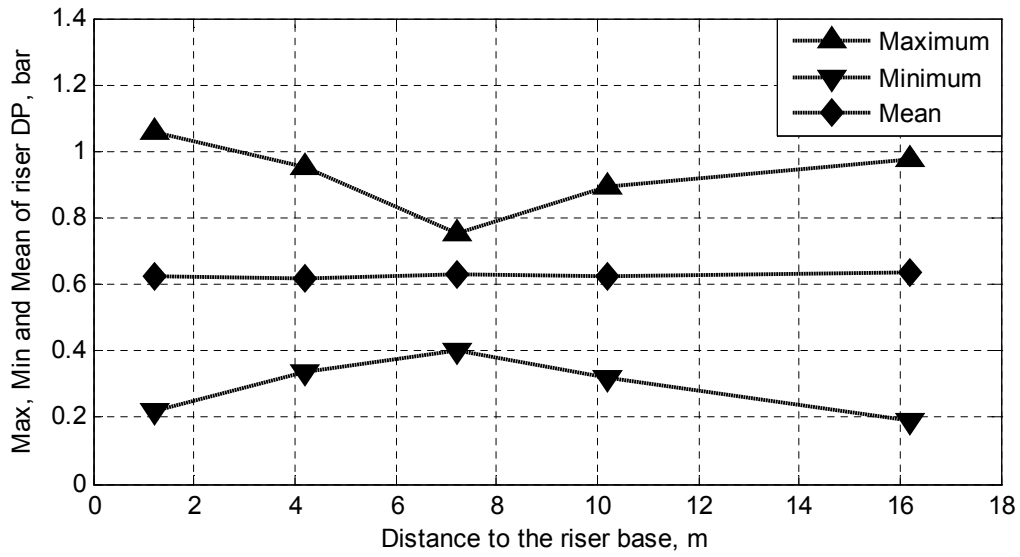
riser DP firstly drops to 0.75 bar from 1.05 bar then increases to 0.97 bar; (2) the minimum riser DP firstly increases to 0.40 bar from 0.22 bar then drops to 0.19 bar; (3) the mean riser DP remains almost unchanged, about 0.63 bar. The lowest fluctuation amplitude and maximum riser DP are obtained with the wavy pipe at Location III. The lower fluctuation amplitude and maximum riser DP indicate a shorter equivalent slug in the riser at the liquid buildup stage of the oscillation flow. Therefore, Location III (7.2 m to the riser base, 71.3d) is the most desirable location, where the wavy pipe is the most effective on reducing the slug length/severity of the flow.

The cycle time of the flow process in the pipeline/wavy-pipe/riser system firstly drops to 36 s from 50 s then increases to 39 s with the increase of the distance between the riser base and wavy pipe outlet. Comparing Figure 4-24 (b) and (c) we can see that the cycle time varies in a similar manner with the standard deviation of the riser DP. The minimum cycle time is obtained with the wavy pipe at Location III, where the minimum fluctuation amplitude of the riser DP appears. A smaller cycle time means a higher slug frequency, which indicates that the equivalent slug in the riser is shorter. This confirms that at Location III the wavy pipe is the most effective on reducing the slug length/severity of the flow.

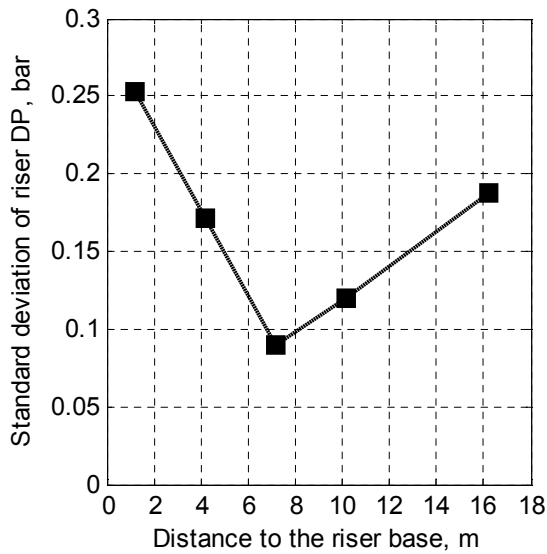


Location I: offset 1 bar; Location II: offset 2 bar; Location III: offset 3 bar; Location IV: offset 4 bar; Location V: offset 5 bar

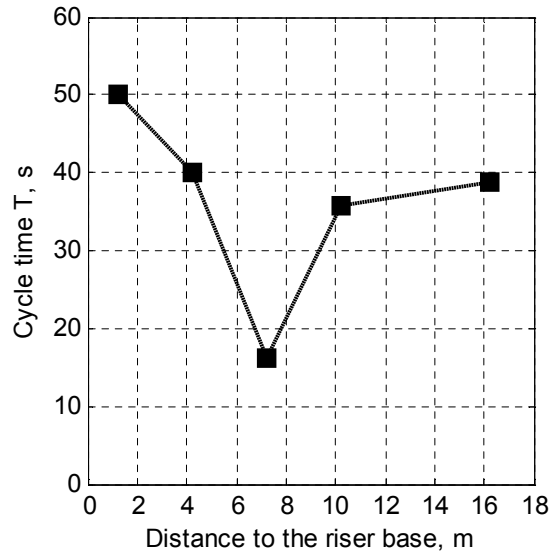
Figure 4-23 Time traces of the riser DP for the plain riser system and pipeline/wavy-pipe/riser systems with Wavy III of 7 bends at Location I to V



(a) Maximum, minimum and mean



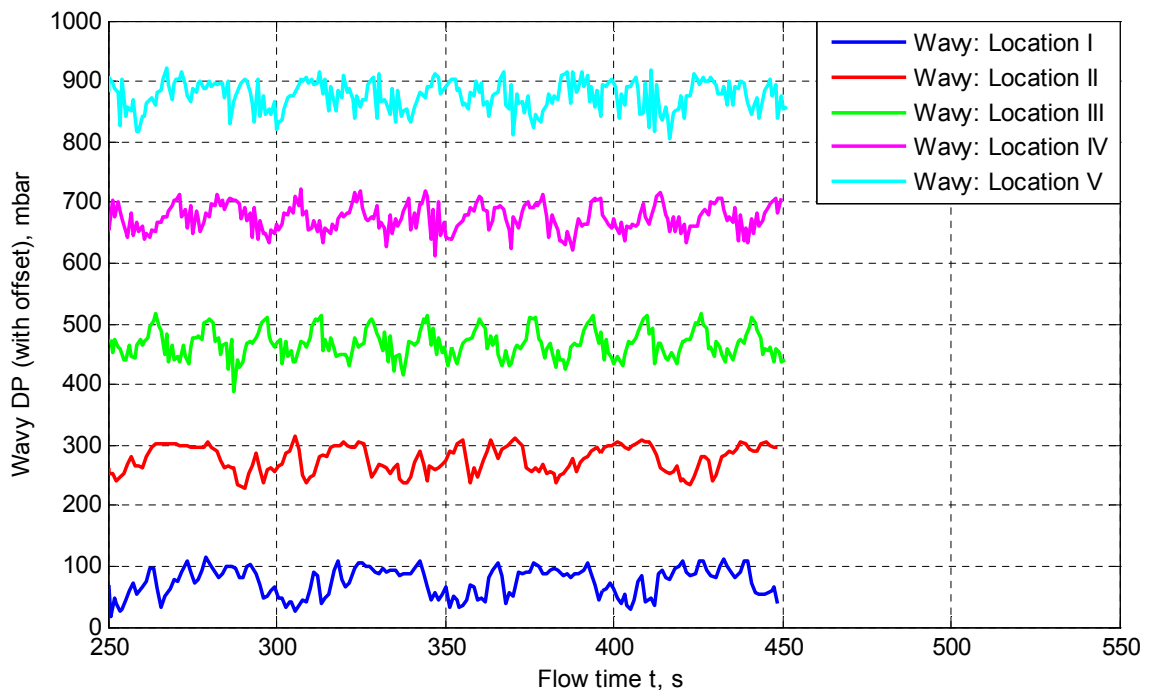
(b) Standard deviation



(c) Cycle time

Figure 4-24 Statistical parameters of the riser DP and the cycle time of the flow process in the pipeline/wavy-pipe/riser systems with Wavy III of 7 bends at Location I to V

The wavy DP for Wavy III at Location I to V is compared in Figure 4-25. It needs to be noted that the wavy DP has been plotted with offsets 200 mbar, 400 mbar, 600 mbar and 800 mbar for Location II, III, IV and V, respectively. The statistical parameters of the wavy DP are plotted against the distance to the riser base from the wavy pipe outlet in Figure 4-26. The maximum, minimum and mean of the wavy DP are not affected significantly by the location of the wavy pipe. The fluctuation amplitude of the wavy pipe tends to increase slightly with the increase of the distance to the riser base from the wavy pipe outlet. As the cycle time of the wavy DP is highly dependent on that of the riser DP, the cycle time of the wavy DP varies in a similar manner to that of the riser DP. Therefore, it is concluded that the wavy DP is not affected by the location of the wavy pipe significantly.



Location II: offset 200 mbar; Location III: offset 400 mbar; Location IV: offset 600 mbar; Location V: offset 800 mbar

Figure 4-25 Time traces of the wavy DP for Wavy III of 7 bends at Location I to V

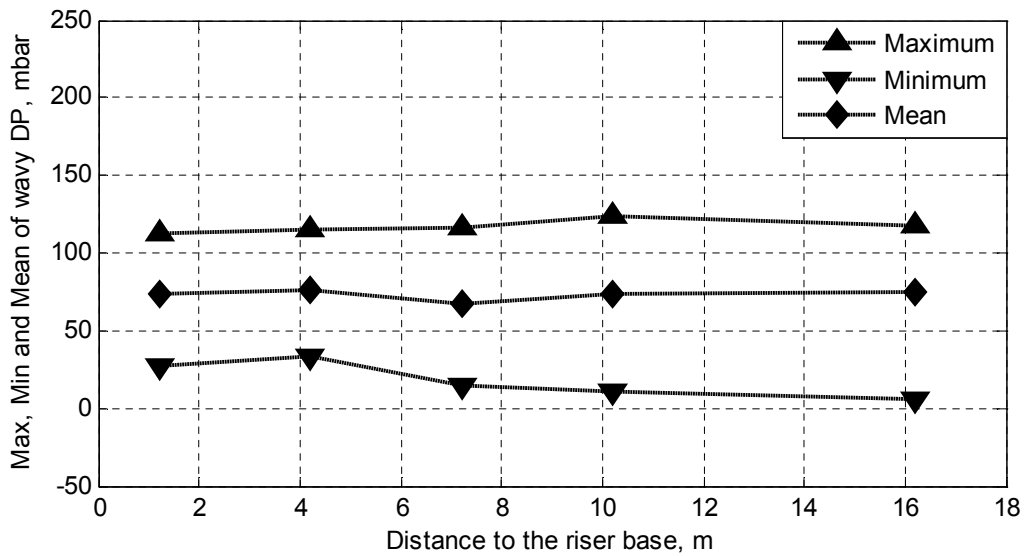
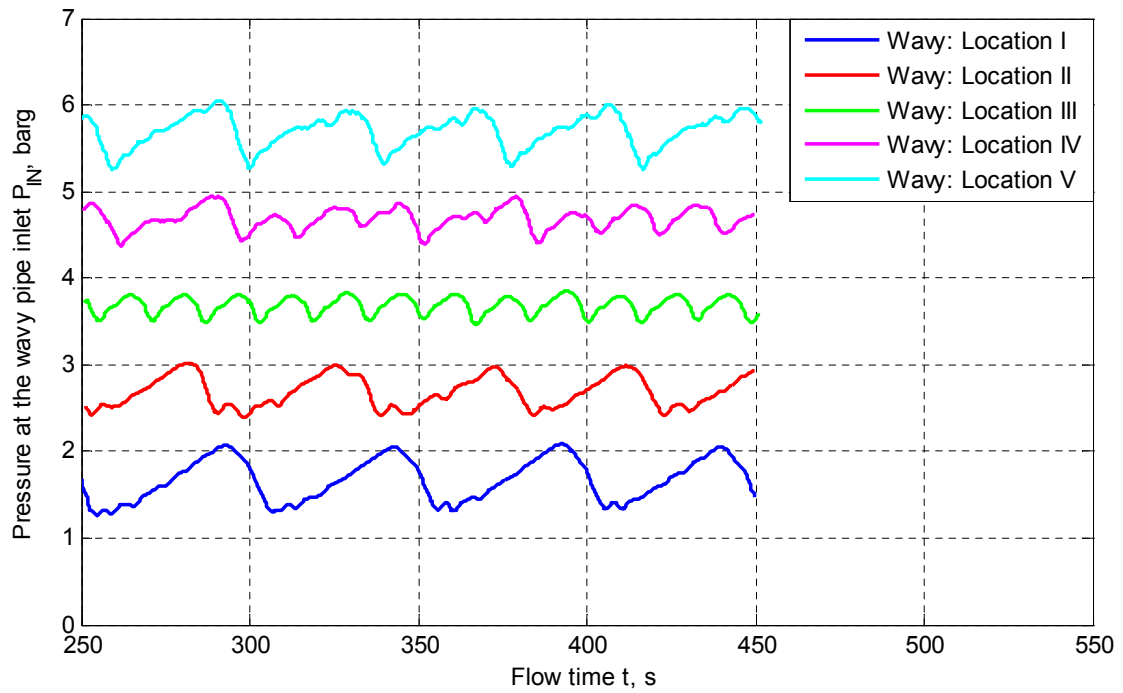


Figure 4-26 Maximum, minimum and mean of the wavy DP with Wavy III of 7 bends at Location I to V

The pressure at the inlet of the wavy pipe at Location I to V is compared in Figure 4-27. The offsets of the plotted pressure in Figure 4-27 are 1 barg, 2 barg, 3 barg and 4 barg for Location II, III, IV and V, respectively. The mean, maximum, minimum and standard deviation of the pressure are plotted against the distance to the riser base from the wavy pipe outlet in Figure 4-28. The effects of the location on the pressure at the inlet of the wavy pipe are similar to those on the wavy DP. That is reasonable because the wavy DP is not affected by the location of the wavy pipe significantly. It can be seen clearly that the lowest maximum and fluctuation amplitude of the pressure upstream of the wavy pipe can be obtained when locating the wavy pipe at Location III. Hence the most stable pressure at the inlet of the wavy pipe is obtained with the wavy pipe at Location III.



Location II: offset 1 barg; Location III: offset 2 barg; Location IV: offset 3 barg;
 Location V: offset 4 barg

Figure 4-27 Time traces of the pressure at the inlet of Wavy III of 7 bends at Location I to V

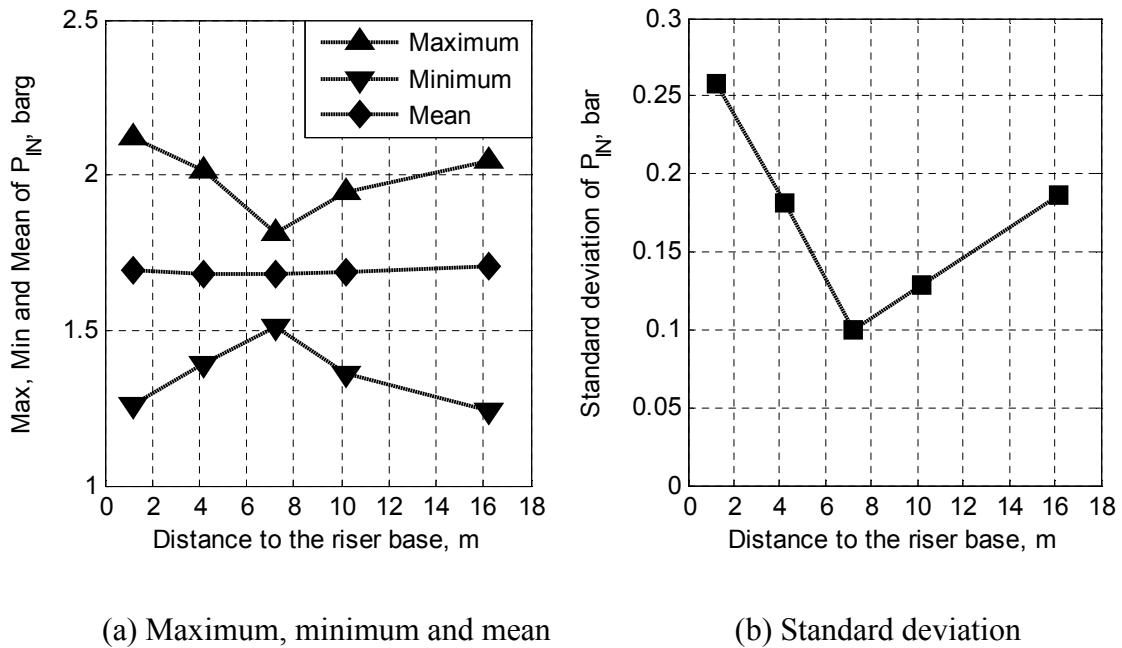


Figure 4-28 Maximum, minimum, mean and standard deviation of the pressure at the inlet of Wavy III of 7 bends at Location I to V

To sum up, the effects of the location of the wavy pipe have been examined by inspecting the riser DP, wavy DP and pressure at the inlet of the wavy pipe. The wavy pipe, Wavy III of 7 bends, has been tested at Location I (1.2 m upstream of the riser base), II (4.2 m), III (7.2 m), IV (10.2 m) and V (15.2 m). It has been found that:

- (1) with the increase of the distance between the riser base and wavy pipe outlet, i.e. from Location I to Location V, the maximum and fluctuation amplitude of the riser DP firstly decreases then increases; the lowest maximum and fluctuation amplitude of the riser DP are obtained with the wavy pipe at Location III; the mean riser DP remains almost unchanged; the lowest cycle time, i.e. highest slug frequency, is obtained with the wavy pipe at Location III;
- (2) the wavy DP is not affected by the location of the wavy pipe significantly; the pressure at the inlet of the wavy pipe at different locations behaves similarly to the

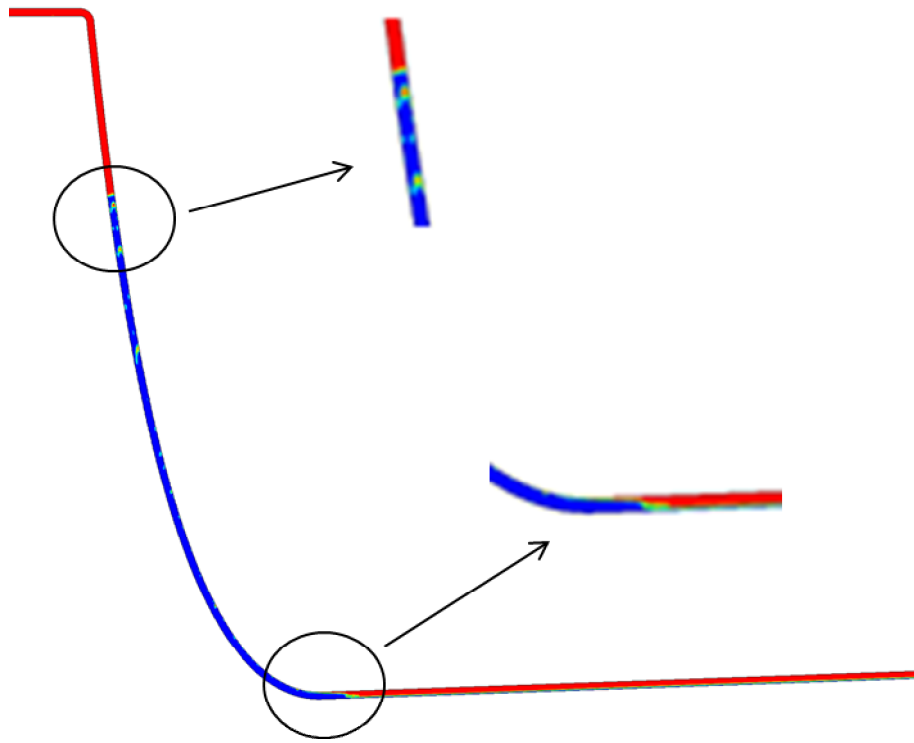
riser DP; the lowest maximum and fluctuation amplitude of the pressure at the wavy pipe inlet can be obtained at Location III.

Therefore, at Location III the wavy pipe is the most effective on reducing the slug length/severity of the flow. It is concluded that an appropriate location to place a wavy pipe exists to obtain the best performance of the wavy pipe on slug mitigation.

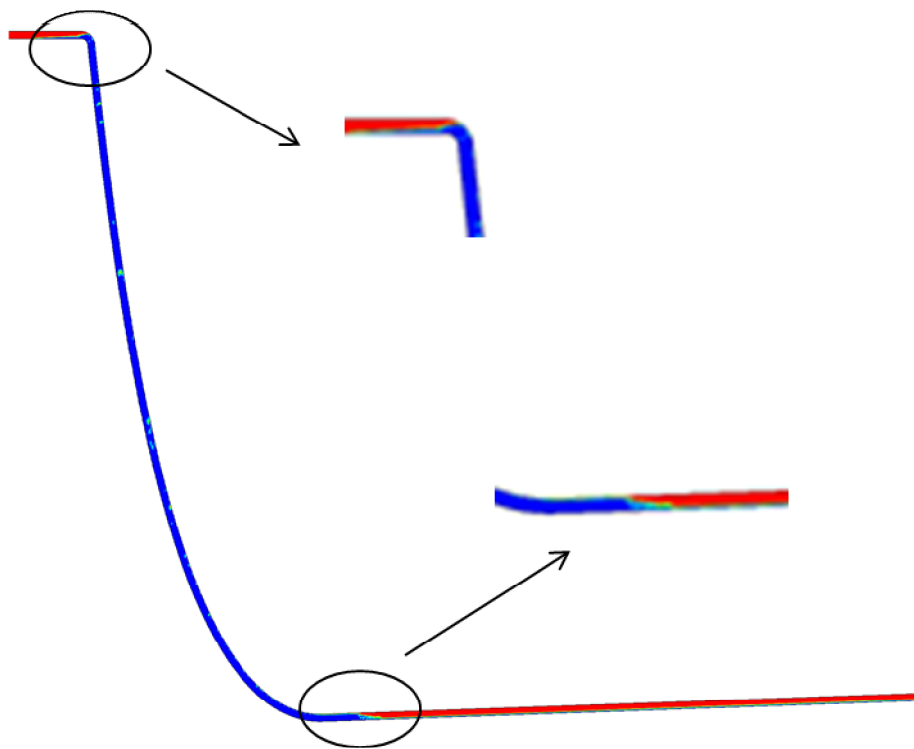
4.4.6 Phase Distribution in the Pipeline/Wavy-Pipe/Riser Systems

The effects of the geometrical parameters and the location of the wavy pipe on slug mitigation have been discussed in the above sections (Section 4.4.3, 4.4.4 and 4.4.5). To obtain an understanding of how the performance of the wavy pipe being affected, it is of essential importance to inspect the phase distribution in the plain riser and pipeline/wavy-pipe/riser systems.

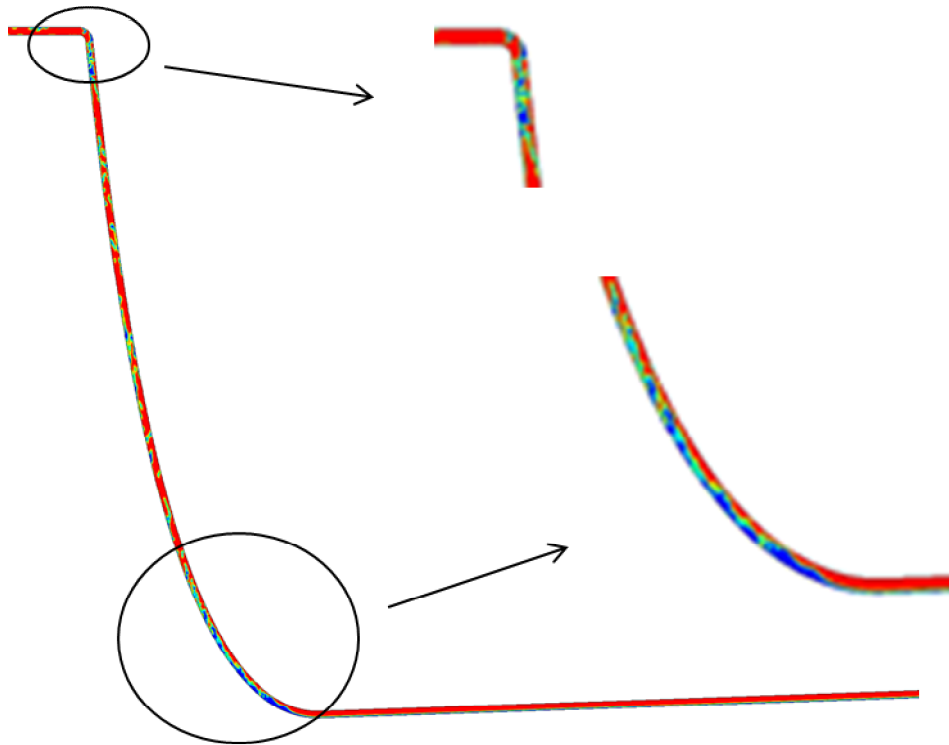
The phase distribution of air and water in the plain riser system is illustrated in Figure 4-29. For severe slugging the liquid slug grows in both of the riser and pipeline at the liquid buildup stage and there is little gas penetrating into the riser. At the end of the liquid buildup stage the riser is almost filled with the liquid phase. Consequently the riser DP, mainly induced by the hydrostatic pressure of the liquid column, arrives at its maximum. Most of the liquid phase has been pushed out of the riser at the end the gas-blowdown/liquid-fallback stage, as a result, the riser DP arrives at its minimum.



(a) Liquid buildup stage



(b) End of liquid buildup stage



(c) End of gas-blowdown/liquid-fallback stage

■: Water; ■: Air

Figure 4-29 Phase distribution in the plain riser at the liquid buildup stage, the end of the liquid buildup stage and the gas-blowdown/liquid-fallback stage

The flow behaviour in the pipeline/wavy-pipe/riser systems is discussed through the comparison with that in the plain riser as illustrated in Figure 4-29.

Wavy pipes of different amplitudes: Wavy I and Wavy III; 7 bends; Location III

It has been concluded in Section 4.4.3 that the slug length and severity of the flow can be reduced further as indicated by the lower maximum and fluctuation amplitude of the riser DP with a higher-amplitude wavy pipe. The phase distribution in the pipeline/wavy-pipe/riser systems with Wavy I and Wavy III is compared. Figure 4-30, 4-31 and 4-32 show the phase distribution at the liquid buildup stage, the end of the liquid buildup stage and the gas-blowdown/liquid-fallback stage, respectively. The

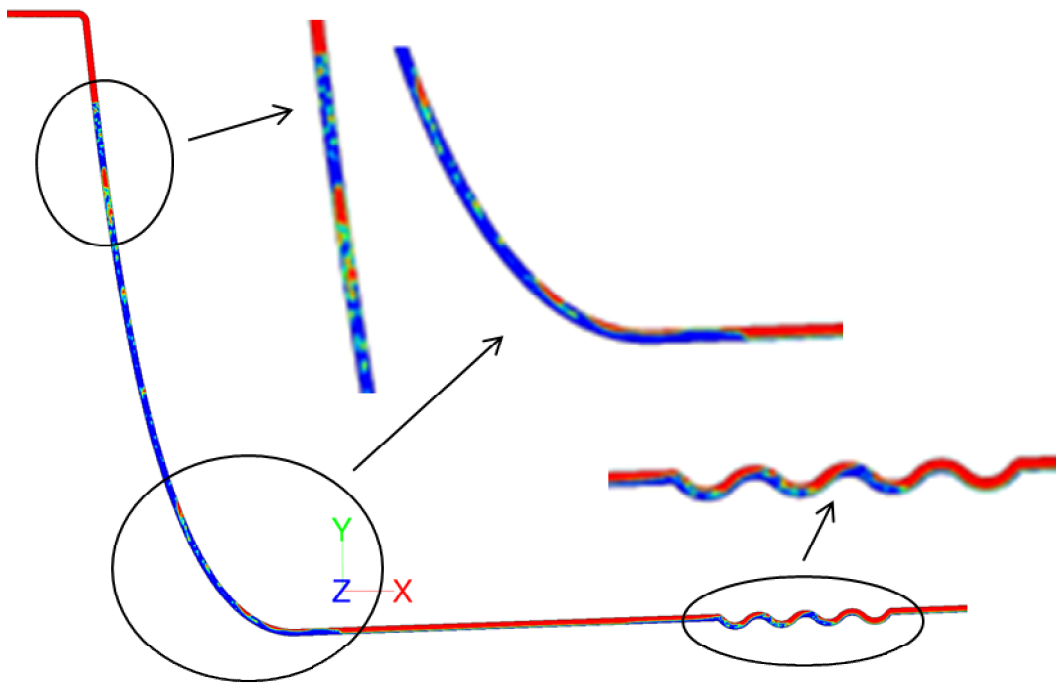
following discussion explains how the higher-amplitude wavy pipe works to reduce the slug length further.

Different from the plain riser system in Figure 4-29 there is no possibility for a slug as long as the riser to form in the pipeline/wavy-pipe/riser system. It can be observed in Figure 4-30 that some large bubbles have penetrated into the liquid slug in the riser at the liquid buildup stage. The gas bubbles come directly from the trapped gas in the pipe section between the riser base and the wavy pipe outlet. With a wavy pipe applied in the pipeline, a certain amount of gas is trapped in the pipe section between the riser base and the wavy pipe outlet and in the wavy pipe. As can be seen in Figure 4-30 the gas is mainly trapped in the top of the Λ sections and the downward limbs of the wavy pipe (looking in the direction of the flow to the riser base) and the liquid accumulates in the dips of the V sections and the upward limbs forming 'mini slugs'. With the gas and liquid coming from the inlet of the pipeline continuously, the pressure upstream of the wavy pipe increases. Then some gas penetrates into the mini slugs in the wavy pipe and then arrives at the wavy pipe outlet. As more and more gas moves into the pipe section between the riser base and wavy pipe outlet the pressure in the pipe section increases. When the pressure is high enough the trapped gas penetrates into the liquid column in the riser in the form of large bubbles. The penetration of the gas bubbles reduces the effective density of the liquid column in the riser then reduces the hydrostatic pressure at the riser base. Consequently it becomes easier for the subsequent large bubbles to penetrate into the riser.

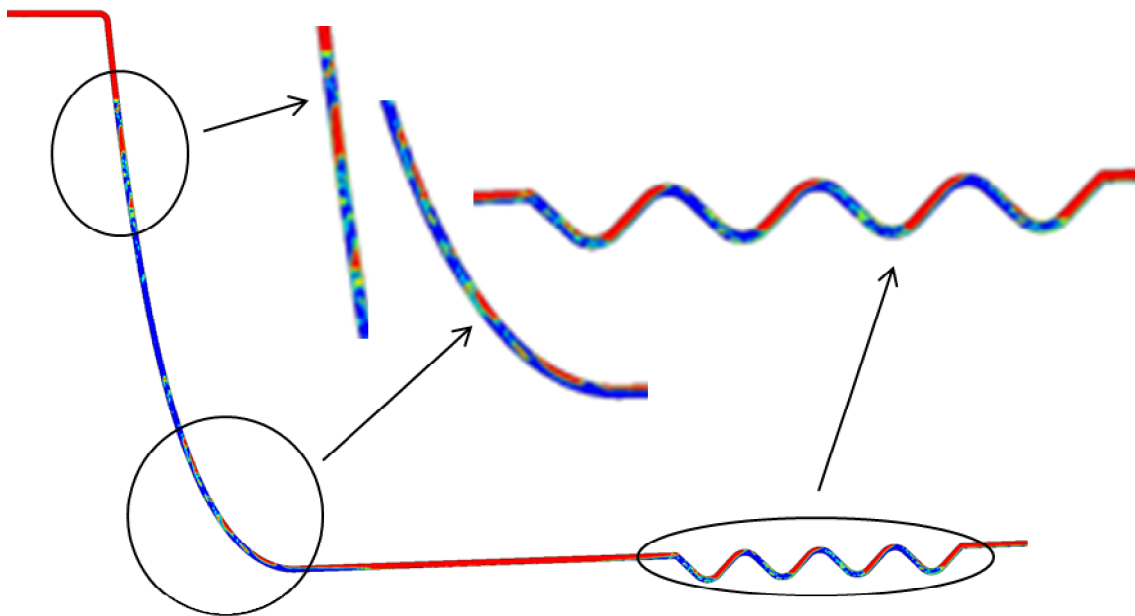
With the increase of the amplitude of the wavy pipe the length of each limb increases. The longer limbs allow for longer mini slugs to form and provide more space for more gas to be trapped in. As can be seen in Figure 4-30 there are 3 short mini slugs in Wavy I and 4 longer mini slugs in Wavy III. More gas penetration can be induced by more trapped gas upstream of the riser base. It can be seen in Figure 4-31 that more gas has penetrated into the riser with Wavy III than Wavy I. Consequently, a lower maximum riser DP, i.e. shorter slug in the riser, is obtained with Wavy III than Wavy I at the end of the liquid buildup stage.

The minimum riser DP with Wavy III is higher than that with Wavy I. The minimum riser DP appears at the end of the gas-blowdown/liquid-fallback stage as shown in

Figure 4-32. The stratified flow prevails in the pipeline including Wavy I, while in the pipeline with Wavy III there are still packages of liquid in the wavy pipe. Then the liquid packages move into the riser and form aerated slugs. Therefore, at the end of the gas-blowdown/liquid-fallback stage, the two-phase flow in the riser with Wavy III still takes the form of highly aerated slugs. However, in the pipeline/wavy-pipe/riser system with Wavy I in Figure 4-32 (a) or the plain riser system in Figure 4-29 (c), most of the liquid in the riser attaches onto the wall and no liquid slugs form to block the gas path. To summarise, the minimum riser DP is mainly induced by the aerated slugs and gas flow with Wavy III and Wavy I, respectively. Therefore, the riser DP with Wavy III is higher than that with Wavy I. It is concluded that a lower fluctuation amplitude of the riser DP can be obtained with Wavy III.



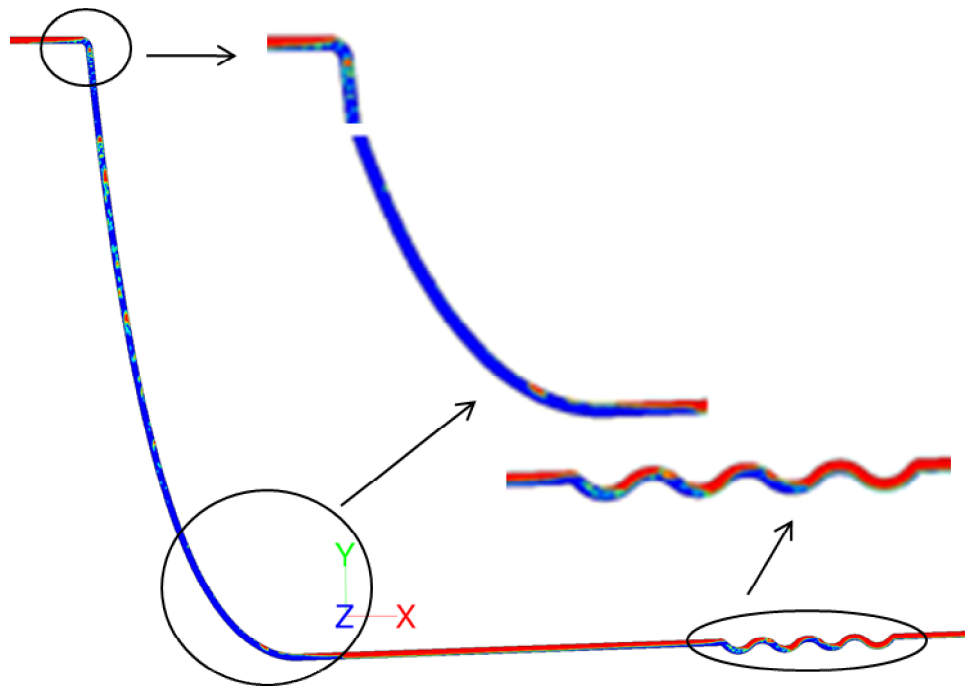
(a) Wavy I



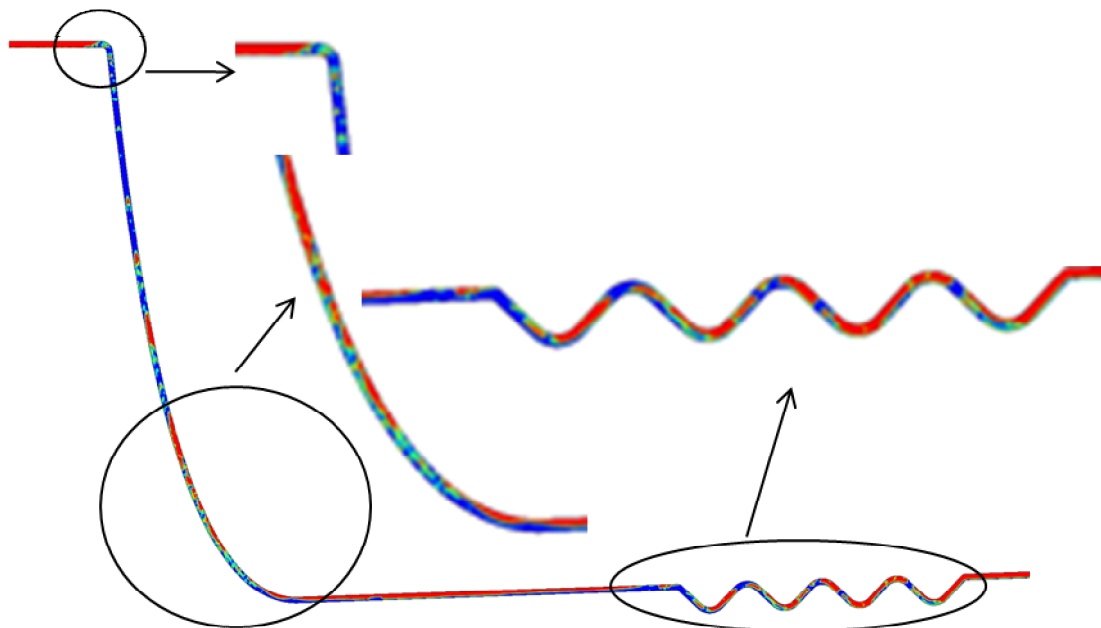
(b) Wavy III

■: Water; ■: Air

Figure 4-30 Phase distribution at the liquid buildup stage with Wavy I and Wavy III at Location III



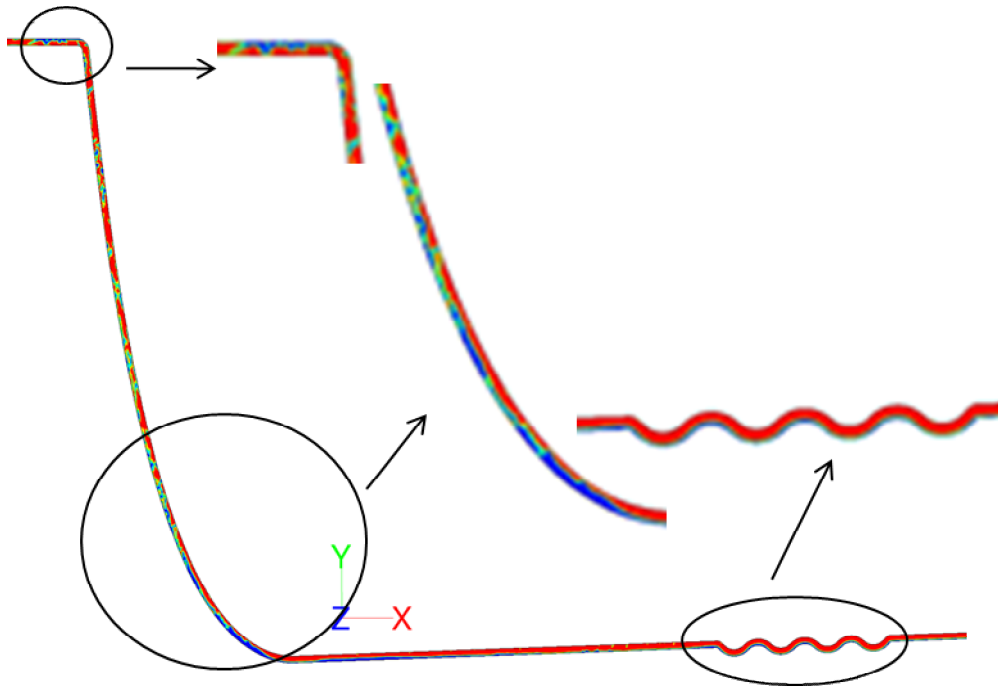
(a) Wavy I



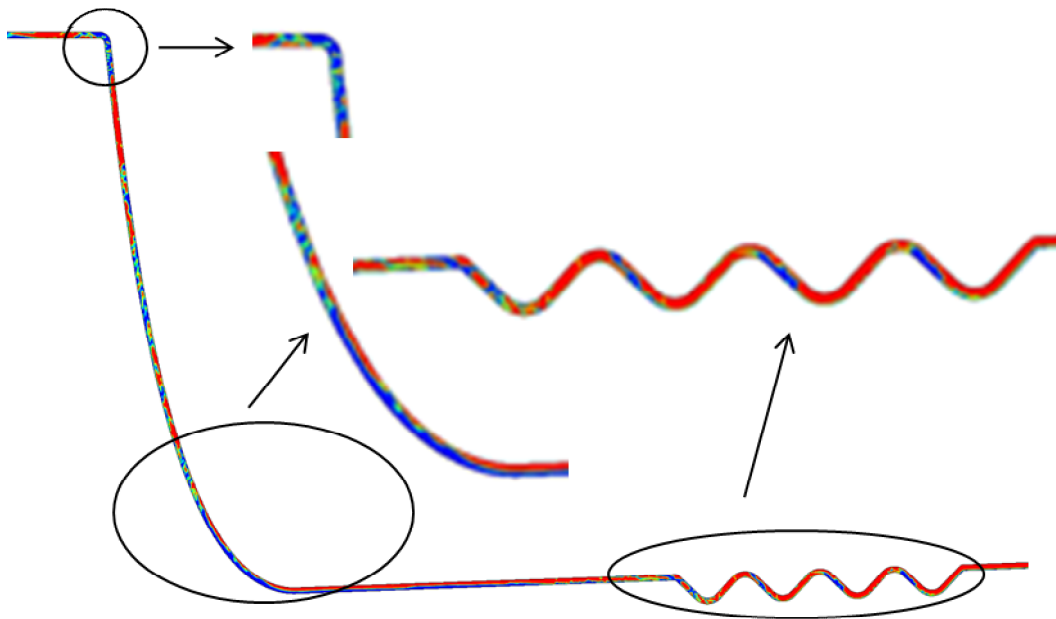
(b) Wavy III

■: Water; ■: Air

Figure 4-31 Phase distribution at the end of the liquid buildup stage with Wavy I and Wavy III at Location III



(a) Wavy I



(b) Wavy III

■: Water; ■: Air

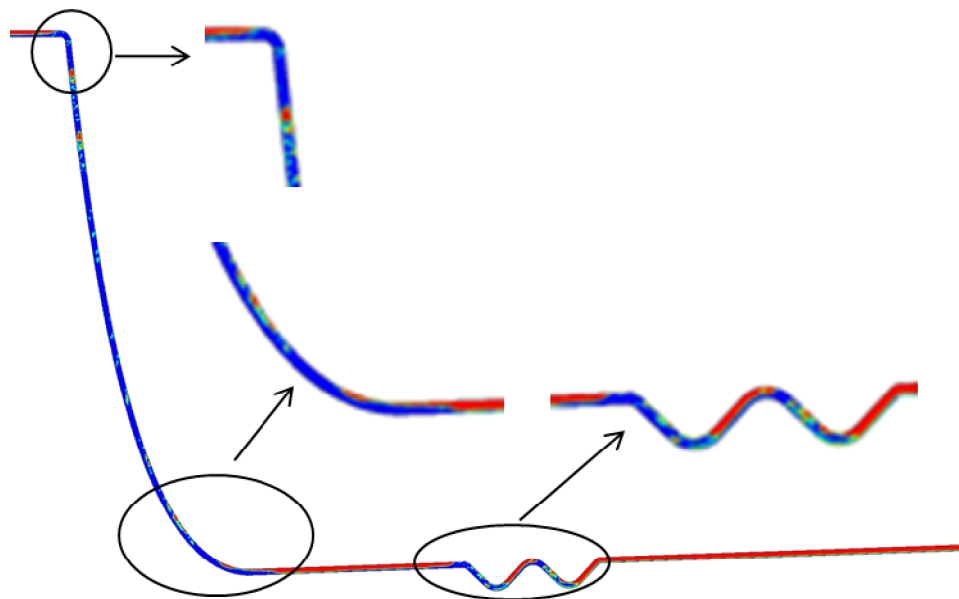
Figure 4-32 Phase distribution at the end of the gas-blowdown/liquid-fallback stage with Wavy I and Wavy III at Location III

Wavy pipes of different lengths: 3 and 11 bends; Wavy III; Location II

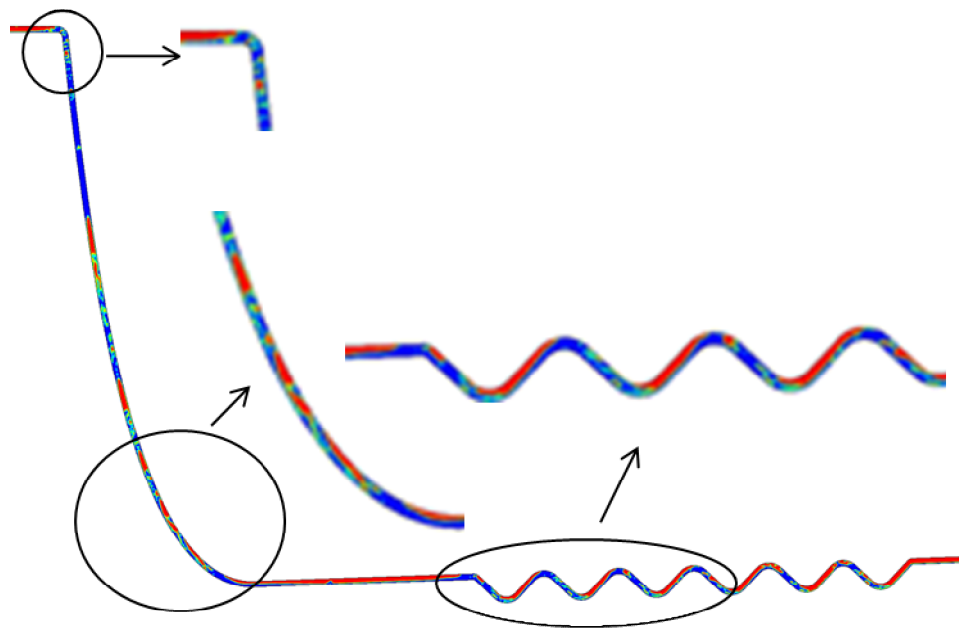
It has been concluded in Section 4.4.4 that the slug length and severity of the flow can be reduced further by applying a wavy pipe of more bends. The phase distribution in the pipeline/wavy-pipe/riser systems with Wavy III of 3 and 11 bends at Location II is shown in Figure 4-33 and Figure 4-34. The following discussion explains how the longer wavy pipe works to reduce the slug length further.

Figure 4-33 compares the phase distribution in the pipeline/wavy-pipe/riser systems with 3-bend and 11-bend wavy pipes at the end of the liquid buildup stage, when the maximum riser DP appears. It can be seen that much more gas has penetrated into the liquid slug in the riser with the 11-bend wavy pipe than that with the 3-bend wavy pipe. Thus the maximum riser DP with the 11-bend wavy pipe is much lower than that with the 3-bend wavy pipe. The 11-bend wavy pipe allows for more gas to be trapped and more mini slugs forming in it. Then the trapped gas and newly formed mini slugs in the wavy pipe move into the riser at the liquid buildup stage.

Figure 4-34 compares the phase distribution in the pipeline/wavy-pipe/riser systems with 3-bend and 11-bend wavy pipes at the end of the gas-blowdown/liquid-fallback stage, when the minimum riser DP appears. As we can see there are short and highly aerated slugs in the riser and small pockets of liquid in the 3-bend wavy pipe; while with the 11-bend wavy pipe, there are more and longer liquid slugs in the riser and more pockets of liquid in the wavy pipe. The longer liquid slugs in the riser result in a higher riser DP, i.e. a higher minimum riser DP in a cycle. The longer slugs in the riser mainly result from the more mini slugs in the wavy pipe of more bends (11 bends).



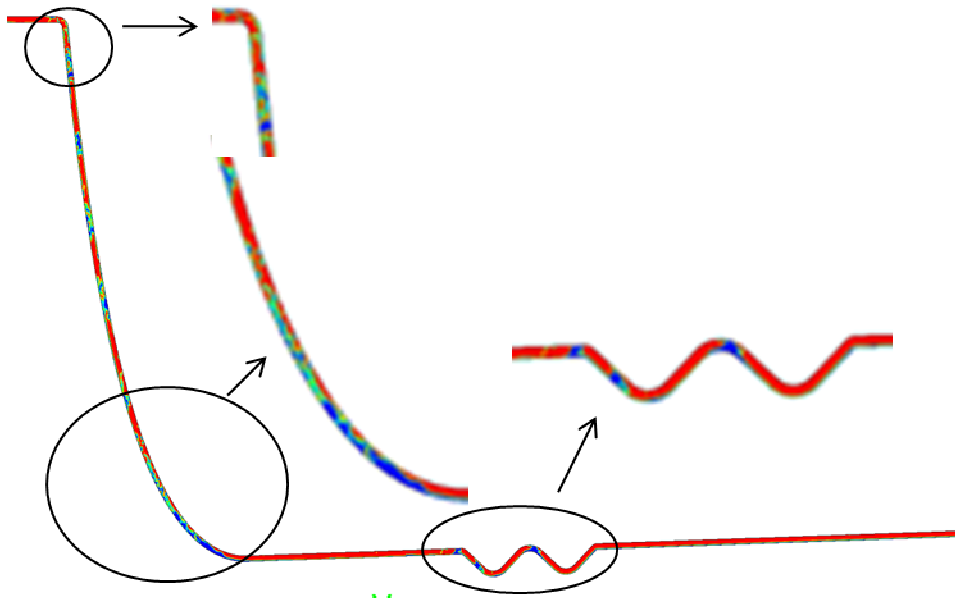
(a) 3 bends



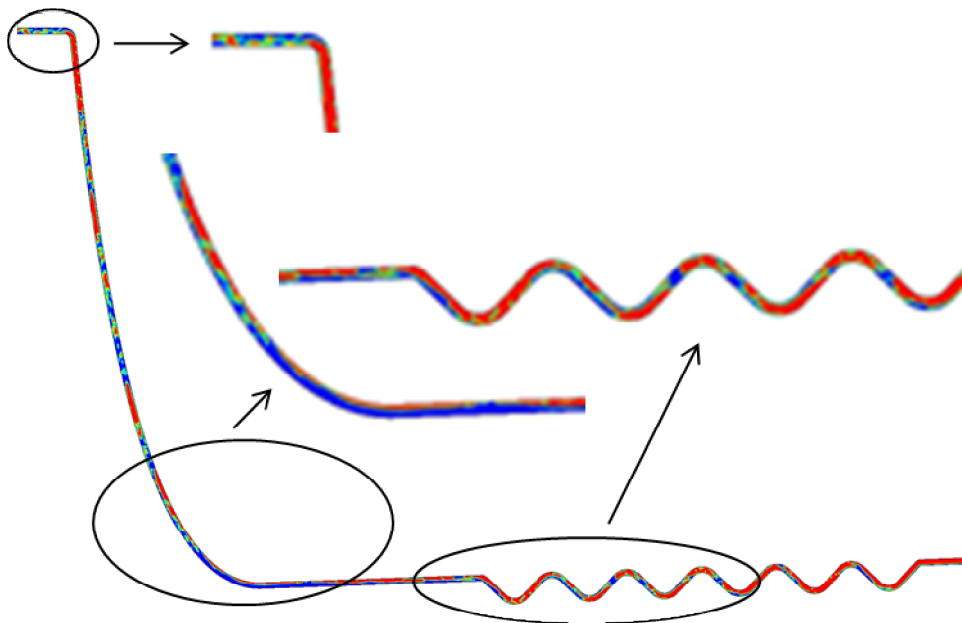
(b) 11 bends

■: Water; ■: Air

Figure 4-33 Phase distribution at the end of the liquid buildup stage with Wavy III of 3 bends and 11 bends at Location II



(a) 3 bends



(b) 11 bends

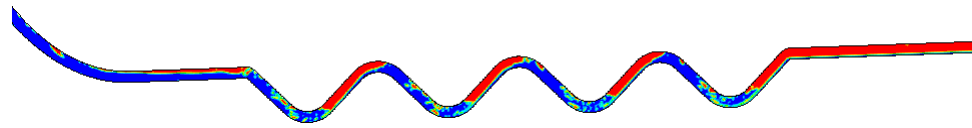
■: Water; ■: Air

Figure 4-34 Phase distribution at the end of the gas-blowdown/liquid-fallback stage with Wavy III of 3 bends and 11 bends at Location II

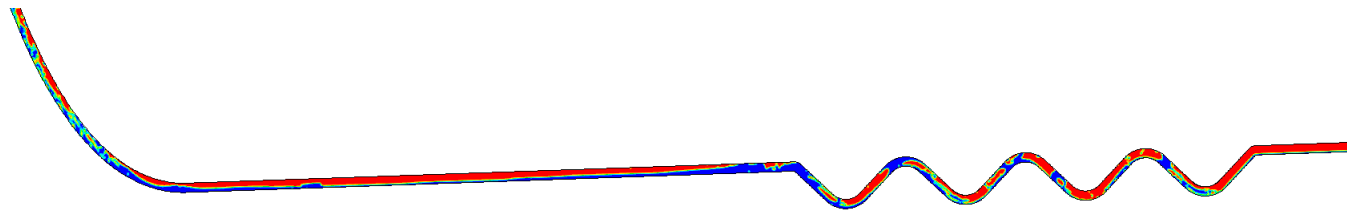
Wavy pipes at different locations: Location I, III and V; Wavy III; 7 bends

The wavy pipe, Wavy III, of 7 bends has been installed at five locations in the pipeline and the effects of the location have been discussed in Section 4.4.5. The experimental data have revealed that Location III is the most desirable location among Location I to V. The distance between the riser base and the wavy pipe outlet is 1.2 m, 4.2 m, 7.2 m, 10.2 m and 16.2 m for Location I to V, respectively.

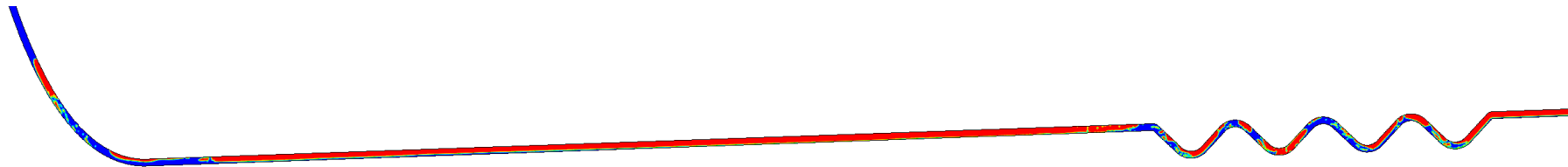
Figure 4-35 shows the phase distribution in the lower part of the riser and the wavy pipe at Location I, III and V at the end of the liquid buildup stage. As presented in Section 4.4.5 the lowest maximum riser DP is obtained with the wavy pipe at Location III. A lower riser DP indicates that more gas has penetrated into the riser at the liquid buildup stage. The bubble penetration into the slug body in the riser only happens when the pressure behind the slug tail is high enough. The high pressure is induced by the compression of the gas. Thus a sufficient amount of gas and an appropriate space for the gas to be stored and compressed are the two key factors to initiate the bubble penetration process. The pipe section between the riser base and the wavy pipe outlet can provide a space for the gas to be stored and compressed. With a short pipe section, i.e. 1.2 m for Location I as shown in Figure 4-35 (a), a majority of the pipe section is occupied by the liquid phase. The space left for the gas to be stored and compressed is quite limited. With a very long pipe section, i.e. 16.2 m for Location V as shown in Figure 4-35 (c), a much larger space has been provided. However, to obtain the same pressure high enough to initiate the bubble penetration process, much more gas is required by a longer pipe section than that by a shorter one. It is postulated that the amount of the gas trapped in the pipe section and the subsequent addition from the wavy pipe is not enough with the wavy pipe at Location V for the test case in Section 4.4.5. Therefore, a pipe section of an appropriate length is required to initiate the bubble penetration process. A better performance of the wavy pipe has been obtained with the wavy pipe at Location III with the pipe section of 7.2 m than that at Location I and V. As can be seen in Figure 4-35 (b) more gas has penetrated into the slug in the riser and the slug becomes more aerated. Consequently, the effective slug length is shorter than that with the wavy pipe at Location I and V.



(a) Location I



(b) Location III



(c) Location V

■: Water; ■: Air

Figure 4-35 Phase distribution at the end of the liquid buildup stage with Wavy III of 7 bends at Location I, III and V

4.4.7 Discussions

The pipeline/wavy-pipe/riser system has been simulated through a 2-D CFD model. Three groups of numerical tests have been carried out to examine the effects of the geometrical parameters and locations of the wavy pipe on mitigating the severity of the flow. The severity of the flow regimes, such as severe slugging and oscillation flow, can be assessed by the length of the liquid slug in the pipeline/riser system. The maximum and minimum riser DP can be used to estimate the maximum and minimum length (or equivalent length) of the liquid column in the riser.

The differential pressure across the wavy pipe, wavy DP, is of concern because the additional pressure loss induced by the application of a wavy pipe needs to be understood. The pressure upstream of the wavy pipe is an important parameter because the flowrates at the inlet of the pipeline are highly dependent on it in the field production systems. Mechanical oscillations of the wavy pipe can be induced by the gas/liquid two-phase flow passing through the up and down limbs. The forces on the wavy pipe need to be known when designing the pipe supporting system for the pipeline.

With a higher-amplitude wavy pipe applied the slug length in the riser can be reduced further; the fluctuation amplitude of the riser DP and the pressure upstream of the wavy pipe become lower; however, the mean, maximum and fluctuation amplitude of the drag and lift forces on the wavy pipe increase sharply. The forces on the wavy pipe have to be taken into account when designing a pipeline/wavy-pipe/riser system and the corresponding pipe supporting system. For a given pipeline/riser system experiencing severe slugging, the flow regime induced instability can be reduced further by applying a higher-amplitude wavy pipe, but the instability induced by the forces on the wavy pipe rises. Similar effects of increasing wavy pipe amplitude have been found when increasing the length of the wavy pipe. With the increase of the length of the wavy pipe the slug length in the riser can be reduced further; however, the mean, maximum and fluctuation amplitude of the wavy DP increases sharply.

The location of the wavy pipe has significant effects on its performance of slug mitigation. The reduction of the slug length, i.e. reduction of the severity of the flow, is achieved by the bubble penetration at the liquid buildup stage. With the wavy pipe

placed at an appropriate location the bubble penetration process can be initiated earlier and more gas can be pushed into the riser at the liquid buildup stage than that with the wavy pipe located elsewhere. The length of the pipe section between the riser base and the wavy pipe outlet is very important, because it provides a space for the gas to be stored and compressed. To obtain a high-enough pressure for the bubble penetration, a sufficient amount of gas and an appropriate volume of space are crucial. The required amount of gas and volume of space are affected by the geometries and dimensions of the pipeline/riser and wavy pipe and the operating conditions. For a pipeline/riser system and a wavy pipe at given operating conditions, an optimum length of the pipe section between the riser base and the wavy pipe outlet exists.

4.5 Summary

The gas/liquid two-phase flow in the pipeline/riser and pipeline/wavy-pipe/riser systems has been simulated applying CFD. Firstly, a 2-D CFD model of the pipeline/riser system was developed and the model predictions were verified by the experimental data. Secondly, the CFD model was applied to assess the performance of two classical severe slugging mitigation techniques. Thirdly, the CFD model was extended to include the wavy pipe to examine the effects of the geometrical parameters and location in the pipeline of the wavy pipe on its performance of slug mitigation.

Validated by the experimental data the proposed 2-D CFD model of the pipeline/riser system is able to predict the flow regime transition and slug frequency reasonably well. It has been found that the discrepancy between model predictions and experimental data are flow conditions dependent such as water flowrate and flow regime. The minimum riser DP is under predicted by the CFD model consistently. The major reason is that the resistance in the system is not represented adequately by the 2-D model. Qualitative agreement with the experimental results has been obtained when two classical slug mitigation methods, i.e. increasing back pressure and choking riser outlet valve, are applied to the CFD model. This shows the potential of the proposed CFD model for evaluating the performance of severe slugging mitigation techniques. The encouraging results from the CFD model of the pipeline/riser system give confidence in applying the proposed model to the pipeline/wavy-pipe/riser system.

The CFD modelling provides a feasible way to examine the effects of the amplitude, length and location of the wavy pipe on its performance of slug mitigation in detail. With a higher-amplitude wavy pipe applied the slug length in the riser can be reduced further; the fluctuation amplitude of the riser DP and the pressure upstream of the wavy pipe become lower; however, the mean, maximum and fluctuation amplitude of the drag and lift forces on the wavy pipe increase sharply. The forces on the wavy pipe have to be taken into account when designing a pipeline/wavy-pipe/riser system and the corresponding pipe supporting system. For a given pipeline/riser system experiencing severe slugging, the flow regime induced instability can be reduced further by applying a higher-amplitude wavy pipe, but the instability induced by the forces on the wavy pipe rises. Similar effects of increasing wavy pipe amplitude have been found when increasing the length of the wavy pipe. With the increase of the length of the wavy pipe the slug length in the riser can be reduced further; however, the mean, maximum and fluctuation amplitude of the wavy DP increases sharply.

The location of the wavy pipe has significant effects on slug mitigation. The reduction of the slug length, i.e. reduction of the severity of the flow, is achieved by the bubble penetration at the liquid buildup stage. With the wavy pipe placed at an appropriate location the bubble penetration process can be initiated earlier and more gas can be pushed into the riser at the liquid buildup stage. The length of the pipe section between the riser base and the wavy pipe outlet is very important, because it provides a space for the gas to be stored and compressed. To obtain a high-enough pressure for bubble penetration, a sufficient amount of gas and an appropriate volume of space are crucial. The required amount of gas and volume of space are affected by the geometries and dimensions of the pipeline/riser and wavy pipe and the operating conditions. For a pipeline/riser system and a wavy pipe at given operating conditions, an optimum length of the pipe section between the riser base and the wavy pipe outlet exists.

5 EXPERIMENTAL STUDY ON HYDRODYNAMIC SLUG FLOW MITIGATION USING WAVY PIPES IN HORIZONTAL PIPELINES

5.1 Introduction

It has been demonstrated in Chapter 3 and 4 that the wavy pipe is effective on mitigating severe slugging in pipeline/riser systems. The effects of the wavy pipe on hydrodynamic slug flow are investigated experimentally in this Chapter. The experiment was conducted on a horizontal two-phase (air/water) test facility in PSE Laboratory. A 2” wavy pipe of 7 bends was installed in the test section. A wide range of superficial air and water velocities was tested. Firstly the flow regimes in this test rig were observed; secondly the flow behaviour upstream of the wavy pipe, in the wavy pipe and downstream of the wavy pipe was analysed; finally the performance of the wavy pipe on hydrodynamic slug mitigation and how the wavy pipe works were discussed. The experimental data are also used for the development and validation of the simulation models in Chapter 6.

5.2 Experimental Campaign

5.2.1 Two-Phase Test Facility

The experiment was conducted on a 2” air/water two-phase test facility in PSE Laboratory. The schematic of the test facility is shown in Figure 5-1.

The water was pumped into the flowline from a water tank of capacity 4.4 m³. A Worthington Simpson centrifugal pump with a maximum capacity of 40 m³/h and a maximum discharge pressure of 5 barg was employed. The water flow to the flowline was controlled by two valves located in the flowline and bypass line, respectively. The bypass line could direct a portion of the water from the pump outlet back to the tank. The other portion of the water passed the liquid metering station then mixed with the air flow at the mixing point. The air was supplied by a Screw Engineering compressor with a maximum supply capacity of 400 m³/h and a maximum discharge pressure of 10 barg.

The compressed air accumulated in a tank receiver of capacity 2.5 m³ to reduce the pressure fluctuation induced by the compressor. Then the air from the receiver flowed to the gas metering station through a needle valve.

At the mixing point the air was fed into the water flow perpendicularly on the top of the pipeline. The air/water two-phase mixture flowed through the test section located 15 m downstream of the mixing point. Then the two-phase flow returned to the water tank open to the atmosphere.

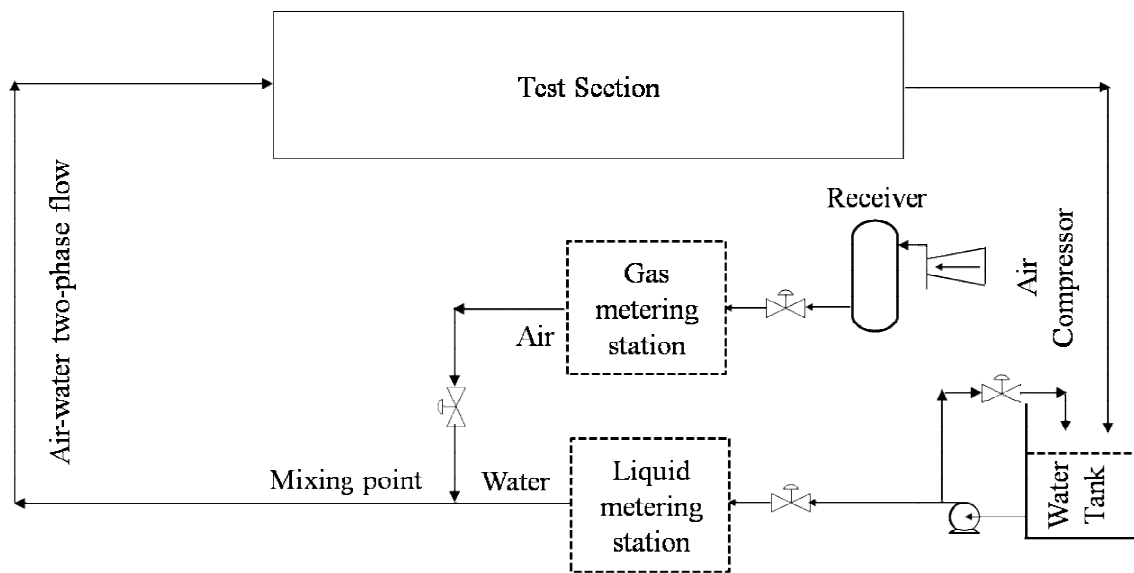
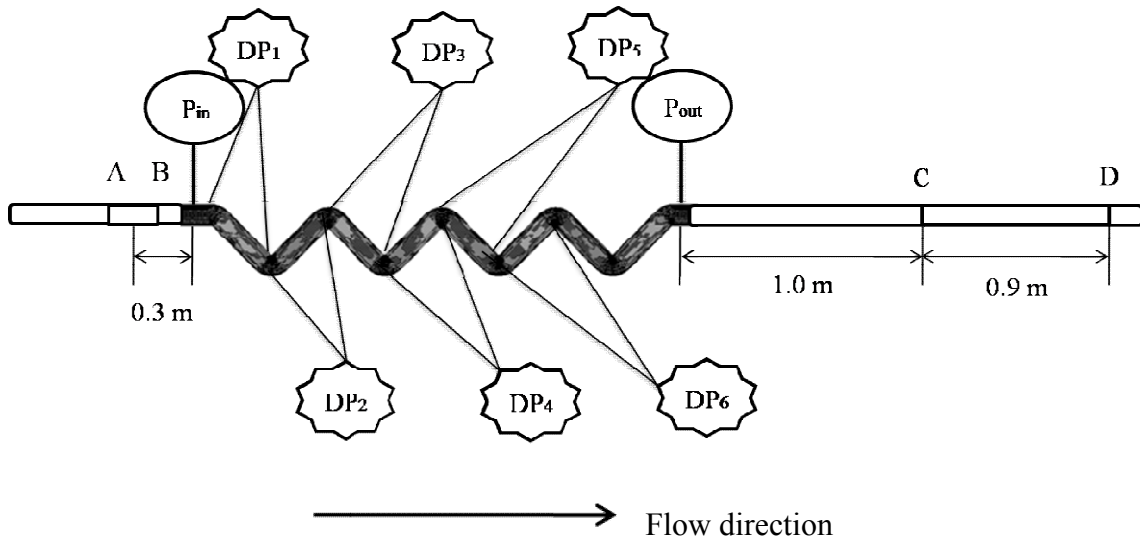


Figure 5-1 Schematic of the two-phase test facility

The water flow was metered by an electromagnetic flow meter (Khrone Altopflux Series electromagnetic K280/0 AS model) with a range of 0-4.524 m³/h and an uncertainty of $\pm 1\%$ of full scale. The air flow was metered by two Quadrina gas turbine flow meters (QFG/13B/EP1 and QFG/25B/EP1) for low and high flowrates, respectively. They had measuring ranges of 1-8 m³/h and 6-60 m³/h respectively and the same uncertainty of $\pm 1\%$ of full scale. At the gas metering station the temperature and pressure were measured by pressure transducers (range 0-5 barg, uncertainty $\pm 1\%$ of full scale) and thermocouples (range 0-100 °C, uncertainty $\pm 1\%$ of full scale), respectively.

5.2.2 Test Section with a Wavy Pipe

The test section consisted of a 2" wavy pipe of 7 bends and a view section downstream. A series of instruments was distributed along the wavy pipe and view section. In order to monitor the liquid holdup conductivity cells were allocated upstream and downstream of the wavy pipe, respectively. To monitor the pressures at the inlet/outlet and differential pressures across the limbs of the wavy pipe, two pressure transducers and six differential pressure transducers were installed. The instrument configuration in the test section, i.e. the wavy pipe and view section, are illustrated in Figure 5-2.



A, B, C and D: Conductivity cells; P_{in} and P_{out} : Pressure transducer;

DP₁ to DP₆: Differential pressure transducers

Figure 5-2 Schematic of the test section with instruments

The pipe section between the mixing point and the inlet of the wavy pipe is 15 m long (about $300d$, $d = 0.052$ m, the pipe diameter) and the downstream section between the wavy pipe outlet and water tank is 3.5 m. In order to examine the effects of the wavy pipe on the two-phase flow behaviour a series of flow parameters were measured. The liquid holdup and pressure upstream and downstream of the wavy pipe were measured

by conductivity cells and pressure transducers (PMP 4070, range 0-1.5 barg and 0-1.0 barg for inlet and outlet, uncertainty $\pm 0.04\%$ of full scale). The differential pressure across each limb of the bends was measured by differential pressure transducers (PMP 4170, range from -200 to 200 mbar, uncertainty $\pm 0.04\%$ of full scale). The conductivity cells (A, B, C and D) provide a continuous measurement of the liquid holdup. Each set of the conductivity cell employed in the experiment included one pair of ring electrodes flush mounted to the pipe wall. The ring electrodes with a width of 3.7 mm each were made of stainless steel and spaced 17 mm apart to form one cell (Al-lababidi, 2006; Adedigba, 2007).

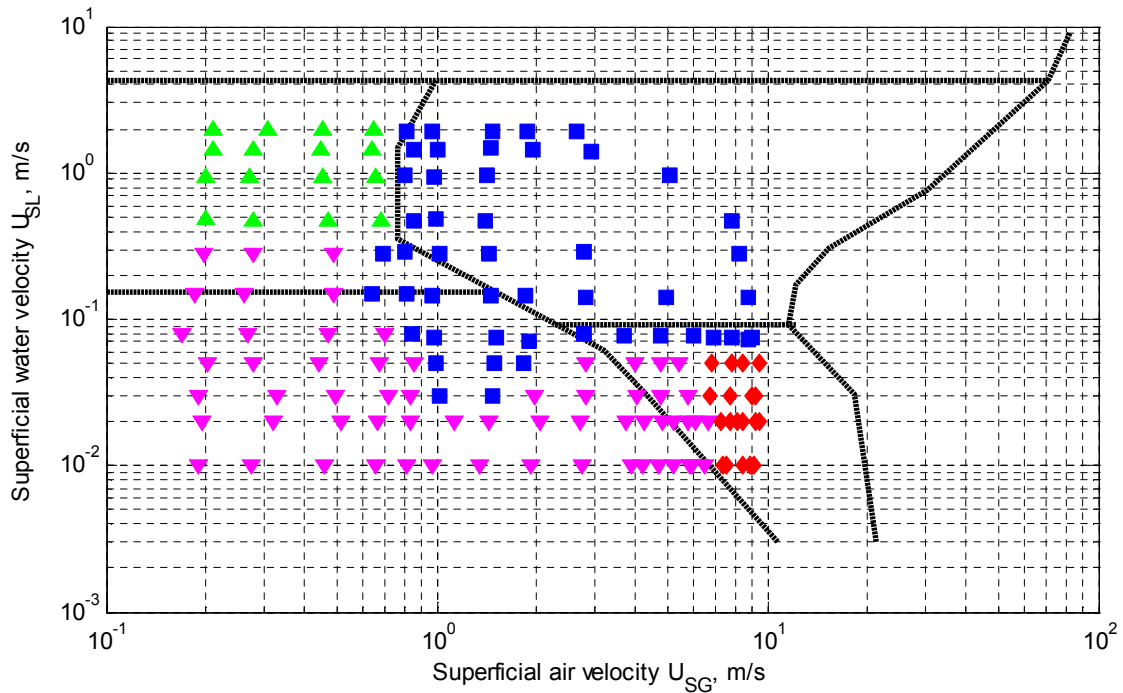
The outputs of all the instruments were connected to a PC where the data were recorded using a Labview[®] data acquisition programme. The sampling rate of all the data was set to be 20 Hz.

5.3 Flow Behaviour in the Horizontal Wavy-Pipe System

5.3.1 Flow Regime Upstream of the Wavy Pipe

The flow regimes upstream of the wavy pipe were observed visually during the tests and then confirmed by the liquid holdup time traces obtained by the conductivity cells A and B (see Figure 5-2). The flow regime map proposed by Mandhane *et al.* (1974) has been used as a reference for flow regime identification. The flow regimes under consideration are mainly stratified flow, wave flow, elongated bubble flow and slug flow in Mandhane flow regime map. No dispersed flow, annular and annular-mist flow were produced as they are out of the scope of this work.

A wide range of flow conditions in terms of superficial water and air velocities have been tested. The superficial water velocity, U_{SL} , ranges from 0.01 m/s to 2.0 m/s and superficial air velocity, U_{SG} , ranges from 0.2 m/s to 10.0 m/s. The test points are plotted in Mandhane flow regime map as shown in Figure 5-3. The flow regimes observed in the experiment are distinguished by different colours.



■ Slug flow
 ▲ Elongated bubble flow
 ▼ Stratified flow with low-frequency and high-amplitude waves
 ◆ Stratified flow with high-frequency and low-amplitude waves

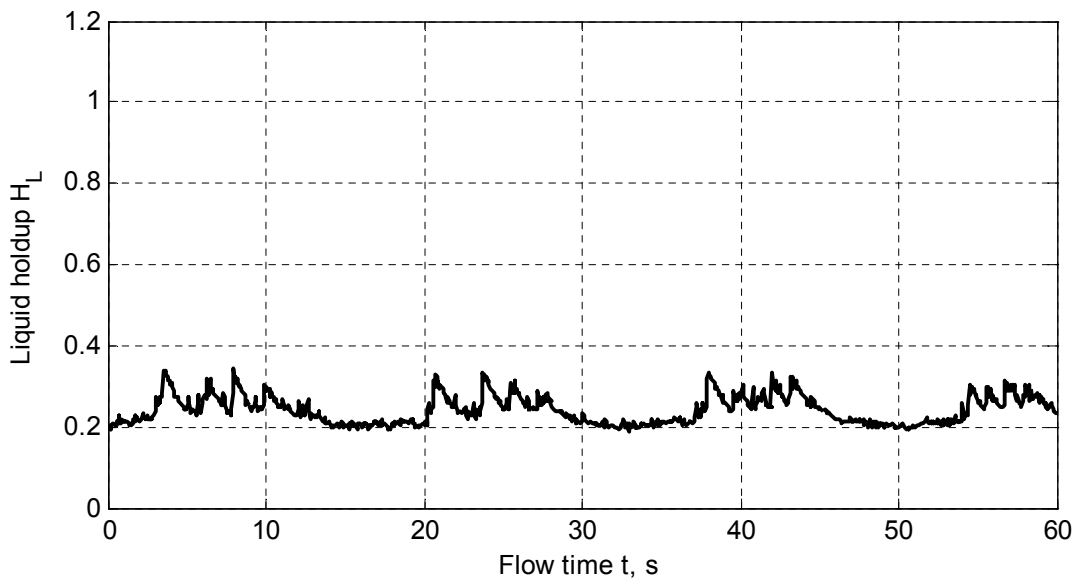
Figure 5-3 Test points and flow regimes in the 2” test rig on Mandhane flow regime map (Mandhane *et al.*, 1974)

Stratified flow with low-frequency and high-amplitude waves:

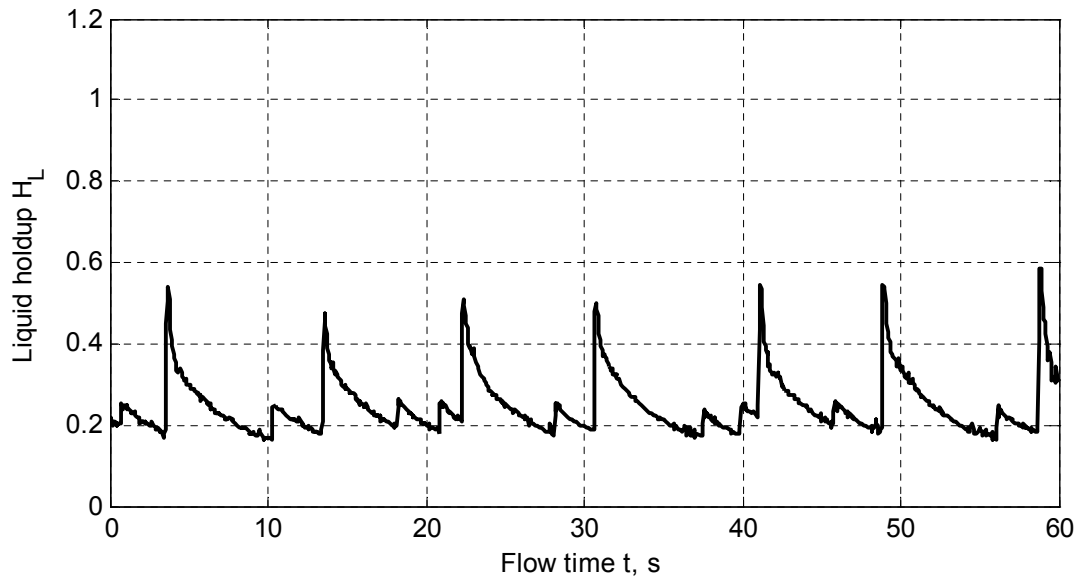
At low superficial gas and liquid velocities the gravitational effects result in a total separation of the two phases. The liquid phase flows along the bottom of the pipe and the gas phase flows along the top. There is a smooth interface between the two phases. However, in the two-phase test rig the stratified smooth flow predicted by Mandhane flow regime map is always accompanied with obvious liquid waves. The liquid waves appear with a low frequency and high amplitude, but they never block the whole cross-section of the pipe. It is postulated that the waves are induced by the two bends (two 90° bends with 0.5 m) in the flow-developing pipe section between the gas/liquid mixing point and test section where the flow regime is monitored. At the bends the liquid

moves towards the outer part of the bend from the bottom due to the centrifugal effect. A chunk of liquid can be produced due to the resistance of the bends. Thus a liquid wave with significantly high amplitude forms from the chunk of liquid downstream of the bends.

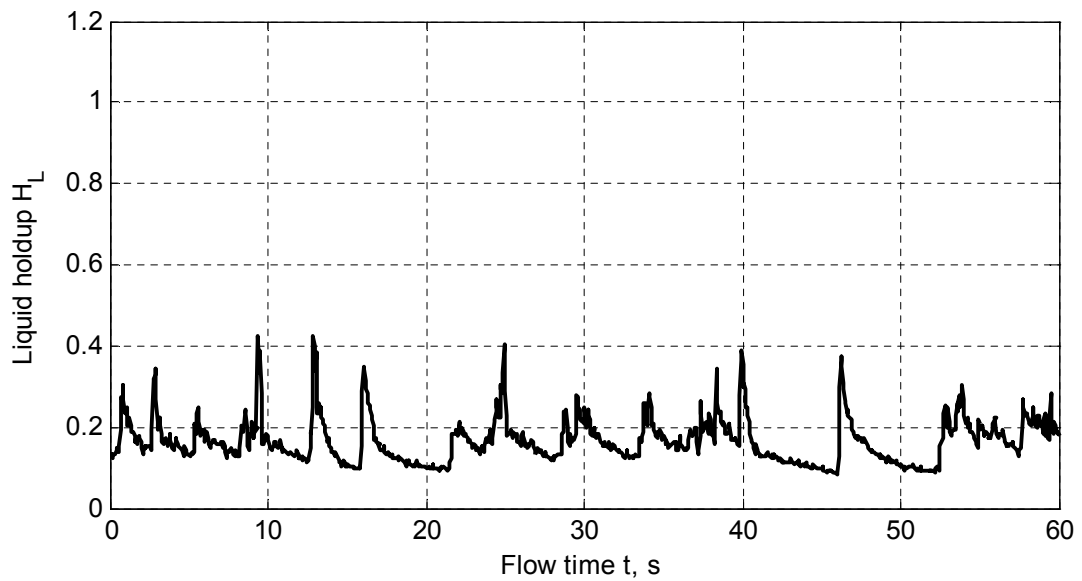
Figure 5-4 shows the liquid holdup time traces of this flow regime at different U_{SG} and the same $U_{SL} = 0.02$ m/s. The wave amplitude increases first then decreases and the frequency increases consistently with the increasing U_{SG} at the same U_{SL} . With the increase of U_{SG} the gas is able to support waves of higher amplitudes, but at even higher U_{SG} the high-amplitude waves tend to be pressed down to the bottom of the pipe as shown in Figure 5-4 (c).



(a) $U_{SL} = 0.02$ m/s $U_{SG} = 0.2$ m/s



(b) $U_{SL} = 0.02$ m/s $U_{SG} = 0.7$ m/s



(c) $U_{SL} = 0.02$ m/s $U_{SG} = 6.0$ m/s

Figure 5-4 Time traces of the liquid holdup for stratified flow with low-frequency and high-amplitude waves

Stratified flow with high-frequency and low-amplitude waves:

The stratified flow with high-frequency and low-amplitude waves appears at low U_{SL} and high U_{SG} . The increase of U_{SG} results in the increase of the interfacial shear force, rippling the liquid surface and producing a wavy interface. Instead of the smooth interface and intermittent high-amplitude waves in the above flow regime, there are continuous waves of low amplitude on the liquid surface. The wave frequency is much higher and the amplitude is much lower than those in the above flow regime. This flow regime occurs within the region of wave flow in Mandhane flow regime map. The time trace of an example case for this flow regime is shown in Figure 5-5.

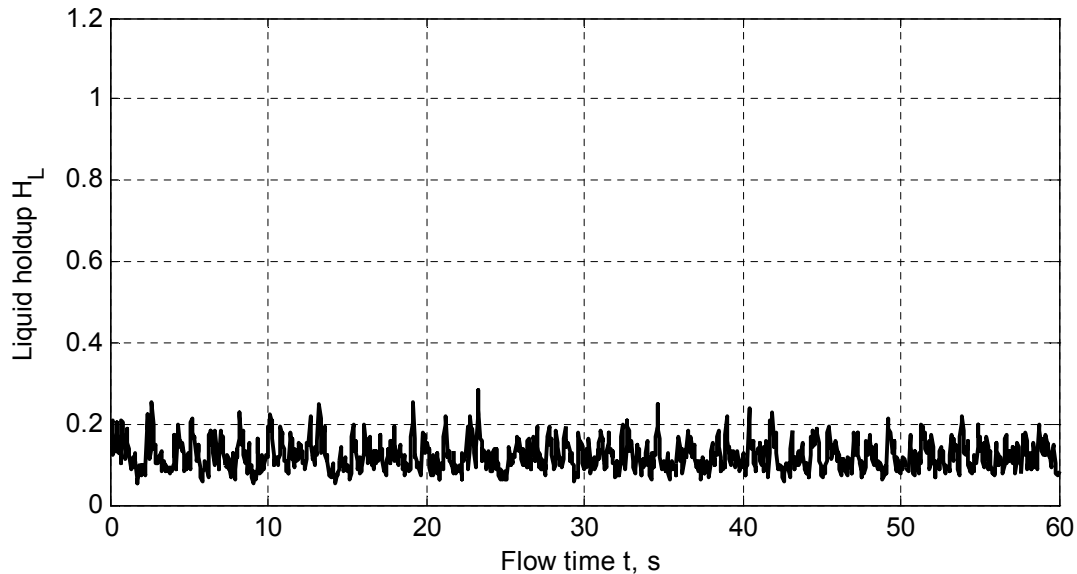


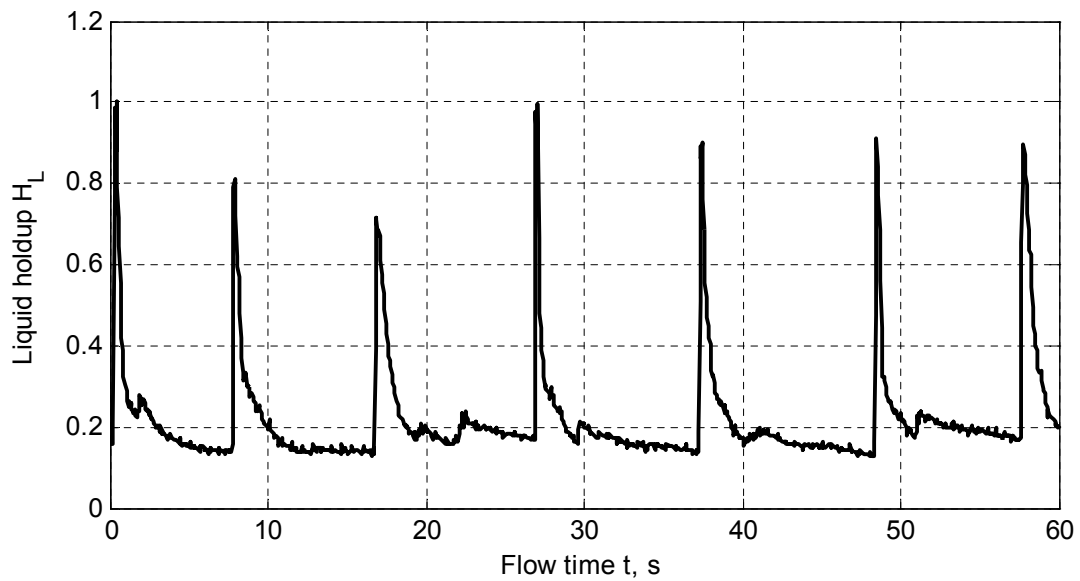
Figure 5-5 Time trace of the liquid holdup for stratified flow with high-frequency and low-amplitude waves ($U_{SL} = 0.02$ m/s, $U_{SG} = 9.0$ m/s)

Slug flow:

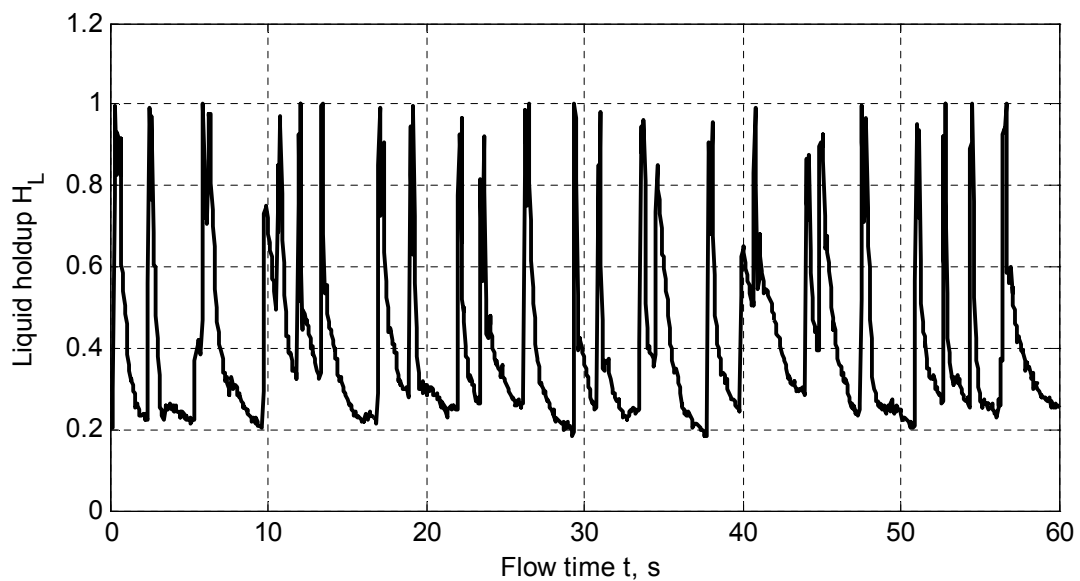
With the increase of U_{SL} and U_{SG} the amplitude of the waves in the stratified flows discussed above becomes progressively higher. Eventually the whole cross-section of the pipe is blocked by a wave forming a liquid slug. Then the slug is accelerated by the gas bubble behind it. Significant gas entrainment in the slug body can be observed in

slug flow. The slug flow region for the present test rig is larger than that in Mandhane flow regime map as indicated in Figure 5-3.

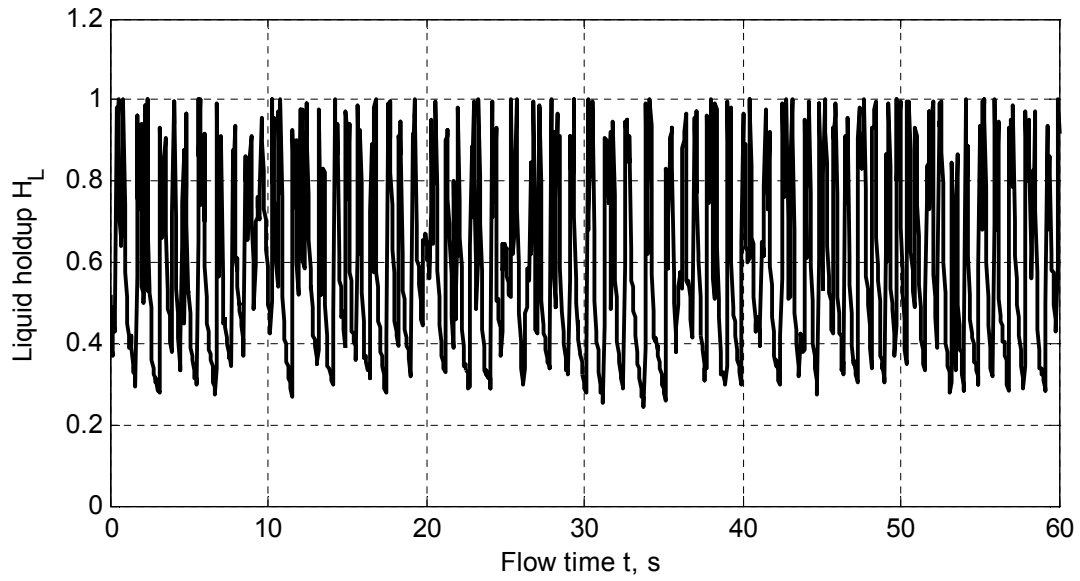
Figure 5-6 show a series of liquid holdup time traces for slug flow cases. The slug frequency increases with the increase of U_{SL} at the same U_{SG} (Figure 5-6 (a) and (b)); the gas entrainment in the slug body (indicated by the reduction of the maximum liquid holdup) increases with the increasing U_{SG} at the same U_{SL} (Figure 5-6 (c) and (d)).



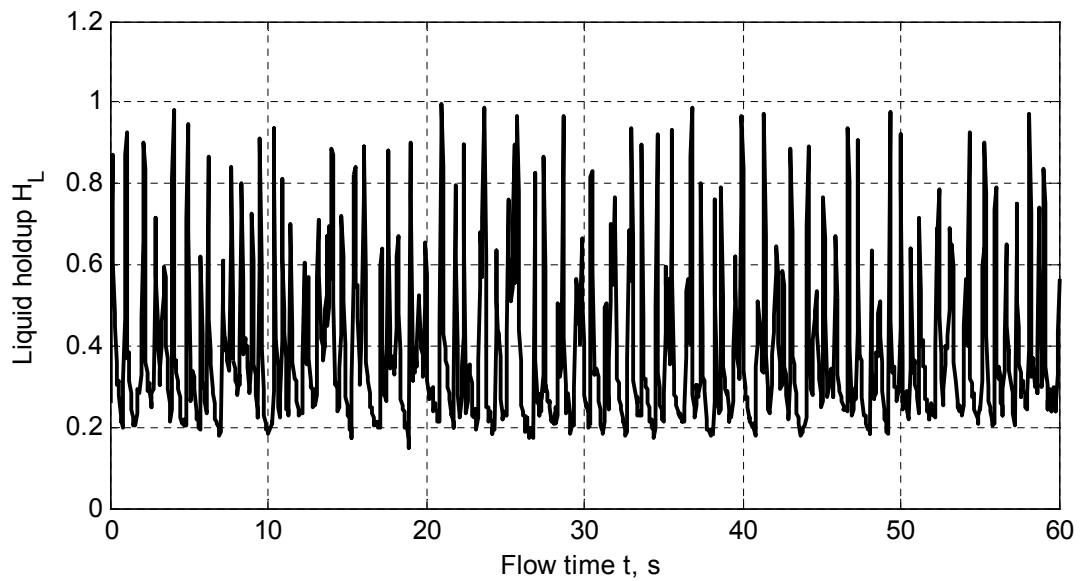
(a) $U_{SL} = 0.03$ m/s $U_{SG} = 1.5$ m/s



(b) $U_{SL} = 0.3$ m/s $U_{SG} = 1.5$ m/s



(c) $U_{SL} = 1.0 \text{ m/s}$ $U_{SG} = 1.5 \text{ m/s}$



(d) $U_{SL} = 1.0 \text{ m/s}$ $U_{SG} = 5.0 \text{ m/s}$

Figure 5-6 Time traces of the liquid holdup for slug flow

Elongated bubble flow (Plug flow):

This flow regime appears at high U_{SL} and low U_{SG} as indicated in Figure 5-3. The lowest U_{SL} for the elongated bubble flow to occur in the present rig is higher than that in

Mandhane flow regime map. In the elongated bubble flow large bullet-shaped bubbles move along the top of the pipe. The gas entrainment in the liquid phase is not as significant as that in slug flow discussed above.

5.3.2 Flow in the Wavy Pipe

Different flow behaviour in the wavy pipe has been observed for different upstream flow regimes. The flow behaviour in the wavy pipe is discussed based on the videos taken in the experiment.

The stratified flow with high-amplitude waves comprises two distinct sections: a section of separated gas and liquid layers with smooth interface in between and a section of liquid wave. The stratified flow persists in the downward limbs when the separated gas and liquid layers flowing in the wavy pipe. The interface can be identifiable as indicated by the red lines in Figure 5-7. However, the liquid phase tends to accumulate in the upward limbs and then is pushed out by the upstream gas to the next downward limb or the wavy pipe outlet. The liquid phase pushed out by the upstream gas takes the form of small pockets. A certain amount of gas can penetrate into the liquid pockets during the push-out process forming an air/water mixture as shown in Figure 5-7. Figure 5-8 shows the flow in the wavy pipe when the high-amplitude waves travelling in the wavy pipe. In the first downward limb the waves tend to decay and drop into the bottom of the bend quickly. The interface is identifiable in the first downward limb. However, as highlighted by the green circle in Figure 5-8, the liquid waves and gas mix together in the following limbs of the wavy pipe. There is no identifiable interface any more in the following limbs. The liquid waves are transformed into gas/liquid mixture occupying the whole pipe cross-section by the wavy pipe.

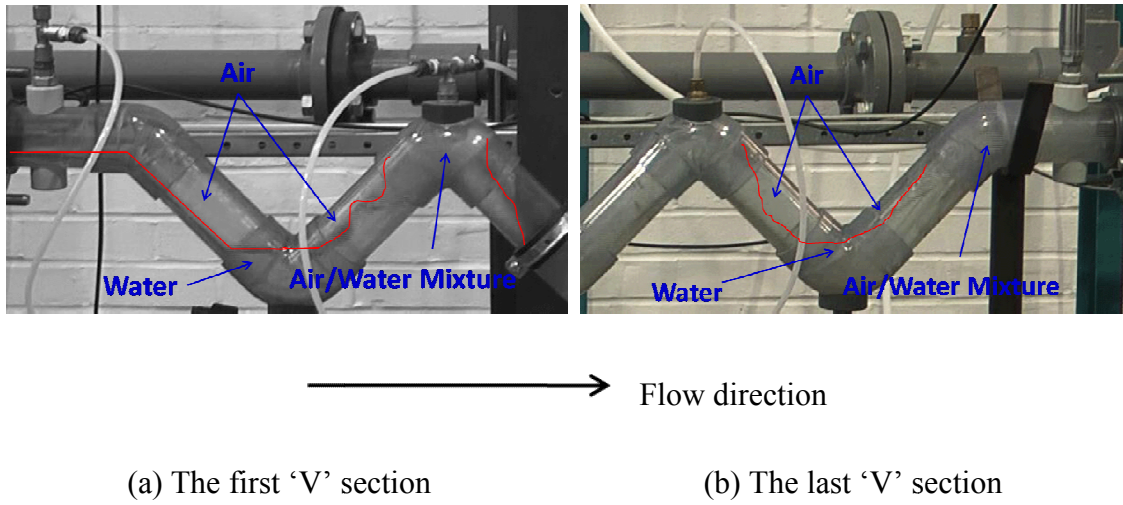


Figure 5-7 Flow in the wavy pipe for the upstream separate gas and liquid layers

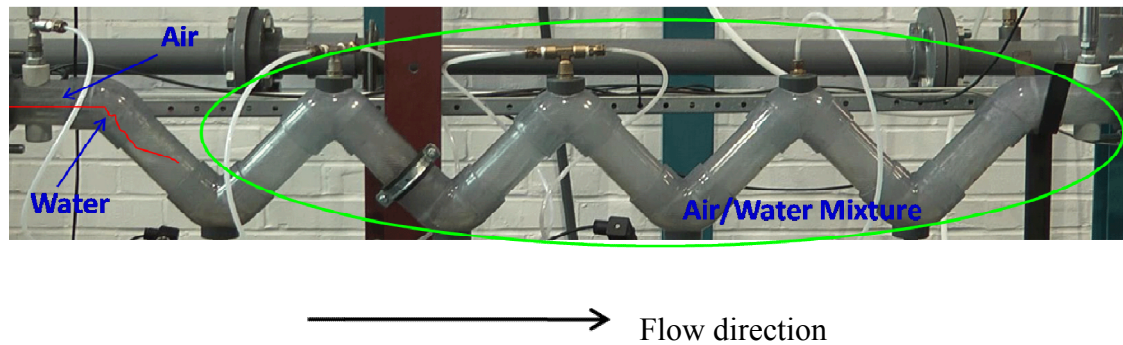


Figure 5-8 Flow in the wavy pipe for the upstream high-amplitude waves

In the stratified flow with low-amplitude waves there are gas and liquid layers with a rougher interface than that in the stratified flow with high-amplitude waves. The phase distribution in the wavy pipe is similar to that when the separated gas and liquid layers in the stratified flow with high-amplitude waves passing through the wavy pipe as shown in Figure 5-7. However, the liquid pockets are pushed out by the upstream gas more frequently due to a higher gas velocity.

Compared with the high-amplitude waves in the stratified flow the liquid slugs in slug flow have a higher liquid holdup and move faster at a higher frequency. No obvious growth and decay of the liquid slugs can be observed visually in the wavy pipe during the experiment. After the slug unit (including slug body and elongated bubble with liquid film) moves into the wavy pipe, the slug body and elongated bubble become undistinguishable any more as shown in Figure 5-9. The liquid holdup in slug body decreases because more gas entrainment has been introduced during the travelling of the slug in the wavy pipe.

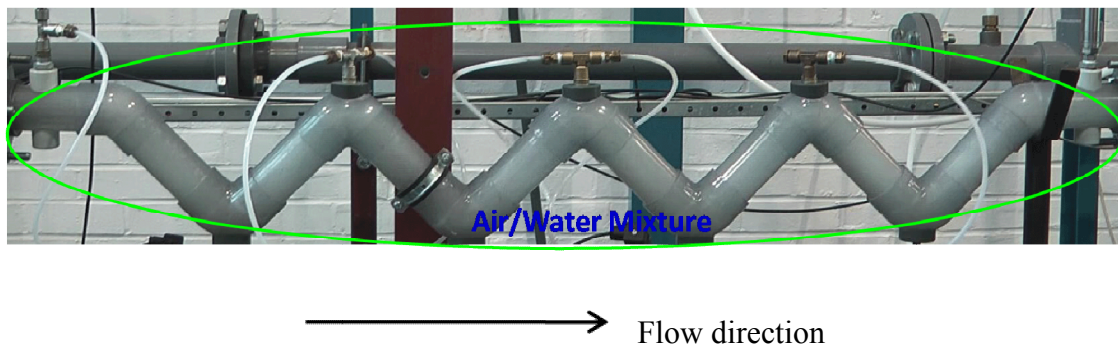


Figure 5-9 Flow in the wavy pipe for the upstream slug flow

In the elongated bubble flow upstream of the wavy pipe there is little gas entrainment in the liquid plugs. But in the wavy pipe more gas entrainment has been introduced into the liquid phase similarly to slug flow. There is no clear interface between the gas/liquid two phases any more in the wavy pipe.

5.3.3 Flow Downstream of the Wavy Pipe

The liquid holdup has been measured at different locations downstream of the wavy pipe as shown in Figure 5-2. It needs to be noted that the downstream pipe section is only 3.5 m long due to the restriction of the space in the laboratory.

In the stratified flow with high-amplitude waves the upstream waves have grown in the wavy pipe and become liquid slugs occupying the pipe cross-section. The wave

frequency at the outlet of the wavy pipe is higher than that upstream. This is attributed to the addition of the newly formed waves in the upward limbs in the wavy pipe as discussed in Section 5.3.2. However, the newly formed waves are much lower in amplitude and shorter in length than the existing ones. Figure 5-10 shows the liquid holdup obtained from conductivity cells A and C at $U_{SL} = 0.02$ m/s and $U_{SG} = 0.7$ m/s. The maximum liquid holdup downstream (C) is higher than that upstream (A), which confirms the wave growth in amplitude in the wavy pipe. Furthermore, we can see that there are several smaller waves with liquid holdup less than 0.5. It is postulated that these smaller waves are newly formed in the wavy pipe. To summarise, there are two effects on the stratified flow with high-amplitude waves induced by the wavy pipe. Firstly the existing waves upstream grow in amplitude then become liquid slugs downstream of the wavy pipe; secondly the smooth interface between the two phases upstream becomes wavy as new waves are produced in the wavy pipe.

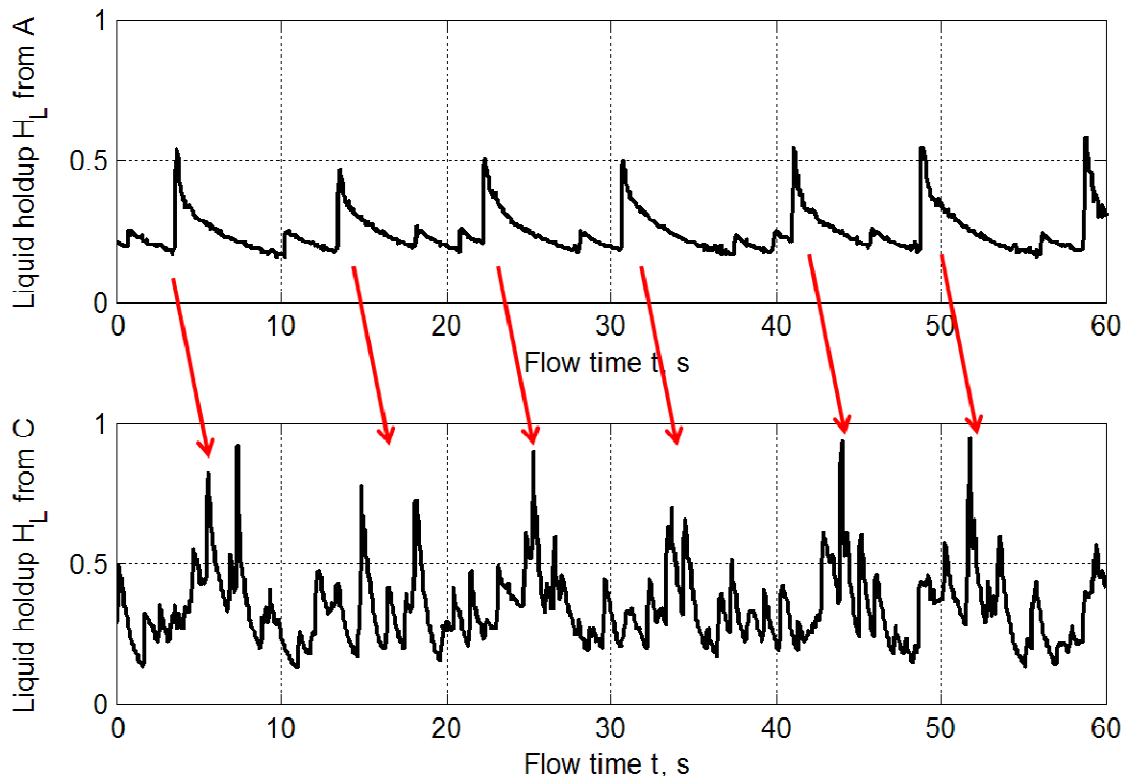


Figure 5-10 Liquid holdup upstream and downstream of the wavy pipe for the upstream stratified flow with high-amplitude waves ($U_{SL} = 0.02$ m/s, $U_{SG} = 0.7$ m/s)

Figure 5-11 shows the liquid holdup time traces from conductivity cells A and C for the stratified flow with high-frequency and low-amplitude waves. The wave growth in the wavy pipe can be observed as indicated by the increase of the maximum liquid holdup from A to C.

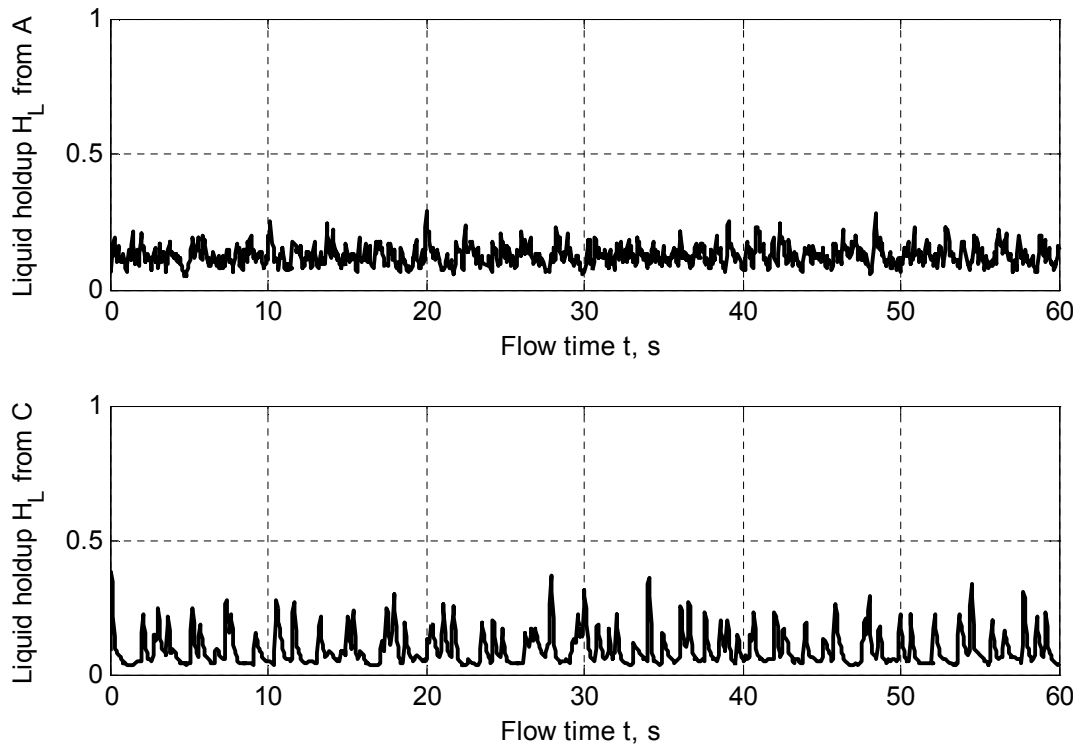
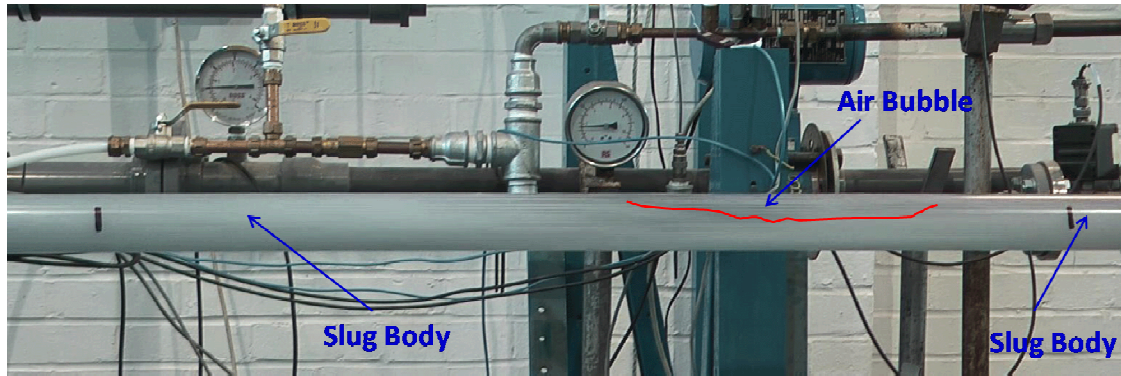


Figure 5-11 Liquid holdup upstream and downstream of the wavy pipe for stratified flow with low-amplitude waves upstream ($U_{SL} = 0.02$ m/s, $U_{SG} = 9.0$ m/s)

The liquid holdup in slug body has been reduced in the wavy pipe for the upstream slug flow. More gas is introduced into the slug body during the interaction between the two phases and wavy pipe. The gas/liquid two phases tend to become ‘homogeneous’ as a number of gas bubbles distribute in the slug body extensively. Figure 5-12 shows a snapshot of the slug unit downstream of the wavy pipe.



—————→ Flow direction

Figure 5-12 Flow downstream of the wavy pipe for the upstream slug flow

As mentioned in Section 5.3.2 more gas entrainment has been introduced into the liquid phase in the wavy pipe for the upstream elongated bubble flow. The elongated bubble flow remains in the downstream pipe section, but with more gas entrainment in the liquid plugs than that upstream.

5.4 Slug Mitigation with Wavy Pipe

As discussed in Section 5.3 more gas entrainment can be introduced into slug body with a wavy pipe applied. Hence the average liquid holdup and thus the effective density of the slug body are reduced. As a result, the impact on the downstream facility induced by the fast moving slugs is mitigated. The performance of the wavy pipe on hydrodynamic slug mitigation and how the wavy pipe works are discussed in this section.

5.4.1 Gas Entrainment and Flow Recovery Downstream

The maximum liquid holdup is an indicator of the minimum gas entrainment in slug body. The reduction of the maximum liquid holdup downstream of the wavy pipe is a measure to evaluate the increase of the gas entrainment in slug body in the wavy pipe. However, the flow tends to recover downstream of the wavy pipe. The liquid holdup at

1.0 m and 1.9 m downstream of the wavy pipe has been measured to monitor the flow recovery.

The effectiveness of the wavy pipe on introducing more gas into slug body varies with different flow conditions, such as inlet U_{SL} and U_{SG} . Figure 5-13 shows the variation of the maximum liquid holdup upstream and downstream of the wavy pipe with different U_{SG} at the same $U_{SL} = 1.0$ m/s. It can be seen that the lowest maximum liquid holdup is obtained at the location C, 1 m downstream of the wavy pipe. The reduction of the liquid holdup at the location C compared with that at the location A indicates that a certain amount of gas has been introduced into the slug body during travelling in the wavy pipe. However, the flow tends to recover as indicated by the higher liquid holdup at the location D, 1.9 m downstream of the wavy pipe, than that at the location C. The difference in the maximum liquid holdup between the location A and C becomes smaller with the increase of U_{SG} . Comparing the maximum liquid holdup at the location C with D we can see that the difference between them at lower U_{SG} ($U_{SG} < 2.0$ m/s) is larger than that at higher U_{SG} ($U_{SG} > 2.0$ m/s). This indicates that the flow recovery is more significant at lower U_{SG} ($U_{SG} < 2.0$ m/s) at the same U_{SL} ($U_{SL} = 1.0$ m/s).

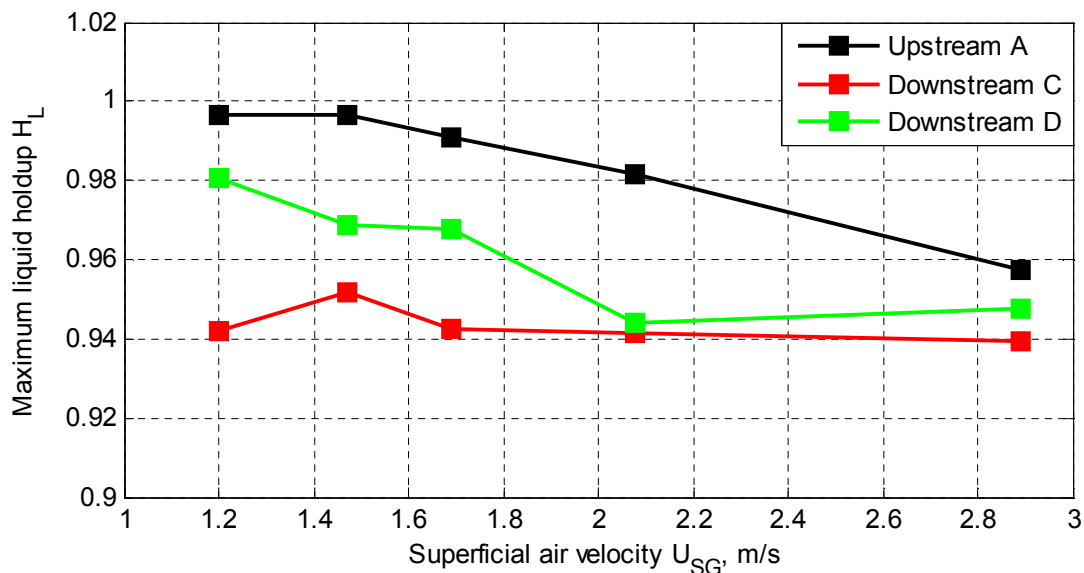


Figure 5-13 Maximum liquid holdup upstream and downstream of the wavy pipe ($U_{SL} = 1.0$ m/s)

Figure 5-14 shows the variation of the maximum liquid holdup upstream and downstream of the wavy pipe with different U_{SL} at the same $U_{SG} = 1.5$ m/s. It can be seen that the lowest maximum liquid holdup is obtained at the location C. The flow tends to recover downstream because the maximum liquid holdup at the location D is higher than that at the location C. Comparing the maximum liquid holdup at the location C with D we can see that the difference between them becomes smaller with the increase of U_{SL} . This indicates that the flow recovery is more significant at lower U_{SL} ($U_{SL} < 1.0$ m/s) at the same U_{SG} ($U_{SG} = 1.5$ m/s).

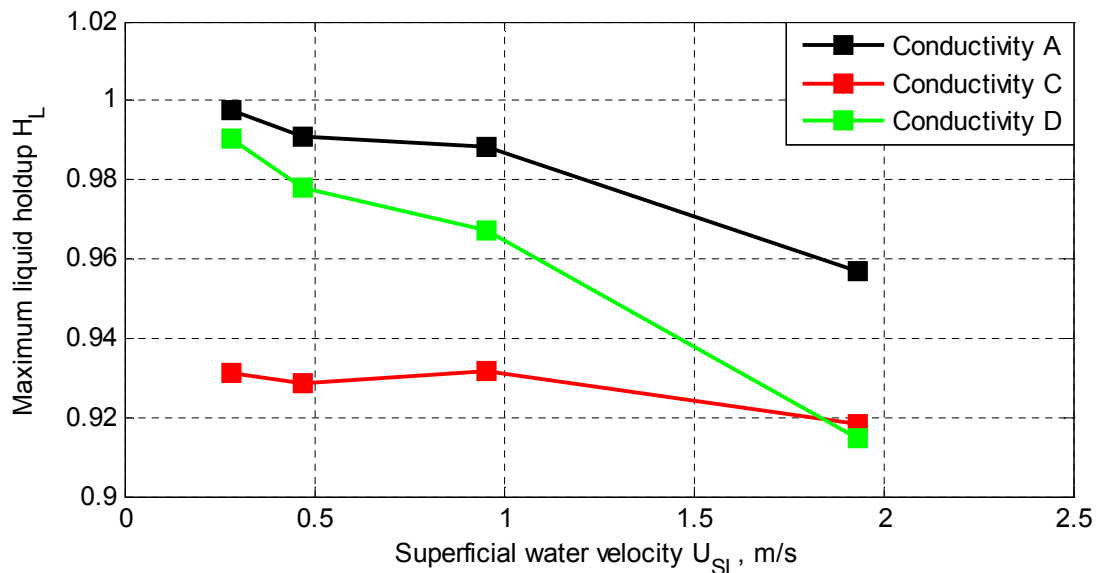


Figure 5-14 Maximum liquid holdup upstream and downstream of the wavy pipe ($U_{SG} = 1.5$ m/s)

5.4.2 Interaction between Slug Flow and Wavy Pipe

The phase distribution in the wavy pipe is of interest because it shows how the two phases interact with each other and with the wavy pipe. As discussed in Section 5.3.2 the two phases mix together with no identifiable interface in between. Therefore, it is difficult to describe the phase distribution based on visual observations. Alternatively the differential pressure (DP) across each of the first 6 limbs of the wavy pipe has been

measured (see Figure 5-2) and analysed. The DP comprises three terms induced by gravity, friction and acceleration, respectively.

Figure 5-15 shows the variation of the average DP with the increase of U_{SG} at the same $U_{SL} = 1.0$ m/s for slug flow upstream of the wavy pipe. The DP across the downward (DP1, DP3 and DP5) and upward (DP2, DP4 and DP6) limbs has been plotted separately for clarity. It needs to be mentioned that the DP is obtained by subtracting the pressure at the top from that at the bottom of the ‘V’ sections of the wavy pipe. The variation of the average DP with the increase of U_{SL} at the same $U_{SG} = 1.5$ m/s is shown in Figure 5-16.

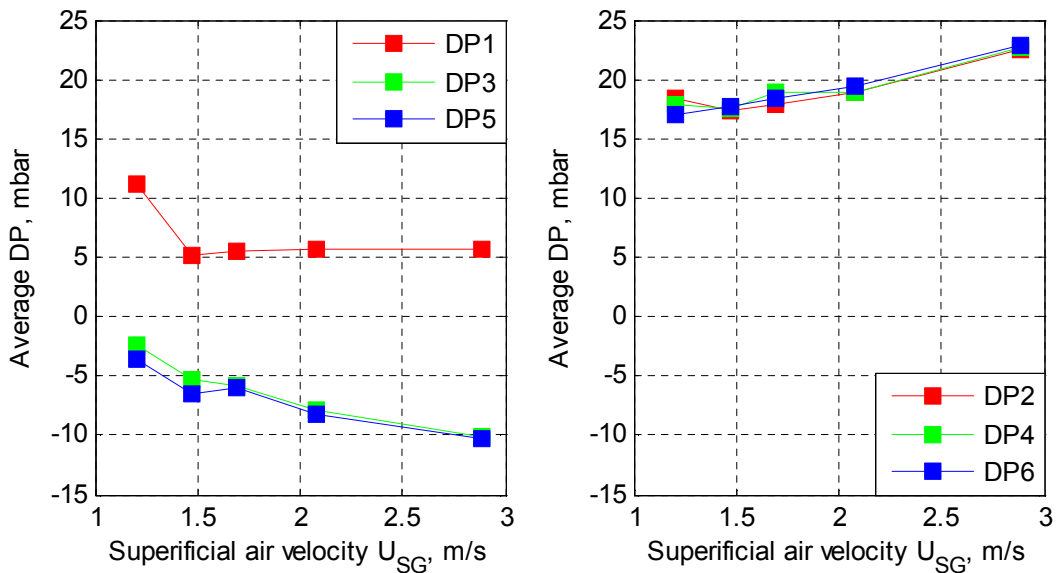


Figure 5-15 Average differential pressures across the first 6 limbs of the wavy pipe
($U_{SL} = 1.0$ m/s)

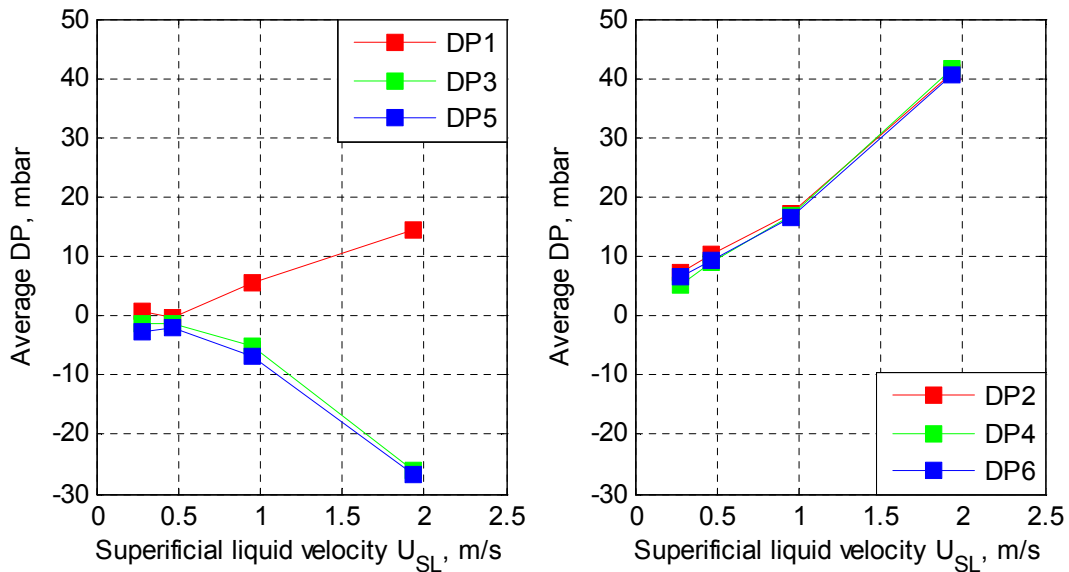


Figure 5-16 Average differential pressures across the first 6 limbs of the wavy pipe ($U_{SG} = 1.5$ m/s)

It can be seen in Figure 5-15 and Figure 5-16 that the DP across the downward limbs is consistently lower than those across the upward limbs at the same U_{SL} and U_{SG} . The higher DP is attributed to the higher hydrostatic pressure induced by the liquid column in the upward limbs, because the liquid phase tends to accumulate in the upward limbs.

The DP across the downward limbs (DP3 and DP5) decreases with the increasing U_{SG} at the same U_{SL} ($U_{SL} = 1.0$ m/s) as shown in Figure 5-15. But DP3 and DP5 actually increase in amplitude because they are negative in ‘direction’ (The ‘direction’ here is used to distinguish the higher or lower pressure end of the DP.). A negative DP indicates that the pressure at the bottom is lower than that at the top. The DP includes three terms induced by friction, acceleration and gravity, respectively. It is postulated that the friction and acceleration terms dominate in DP3 and DP5, and the gravity term is relatively smaller. Furthermore, DP3 is only slightly higher than DP5 and they are almost equal at higher U_{SG} ($U_{SG} > 1.5$ m/s). This indicates that the phase distribution in the limb labeled with DP3 is similar to that in the limb with DP5. However, it needs to be noted that DP1 behaves in a different way from DP3 and DP5. DP1 is positive and

does not increase in amplitude significantly with the increasing U_{SG} at the same U_{SL} ($U_{SL} = 1.0$ m/s). The pressure at the bottom of the first downward limb is higher than that at the top. This indicates that the gravity induced DP is higher than the sum of the friction and acceleration terms. The ‘direction’ change of the DP from DP1 to DP3/DP5 (in the flow direction) indicates the increase of the friction and acceleration terms. It is postulated that the flow has been accelerated in the wavy pipe especially in the first ‘V’ section (from DP1 to DP3), because the velocity increase could result in the increase of both the friction and acceleration induced pressure drop. The DP across the upward limbs (DP2, DP4 and DP6) increases with the increasing U_{SG} at the same U_{SL} ($U_{SL} = 1.0$ m/s). The increase of the DP is mainly attributed to the increase of the friction and acceleration induced pressure drop due to the increase of U_{SG} . It is interesting to note that DP2, DP4 and DP6 are almost equal as shown in Figure 5-15. This indicates that the phase distribution in the three upward limbs is similar.

Comparing Figure 5-15 and Figure 5-16 we can see that DP1 behaves differently with the increasing U_{SL} at the same U_{SG} ($U_{SG} = 1.5$ m/s) from that with the increasing U_{SG} at the same U_{SL} ($U_{SL} = 1.0$ m/s). DP1 increases significantly with the increase of U_{SL} at the same U_{SG} ($U_{SG} = 1.5$ m/s) as shown in Figure 5-16. That is mainly attributed to the increase of the hydrostatic pressure due to higher liquid fraction at higher U_{SL} . Similarly to the analysis of Figure 5-15 DP3 and DP5 also decrease and are almost equal with the increase of the mixture velocity ($U_{SL} + U_{SG}$) at the same U_{SG} . This confirms that the flow in the second and third downward limbs is similar. Furthermore, DP2, DP4 and DP6 also increase and are almost equal with the increase of the mixture velocity ($U_{SL} + U_{SG}$) at the same U_{SG} . But differently from that in Figure 5-15 the increase is attributed to not only the increase of the friction and acceleration induced pressure drop but also the higher hydrostatic pressure due to higher liquid fraction at higher U_{SL} .

5.4.3 Working Principle

The wavy pipe works as a mixer which is able to agitate the gas/liquid two phases by its upward and downward limbs. In the wavy pipe the liquid phase tends to slow down and accumulate in the upward limbs and accelerate in the downward limbs. The gas phase then gains an opportunity to penetrate into the liquid phase while it is slowing down in the upward limbs. For slug flow a certain amount of gas in the elongated bubble can

penetrate into the slug body. The penetrated gas distributes in the slug body extensively due to the agitation effects of the wavy pipe. As a result, the liquid holdup in the slug body at the outlet of the wavy pipe is lower than that upstream. Therefore, the effective density of the slug body decreases thus the impact of the liquid slugs on the downstream facility is reduced. However, the flow tends to recover after a certain distance downstream of the wavy pipe, especially at lower superficial gas and/or liquid velocities ($U_{SG} < 2.0$ m/s at $U_{SL} = 1.0$ m/s; $U_{SL} < 1.0$ m/s at $U_{SG} = 1.5$ m/s in the experiment).

5.5 Summary

A 2" wavy pipe of 7 bends has been installed horizontally in the test section of a two-phase test facility in PSE (Process Systems Engineering) Laboratory. A wide range of superficial air and water velocities has been tested. Firstly the flow regimes in this test rig were observed; secondly the flow behaviour upstream of the wavy pipe, in the wavy pipe and downstream of the wavy pipe was analysed; thirdly the performance of the wavy pipe on slug mitigation and how the wavy pipe works were discussed.

Four flow regimes in the two-phase test rig were identified and discussed based on the visual observations and liquid holdup measurements with Mandhane flow regime map as a reference. The four flow regimes are: stratified flow with low-frequency and high-amplitude waves; stratified flow with high-frequency and low-amplitude waves; slug flow and elongated bubble flow. No stratified flow with smooth interface is observed; instead a stratified flow with low-frequency and high-amplitude waves occurs. It is postulated that the high-amplitude waves are mainly initiated due to the effects of the two bends upstream of the test section.

The stratified flow with high-amplitude waves comprises two distinct sections: a section of liquid wave and a section of separated gas and liquid layers with smooth interface in between. The wavy pipe has different effects on these two sections. Firstly the existing waves upstream grow in amplitude and become liquid slugs downstream of the wavy pipe; secondly the smooth interface upstream becomes wavy as new waves are generated in the wavy pipe. The wave frequency at the outlet of the wavy pipe is higher than that upstream, resulting from the addition of the newly formed waves in the upward limbs in the wavy pipe. The newly formed waves are much lower in amplitude

and shorter than the existing ones. When a slug unit moves into the wavy pipe, the slug body and elongated bubble become indistinguishable. The liquid holdup in slug body decreases because more gas entrainment is induced during the travelling of the slug in the wavy pipe.

The wavy pipe is able to mitigate the impact of slug flow on the downstream facilities. It works as a mixer which is able to agitate the gas/liquid two phases by its upward and downward limbs. In the wavy pipe the liquid phase tends to slow down and accumulate in the upward limbs and accelerate in the downward limbs. The gas phase then gains an opportunity to penetrate into the liquid phase while it is slowing down in the upward limbs. For slug flow a certain amount of gas in the elongated bubble can penetrate into the slug body. The penetrated gas distributes in the slug body extensively due to the agitation effects of the wavy pipe. As a result, the liquid holdup in the slug body at the outlet of the wavy pipe is lower than that upstream. Therefore, the effective density of the slug body decreases thus the impact of the liquid slugs on the downstream facility is reduced. However, the flow tends to recover after a certain distance downstream of the wavy pipe, especially at lower superficial gas and/or liquid velocities ($U_{SG} < 2.0$ m/s at $U_{SL} = 1.0$ m/s; $U_{SL} < 1.0$ m/s at $U_{SG} = 1.5$ m/s in the experiment).

6 MODELLING OF HYDRODYNAMIC SLUG FLOW IN HORIZONTAL WAVY-PIPE SYSTEMS APPLYING STAR-OLGA COUPLING

6.1 Introduction

It is still a challenge to predict the slug flow characteristics accurately for a wide range of pipeline configurations and flow conditions with models. OLGA is a transient one-dimensional (1-D) model suitable for long pipelines. The slug tracking model in OLGA can give predictions of the characteristic parameters of slug flow. However, OLGA models cannot provide details of the phase distribution in the pipeline and forces on the pipe wall. CFD models are able to present the details of the flow field in 2-D and 3-D spaces. However, CFD models are computationally expensive to obtain the time-dependent solutions for slug flows in long pipelines. Recently, a novel co-simulation tool called STAR-OLGA coupling has been proposed by CD-adapco. As a part of the project to explore the CFD-OLGA co-simulation tool, the code of the coupling between OLGA and STAR-CD/STAR-CCM+ is validated in this work. The coupling provides a means of data exchange between 3-D CFD and 1-D OLGA. This allows for a compromise between the speed of the 1-D code and the details of the 3-D code.

In this work the STAR-OLGA coupling was applied to develop simulation models for predicting hydrodynamic slug flow in horizontal wavy-pipe systems. The wavy pipe was modelled using the 3-D CFD code STAR-CCM+ (Release 5.04.006) and the pipelines upstream and downstream of the wavy pipe were modelled using the 1-D code OLGA (Release 5.3.2). A set of wavy pipes of different amplitudes and lengths was tested numerically. The effects of the geometrical parameters of the wavy pipe on hydrodynamic slug flow were examined.

6.2 STAR-OLGA Coupling

The STAR-OLGA coupling tool in STAR-CCM+ is responsible for the data transfer between the 3-D STAR-CCM+ and 1-D OLGA codes. Compared with a pure OLGA model the coupling model is able to provide increased details of a specific part by

replacing that part with a 3-D element. Compared with a pure 3-D STAR-CCM+ model the calculation time can be significantly reduced by applying the high-speed 1-D code OLGA to long pipelines. Thus the coupling provides a good compromise between the speed of the 1-D code and the details of the 3-D code.

6.2.1 Configuration of the Coupling

Two model configurations, i.e. one-point coupling and two-point coupling, can be realised using the STAR-OLGA coupling tool. A schematic of a two-point coupling model is shown in Figure 6-1. In the two-point coupling model the outlet of the upstream OLGA pipe (OUTLET-1) is coupled with the inlet of the STAR pipe and the outlet of the STAR pipe is coupled with the inlet of the downstream OLGA pipe (SOUR-2). The fluids enter the computation domain at the inlet of the upstream OLGA pipe (SOUR-1), flow down the upstream OLGA pipe, into the STAR pipe and finally into the downstream OLGA pipe. The inlet boundary conditions of the coupling model are specified at the SOUR-1 and the outlet boundary conditions are specified at the OUTLET-2. The communications between the internal boundaries of the OLGA and STAR model parts, i.e. OUTLET-1/Inlet and Outlet/SOUR-2, are managed by the coupling tool.

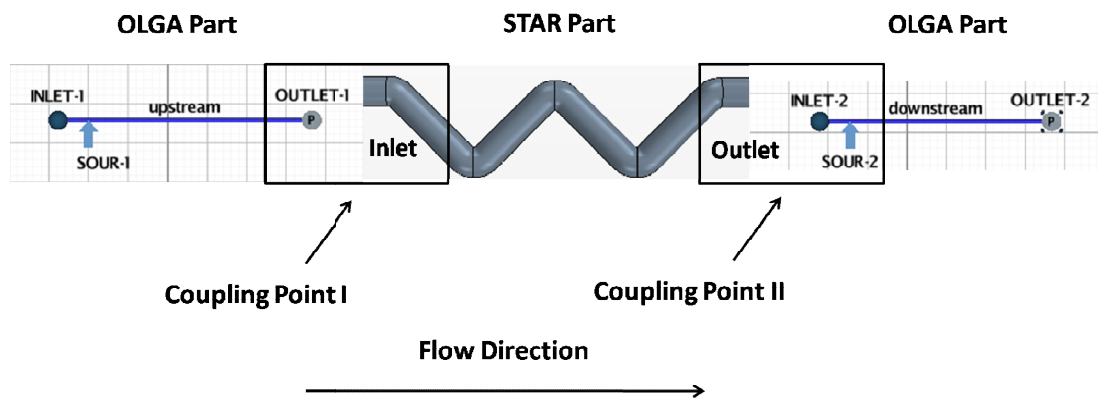


Figure 6-1 Schematic of a two-point STAR-OLGA coupling model

One-point coupling models can be obtained by releasing one of the coupling points of a two-point coupling model.

6.2.2 Key Issues of the Coupling

Three key issues have to be addressed to achieve a successful co-simulation of the 3-D STAR and 1-D OLGA models:

- (1) Consistency of the physical properties of the fluid components in the STAR and OLGA computation domains;
- (2) Transmission of the physical parameters at the coupling points;
- (3) Synchronisation of the time steps in the STAR and OLGA models.

Issue I: Consistency of the physical properties of the fluid components

In a three-phase OLGA simulation there are three species, i.e. gas, oil and water. Each of them must be assigned to an Eulerian phase in the STAR model for the coupled simulation. The three species in the coupled simulation are defined as follows (CD-adapco, 2010):

- **Gas:** a species representing the gas components of the mixture from OLGA;
- **Oil:** a species representing the oil components of the mixture from OLGA;
- **Water:** a species representing the water component of the mixture from OLGA.

The physical properties of the components are specified in a PVT table file, where the properties are tabulated as functions of temperature and pressure. The same PVT table file has to be used by the STAR and OLGA models to ensure that consistent physical properties are specified in both models.

Issue II: Transmission of the physical parameters at the coupling points

The physical parameters exchanged between the STAR and OLGA models are determined by the boundary types. The upstream and downstream OLGA models have the same boundary types, i.e. mass flow inlet and pressure outlet. The STAR model has

a velocity inlet and a pressure outlet. The parameters received by the STAR model from the OLGA models shown in Figure 6-1 include: (1) mass flux, velocity and density of each phase from the upstream; (2) mass flux of each phase (if there is reverse flow from OLGA to STAR), pressure and temperature from the downstream.

At the coupling point I in Figure 6-1 the 1-D data at the outlet boundary of the upstream OLGA model have to be converted into 3-D data for the inlet boundary of the STAR model and the 3-D data at the inlet of the STAR model need to be converted into 1-D data for the outlet boundary of the upstream OLGA model. Similar conversions are required at the coupling point II. The conversion of the 1-D data from the upstream OLGA to 3-D data for the STAR inlet boundary is achieved by assuming that the phases are distributed as stratified layers. The position and occupied area of each phase on the cross-section of the STAR inlet are determined according to their densities and volume fractions. The pressure and temperature from the downstream OLGA are applied uniformly on the cross-section of the STAR outlet boundary. The 3-D data from STAR are averaged then sent to the OLGA models upstream and downstream.

The assumption of the phase distribution as stratified layers on the cross-section at the inlet of the STAR pipe is reasonably realistic for the slug body and slug tail. The slug front has not been represented well due to the high-degree turbulence and more evenly distributed gas bubbles. However, the adverse impacts of this assumption can be alleviated by extending the pipe section between the inlets of the STAR pipe and wavy pipe. In the pipe section upstream of the wavy pipe, the two-phase flow can develop further and the phases can re-distribute themselves before arriving at the wavy pipe.

Issue III: Synchronisation of the time steps

The STAR model usually uses a smaller time step than the OLGA models. The data are exchanged at each time step of the OLGA model. Then the STAR model interpolates the data from OLGA for the intermediate steps.

At the start of the calculation, the STAR solver runs for one time step to generate the boundary values for the OLGA solver. Then OLGA runs for two time steps with Δt apart to generate the data at t_0 and t_1 . After that OLGA is allowed to choose its own time

step within the upper and lower limits specified by the user. Then STAR will step from t_0 to t_1 interpolating the data from OLGA in between for boundary conditions. After the start up procedure the time step synchronisation of STAR and OLGA is shown in Figure 6-2.



Figure 6-2 Schematic of the time step synchronisation (Jonnavithula *et al.* (2009))

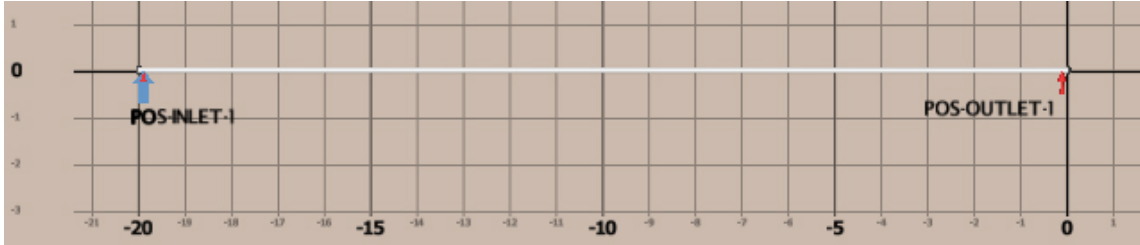
6.3 Development of the Coupling Model

The STAR-OLGA coupling models in this work were developed using STAR-CCM+ (Release 5.04.006) and OLGA (Release 5.3.2). Firstly a straight pipe instead of the wavy pipe was employed in the coupling model. The results obtained from this simple geometry provided a basis for developing the model of the wavy-pipe system. In order to check the mesh dependency of the solutions, both of the STAR and OLGA models were discretised with different levels of meshes. Then the mesh dependency of the solutions for the straight-pipe system was examined. An appropriate mesh level was then determined for the coupling model of the wavy-pipe system. Then the wavy-pipe system was modelled by replacing the straight pipe with a wavy pipe. A group of wavy pipes of different amplitudes and/or lengths was created and tested to examine the effects of the geometrical parameters of wavy pipe on hydrodynamic slug flow.

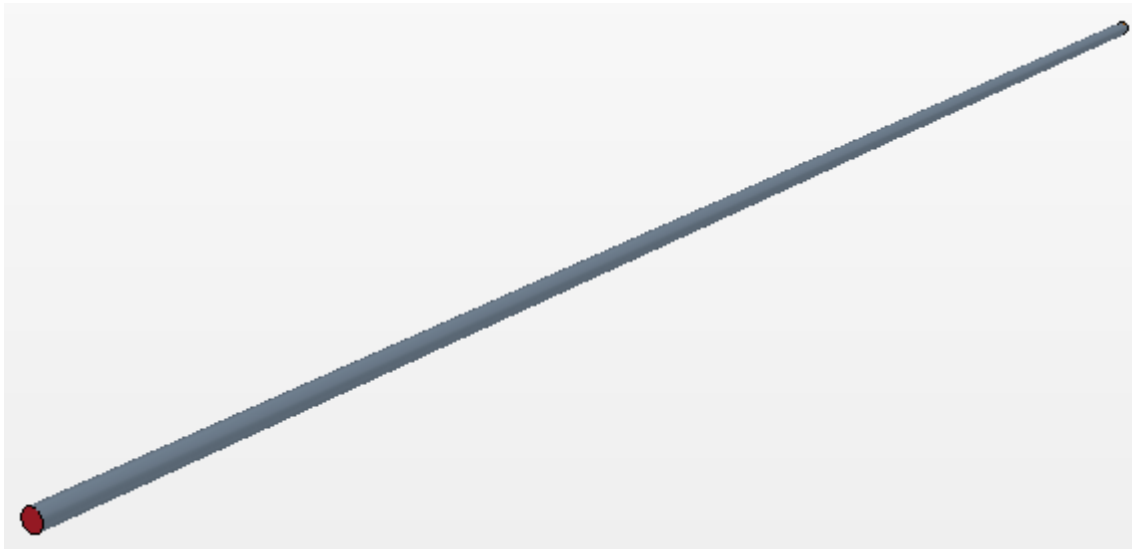
6.3.1 Geometries and Meshes of Straight-Pipe System

The straight-pipe system included 3 parts: upstream pipe, test pipe and downstream pipe. In the STAR-OLGA coupling model the upstream and downstream pipes were modelled in OLGA and the test pipe was modelled in STAR-CCM+. All the pipes were

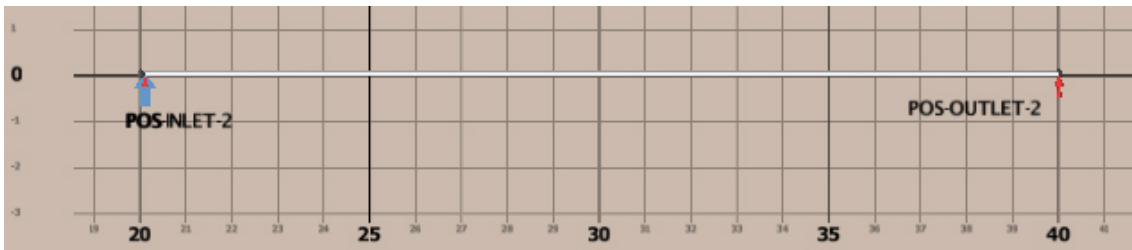
straight and positioned horizontally. The pipe diameter of the straight-pipe system was 0.052 m. Both of the upstream and downstream OLGA pipes were 20 m long and the test pipe in STAR-CCM+ was 6 m long. The profiles of the three pipe sections in the straight-pipe system are shown in Figure 6-3.



(a) Upstream straight pipe in OLGA (20 m)



(b) Straight pipe in STAR-CCM+ (6 m)



(c) Downstream straight pipe in OLGA (20 m)

Figure 6-3 Profiles of the three pipe sections in the straight-pipe system

The OLGA pipes and STAR pipe were discretised with different levels of meshes for numerical calculations. The mesh dependency of the model solutions was then examined. Two sets of tests were carried out: (1) tests on the OLGA model alone to determine the mesh level for the OLGA model parts; (2) tests on the STAR-OLGA coupling model to determine the STAR model part. It needs to be mentioned that only the upstream OLGA model part was discussed then the downstream OLGA model part keeps the same level of mesh with the upstream. The mesh details of the OLGA and STAR models are listed in Table 6-1 and Table 6-2, respectively.

Table 6-1 Meshes of the OLGA models

	Cell count	Cell size (m)
Mesh I	20	1.0
Mesh II	40	0.5
Mesh III	80	0.25
Mesh IV	160	0.125
Mesh V	320	0.0625

Table 6-2 Meshes of the STAR models

	Total cell count	Cell count on cross-section	Average cell size on cross-section ($10^{-6}m^2$)
Level 1	78,000	156	13.6
Level 2	128,000	256	8.30
Level 3	190,000	380	5.59

Firstly the OLGA models of different levels of meshes in Table 6-1 were solved and then the solutions were compared. Based on the comparison an appropriate mesh was selected. Secondly the OLGA model of the selected mesh was solved coupled with the STAR model of different levels of meshes in Table 6-2. Then the solutions of the STAR model were compared and then an appropriate mesh was selected. After that the

selected meshes for the OLGA and STAR models were employed in the coupling model of the wavy-pipe system.

6.3.2 Model Setup

The test fluids in the models were air and water. Constant mass flowrates of the air and water were specified at the inlet of the OLGA pipe. The outlet of the downstream OLGA pipe was specified as the standard atmospheric pressure. For the internal boundaries a slightly higher pressure than the atmospheric pressure was specified at the outlet of the upstream OLGA pipe to drive the flow from upstream to downstream. The boundary conditions of the STAR pipe were set to be provided by the upstream and downstream OLGA pipe, respectively.

The slug tracking module in OLGA was employed to predict the characteristic parameters of slug flow in the upstream pipe. In the STAR model the two-layer realisable k - ε model (CD-adapco, 2010) and VOF model were applied to model the turbulence and track the volume fraction of each phase, respectively. A fixed time-step scheme was used for the implicit unsteady solver in STAR; while the minimum and maximum time steps in OLGA were set properly with the time step in STAR as a reference. For the cases discussed below the time step in the STAR model was 0.001 s and the minimum and maximum time steps in the OLGA model were 0.001 s and 0.003 s respectively.

A series of ‘plane sections’ were created along the STAR pipe. The plane sections took the form of cross-sections at the specified positions of interest. The plane sections were used to monitor the area-averaged pressure and liquid holdup during the calculation. The phase distribution on the pipe wall and longitudinal section of the STAR pipe were also recorded in terms of gas volume fraction contour plots.

6.3.3 Hardware Configuration

The coupling models were solved by computers in a network as shown in Figure 6-4. The calculation of the STAR model was conducted on the computational "Grid" at Cranfield University. The Grid compute nodes are HP DL160G5 servers running Linux. Each node has two Intel Xeon 5272 "Wolfdale" dual-core processors (clock speed 3.4

GHz) with 16 GB of RAM and 80 GB local SATA disk. The STAR model was run on one compute node with 4 cores in parallel. The OLGA model was solved on a Windows desktop with a single-core processor (clock speed 3.0 GHz) and 2.0 GB RAM. The IP address of the Windows desktop running OLGA was specified in the STAR model so that the Windows machine could be recognised by the Grid node running STAR-CCM+. All the data exchanged between the OLGA and STAR models are transmitted through the internet.

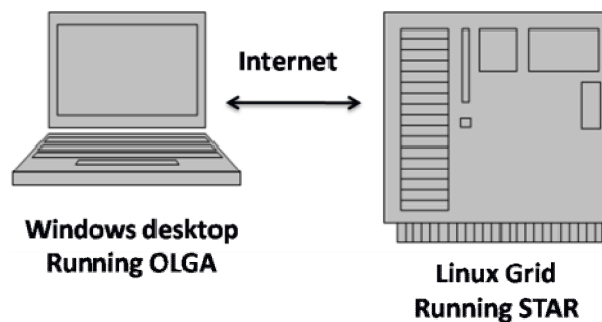


Figure 6-4 Schematic of the hardware configuration for solving the coupling model (after Jonnavithula *et al.* (2009))

6.3.4 Mesh Selection

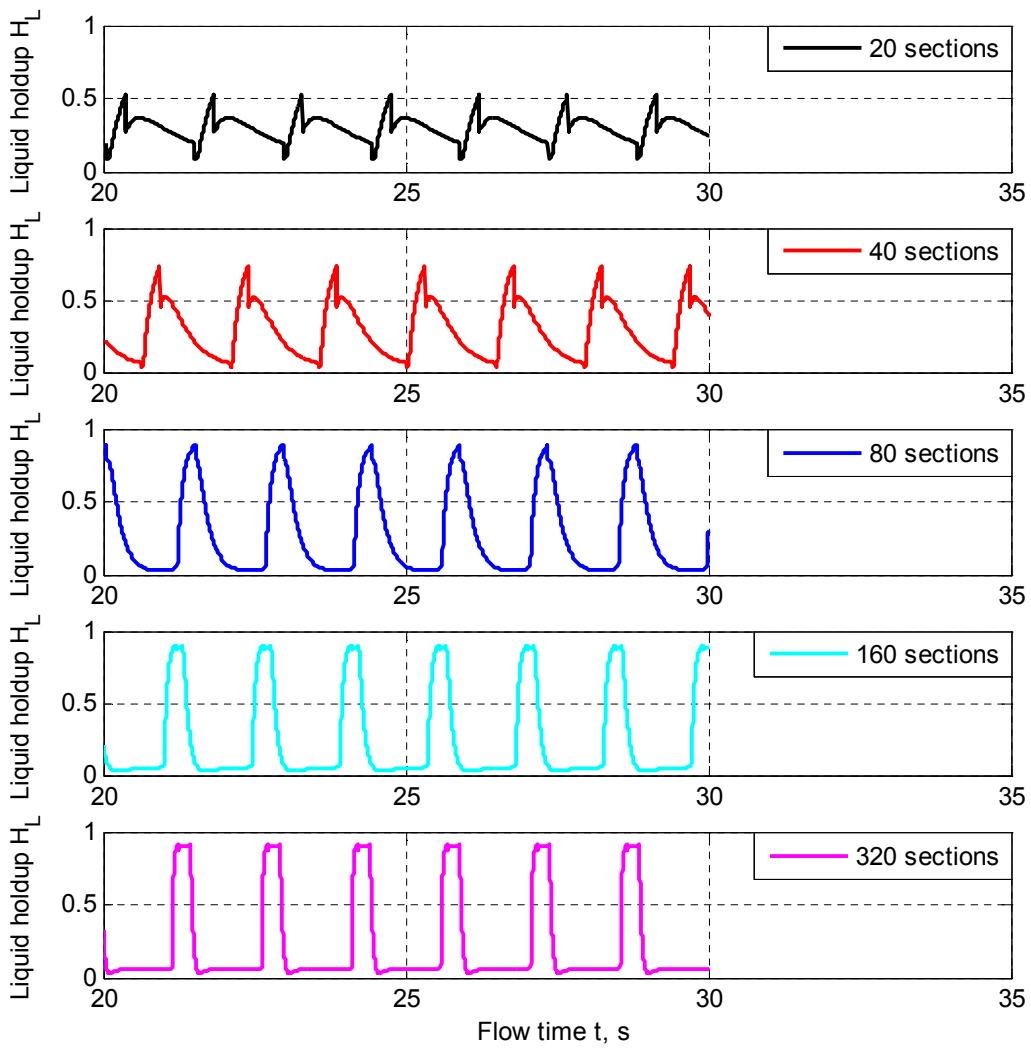
The OLGA models and STAR-OLGA coupling models have been solved with a typical slug flow case. The predictions of the OLGA model alone and the coupling model of different levels of meshes are compared.

The characteristics of the slug flow such as slug frequency, gas entrainment in slug body and liquid film thickness can be obtained from the liquid holdup time traces. Therefore, the liquid holdup is of concern when examining the model solutions. Furthermore, as the outlet of the upstream OLGA pipe is coupled with the downstream STAR pipe, the liquid holdup at the last section of the upstream OLGA pipe is more important.

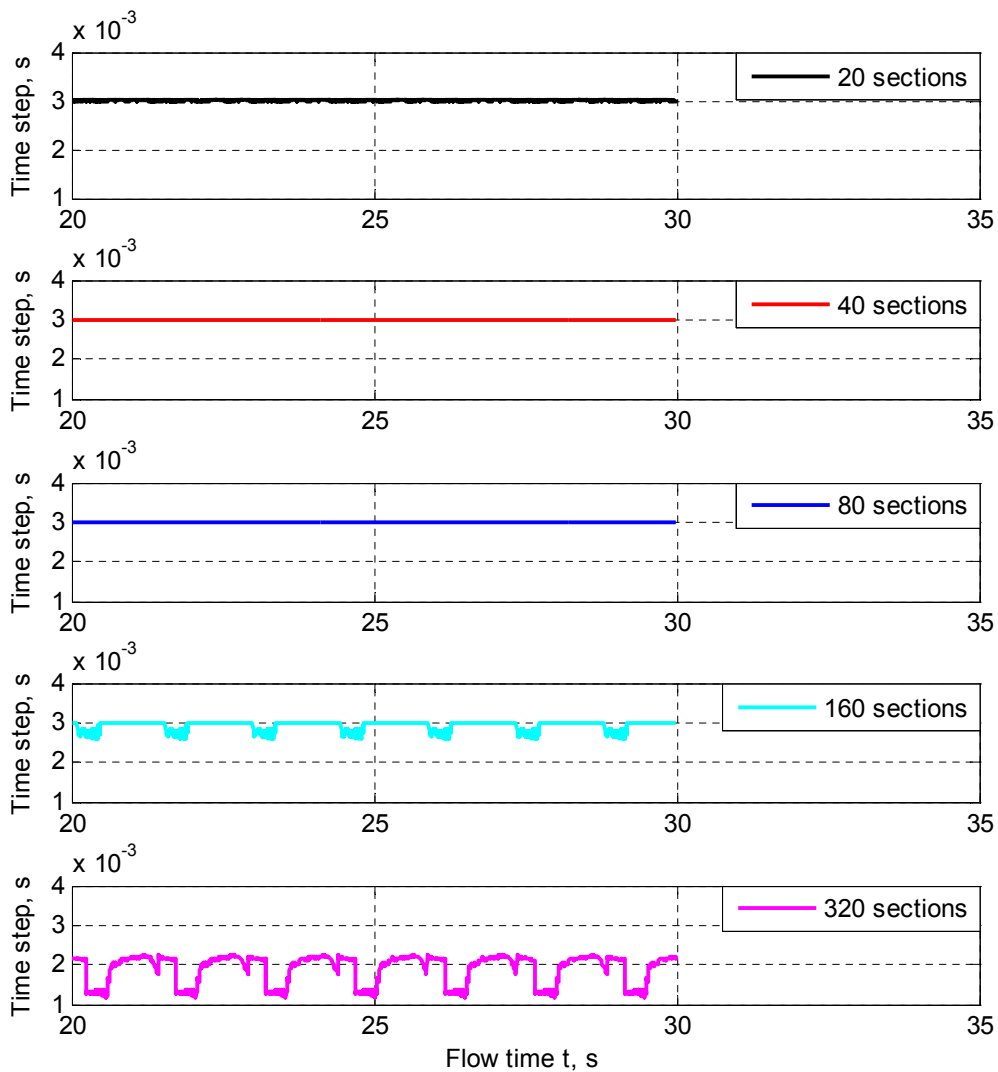
Figure 6-5 (a) compares the liquid holdup at the last section of the OLGA pipe of different levels of meshes. We can see that there are significant differences among the liquid holdup time traces due to different levels of meshes. The model of Mesh I with 20 sections provides the worst predictions of the maximum/minimum liquid holdup compared with the others. The maximum and minimum have been under predicted and over predicted, respectively. Moreover, the distribution of the gas/liquid two phases derived from the liquid holdup shows the distortion of the predicted slug and liquid film shapes. With the increase of the count of the sections until Mesh III with 80 sections the maximum liquid holdup increases and the minimum decreases, and the shapes of the slug and liquid film become reasonable. With the section count doubled and trebled of Mesh III with 80 sections, there is no significant improvement of the maximum/minimum liquid holdup, but only the shape of slugs. Based on the above discussions it is concluded that the upstream OLGA should have at least 80 sections.

Figure 6-5 (b) shows the time step series adopted by the OLGA model of Mesh I to Mesh V during the calculation. A time step control scheme based on the transport criterion of Courant-Friedrich-Levy (CFL) has been used in the OLGA model. Based on the CFL criterion the time step is adjusted to ensure that no mass is transported across a whole section of the OLGA pipe within one time step. This means that a smaller time step is required for a finer mesh with shorter sections. The upper and lower limits of the time step are specified by the user, for example 0.003 s and 0.001 s in the sample case, respectively. It can be seen in Figure 6-5 (b) that the time steps for Mesh I with 20 sections to Mesh III with 80 sections are limited by the user-specified upper limit, 0.003 s. For Mesh IV with 160 sections and Mesh V with 320 sections the time steps vary with the passages of the liquid slugs and films between the user-specified lower and upper limits. Compared with Mesh IV even smaller time steps are required by Mesh V. A ‘smoother’ time step series is more favourable to improve the numerical stability of the coupling model. Furthermore, the time step of the STAR model is usually smaller than that of the OLGA model. Therefore, larger time steps of the OLGA model are preferable to reduce the total computation time of the coupling model. Mesh IV and Mesh V are not recommended for the above reasons.

To summarise, the OLGA model of Mesh III with 80 sections provide reasonable predictions of the liquid holdup (Figure 6-5 (a)) and tend to reduce the computation time of the coupling model compared with Mesh IV and Mesh V. Therefore, Mesh III with 80 sections has been selected for the OLGA model in the STAR-OLGA coupling model below.



(a) Liquid holdup time traces



(b) Time step series

Figure 6-5 Liquid holdup time traces and time step series obtained from the OLGA model of different levels of meshes

The OLGA model of Mesh III was then coupled with the STAR model of different levels of meshes as listed in Table 6-2. Figure 6-6 compares the time traces of liquid holdup in the STAR pipe predicted by the coupling model of different levels of meshes. Four slug units including slug body and liquid film regions have been shown in the figure. It can be observed that the major differences among the three predictions take place in the liquid film regions. The liquid holdup in the slug bodies agree with each

other reasonably well except that the maximum liquid holdup of the last slug from the coarse mesh (level 1) is much lower than that from the other two meshes. It needs to be noted that the liquid holdup in the liquid film regions from the medium mesh (level 2) and fine mesh (level 3) agree with each other reasonably well but the liquid holdup from the coarse mesh behaves differently. To summarise, the coarse mesh is abandoned because the prediction of the liquid holdup in both slug body and liquid film deviates from that from the medium and fine meshes. Compared with the medium mesh the cell count of the fine mesh has increased by about 50 %, but there is only slight improvement on the prediction of liquid holdup in film regions. Therefore, the medium mesh (level 2) has been selected for the STAR model in the STAR-OLGA coupling model below.

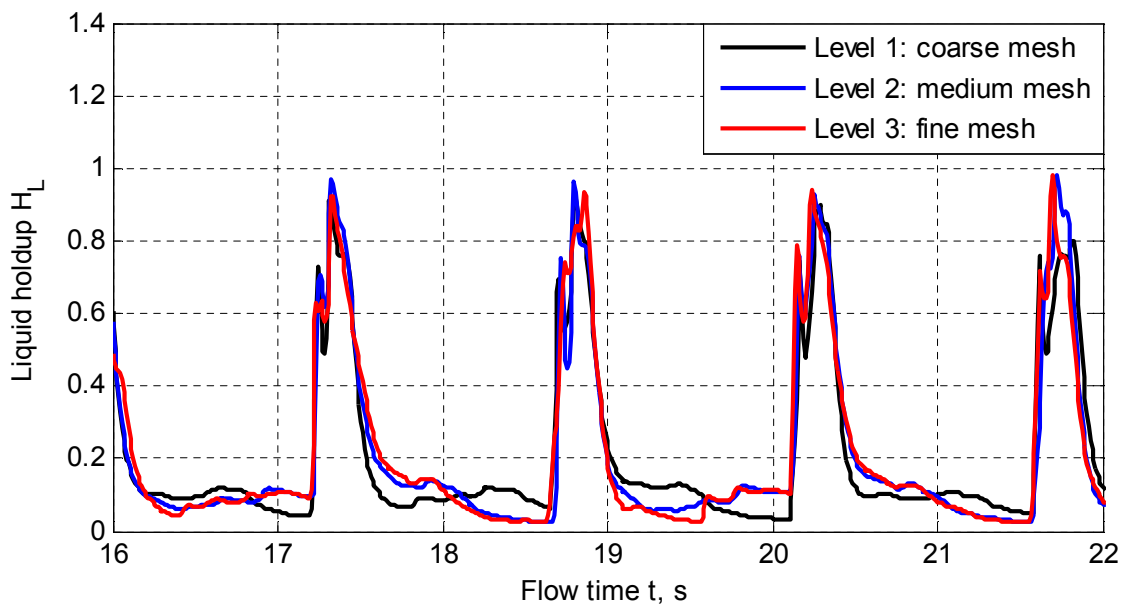


Figure 6-6 Time traces of the liquid holdup in the STAR pipe predicted by the coupling model of different levels of meshes

6.3.5 Geometries of Wavy Pipes

A series of wavy pipes with different amplitudes and lengths were created. Three geometries were created with different amplitudes. Geometry I has the same dimensions

with the tested wavy pipe in the experiment presented in Chapter 5. Geometry II and III are variants of Geometry I. Geometry II and III are obtained by extending each end of the bend in Geometry I by a straight pipe section with a length of $1d$ and $2d$, respectively (d the pipe diameter). The wavy pipes of Geometry I, II and III are denoted as Wavy I, Wavy II and Wavy III, respectively. The amplitudes of Wavy I, Wavy II and Wavy III are 0.057 m, 0.095 m and 0.132 m, with the ratio of amplitude to diameter (A/d) of 1.1, 1.8 and 2.5, respectively. Three wavy pipes of different lengths, with 7, 5 and 3 bends, were created for Wavy I. The lengths of the three wavy pipes are 1.061 m, 0.857 and 0.575, with the ratio of length to diameter (L/d) of 20.4, 16.5 and 11.1, respectively. Figure 6-7 and Figure 6-8 show the schematics of the wavy pipes of different amplitudes and lengths introduced above.

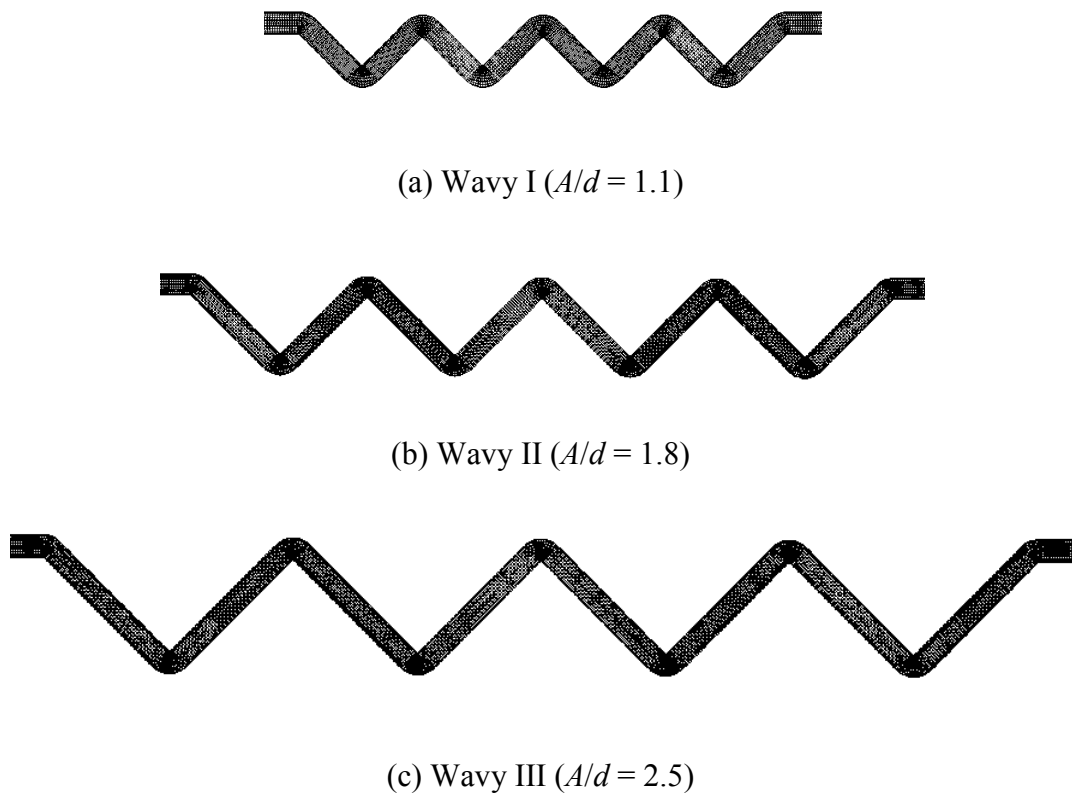
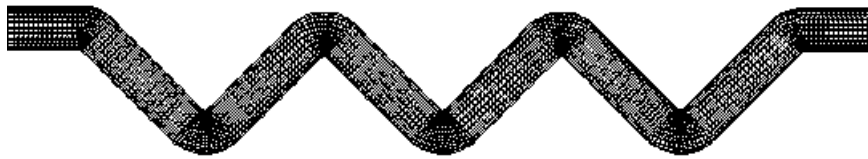


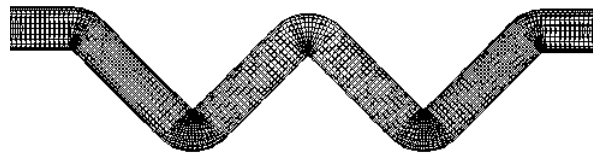
Figure 6-7 Schematics of the wavy pipes of different amplitudes (Wavy I, Wavy II and Wavy III of 7 bends)



(a) 7 bends ($L/d = 20.4$)



(b) 5 bends ($L/d = 16.5$)



(c) 3 bends ($L/d = 11.1$)

Figure 6-8 Schematics of the wavy pipes of different lengths (Wavy I)

It needs to be mentioned that there are two pipe sections of 2 m upstream and downstream of the wavy pipe in the STAR model, respectively. Both of the pipe sections are used to monitor the flow behaviour upstream and downstream of the wavy pipe.

6.4 Slug Flow in the Horizontal Wavy-Pipe System

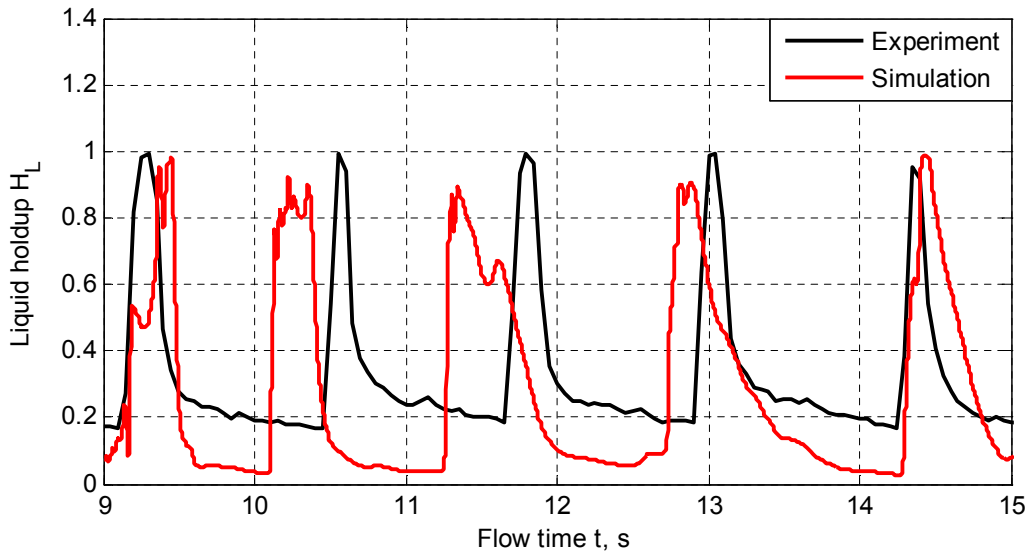
The coupling models of the wavy-pipe systems were solved at different flow conditions. The boundary conditions were specified according to the experimental data presented in Chapter 5. Firstly the coupling model with Wavy I of 7 bends (Figure 6-7 (a)), which has the same dimensions with that in the experiment, was solved and the model

predictions were compared with the experimental data; secondly the other wavy pipes of different amplitudes and lengths were tested and then the effects of the amplitude and length were examined based on the model predictions.

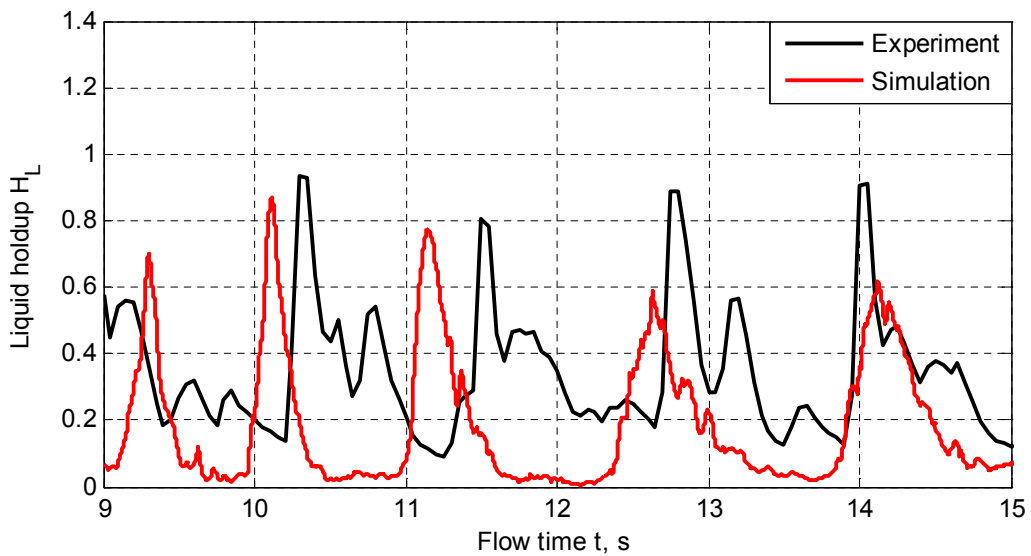
6.4.1 Effects of Wavy Pipe

Slug flow was generated in the upstream OLGA pipe, and then fed into the downstream wavy pipe. The area-averaged pressure and liquid holdup upstream and downstream of the wavy pipe were monitored during the calculation. The phase distribution on the pipe wall and longitudinal section of the STAR pipe were recorded in terms of gas volume fraction contour plots. More information and thus more understanding of the flow behaviour in the wavy pipe system have been obtained from the coupling model than the experiment in Chapter 5.

Figure 6-9 compares the liquid holdup upstream and downstream of the wavy pipe between the model predictions and experimental data. The inlet superficial water and air velocities are 0.47 m/s and 2.05 m/s, respectively, and the outlet pressure is the standard atmospheric pressure.



(a) Upstream



(b) Downstream

Figure 6-9 Comparison of the liquid holdup upstream and downstream of the wavy pipe between the model predictions and experimental data ($U_{SL} = 0.47$ m/s, $U_{SG} = 2.05$ m/s)

It can be seen in Figure 6-9 (a) that the slug frequency predicted by the coupling model agrees with the experimental data reasonably well. For most of the slug units the maximum liquid holdup in slug body and minimum in liquid film are under predicted by the model compared with the experimental data. The predicted minimum liquid holdup in the film region is about 0.03 while in the experimental data it is about 0.17. The lower liquid holdup in the liquid film indicates that a certain amount of liquid has gone into the slug body. Consequently, the predicted liquid slugs are longer than those in the experiment. The longer liquid slugs can be evidenced by the longer duration time of slug body indicated by the liquid holdup time traces in Figure 6-9 (a). Similarly the maximum and minimum liquid holdup downstream of the wavy pipe are also under predicted by the coupling model as shown in Figure 6-9 (b).

Comparing Figure 6-9 (a) and (b) we can see that: (1) the maximum liquid holdup in slug body downstream is lower than that upstream; (2) the same trend has been predicted by the coupling model. The reduction of the maximum liquid holdup in slug body reflects an increase of the gas entrainment in slug body. However, the gas entrainment into slug body tends to be over predicted by the model compared with the experimental data. To summarise, the coupling model can predict the phenomenon that an increase of the gas entrainment into slug body is induced by a wavy pipe, although tend to over predict the effects.

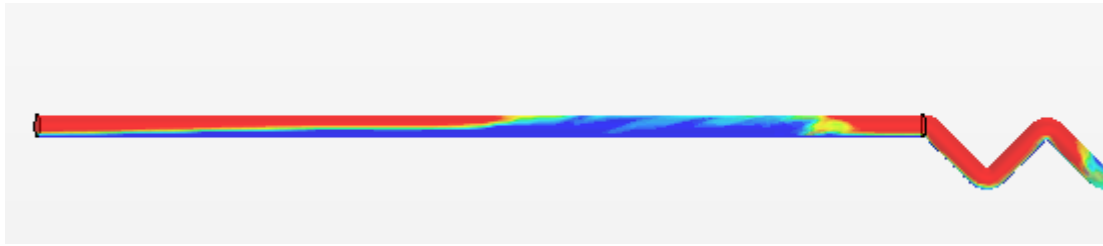
The phase distribution in the wavy pipe and upstream/downstream pipe sections has been examined to show how the two phases interact with the wavy pipe and the effects of the wavy pipe. It is still a challenge to measure the phase distribution on the cross-sections in the experiment; however, this can be achieved by monitoring the phase fraction in the STAR model part of the coupling model. The contour plots of gas volume fraction when a liquid slug appears upstream of the wavy pipe, in the wavy pipe and downstream of the wavy pipe are shown in Figure 6-10, 6-11 and 6-12, respectively. In each figure there are two contour plots showing the gas volume fraction on the pipe wall and on the longitudinal section of the pipe, respectively.

The slug flow is generated in the upstream OLGA pipe and then fed into the STAR pipe. A liquid slug followed by a liquid film in the pipe section upstream of the wavy pipe is

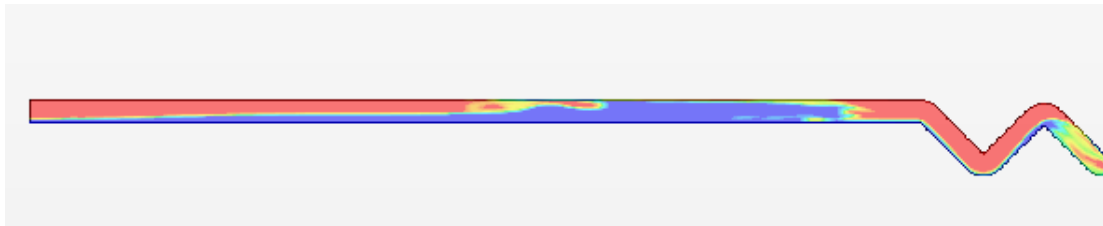
shown in Figure 6-10. The gas phase in the slug body is mainly located at the top and significant gas entrainment in the slug front can be observed in Figure 6-10 (a).

After the slug body moves into the wavy pipe the liquid phase tends to slow down and accumulate in the first upward limb. Consequently the flow path of the gas in the following liquid film region is blocked at the trough of the bend. However, the blockage cannot maintain because the gas keeps moving in and accumulates there. Soon the liquid in the first upward limb is pushed out into the next bend. The two phases tend to mix together during the push-out process. The mixing effect is then enhanced by the following bends. Eventually a highly aerated slug comes out of the wavy pipe as shown in Figure 6-11.

The highly aerated slug can be identified as a 'liquid dense zone' downstream of the wavy pipe as shown in Figure 6-12. The 'liquid dense zone' refers to a fluid region downstream of the wavy pipe, where the liquid holdup is higher than that in the liquid film region of the corresponding slug unit (including slug body and liquid film regions) upstream. The 'liquid dense zone' is longer than the corresponding slug body upstream; hence the average density of the 'liquid dense zone' is lower than that of the slug body. Furthermore, the 'liquid dense zone' can be divided into two sub-zones: Zone I and Zone II. As can be observed in Figure 6-12 Zone I is occupied by a gas/liquid mixture while Zone II is characterised of a swirling flow of liquid and gas/liquid mixture, and a gas core. Figure 6-13 shows the contour plots of the gas volume fraction on two cross-sections in Zone I (1.9 m downstream) and Zone II (1.0 m downstream), respectively. In Zone I the cross-section is occupied by a mixture of the two phases with higher gas volume fraction on the top. In Zone II we can see that: (1) a liquid film attaches to the pipe wall; (2) a gas core forms in a region close to the pipe centre; (3) a two-phase mixture of swirling behaviour is located between the gas core and liquid film. The swirling flow of liquid and gas/liquid mixture occurs as a result of the interaction between the gas/liquid two phases and the bends of the wavy pipe. In the swirling flow the liquid phase tends to move towards the pipe wall due to its higher density and decelerates due to the friction of the wall. Consequently a thin liquid film forms and a 'liquid dense zone' longer than the corresponding slug body is produced.



(a) Pipe wall (upstream of the wavy pipe)



(b) Longitudinal section (upstream of the wavy pipe)

→ Flow direction

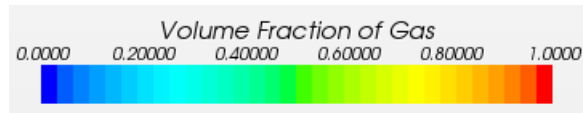
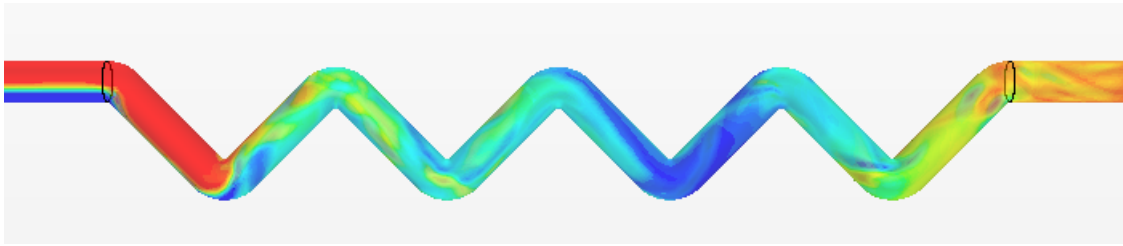
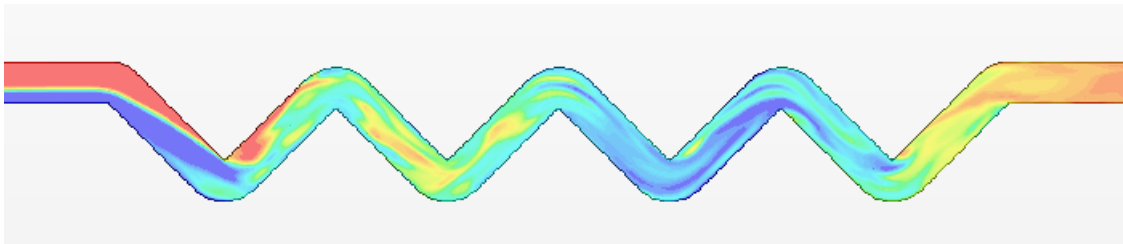


Figure 6-10 Contour plots of the gas volume fraction upstream of the wavy pipe
($U_{SL} = 0.47$ m/s, $U_{SG} = 2.05$ m/s)



(a) Pipe wall (in the wavy pipe)



(b) Longitudinal section (in the wavy pipe)

→ Flow direction



Figure 6-11 Contour plots of the gas volume fraction in the wavy pipe ($U_{SL} = 0.47$ m/s, $U_{SG} = 2.05$ m/s)

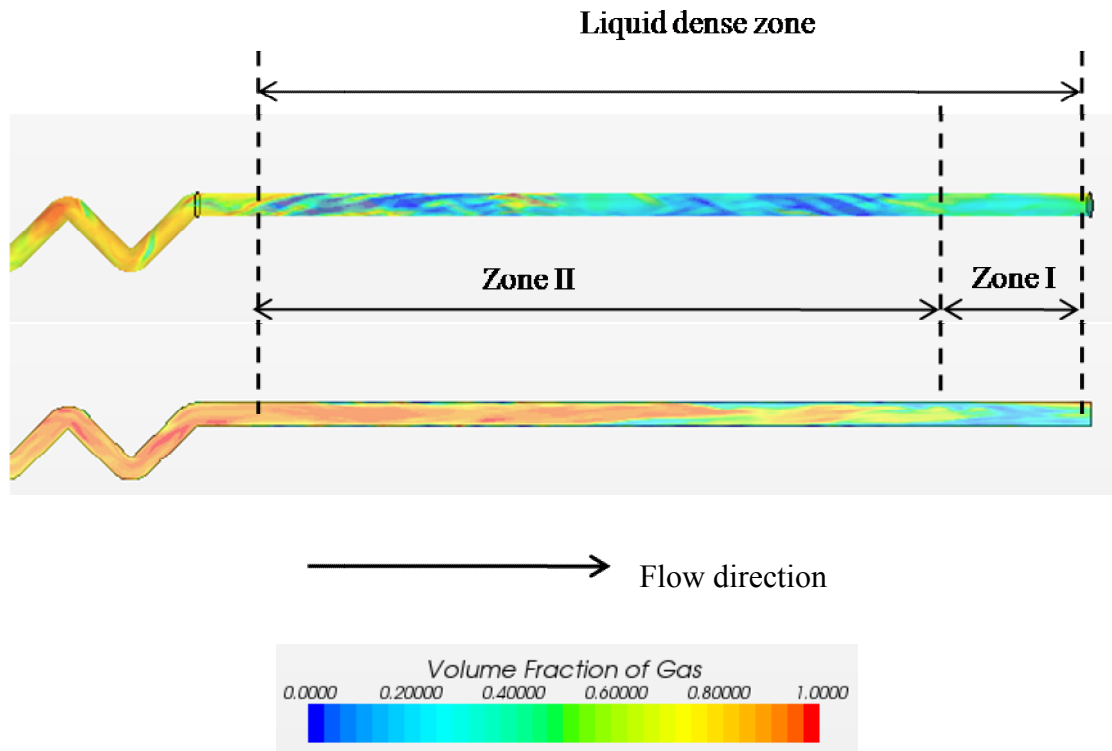
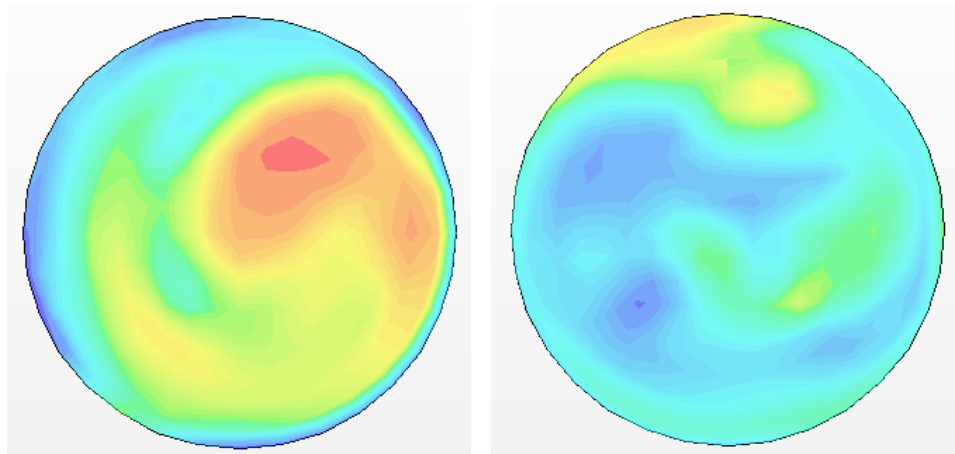


Figure 6-12 Contour plots of the gas volume fraction downstream of the wavy pipe
 ($U_{SL} = 0.47$ m/s, $U_{SG} = 2.05$ m/s)



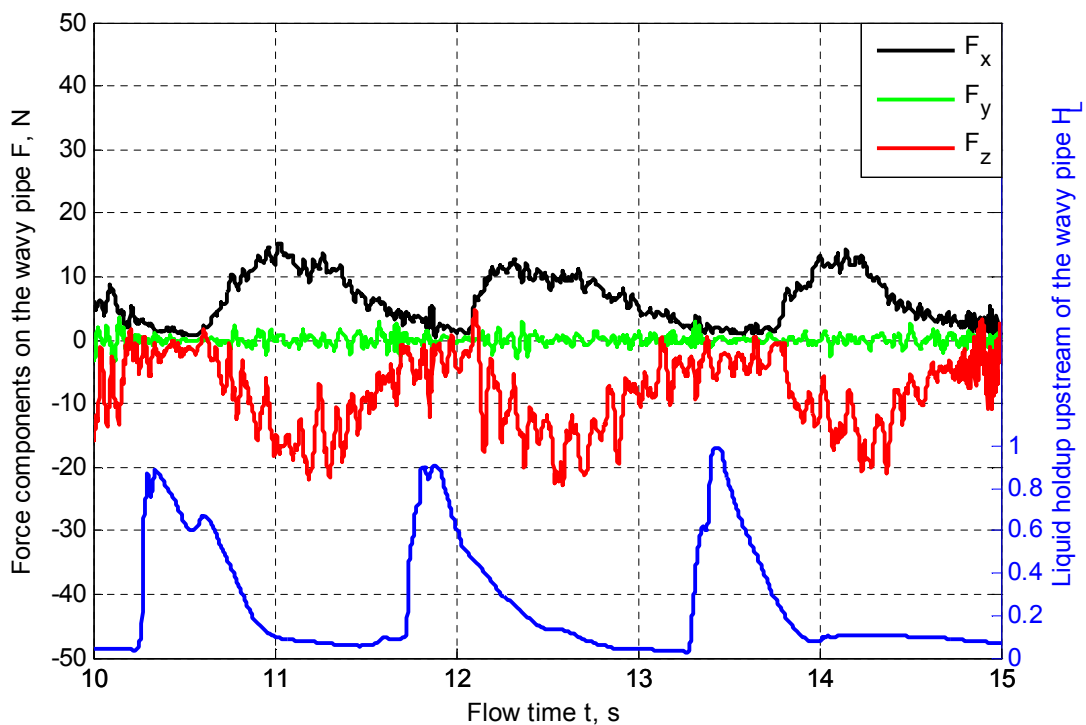
(a) Zone II (cross-section 1.0 m)

(b) Zone I (cross-section 1.9 m)



Figure 6-13 Contour plots of the gas volume fraction in Zone I and Zone II
 downstream of the wavy pipe ($U_{SL} = 0.47$ m/s, $U_{SG} = 2.05$ m/s)

It has been observed in the experimental campaign that the wavy pipe oscillates when the slug units are travelling in it. It is postulated that the oscillation of the wavy pipe is induced by the pseudo-cyclic forces acting on the bends of the wavy pipe. The liquid slug can exert forces on the humps and troughs of the bends where the flow direction changes. The forces on the wavy pipe have been monitored in the STAR model. Figure 6-14 shows the time traces of the force components in the x direction (flow direction), y direction and z direction (the opposite of the gravity direction).



x: Flow direction; z: Opposite of the gravity direction

Figure 6-14 Time traces of the force components on the wavy pipe and liquid holdup upstream of the wavy pipe predicted by the coupling model ($U_{SL} = 0.47$ m/s, $U_{SG} = 2.05$ m/s)

It needs to be mentioned that the liquid holdup shown in Figure 6-14 is obtained from the pipe section upstream of the wavy pipe, thus there is a time delay for the forces on the wavy pipe to increase. Actually the force components in the x and y directions start

to rise once the liquid slug moves into the wavy pipe and drop when the liquid film moves in. Hence the slug induced force has the same cycle time with that of the corresponding slug unit. The amplitudes of the force components in the x and z directions are similar and much higher than that in the y direction. The average force in the y direction is almost zero. The cyclic force on the wavy pipe needs to be taken into consideration when designing a wavy pipe system. An appropriate piping support system is required to stabilise the wavy pipe experiencing slug flow.

The effects of the wavy pipe on slug flow identified from the model predictions can be confirmed by the experimental data presented in Chapter 5. This provides more confidence in applying this coupling model to wavy pipe systems with wavy pipes of different configurations. The effects of the amplitude and length of the wavy pipe are examined through the coupling model and discussed in Section 6.4.2 and Section 6.4.3, respectively.

6.4.2 Effects of the Amplitude of Wavy Pipe

The three wavy pipes of different amplitudes, i.e. Wavy I, Wavy II and Wavy III of 7 bends shown in Figure 6-7, have been tested applying STAR-OLGA coupling models. The liquid holdup and phase distribution downstream of the wavy pipes are compared among the three wavy pipe systems. The superficial water and air velocities at the inlet of the systems are $U_{SL} = 0.95$ m/s and $U_{SG} = 2.14$ m/s, respectively. The same flow conditions have been achieved upstream of the three wavy pipes, therefore, the effects of the amplitude of the wavy pipe can be identified by analysing the differences in the flow behaviour downstream.

The time traces of the liquid holdup downstream of the wavy pipe are compared in Figure 6-15 for the three wavy pipe systems. The maximum liquid holdup in slug body is an indicator of the gas entrainment. The lower maximum liquid holdup indicates that more gas entrainment is introduced into the slug body. Therefore, the effective density of the slug is reduced. It can be seen in Figure 6-15 that, for most cases, the highest maximum liquid holdup appears with Wavy III and the lowest can be obtained with Wavy II. The maximum liquid holdup decreases and then increases with the increase of the wavy pipe amplitude from $1.1d$ to $1.8d$ until $2.5d$, i.e. from Wavy I to Wavy III.

Therefore, the amplitude of the wavy pipe needs to be selected properly to obtain a better performance of the wavy pipe. It is reasonable that the wavy pipe of excessively higher amplitude is less effective on introducing more gas entrainment into the slug body, because the liquid phase tends to accumulate in the longer upward limbs.

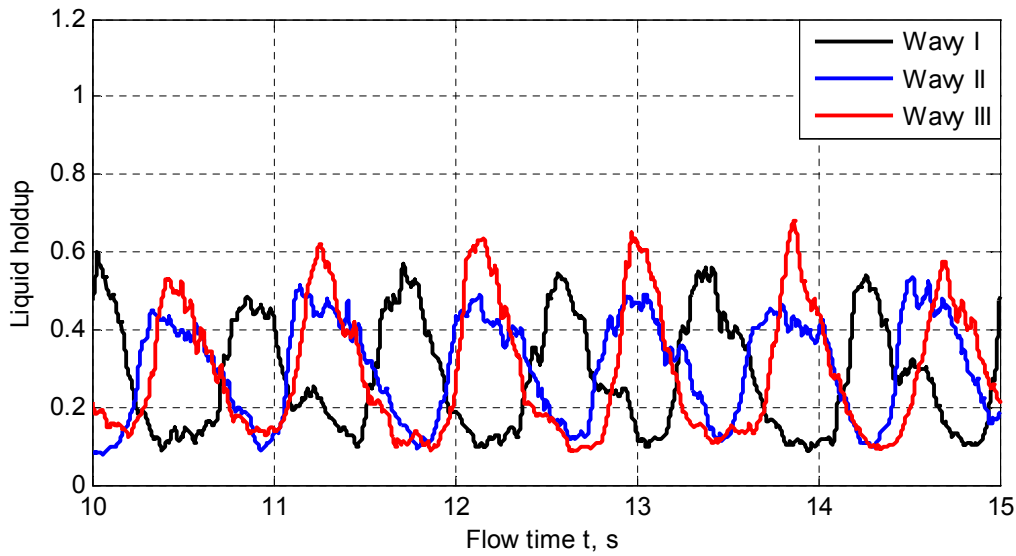


Figure 6-15 Comparison of the liquid holdup time traces downstream of the wavy pipes of different amplitudes ($U_{SL} = 0.95$ m/s, $U_{SG} = 2.14$ m/s)

As concluded in Section 6.4.1, during the travelling in the wavy pipe, the gas and liquid two phases tend to mix and more gas can be introduced into the slug body. As a result, the upstream liquid slug has degenerated to a ‘liquid dense zone’ downstream of the wavy pipe. Figure 6-16 compares the ‘liquid dense zones’ downstream of Wavy I, Wavy II and Wavy III. The three ‘liquid dense zones’ in Figure 6-16 are those with the maximum liquid holdup appearing between $t = 13$ s and $t = 14$ s in Figure 6-15. Those ‘liquid dense zones’ correspond to the same slug upstream of the wavy pipes. Therefore, the effects of the wavy pipe amplitude can be examined by comparing the characteristics of the ‘liquid dense zones’.

It can be observed in Figure 6-16 that the longest ‘liquid dense zone’ appears downstream of Wavy II, followed by that of Wavy I and the shortest of Wavy III. The

length of the ‘liquid dense zone’ increases and then decreases with the increase of the wavy pipe amplitude from $1.1d$ to $1.8d$ until $2.5d$, i.e. from Wavy I to Wavy III. The downstream ‘liquid dense zones’ originate from the same upstream slug. Therefore, the longer the ‘liquid dense zone’ is the more gas is entrained in it, as a result, the lower the effective density of the ‘liquid dense zone’ is. Hence it is concluded that Wavy II is more effective than Wavy I and Wavy III of lower and higher amplitudes, respectively.

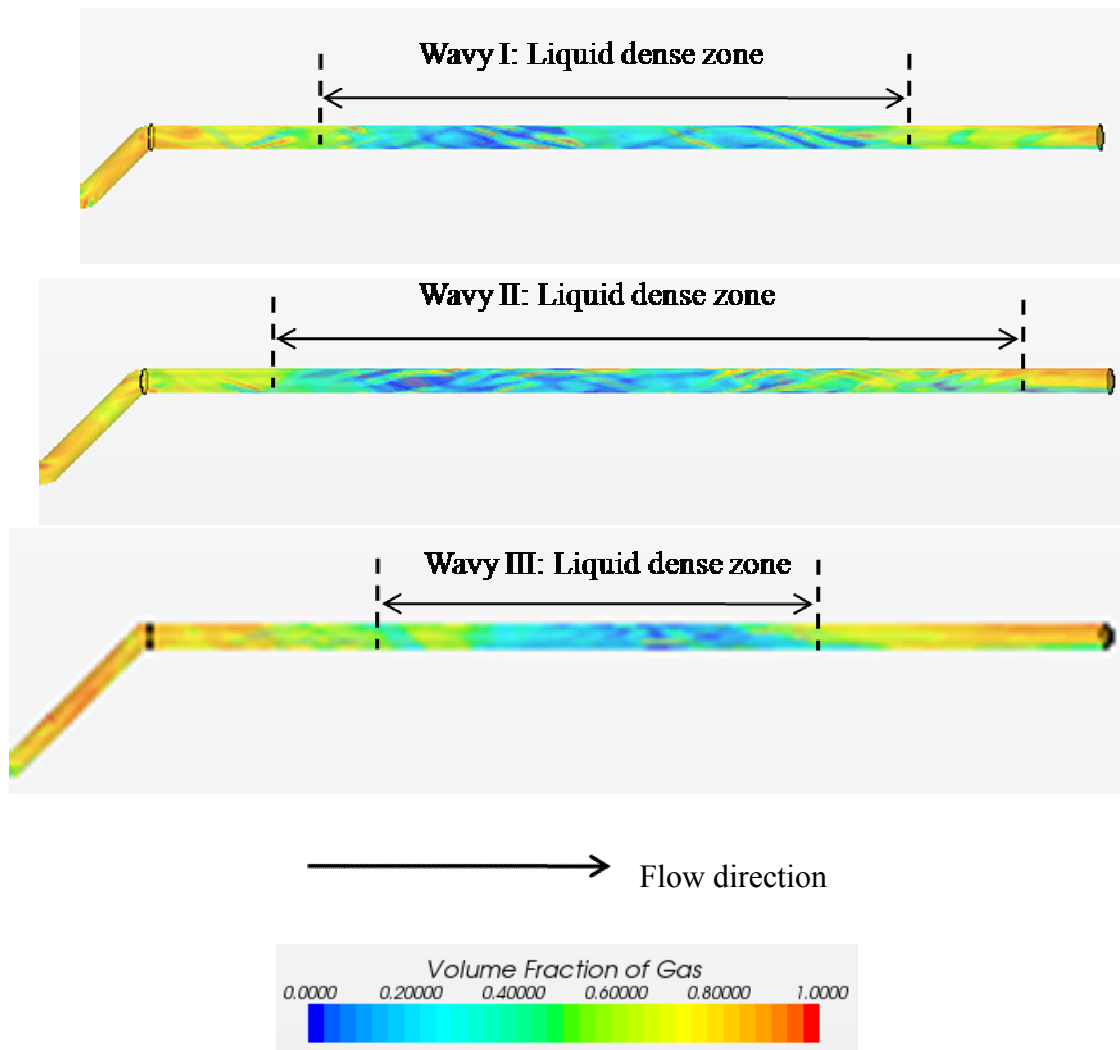


Figure 6-16 Contour plots of the gas volume fraction downstream of Wavy I, Wavy II and Wavy III ($U_{SL} = 0.95$ m/s, $U_{SG} = 2.14$ m/s)

6.4.3 Effects of the Length of Wavy Pipe

The wavy pipe of different lengths, i.e. 7 bends, 5 bends and 3 bends shown in Figure 6-8, have been tested. The liquid holdup and phase distribution downstream of the wavy pipes are compared among the three wavy pipe systems. The superficial water and air velocities are $U_{SL} = 0.95$ m/s and $U_{SG} = 2.14$ m/s, respectively. The same flow conditions have been achieved upstream of the three wavy pipes, however, there are significant differences in the flow behaviour downstream induced by the lengths of the wavy pipes.

The time traces of the liquid holdup downstream of the wavy pipes are compared in Figure 6-17 for Wavy I of 7 bends, 5 bends and 3 bends. For most cases the highest maximum liquid holdup appears with 3-bend wavy pipe and the lowest can be obtained with 7-bend wavy pipe. The maximum liquid holdup decreases with the increasing length of wavy pipe.

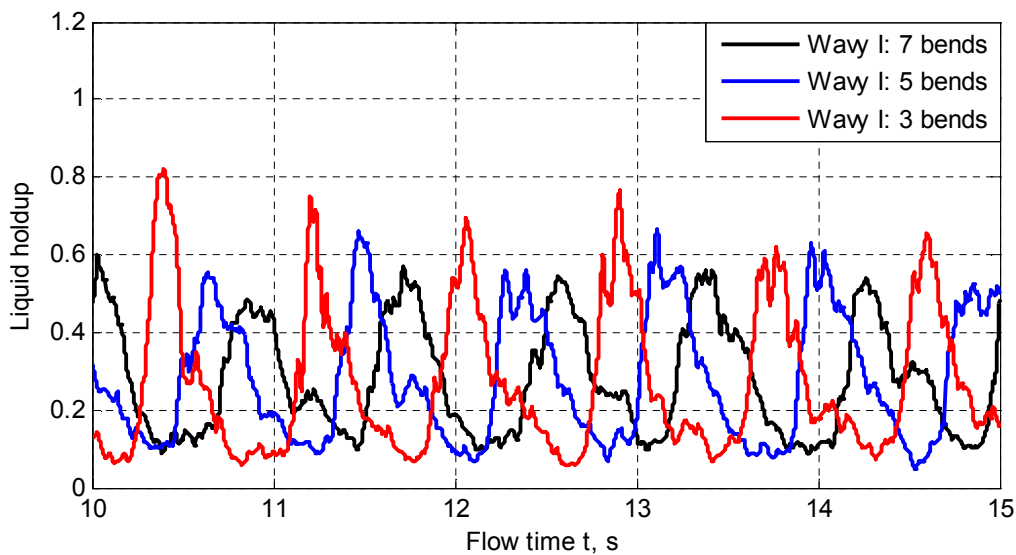


Figure 6-17 Comparison of the liquid holdup time traces downstream of Wavy I of 7 bends, 5 bends and 3 bends ($U_{SL} = 0.95$ m/s, $U_{SG} = 2.14$ m/s)

The ‘liquid dense zones’ downstream of Wavy I of different lengths are compared in Figure 6-18. The three ‘liquid dense zones’ are those with the maximum liquid holdup appearing between $t = 10$ s and $t = 11$ s in Figure 6-17, which correspond to the same slug upstream of the wavy pipes. It can be observed that the longest ‘liquid dense zone’ is obtained with the 7-bend wavy pipe, followed by the 5-bend wavy pipe and the shortest appears downstream of the 3-bend wavy pipe. The length of the ‘liquid dense zone’ increases with the increase of the length of the wavy pipe, i.e. from 3 bends to 7 bends. A longer ‘liquid dense zone’ results in a lower effective density of it. Therefore, a longer wavy pipe of more bends (7 bends, $L/d = 20.4$) is more effective on reducing the effective density of the upstream liquid slugs than shorter ones (5 bends, $L/d = 16.5$; 3 bends, $L/d = 11.1$).

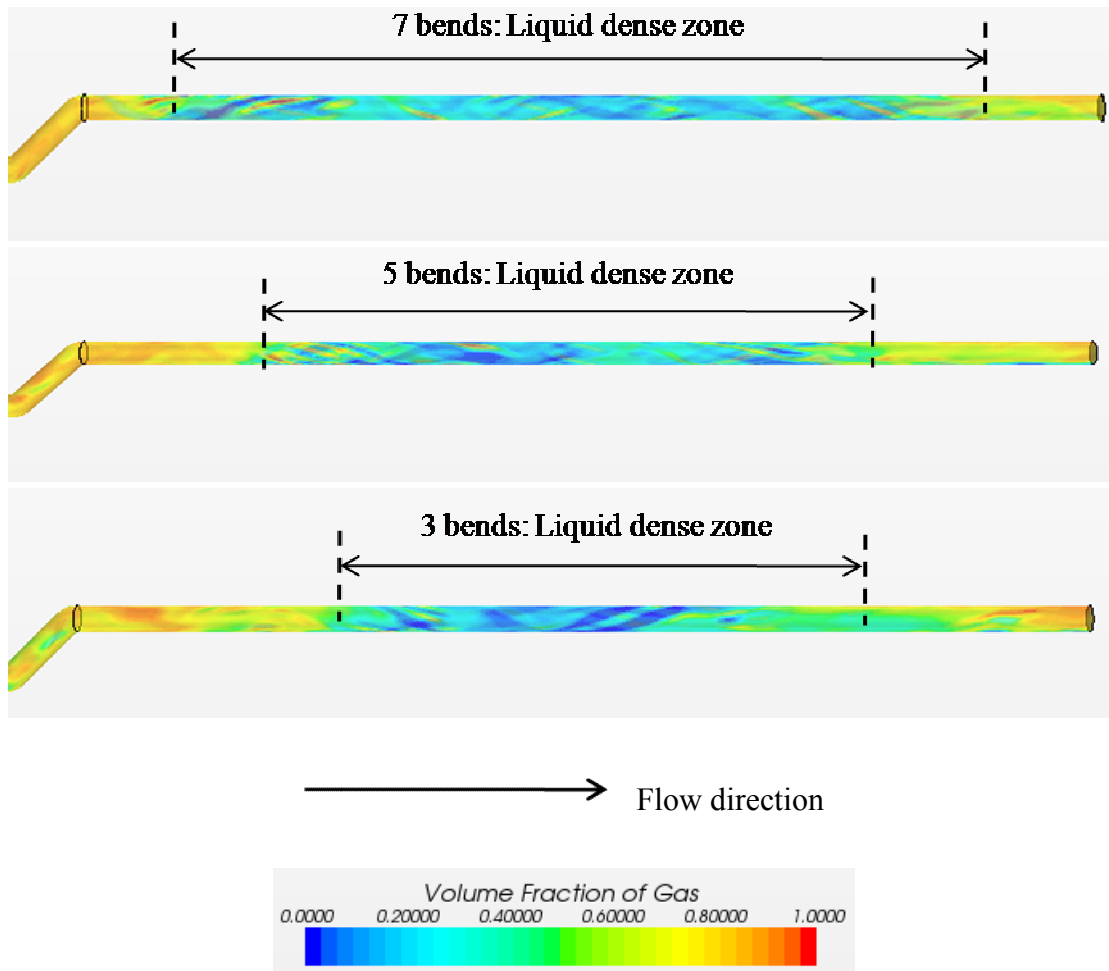


Figure 6-18 Contour plots of the gas volume fraction downstream of Wavy I of 7 bends, 5 bends and 3 bends ($U_{SL} = 0.95$ m/s, $U_{SG} = 2.14$ m/s)

6.4.4 Discussions

The effects of the wavy pipe on hydrodynamic slug flow have been presented in Section 6.4.1. It has been observed that, in the wavy pipe, the liquid phase tends to slow down and accumulate in the first upward limb. Consequently the flow path of the gas in the following liquid film region is blocked at the trough of the bend. However, the blockage cannot maintain because the gas keeps moving in and accumulates there. Soon the liquid in the first upward limb is pushed out into the next bend. The two phases tend to mix together during the push-out process. The mixing effect is then enhanced by the following bends. As a result, the upstream slug degenerates to a ‘liquid dense zone’ with a longer length downstream of the wavy pipe. The ‘liquid dense zone’ can be further divided into Zone I and Zone II. Zone I is occupied by a gas/liquid mixture while Zone II is characterised of a swirling flow of liquid and gas/liquid mixture, and a gas core. The swirling flow occurs as a result of the interaction between the gas/liquid two phases and the bends of the wavy pipe. In the swirling flow the liquid phase tends to move towards the pipe wall due to its higher density and decelerates due to the friction of the wall. Consequently a thin liquid film forms and a ‘liquid dense zone’ longer than the corresponding slug body is produced. The slug flow tends to re-establish downstream of the wavy pipe as observed in the experiment (see Section 5.4.1). It is postulated that the swirling flow downstream of the wavy pipe can delay the recovery of slug flow, because the liquid phase mainly exists in the form of film on the wall or gas/liquid mixture rather than a chunk of liquid at the bottom of the pipe (a precursor of a slug body).

The wavy pipe works by mixing the gas and liquid two phases together. The mixing effects are affected by the geometrical parameters of the wavy pipe such as amplitude and length presented in Section 6.4.2 and 6.4.3. A wavy pipe of higher amplitude does not always introduce better mixing effects to slug flow. The maximum liquid holdup downstream decreases and then increases with the increase of the wavy pipe amplitude from $1.1d$ to $1.8d$ until $2.5d$ (d the pipe diameter). The upward limbs in a wavy pipe of higher amplitude are longer. It is postulated that the longer upward limbs allow for more liquid to accumulate and the slug tends to reform there. A longer wavy pipe of more bends is more favourable to mix the two phases. A longer wavy pipe (7 bends, $L/d =$

20.4) provides more space and time for the gas/liquid two phases to interact with each other than shorter ones (5 bends, $L/d = 16.5$; 3 bends, $L/d = 11.1$). Consequently more gas can penetrate into the slug and reduce the effective density of the slug body during the journey in the wavy pipe.

6.5 Summary

As a part of the project to explore the CFD-OLGA co-simulation tool, in this work the STAR-OLGA coupling was applied to model the hydrodynamic slug flow in horizontal wavy-pipe systems. The wavy pipe was modelled using 3-D CFD code STAR-CCM+, while the upstream and downstream pipelines were modelled using 1-D code OLGA. The slug flow was generated in the upstream OLGA model part and then fed into the wavy pipe and downstream OLGA pipe. The effects of the wavy pipe on hydrodynamic slug flow were investigated.

The STAR-OLGA coupling was introduced briefly then a simple case with a straight pipe modelled with STAR-CCM+ was tested. The dependency of the model solutions on the meshes of OLGA and STAR models was examined, based on which appropriate meshes for the coupling models of the wavy-pipe systems were selected.

The liquid phase in slug body tends to slow down and accumulate in the first upward limb of the wavy pipe. Consequently the flow path of the gas in the following liquid film region tends to be blocked at the trough of the bend. However, the blockage cannot maintain because the gas keeps moving in and accumulates there. Soon the liquid in the first upward limb is pushed out into the next bend. The two phases tend to mix together during the push-out process. The mixing effect is then enhanced by the following bends. As a result, the upstream slug degenerates to a 'liquid dense zone' downstream of the wavy pipe. The 'liquid dense zone' can be further divided into Zone I and Zone II. Zone I is occupied by a gas/liquid mixture while Zone II is characterised of a swirling flow of liquid and gas/liquid mixture, and a gas core. The effective density in the 'liquid dense zone' is less than that in the upstream slug, thus the severity of the slug flow is mitigated by the wavy pipe.

The wavy pipe works as a mixer, which makes the gas/liquid two phases tend to mix together. A wavy pipe of higher amplitude does not always introduce better mixing effects to slug flow. The maximum liquid holdup downstream decreases and then increases with the increase of the wavy pipe amplitude from $1.1d$ to $1.8d$ until $2.5d$ (d the pipe diameter). The upward limbs in a wavy pipe of higher amplitude are longer. It is postulated that the longer upward limbs allow for more liquid to accumulate and thus slugs to reform there. A longer wavy pipe of more bends is more favourable to mix the two phases. A longer wavy pipe (7 bends, $L/d = 20.4$) provides more space and time for the gas/liquid two phases to interact with each other than the shorter ones (5 bends, $L/d = 16.5$; 3 bends, $L/d = 11.1$). Consequently more gas can penetrate into the slug body during the journey in the wavy pipe and the severity of the slug flow is further mitigated.

7 INVESTIGATION OF SLUG FLOW INDUCED FORCES ON PIPE BENDS APPLYING STAR-OLGA COUPLING

7.1 Introduction

Cyclic forces on the wavy pipe can be induced by gas/liquid slug flow. The liquid slugs can exert large forces on the pipe bends where the flow direction changes. The forces result in violent oscillations, which have been observed in the experiment (Chapter 5). However, the forces were not measured in the experiment due to the lack of proper instruments. It has been demonstrated in Chapter 6 that the STAR-OLGA coupling model can predict the cyclic forces exerted on the wavy pipe due to slug flow. The model predictions were not verified due to the lack of experimental data.

In this work the forces on a single pipe bend induced by slug flow were investigated in detail applying STAR-OLGA coupling. The model predictions were verified by the experimental data in the literature. In this chapter, firstly a literature review on the previous studies of slug forces on pipe bends is presented; secondly the development of the coupling model of the bend system is introduced; thirdly the forces and force components on the bend are presented. The objectives are: (1) to verify the forces predicted by the coupling model by experimental data; (2) to attain more understanding of the force distribution on the pipe wall of the bend.

7.2 Previous Investigations of Slug Forces on Pipe Bends

Gas/liquid slug flow is a frequently encountered flow regime in oil and gas flowlines. The fast-moving liquid slugs can exert large forces on the pipe bends where the flow direction changes sharply. Excessive forces induced by slug flows can impose great structural instability on the piping and piping support systems. An understanding of the force characteristics is very important when designing the piping and piping support systems to ensure the integrity of the flowlines. However, limited studies on the characteristics of the forces induced by gas/liquid slug flows in large diameter pipelines have been found in the open literature.

Fairhurst (1983) conducted experiments on an 80° near horizontal-to-vertical bend with an internal diameter of 54 mm subjected to gas/liquid slug flows. The test section also included a 10 m long upstream horizontal pipe and an 8 m long riser discharging to the atmosphere. Along with the experiment a steady-state model in the form of Equation (7-1) and (7-2) was proposed to estimate the largest force on the bend based on the steady-state momentum equation.

$$F_x = \rho AU_s^2(1 - \cos\beta) \quad (7-1)$$

$$F_z = \rho AU_s^2(\sin\beta) \quad (7-2)$$

where F_x and F_z were the magnitudes of the force components in the x and z directions, i.e. the horizontal and vertical directions, respectively, ρ was the density of the liquid slug, A was the cross-sectional area, U_s was the slug velocity calculated by U_{SG}/H_G and β was the angle of the bend. The U_{SG} was the superficial gas velocity and H_G was the average void fraction of the slug flow estimated through the correlation proposed by Beggs and Brill (1973). It was reported that the forces predicted by the above model were 17 % - 56 % higher than the experimental data for the gas free liquid slugs and slugs with void fraction of 25 %. It needs to be noted that the contribution to the force by the pressure at the bend was not taken into account in the above model. Although the riser was discharging into the atmosphere, the hydrostatic pressure induced by the liquid column in the riser was still noticeable.

In the experiment conducted by Sánchez *et al.* (1998) a long radius 90° elbow was positioned horizontally. The internal diameter of the elbow was 41 mm and the radius of the elbow was 280 mm. The pipes upstream and downstream of the elbow were 33 m and 5 m long respectively. Air-water slug flow conditions were tested. They developed a model to calculate the forces on the bend as below:

$$F_x = \rho Au_x^2 + (P_x - P_a)A \quad (7-3)$$

$$F_y = \rho Au_y^2 + (P_y - P_a)A \quad (7-4)$$

where u_x and u_y were the velocities in the x and y directions respectively, P_a was the ambient pressure (atmospheric pressure in the experiment), P_x and P_y were the absolute

pressures at the inlet and outlet of the bend respectively, $P_x A$ and $P_y A$ were the pressure-area forces at the inlet and outlet of the bend respectively. Compared with the model proposed by Fairhurst (1983) the pressure induced force on the bend was taken into account by Sánchez's model. It was claimed that a good agreement between the model predictions and experimental data was achieved. However, no detailed information was provided to explain how the time-dependent parameters, i.e. u_x , u_y , P_x , and P_y , in Equation (7-3) and (7-4) were calculated.

Tay and Thorpe (Tay, 2002; Tay and Thorpe, 2002) conducted an experimental and theoretical investigation into the time-dependent forces on a horizontal bend experiencing gas/liquid slug flows. In their experiment a 90° stainless steel bend with a radius of 105 mm and an internal diameter of 70 mm was tested. The bend was isolated from the upstream and downstream pipes by metal bellows to minimise the mechanical transmission to and from the bend. In their experiment the time-dependent force on the bend, liquid holdup and pressure upstream and downstream of the bend were measured simultaneously. The effects of the liquid physical properties on the slug flow induced force were also examined. It was concluded that no significant effects on the forces acting on the bend were observed when the liquid surface tension was reduced by 32 % or the liquid viscosity was increased by a factor of 2.62 (Tay and Thorpe, 2004). A one-dimensional transient model called Piston Flow Model (PFM) was proposed to predict the transient hydrodynamic force on the horizontal pipe bend for gas/liquid slug flow. The PFM was developed based on the unsteady-state momentum equation and could predict the time-dependent force on the bend including three terms: momentum term, change rate of momentum and pressure-area term. A method for calculating the time-dependent pressures at the inlet and outlet of the bend was also proposed under the PFM. It was concluded that the predictions of the maximum force agreed with their experimental measurements very well and could account for the effects of the increased gas/liquid ratio and reduced liquid surface tension by adjusting the liquid holdup in liquid slugs accordingly.

However, it needs to be noted that the slug length was an important input parameter to the PFM as it would be used for predicting the pressure drop and density then the maximum slug force. The requirement for an accurate prediction of the average slug

length could limit the application range of the PFM because the slugs usually have a distribution of lengths (Brill *et al.*, 1981; Barnea and Taitel, 1993). In addition some assumptions had to be made in developing the PFM. The major assumptions were: (1) a hypothetical slug flow consisting of a piston flow of pure gas followed by a piston flow of pure liquid; (2) only a gas bubble or a liquid slug confined in the bend control volume; (3) the gas bubbles and liquid slugs flowing at a constant and uniform velocity, slug velocity U_s , obtained from the following equation:

$$U_s = C(U_{SG} + U_{SL}) + U_{drift} \quad (7-5)$$

where C was a constant, U_{SG} and U_{SL} were the superficial gas and liquid velocities respectively and U_{drift} was the drift velocity. The coefficient C and U_{drift} were obtained through linear regression on their experimental data. Extra care needs to be taken when the PFM is applied to other bend configurations as the estimation of the slug velocity affects the accuracy of the force prediction significantly.

The issues related to the application of the PFM mainly arise from the characterisation of the slug flow upstream of the bend. It has been recognised that it is still a challenge to predict the slug flow characteristics accurately for a wide range of pipe configurations and flow conditions with simulation models.

7.3 Development of the Coupling Model

The experimental apparatus reported by Tay (2002) was modelled applying STAR-OLGA coupling. In their experiment a 90° stainless steel bend with a radius of 105 mm and an internal diameter of 70 mm was tested and the time-dependent force acting on the bend was measured. In the STAR-OLGA coupling model the bend was modelled in STAR-CCM+ and the upstream and downstream pipelines were modelled in OLGA.

7.3.1 Model Geometry

The upstream and downstream pipes of the experimental rig were approximately 9.0 m and 2.6 m long respectively. However, in the OLGA model the upstream pipe was extended to 20 m to allow for the establishment of a steady hydrodynamic slug flow and increase the numerical stability of the model. The OLGA pipe was divided into 80

sections with 0.25 m for each section. Two coupling configurations, i.e. one-point coupling and two-point coupling, were employed. In the one-point coupling model the downstream pipe was not taken into account as it was too short to be modelled in OLGA. A 1 m long downstream pipe was created in the CFD model instead. The two-point coupling model was created to examine the effects of the downstream pipe on the force exerted on the bend. Figure 7-1 shows a schematic of the two-point coupling model.

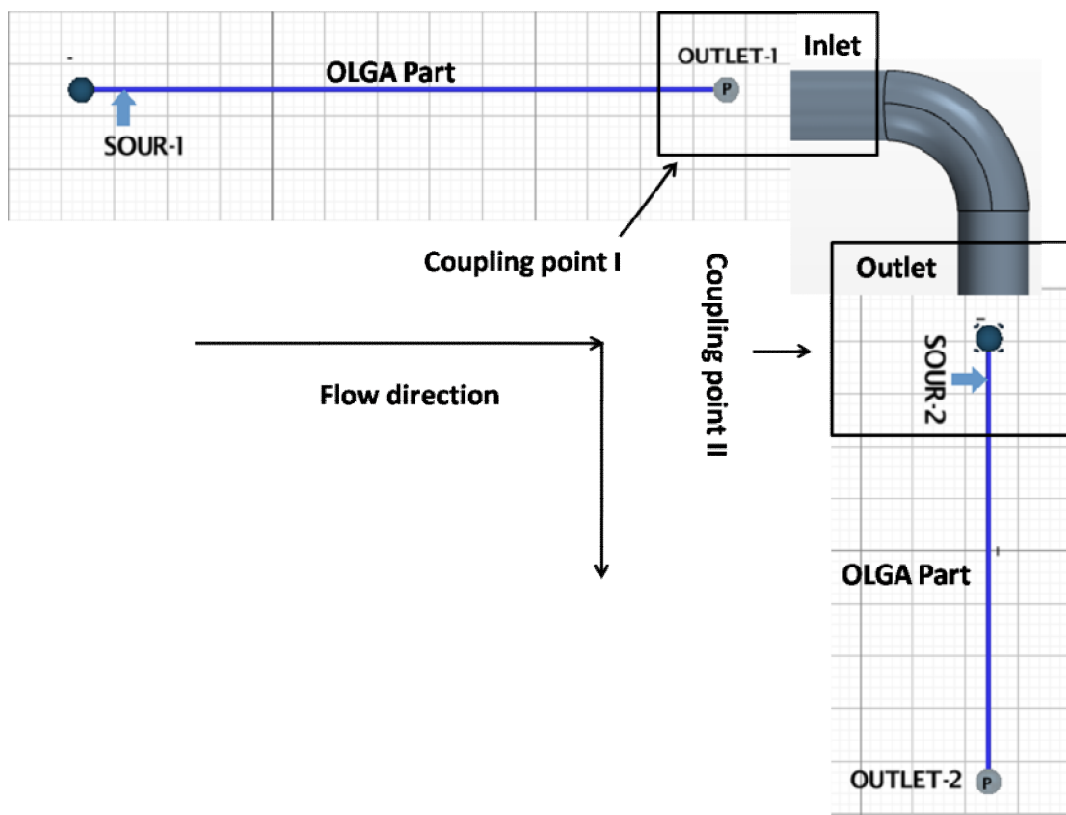
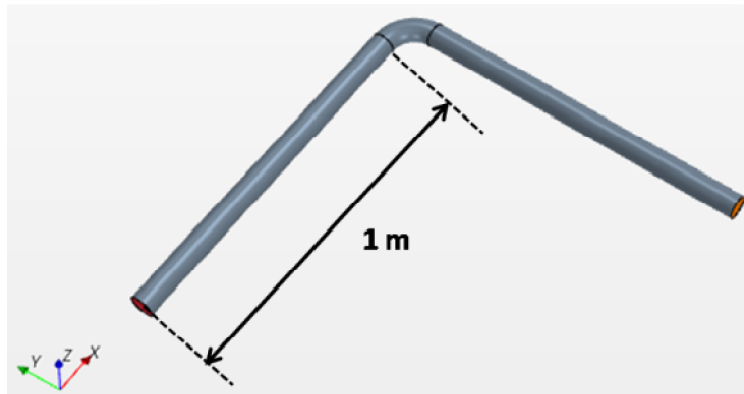


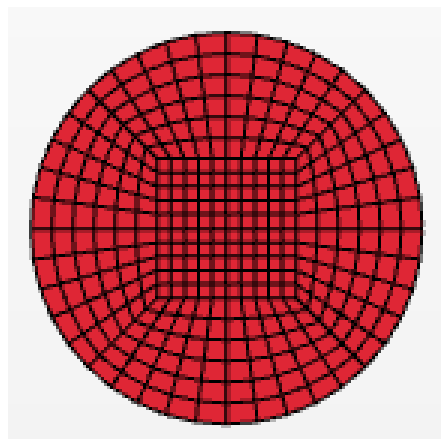
Figure 7-1 Schematic of the two-point STAR-OLGA coupling model

The CFD model in STAR-CCM+ included a 1 m long upstream pipe section, a 90° bend with a radius of 105 mm and a 1 m long downstream pipe section. The geometry of the STAR model and the mesh used to discretise the cross-section of the pipe are shown in Figure 7-2. There are 340 cells on the cross section with the minimum and maximum area of $2.5 \times 2.5 \text{ mm}^2$ and $5.5 \times 3.0 \text{ mm}^2$ respectively. A uniform axial mesh was used

for the upstream and downstream pipes with a length 4 mm for each cell in the axis-direction. The STAR model had 154,700 cells in the computation domain.



(a) Geometry of the STAR model



(b) Mesh on the cross-section

Figure 7-2 Geometry of the STAR model and mesh on the cross-section

7.3.2 Model Setup

The flow conditions of the test cases were consistent with the experimental data collected by Tay (2002). The test fluids in the experiment were air and water. The mass flowrates of the two phases at the inlet of the upstream OLGA pipe were constant and the outlet of the STAR pipe for the one-point coupling model was specified as the

atmospheric pressure. In the two-point coupling model the outlet of the downstream OLGA pipe was specified as the atmospheric pressure. For the internal boundaries a slightly higher pressure than the atmospheric pressure was specified at the outlet of the upstream OLGA pipe. The inlet boundary conditions of the STAR pipe were provided by the upstream OLGA pipe in the one-point model, while in the two-point coupling model the outlet boundary conditions of the STAR pipe were also provided by the downstream OLGA pipe.

The slug tracking module in OLGA was applied to predict the characteristic parameters of the slug flow in the upstream pipe. In the STAR model the two-layer realisable $k-\epsilon$ model (generally used and recommended for a wide range of flows and meshes) and VOF model were adopted to model the turbulence and track the volume fraction of each phase, respectively. The fixed time-step scheme was used for the implicit unsteady solver in STAR; while the minimum and maximum time steps in OLGA were set properly with the time step in STAR as a reference. For the cases discussed in this section the time step for the STAR model was 0.001 s and the minimum and maximum time steps for the OLGA model were 0.001 s and 0.003 s, respectively.

7.3.3 Model Outputs

The forces acting on the bend, liquid holdup in the bend and pressure on the bend wall can be provided by the STAR model. To examine the forces on different locations of the pipe bend individually the wall around the bend was divided into 4 portions as illustrated in Figure 7-3. The ‘inner part of the bend’ was defined as the combination of C and D; while the ‘outer part of the bend’ was the combination of A and B. The division of the bend into the inner and outer parts allows for the presentation of the force distribution on them individually. The pressure distribution on the inner and outer parts of the bend was recorded as contour plots at every 0.1 s during the calculation. The components of the time-dependent force in the x, y and z directions were monitored on the inner part, outer part and the whole bend individually. Then the magnitude of the resultant force on the inner part, outer part and the whole bend can be calculated by:

(7-6)

where F_R , F_x , F_y and F_z are the magnitudes of the resultant force and force components in the x, y and z directions, respectively.

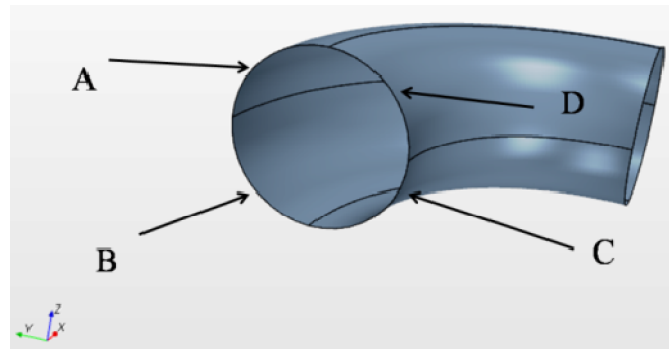


Figure 7-3 Division of the bend wall into 4 portions

A series of ‘plane sections’ were created along the straight sections and around the bend of the STAR pipe. The plane sections took the form of cross-sections at the specified positions of interest. The plane sections were used to monitor the field variables. The area-averaged pressure and liquid holdup on the plane sections were recorded during the calculation. The plane sections created around the bend are illustrated in Figure 7-4. The 90° bend was equally divided into 6 portions with 7 boundaries. The cross-sections of the boundaries are located at central angles $\alpha = 0^\circ, 15^\circ, 30^\circ, 45^\circ, 60^\circ, 75^\circ$ and 90° , respectively.

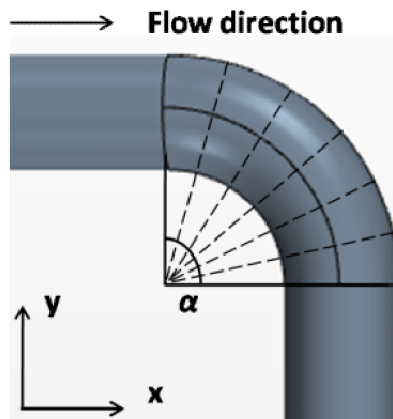


Figure 7-4 Creation of the plane sections in the bend

7.4 Results and Discussions

The STAR-OLGA coupling model developed in Section 7.3 has been validated with a series of tests. Firstly the STAR model was used to predict forces on the bend induced by single-phase water flows. The predicted forces were compared with theoretical analysis. Secondly the coupling model was applied to predict the slug flow induced forces. The model predictions were compared with the experimental data collected by Tay (2002).

The force components F_x , F_y and F_z acting on the inner part, outer part and the whole bend were predicted by the model directly. Then the resultant forces were calculated by integrating the force components. In the following discussions the resultant force was obtained by integrating the components F_x and F_y , thus the direction of the resultant force was in the horizontal direction. The force component F_z was not taken into account when calculating the resultant force as it was mainly induced by the gravitational force of the fluids.

7.4.1 STAR Model with Single-Phase Flow

The force acting on the bend is mainly induced by the momentum change of the fluid passing through the bend. Based on the steady-state momentum equation for a single

phase flow the force components in the x and y directions can be computed using Equation (7) and (8) for a horizontal bend. The flow direction is in the positive x direction as shown in Figure 7-4. The inlet and outlet cross-sections of the bend are at central angles $\alpha = 90^\circ$ and 0° , respectively.

$$F_x = \rho AU_x^2 + (P_{in} - P_a)A \quad (7-7)$$

$$F_y = \rho AU_y^2 + (P_{out} - P_a)A \quad (7-8)$$

where F_x and F_y are the force components in the x and y directions respectively, ρ is the fluid density, A is the cross-sectional area, U_x and U_y are the area-averaged velocities at the inlet (in the x direction) and outlet (in the y direction) of the bend, respectively, P_{in} and P_{out} are the area-averaged absolute pressures at the inlet and outlet of the bend respectively, P_a is the ambient pressure (atmospheric pressure for this case). The magnitude of the resultant force on the bend is:

$$F_R = \sqrt{F_x^2 + F_y^2} \quad (7-9)$$

The inlet water velocities for the test cases are 1 m/s, 2 m/s and 3 m/s respectively and the outlet boundary is specified as the standard atmospheric pressure. Table 7-1 lists the velocities, pressures, theoretical forces, predicted forces by the STAR model and the percentage relative error between the theoretical and predicted forces. Uniform velocity and pressure profiles on the cross-sections of the bend inlet and outlet are assumed in computing the theoretical forces. The area-averaged pressures P_{in} and P_{out} in Equation (7-7) and (7-8) are obtained from the model predictions. The percentage relative error, E_R , is calculated as follows:

$$E_R = \frac{F_{RP} - F_{RT}}{F_{RT}} \times 100 \% \quad (7-10)$$

where F_{RP} and F_{RT} are the resultant forces predicted by the STAR model and obtained from Equation (7-9), respectively.

Table 7-1 Theoretical and predicted forces

Case NO.	U_x (m/s)	U_y (m/s)	$P_{in} - P_a$ (Pa)	$P_{out} - P_a$ (Pa)	F_{RT} (N)	F_{RP} (N)	E_R (%)
1	1.0	1.0	230	179	6.54	6.11	-6.6
2	2.0	2.0	796	617	25.56	23.73	-7.1
3	3.0	3.0	1650	1276	56.80	52.61	-7.4

It can be seen that the theoretical forces calculated by Equation (7-9) are consistently higher than those predicted by the STAR model. The discrepancy mainly results from the assumption of uniform velocity and pressure profiles on the cross-sections of the bend inlet and outlet in calculating the theoretical forces. In the assumption the velocity component in the x direction at the outlet of the bend is 0, i.e. cross flow at the bend outlet is zero. However, there is a positive velocity component in the x direction at the bend outlet due to the centrifugal effect of the bend. The momentum induced by the velocity component is not deducted from the momentum term in Equation (7-7). Consequently the theoretical forces tend to be larger. Figure 7-5 shows the velocity profile on the the transverse section of the bend for Case 2 (inlet velocity 2 m/s). It can be seen that the maximum velocity is as high as 2.65 m/s in the bend centre and the velocity profile at the bend outlet is not as uniform as that at the inlet.

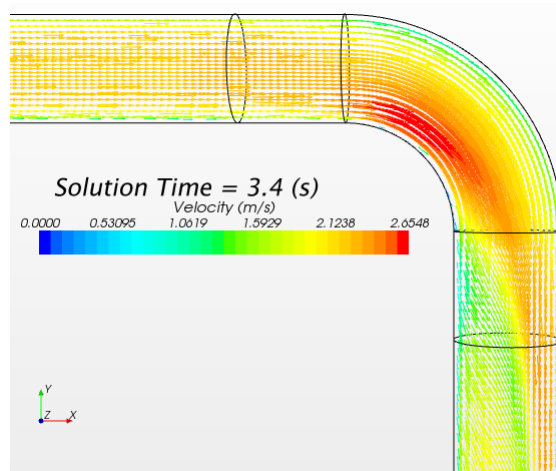


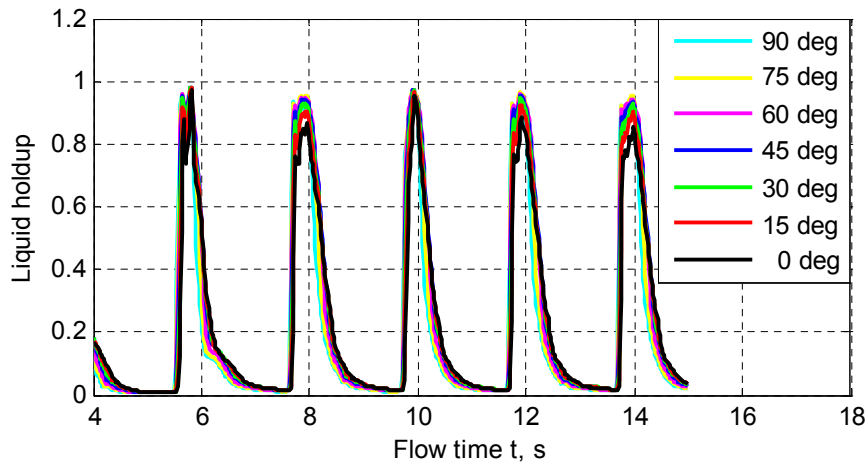
Figure 7-5 Velocity distribution on the transverse section of the bend (Case 2)

In conclusion the CFD model can give a reasonable prediction of the forces acting on the bend induced by single-phase flows. This encouraging result gives confidence in applying CFD coupled with OLGA in the STAR-OLGA coupling models to predict slug induced forces discussed below.

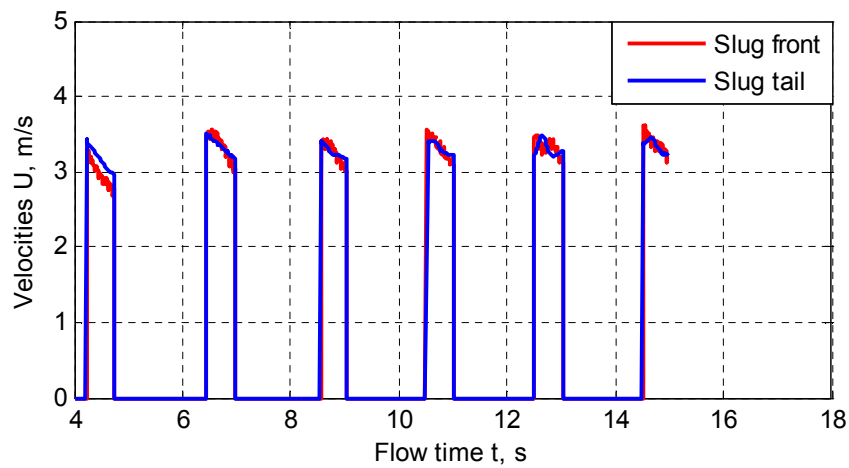
7.4.2 One-Point Coupling Model with Two-Phase Slug Flow

The one-point coupling model includes an upstream OLGA pipe and a STAR pipe with a bend. The upstream OLGA pipe is used to produce the required slug flow for the downstream bend. The results discussed below correspond to the test case of $U_{SG} = 2.02$ m/s and $U_{SL} = 0.6$ m/s in Tay's experiment (Tay, 2002). Figure 7-6 (a) and (b) shows a series of time traces of the area-averaged liquid holdup on the plane sections around the bend and velocities of the slug front and tail upstream of the bend, respectively. The liquid holdup and slug front/tail velocities are predicted by the STAR and OLGA model parts, respectively.

It can be seen in Figure 7-6 that there are 5 liquid slugs passing through the bend between $t = 5$ s and $t = 15$ s. The average slug frequency is 0.5 Hz, the same with the experimental data (Tay, 2002). The average slug velocity measured by Tay (2002) was 3.55 m/s. The slug front and tail velocities are provided by OLGA. The predicted velocities of slug front and tail range from 2.80 m/s to 3.60 m/s and 2.97 m/s to 3.52 m/s, respectively.



(a) Liquid holdup on the cross-sections around the bend

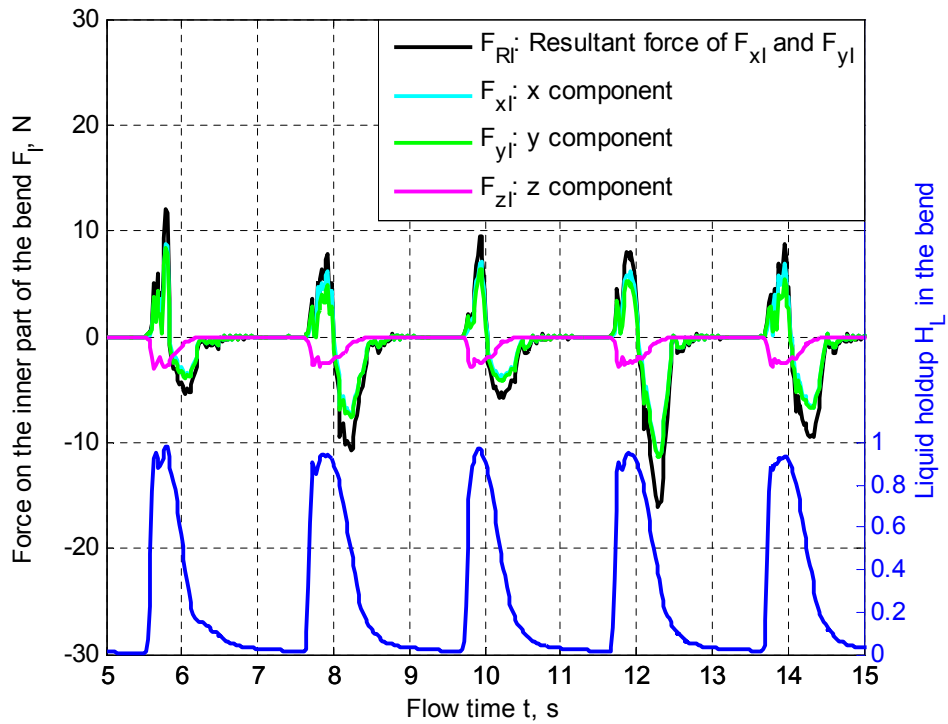


(b) Velocities of the slug fronts and slug tails

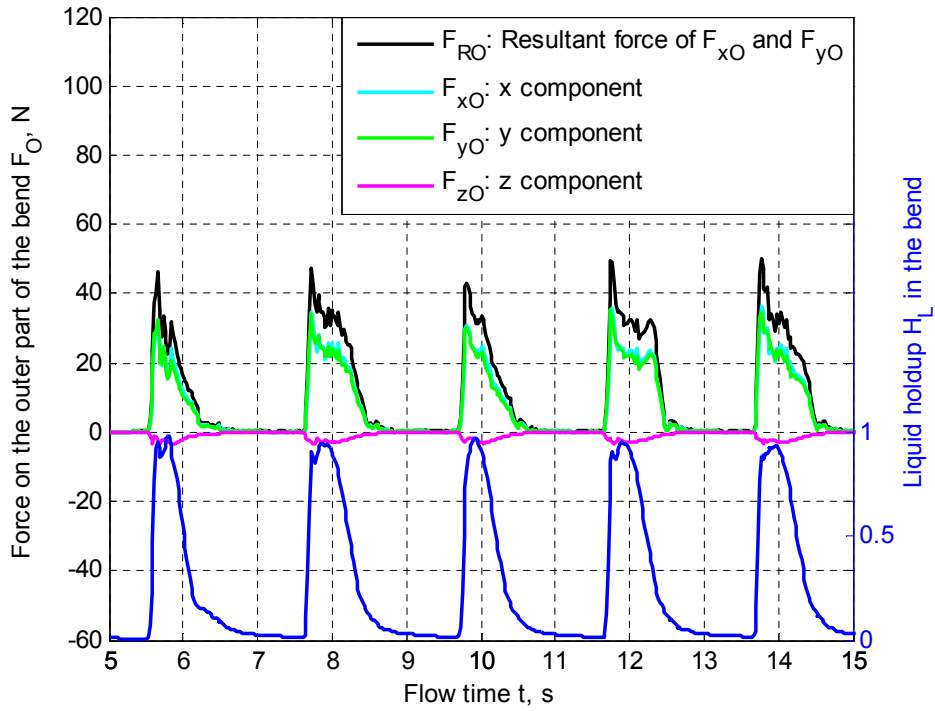
Figure 7-6 Liquid holdup in the bend and velocities of the slug front and tail predicted by the STAR-OLGA coupling model

The liquid slugs produced in the upstream OLGA pipe move into the STAR pipe and then hit the bend. The x, y and z components of the forces on the inner part, outer part and the whole bend are plotted together with the liquid holdup on the central plane section in the bend (the central angle $\alpha = 45^\circ$) in Figure 7-7. In the discussions below two similar terms, i.e. peak force (F_{peak}) and maximum force (F_{max}), are employed to

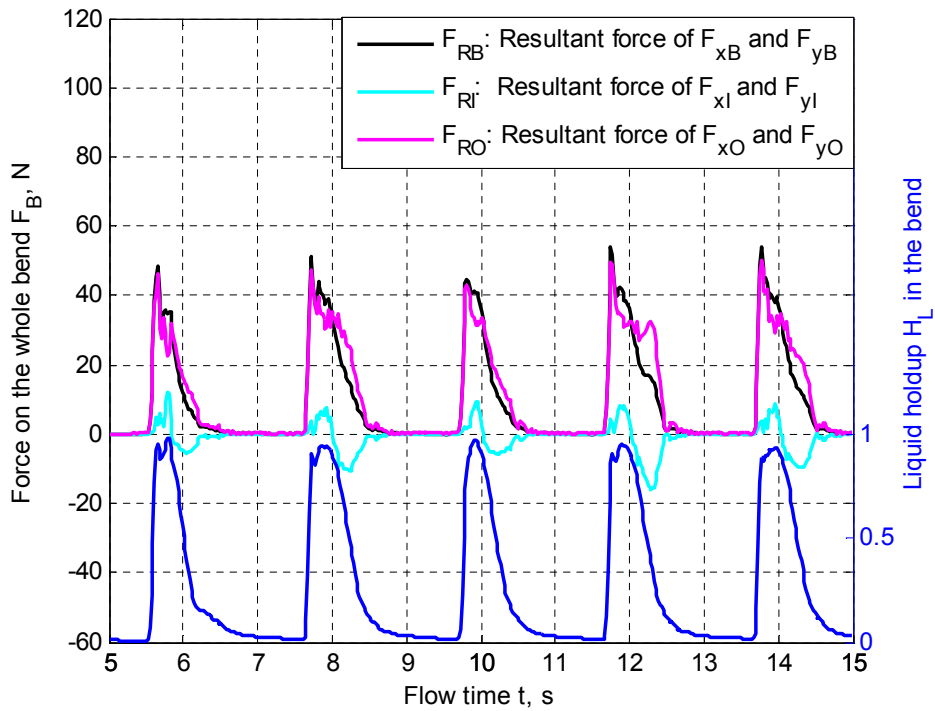
characterise the slug flow induced force. The F_{peak} is the maximum magnitude of the force for one slug unit (including one liquid slug and bubble/film) while the F_{max} is the maximum force in a period of flow time including several slug units. The direction of the force is described in accordance to the coordinate system indicated in Figure 7-2 and 7-3.



(a) Resultant force and force components on the inner part of the bend



(b) Resultant force and force components on the outer part of the bend



(c) Resultant forces on the whole bend, inner part and outer part of the bend

Figure 7-7 Forces on the inner part, outer part and the whole bend with liquid holdup in the bend centre

As can be seen in Figure 7-7 (a) the x and y components of the force on the inner part of the bend, F_{xI} and F_{yI} , behave like a ‘sine wave’ while one liquid slug is travelling in the bend. The F_{xI} and F_{yI} change their directions when the slug tail arrives at the central plane section with $\alpha = 45^\circ$. Before changing their directions the F_{xI} and F_{yI} are in the positive direction indicating that the pressure on the internal wall of the inner part of the bend is lower than the ambient pressure, i.e. standard atmospheric pressure. The lower pressure is attributed to the centrifugal effect of the bend as shown in Figure 7-5. After the slug tail leaves the central plane section the fluids exert a force on the inner part of the bend. The z component, F_{zI} , increases in the direction of gravity when the slug body is travelling in the bend as expected. The F_{peak} of the resultant force of x and y components on the inner part of the bend, F_{RI} , ranges from 7.8 N to 12.1 N and from -5.4 N to -15.8 N in the positive and negative directions, respectively. Thus the maximum force F_{max} between $t = 5$ s and $t = 15$ s is 15.8 N.

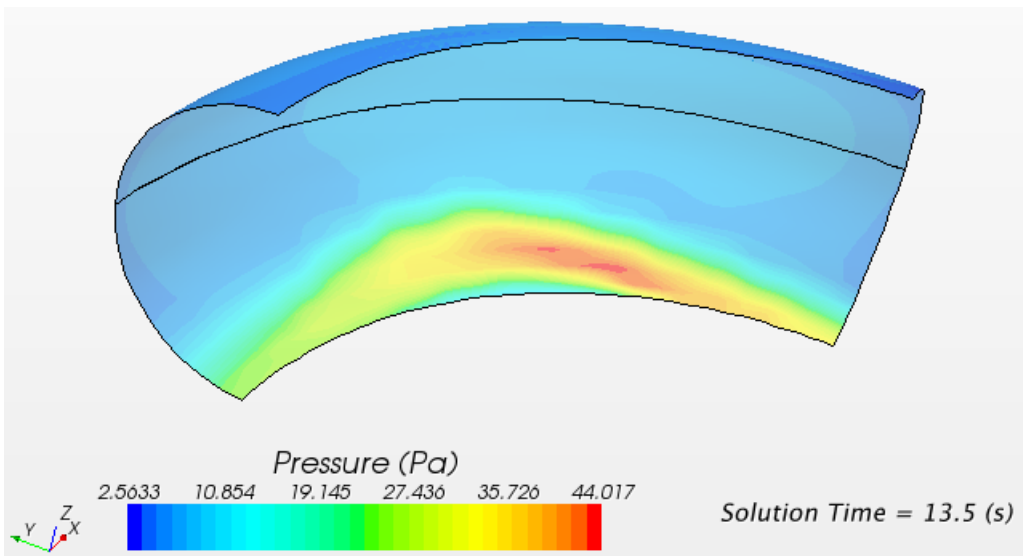
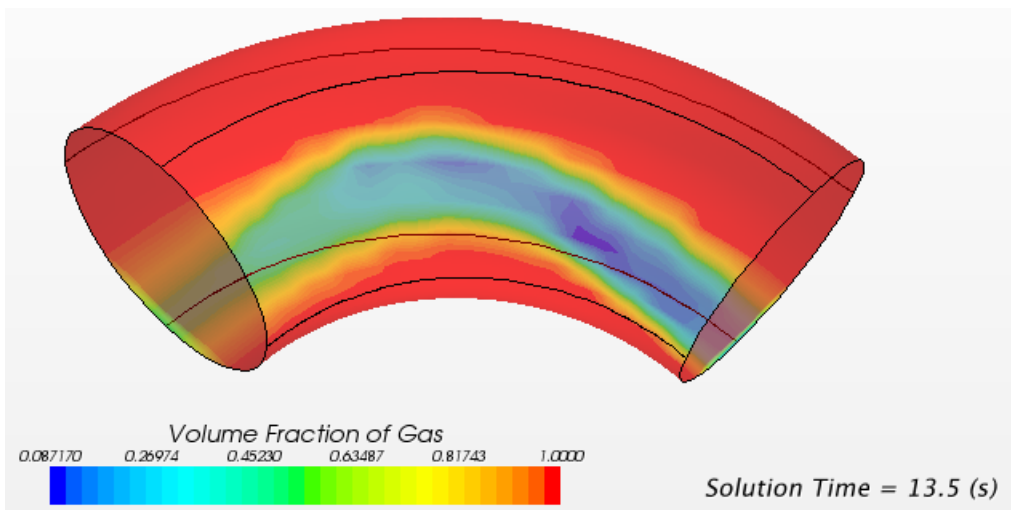
The forces on the outer part of the bend behave differently. Both of the x and y components, F_{xO} and F_{yO} , are in the positive direction as shown in Figure 7-7 (b). Thus the fluids exert forces on the outer part of the bend consistently. The F_{peak} of the resultant force of x and y components on the outer part of the bend, F_{RO} , ranges from 43.1 N to 49.9 N, thus the F_{max} is 49.9 N. The peak force appears when the highly turbulent slug front arrives at the bend centre hitting the bend in the wall.

The force components in the x, y and z directions on the whole bend, i.e. R_{xB} , R_{yB} and R_{zB} , have also been monitored during the calculation. The resultant force on the whole bend in the horizontal direction, F_{RB} , can be obtained by integrating either R_{xB} and R_{yB} or F_{RI} and F_{RO} . The F_{RB} , F_{RI} and F_{RO} are compared in Figure 7-7 (c). It can be seen that the contribution of the F_{RO} to the F_{RB} is much higher than that of the F_{RI} . Therefore, the F_{RB} behaves in a similar manner with the F_{RO} . The F_{peak} of the F_{RB} appears when the F_{RO} is at a peak. The F_{peak} of the F_{RB} ranges from 44.4 N to 54.2 N and the F_{max} is 54.2 N. The measured F_{peak} in Tay’s experiment ranged from 40 N to 60 N (Tay, 2002). In conclusion the predicted peak forces agree with the experimental data reasonably well.

The forces on the inner part, outer part and the whole bend have been examined together with the liquid holdup time traces. The maximum resultant force has been identified because it is an important parameter in designing the piping and piping support systems.

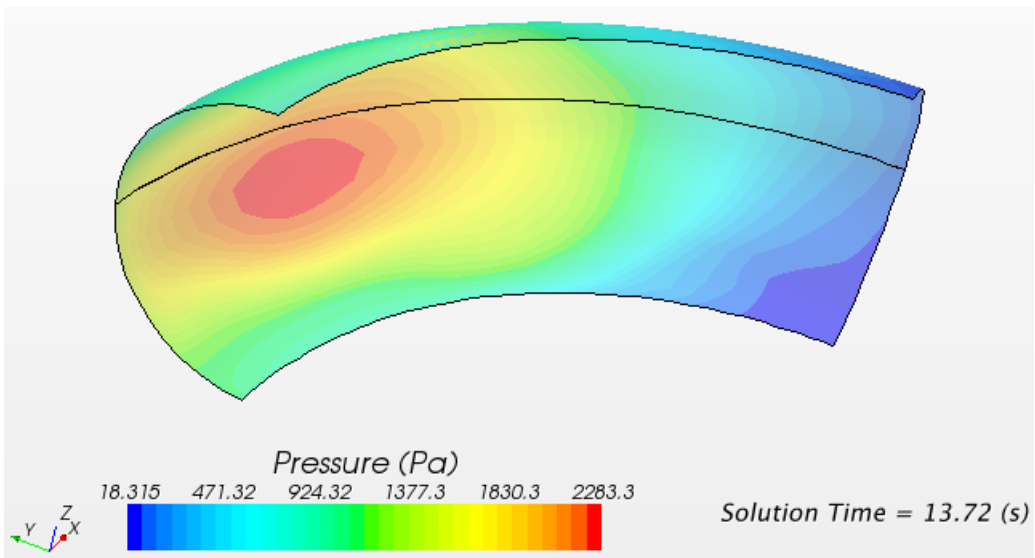
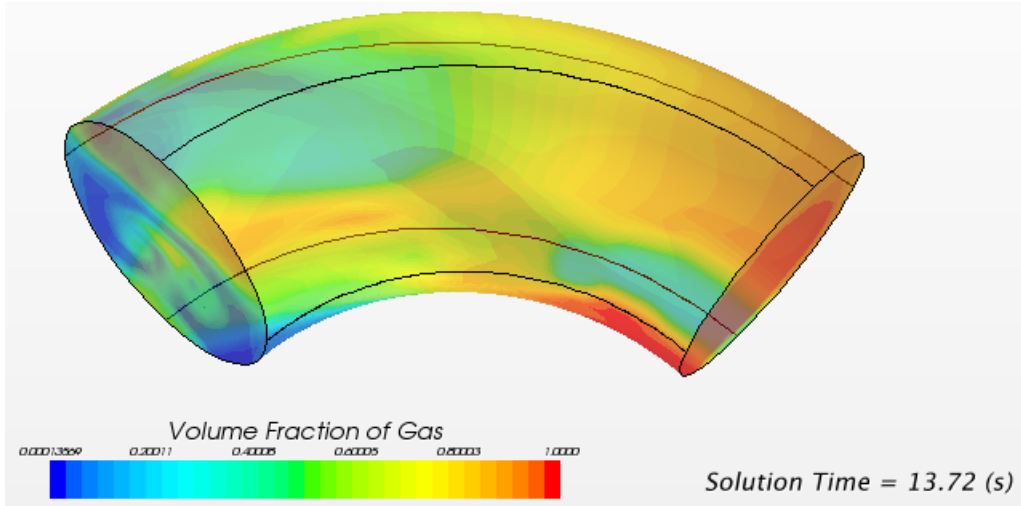
The distribution of the force on the bend wall is also of great importance. The area on the wall experiencing large forces tends to become weak and is vulnerable to mechanical damage.

The force acting on the bend wall includes two parts, i.e. pressure force and shear force. The pressure force is perpendicularly applied on the wall while the shear force is applied in parallel with the wall surface. Because the shear force is much smaller than the pressure force in magnitude, only the pressure force distribution is discussed below. The contour plots of the pressure on the outer part of the bend and gas volume fraction in the bend have been recorded during the simulation. Taking the liquid slug between $t = 13$ s and $t = 15$ s for example, Figure 7-8 presents a series of contour plots when the liquid slug and gas bubble with liquid film is travelling in the bend.



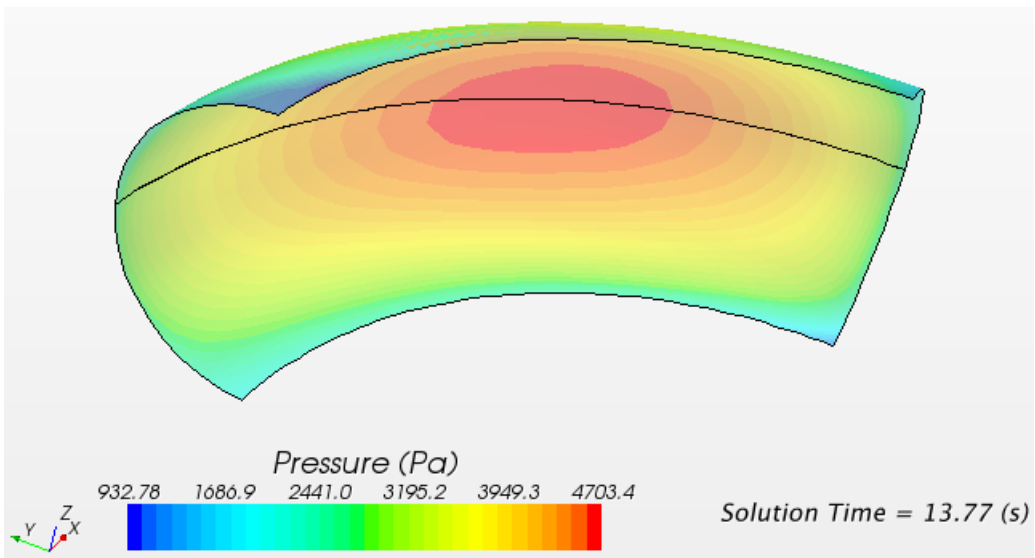
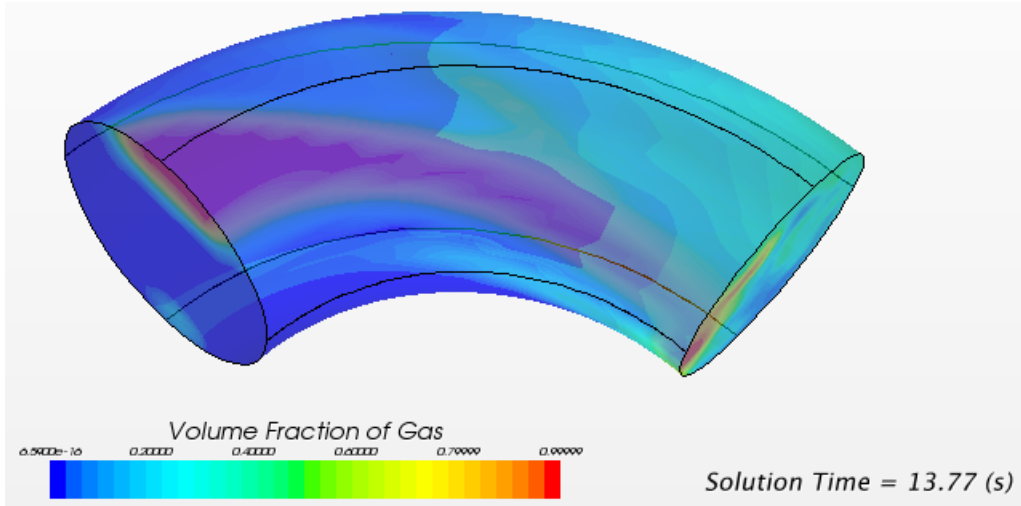
→ Flow direction

(a) $t = 13.50$ s: gas bubble with liquid film travelling in the bend



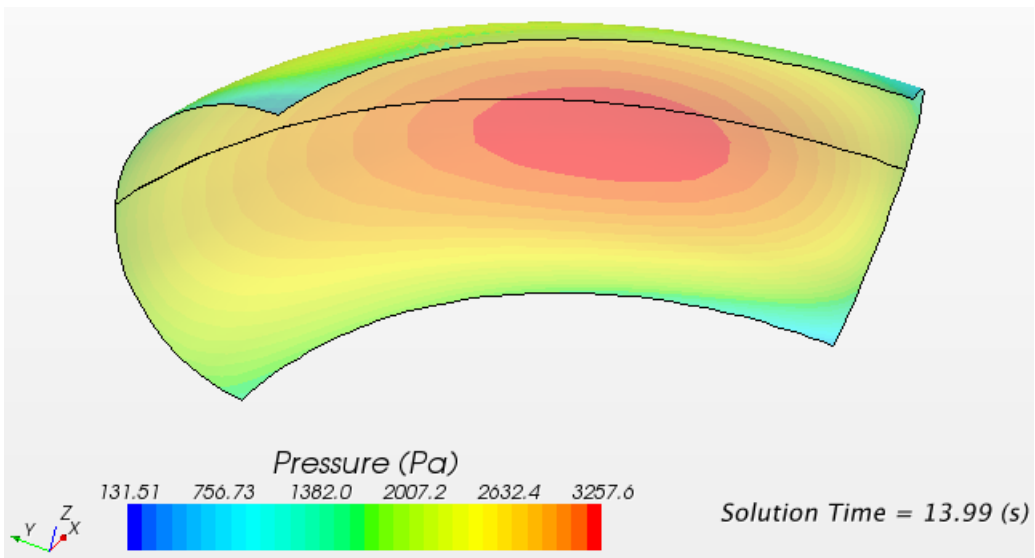
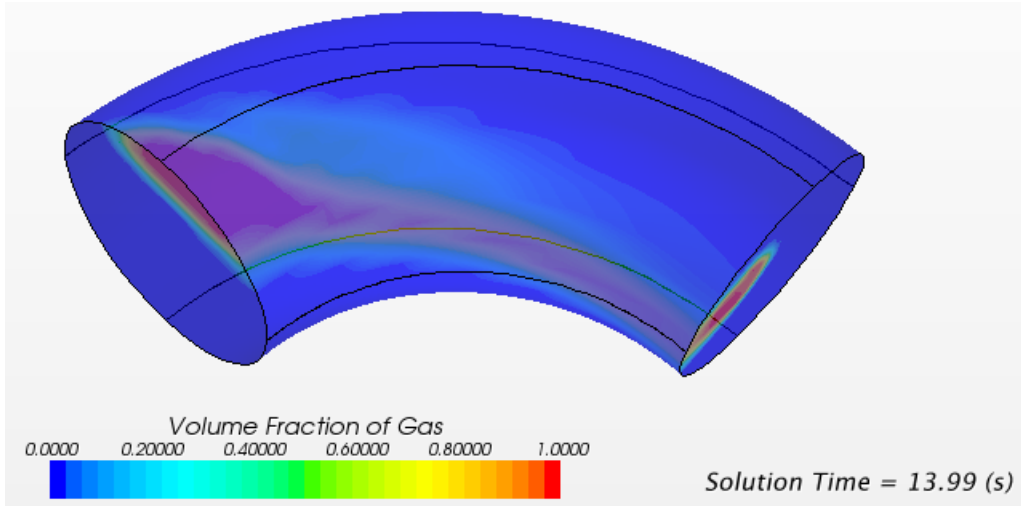
→ Flow direction

(b) $t = 13.72$ s: slug front moving into the bend



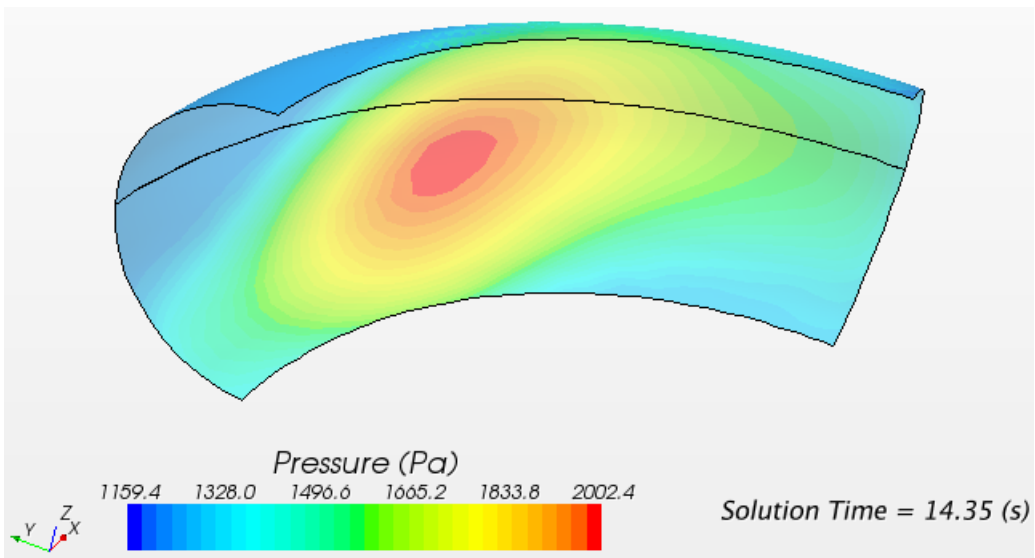
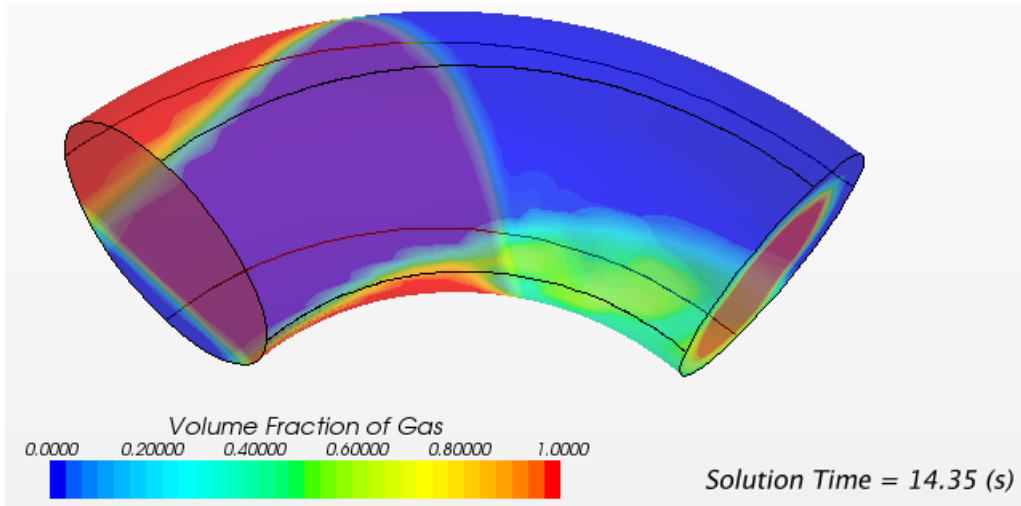
→ Flow direction

(c) $t = 13.77$ s: slug front arriving at the bend centre



→ Flow direction

(d) $t = 13.99$ s: slug body travelling in the bend



→ Flow direction

(e) $t = 14.35$ s: slug tail leaving the bend centre

Figure 7-8 Phase distribution in the bend and pressure (gauge pressure) distribution on the outer part of the bend

As illustrated in Figure 7-8 (a) the liquid film moves towards the outer part of the bend due to the centrifugal effect while the gas bubble with liquid film is travelling in the bend. The pressure on the outer part of the bend is relatively low due to the low average density of the fluids, i.e. low density gas and thin liquid film, in the bend. A higher pressure is induced by the increase of the average density when the slug front moves into the bend in Figure 7-8 (b). As the slug front moves forward and the slug body enters the bend the pressure increases sharply. The maximum pressure appears when the slug front arrives at the bend centre hitting the bend in the wall in Figure 7-8 (c). The maximum pressure is about 4703 Pa, which is much higher than 44 Pa and 2283 Pa indicated in Figure 7-8 (a) and (b) respectively. The significantly high pressure distributes on a certain area of the outer part of the bend, as a result, a large pressure force is induced. After the slug front passes the bend centre a pressure decrease is observed. However, as shown in Figure 7-8 (d) the pressure is still significantly high while the slug body is travelling in the bend due to the high liquid holdup in the slug body. A further decrease of the pressure can be found when the slug tail moves into the bend followed by a gas bubble and liquid film in Figure 7-8 (e). Then the pressure drops sharply after the slug tail leaves the bend centre, which can be confirmed by the time traces of the force on the outer part of the bend and liquid holdup in the bend centre in Figure 7-7 (b).

It needs to be stressed that the significantly large force acts on a certain area of the outer part of the bend as shown in Figure 7-8 (c) and (d). That area is the most vulnerable part prone to mechanical damage; hence more attention needs to be paid to it.

7.4.3 Two-Point Coupling Model with Two-Phase Slug Flow

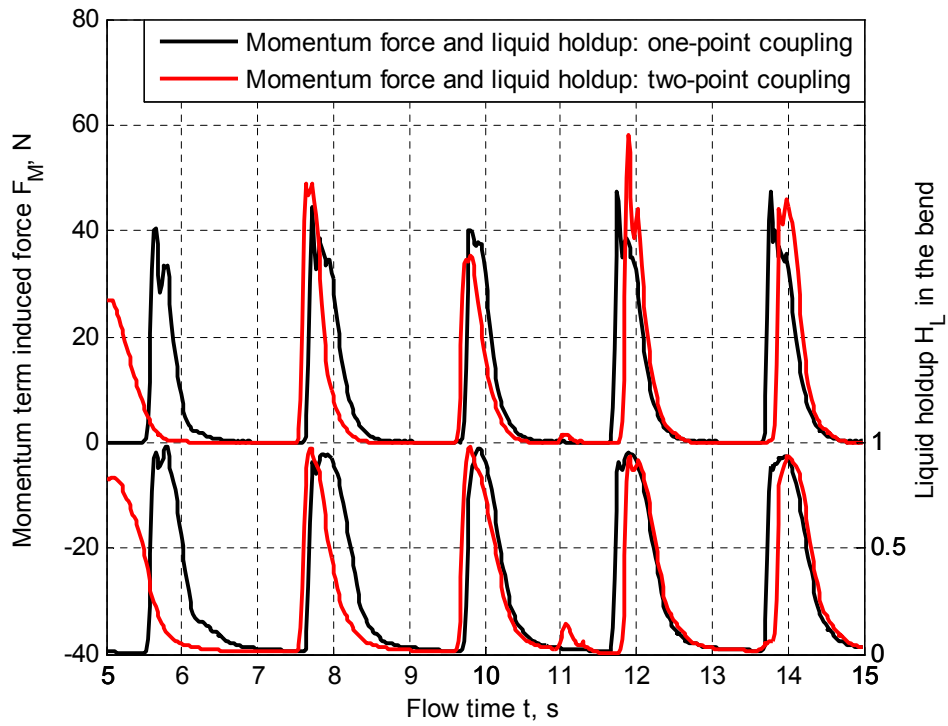
The effects of the downstream pipe on the forces applied on the bend were not taken into account by the one-point coupling model presented in Section 7.4.2. There is a pressure loss along the downstream pipe, thus the pressure at the outlet of the STAR model is higher than that at the outlet of the downstream OLGA pipe. Consequently the force acting on the bend is expected to be higher according to Equation (7-3) and (7-4), if the downstream OLGA pipe has the same outlet pressure. A two-point coupling model shown in Figure 7-1 was created with the same upstream pipe in the one-point coupling model and a 20 m long downstream pipe. It needs to be noted that the outlet of

the downstream pipe has become the outlet of the two-point coupling model with the atmospheric pressure specified. The two-point coupling model was tested using the same case with that in Section 7.4.2, i.e. $U_{SG} = 2.02$ m/s and $U_{SL} = 0.6$ m/s.

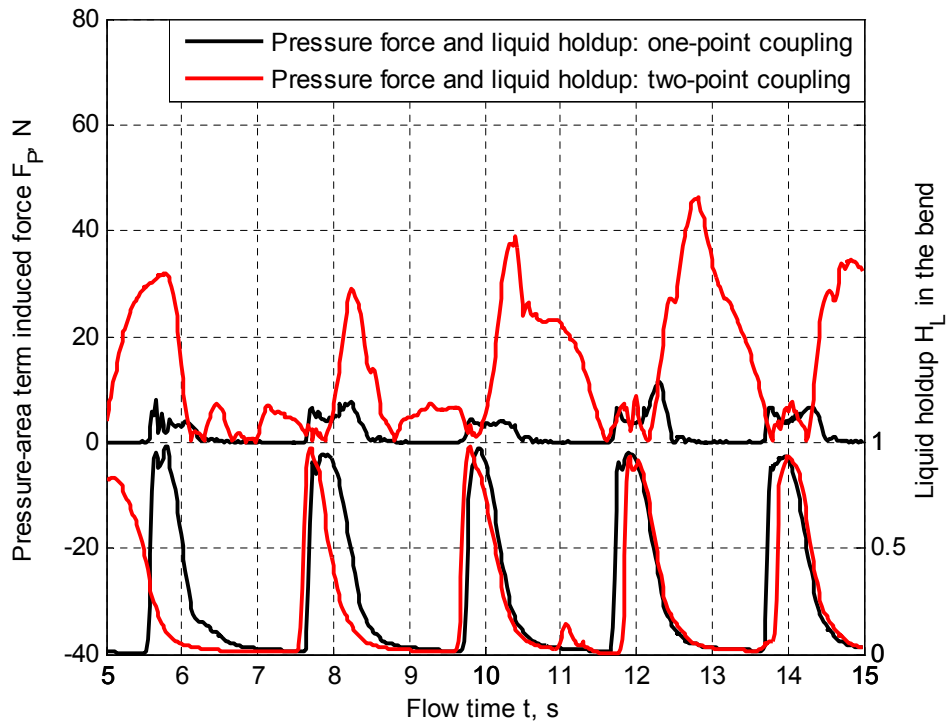
As indicated by Equation (7-3) and (7-4) the resultant force on the bend mainly includes two terms, i.e. momentum term and pressure-area term. The force components induced by the momentum change and pressure have been computed by Equation (7-3) and (7-4). Figure 7-9 compares the force components and resultant force on the bend from the one-point coupling and two-point coupling models.

It can be seen in Figure 7-9 (a) that the time traces of the momentum term induced force predicted by the two models behave in a similar way. Thus the extension of the downstream pipe does not affect the momentum term induced force significantly. It is very interesting to note that there is much difference in the pressure-area induced force on the bend between the two models as shown in Figure 7-9 (b). The pressure-area induced force in the two-point coupling model with a 20 m long pipe downstream is much higher than that in the one-point coupling model. The higher force is mainly attributed to the higher pressure in the bend. As the pressure at the outlets of the two modes is the same, the difference in pressure at the bends results from the pressure drop along the downstream OLGA pipe in the two-point coupling model. It is not surprising to see the disagreement of the resultant forces on the bends between the two models in Figure 7-9 (c). There are two separate peaks in the resultant force time trace corresponding to one slug unit predicted by the two-point coupling model. Comparing with Figure 7-9 (a) and (b) we can understand that the first peak is attributed to both of the momentum induced force and pressure-area induced force, while the second peak is only contributed by the pressure-area induced force.

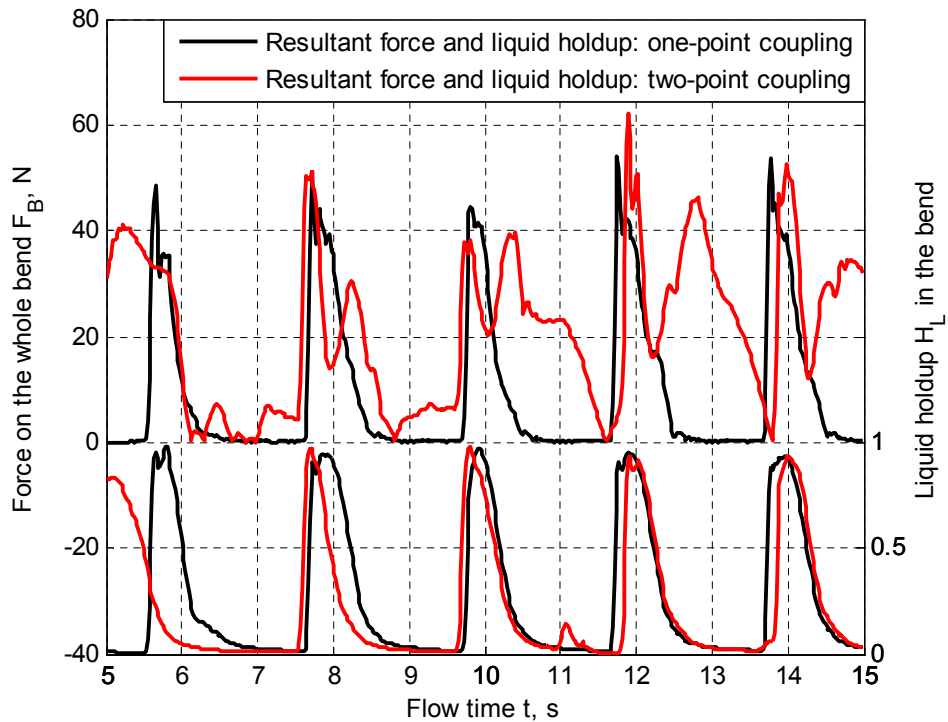
The pressure at the bend increases with the increasing length of the pipe downstream because the pressure increase is equal to the pressure drop along the downstream pipe. Therefore, a longer downstream pipe can result in higher pressure-area induced force on the bend.



(a) Momentum term induced force and liquid holdup



(b) Pressure-area term induced force and liquid holdup



(c) Resultant force and liquid holdup

Figure 7-9 Comparison of the forces predicted by the one-point and two-point coupling models

7.5 Summary

A numerical study of the slug flow induced forces on pipe bends was carried out applying STAR-OLGA coupling. The pipe bend was modelled using 3-D CFD code STAR-CCM+ and the pipelines upstream and downstream of the bend were modelled using 1-D code OLGA. The effects of the downstream pipe on the forces were examined.

The time-dependent forces and force components on different areas of the bend wall can be presented by the STAR model part in the coupling model. The peak force in a slug unit appears when the highly turbulent slug front arrives at the bend centre hitting the bend in the wall. The force distribution contour plots illustrate that large forces act on a

certain area of the bend wall, which is the most vulnerable part prone to mechanical damage. The pressure at the bend increases with the increase of the length of the downstream pipe because the pressure increase is equal to the pressure drop along the downstream pipe. Hence a longer downstream pipe can result in a higher pressure-area induced force on the bend.

8 CONCLUSIONS AND RECOMMENDATIONS FOR THE FUTURE WORK

Slug flow is frequently encountered in the transportation of oil and gas in offshore field development. The long liquid slugs and violent gas surges of slug flow may result in serious problems. Slug flow poses a great challenge to the steady operation of the production system, the mechanical integrity of the structure and the efficient management of the reservoir. This work is dedicated to develop a passive slug mitigation technique based on a novel flow conditioner, wavy pipe, through laboratory experiment and numerical simulation. The wavy pipe has been applied to two types of slug flows: severe slugging in pipeline/riser systems and hydrodynamic slug flow in horizontal pipelines. In this chapter conclusions are drawn from the work presented in this thesis and recommendations for the future work are made. This chapter has two sections for the conclusions and recommendations, respectively. Furthermore, both of the conclusions and recommendations are presented in two subsections for the applications of the wavy pipe to severe slugging in pipeline/riser systems and hydrodynamic slug flow in horizontal pipelines, respectively.

8.1 Conclusions

8.1.1 Severe Slugging Mitigation with Wavy Pipes in Pipeline/Riser Systems

The experiment was conducted on the 2” and 4” pipeline/riser systems in the Three-Phase Test Facility in PSE (Process Systems Engineering) Laboratory. Firstly, the flow behaviour in the pipeline/riser systems without wavy pipes was characterised; secondly, the pipeline/wavy-pipe/riser systems were tested with different configurations of wavy pipes. In parallel with the experimental investigation, CFD models of the 4” pipeline/riser and pipeline/wavy-pipe/riser systems were developed in Fluent (Release 6.3.26) and validated by the experimental data. The effects of the location in the pipeline and geometrical parameters of the wavy pipe on slug flow mitigation were investigated numerically.

Experimental Study

- (1) The flows in the pipeline/riser systems are classified into four categories: severe slugging (SS), transitional severe slugging (TSS), oscillation flow (OSC) and continuous flow (CON). They appear in sequence with the increasing gas flowrate at a fixed liquid flowrate. All of SS, TSS and OSC exhibit cyclic flow behaviour. The slug of SS is longer than the riser, while TSS is characterised by the absence of the slug production stage in SS and the slug length equal to the riser. For OSC more than one aerated slugs coexist in the riser separated by gas packets. No liquid slugs can be observed in the riser in CON.
- (2) The effectiveness of the wavy pipe on severe slugging mitigation is assessed in terms of the flow regime transition boundary and characteristic parameters of riser DP (the differential pressure across the riser). A flow regime transition boundary is placed where the TSS is expected to occur in a flow regime map with superficial gas and liquid velocities (U_{SG} and U_{SL}) as the coordinates. The characteristic parameters include magnitude parameters (M_{MAX} , M_{MIN} , M_{AMP} , M_{AVE}) and time parameters (T_{BUL} , T_{PRO} , T_{BFB} , T_{CYC}). The M_{MAX} , M_{MIN} , M_{AMP} and M_{AVE} refer to the maximum, minimum, fluctuation amplitude and time average of the riser DP, respectively; while the T_{BUL} , T_{PRO} , T_{BFB} and T_{CYC} are the time period of the liquid buildup stage, slug production stage, bubble-penetration/gas-blowdown/liquid-fallback stages and total cycle time, respectively.
- (3) The flow regime transition boundary is shifted to the SS region (SS is changed into OSC) with a wavy pipe installed in the pipeline. Consequently the region in the flow regime map for SS to occur is reduced. In the regions where the flow regimes, i.e. SS and OSC, have not been changed by employing a wavy pipe, the severity of the flow is reduced instead. The average riser DP (M_{AVE}) is consistently lower in the pipeline/wavy-pipe/riser systems than that in the plain riser system without a wavy pipe. For the SS cases the reduction of M_{AVE} is attributed to the reduction of the slug production time (T_{PRO}), while for the OSC cases it is due to the reduction of the maximum riser DP (M_{MAX}). The fluctuation amplitude of the riser DP (M_{AMP}) decreases due to the reduction of M_{MAX} for OSC.

- (4) The effects of the wavy pipe discussed in (3) are summarised as reducing the slug length in the pipeline/riser system. When SS is transformed into OSC with a wavy pipe applied, the long severe slug (longer than the riser) is split into more than one short slugs (shorter than the riser). When there is no flow regime change with a wavy pipe employed: (a) the lower M_{MAX} and M_{AMP} of OSC indicate a shorter maximum equivalent slug in the riser at the liquid buildup stage and a shorter slug produced out of the riser at the gas blowdown stage, respectively; (b) a smaller T_{PRO} of SS means a shorter slug produced out of the riser at the slug production stage; (c) a smaller T_{CYC} indicates a higher slug frequency thus shorter slugs.
- (5) The wavy pipe reduces the severe slug length of SS by acting as an ‘accelerator’ and the equivalent slug length of OSC by acting as a ‘mixer’. In SS the wavy pipe accelerates the movement of the gas in the pipeline to the riser base to initiate the bubble penetration stage, as a result, both the production time and the length of the severe slug is reduced. SS is transformed into OSC when the slug production time becomes zero and also the original severe slug becomes shorter than the riser. In OSC the wavy pipe mixes the gas/liquid two phases and turns the original stratified flow into highly aerated slug flow or even homogenous flow moving towards the riser base in the pipeline. Thus even shorter slugs tend to form at the riser base and in the riser.

Modelling with CFD

- (1) The CFD modelling provides a feasible way to examine the effects of the amplitude, length and location of the wavy pipe on its performance of severe slugging mitigation. The proposed 2-D CFD model of the pipeline/riser system is able to predict the flow regime transition and slug frequency reasonably well compared with the experimental data. The phase distribution of the gas/liquid two phases and interaction between them in pipeline/wavy-pipe/riser systems can be presented by CFD models in detail.
- (2) For a given pipeline/riser system experiencing severe slugging, the flow regime induced instability can be reduced further but the instability induced by the forces on the wavy pipe rises when applying a higher-amplitude wavy pipe. The slug

length in the pipeline/riser system is further reduced with the increase of the wavy pipe amplitude; the fluctuation amplitude of the riser DP and the pressure upstream of the wavy pipe become lower; however, the mean, maximum and fluctuation amplitude of the drag and lift forces on the wavy pipe increase sharply. Similar effects can be achieved by increasing the length of the wavy pipe. The effects are attributed to the more space provided by the longer limbs and more bends, where more gas is trapped and mini slugs form.

- (3) For a pipeline/wavy-pipe/riser system at given operating conditions, an optimum length of the pipe section between the riser base and wavy pipe outlet exists. The slug length in the pipeline/riser system decreases then increases with the increase of the length of that pipe section. The pipe section is used to provide a space for the gas to be stored and compressed. The compressed gas and a high-enough pressure are essential for the bubble penetration to the riser, by which the slug length is reduced. The optimum length of the pipe section is affected by the geometries and dimensions of the pipeline/riser and wavy pipe and the operating conditions.

8.1.2 Hydrodynamic Slug Mitigation with Wavy Pipes in Horizontal Pipelines

The experiment was conducted on a two-phase test facility in PSE (Process Systems Engineering) Laboratory. Firstly the flow regimes in this test rig were observed; secondly the flow behaviour upstream of the wavy pipe, in the wavy pipe and downstream of the wavy pipe was analysed; thirdly the performance and working principle of the wavy pipe on hydrodynamic slug mitigation were discussed. As a part of the project to explore a CFD-OLGA co-simulation tool, in this work the STAR-OLGA coupling was applied to model the horizontal wavy-pipe systems under hydrodynamic slug flow. The wavy pipe was modelled with the 3-D CFD code STAR-CCM+ (Release 5.04.006), while the upstream and downstream pipelines were modelled with the 1-D code OLGA (Release 5.3.2). The effects of the geometrical parameters of the wavy pipe, i.e. amplitude and length, on hydrodynamic slug mitigation were examined. The forces acting on a single bend induced by hydrodynamic slug flow were investigated applying STAR-OLGA coupling models, in which the bend was modelled with STAR-CCM+.

Experimental Study

- (1) The flow regimes identified in the two-phase test rig are: stratified flow with low-frequency and high-amplitude waves; stratified flow with high-frequency and low-amplitude waves; slug flow and elongated bubble flow. No stratified flow with smooth interface is observed; instead a stratified flow with low-frequency and high-amplitude waves occurs. It is postulated that the high-amplitude waves are mainly initiated due to the effects of the two bends upstream of the test section.
- (2) The stratified flow with high-amplitude waves comprises two distinct sections: a section of liquid wave and a section of separated gas and liquid layers with smooth interface in between. The wavy pipe has different effects on these two sections. Firstly the existing waves upstream grow in amplitude and become liquid slugs downstream of the wavy pipe; secondly the smooth interface upstream becomes wavy as new waves are generated in the wavy pipe. The wave frequency at the outlet of the wavy pipe is higher than that upstream, resulting from the addition of the newly formed waves in the upward limbs in the wavy pipe. The newly formed waves are much lower in amplitude and shorter than the existing ones. When a slug unit moves into the wavy pipe, the slug body and elongated bubble become indistinguishable. The liquid holdup in slug body decreases because more gas entrainment is induced during the travelling of the slug in the wavy pipe.
- (3) The wavy pipe is able to reduce the severity of hydrodynamic slug flow. It works as a mixer agitating the gas/liquid two phases by its upward and downward limbs. In the wavy pipe the liquid phase tends to slow down and accumulate in the upward limbs and accelerate in the downward limbs. The gas phase then gains an opportunity to penetrate into the liquid phase while it is slowing down in the upward limbs. The penetrated gas distributes in the slug body extensively due to the agitation effects of the wavy pipe. As a result, the liquid holdup in the slug body at the outlet of the wavy pipe is lower than that upstream. Therefore, the effective density of the slug body decreases thus the impact of the liquid slugs on the downstream facility is reduced. However, the flow tends to recover after a certain distance downstream of the wavy pipe, especially at lower superficial gas and/or

liquid velocities ($U_{SG} < 2.0$ m/s at $U_{SL} = 1.0$ m/s; $U_{SL} < 1.0$ m/s at $U_{SG} = 1.5$ m/s in the experiment).

Modelling with STAR-OLGA Coupling

- (1) The liquid phase in slug body tends to slow down and accumulate in the first upward limb of the wavy pipe. Consequently the flow path of the gas in the following liquid film region tends to be blocked at the trough of the bend. However, the blockage cannot maintain because the gas keeps moving in and accumulates there. Soon the liquid in the first upward limb is pushed out into the next bend. The two phases tend to mix together during the push-out process. The mixing effect is then enhanced by the following bends. As a result, the upstream slug degenerates to a ‘liquid dense zone’ downstream of the wavy pipe. The ‘liquid dense zone’ can be further divided into Zone I and Zone II. Zone I is occupied by a gas/liquid mixture while Zone II is characterised of a swirling flow of liquid and gas/liquid mixture, and a gas core. The effective density in the ‘liquid dense zone’ is less than that in the upstream slug body, thus the severity of the slug flow is mitigated by the wavy pipe. The mixing effects of the wavy pipe on gas/liquid two-phase flow identified in the experiment can be presented by the coupling model reasonably well.

- (2) A wavy pipe of higher amplitude does not always introduce better mixing effects to slug flow. The maximum liquid holdup downstream decreases and then increases with the increase of the wavy pipe amplitude from $1.1d$ to $1.8d$ until $2.5d$ (d the pipe diameter). The wavy pipe with amplitude of $1.8d$ is more desirable than those of $1.1d$ and $2.5d$. The upward limbs in a wavy pipe of higher amplitude are longer. It is postulated that the longer upward limbs allow for more liquid to accumulate and thus slugs to reform there. A longer wavy pipe of more bends is more favourable to mix the two phases. A longer wavy pipe (7 bends, $L/d = 20.4$) provides more space and time for the gas/liquid two phases to interact with each other than the shorter ones (5 bends, $L/d = 16.5$; 3 bends, $L/d = 11.1$). Consequently more gas can penetrate into the slug body during the journey in the 7-bend wavy pipe and the severity of the slug flow is further mitigated.

- (3) The time-dependent forces and force components on different areas of the bend wall can be presented by the STAR model in detail. The predicted peak force on the bend agrees with the experimental data in the literature. The peak force in a slug unit appears when the highly turbulent slug front arrives at the bend centre hitting the bend in the wall. The force distribution contour plots illustrate that large forces act on a certain area of the bend wall, which is the most vulnerable part prone to mechanical damage.

8.2 Recommendations for the Future Work

8.2.1 Severe Slugging Mitigation with Wavy Pipes in Pipeline/Riser Systems

- (1) In the experiment on pipeline/wavy-pipe/riser systems, the wavy pipe has been placed with the top aligned with the pipeline and the downstream pressure of the pipeline/riser system is 1 barg. It is of interest to examine the effectiveness of the wavy pipe on severe slugging mitigation when the bottom is aligned with the pipeline. The physical properties of the gas phase are affected by the system pressure significantly. It is worth investigating how the wavy pipe works under different system pressures especially higher pressures, because the system pressure in the field application may be much higher than that in the current experiment. Therefore, two test configurations are suggested: (a) pipeline/wavy-pipe/riser systems with the wavy pipe rotated by 180°; (b) pipeline/wavy-pipe/riser systems with higher downstream pressure. The CFD modelling of these test configurations are also recommended to obtain more understanding of the flow behaviour.
- (2) The STAR-OLGA coupling is a potential engineering tool for designing pipeline/wavy-pipe/riser systems. However, it is still a challenge to simulate the severe slugging flow regime in the pipeline/wavy-pipe/riser system applying this tool. Usually the wavy pipe is modelled in STAR-CCM+ and the upstream pipeline and downstream riser are modelled in OLGA. When severe slugging occurs the liquid slug grows in the pipeline and riser starting from the riser base. Thus there is reverse flow from the downstream OLGA pipe to the wavy pipe in STAR-CCM+ and then to the upstream OLGA pipe (if the severe slug is long enough). However, in the current code of STAR-OLGA coupling the reverse flow has not been dealt

with properly and thus the simulation cannot proceed successfully. The STAR-OLGA coupling tool needs to be improved to model the reverse flow.

8.2.2 Hydrodynamic Slug Mitigation with Wavy Pipes in Horizontal Pipelines

- (1) The two-phase test rig in this work has a short pipe section downstream of the wavy pipe due to the restriction of the space in the laboratory. Thus it has not been observed in the experiment that the downstream slug flow recovers to that upstream of the wavy pipe. Experimental data are required to characterise the flow recovery downstream of the wavy pipe under different flow conditions.
- (2) In the current code of STAR-OLGA coupling the conversion of the 1-D data at the outlet of the upstream OLGA to the 3-D data for the STAR inlet boundary is achieved by assuming that the phases are distributed as stratified layers. Under this assumption the slug body with entrained gas in hydrodynamic slug flow regime has been modelled as two layers: one liquid layer at the bottom and one gas layer on the top. It is required to take into account of the actual flow regime during the conversion of the 1-D data to 3-D data.

REFERENCES

- Adedigba, A. G. (2007). *Two-Phase Flow of Gas-Liquid Mixtures in Horizontal Helical Pipes*. PhD Thesis, Cranfield University, UK.
- Al-lababidi, S. (2006). *Multiphase Flow Measurement in the Slug Regime Using Ultrasonic Measurements Techniques and Slug Closure Model*. PhD Thesis, Cranfield University, UK.
- Almeida, A. R. and Gonçalves M. A. L. (1999 a). Venturi for severe slugging elimination. In: *9th International Conference Multiphase Production*, 16-18 June 1999, Cannes, France, BHRG, p. 149-158.
- Almeida, A. R. and Gonçalves M. A. L. (1999 b). Device and method for eliminating severe slugging in multiphase-stream flow lines. *US Patent*, US6041803.
- Andritsos, N. and Hanratty, T. J. (1987). Interfacial instabilities for horizontal gas-liquid flows in pipelines. *International Journal of Multiphase Flow*, 13(5), p. 583-603.
- ANSYS (2006). *Fluent 6.3 Documentation*. ANSYS Inc..
- Anthony, N.R., Ronalds, B.F. and Fakas, E. (2000). Platform decommissioning trends. In: *SPE Asia Pacific Oil and Gas Conference and Exhibition*, 16-18 October 2000, Brisbane, Austria, Society of Petroleum Engineers, p. 747-754 (SPE 64446).
- Bai, Y. and Bai, Q. (2005). *Subsea Pipelines and Risers*. Elsevier Science Ltd., p. 263-562.
- Baliño, J. N., Burr, K. P. and Nemoto, R. H. (2010). Modelling and simulation of severe slugging in air-water pipeline-riser systems. *International Journal of Multiphase Flow*, 36(8), p. 643-660.
- Barnea, D. and Taitel, Y. (1993). A model for slug length distribution in gas-liquid slug flow. *International Journal of Multiphase Flow*, 19(5), p. 829-838.
- Beggs, H. D. and Brill, J. P. (1973). A study of two-phase flow in inclined pipes. *Journal of Petroleum Technology*, 25(5), p. 607-617.

Bendiksen, K. H. and Espedal, M. (1984). Onset of slugging in horizontal gas-liquid pipe flow. *International Journal of Multiphase Flow*, 18(2), p. 237-247.

Bendiksen, K. H. (1984). An experimental investigation of the motion of long bubbles in inclined tubes. *International Journal of Multiphase Flow*, 10(4), p. 467-483.

Bendiksen, K.H., Malnes, D., Moe, R. and Nuland, S. (1991). The dynamic two-fluid model OLGA: theory and application. *SPE Production Engineering*, 6(2), p. 171-180.

Bendiksen, K.H., Malnes, D. and Nydal, O. J. (1996). On the modelling of slug flow. *Chemical Engineering Communications*, 141-142, p. 71-102.

Bendiksen, K.H., Malnes, D., Straume, T. and Hedne, P. (1990). A non-diffusive numerical model for transient simulation of oil-gas transportation systems. In: *European Simulation Multi-conference*, 10-13 June 1990, Nuremberg, Germany, Society for Computer Simulation, p. 508-515.

Bøe, A. (1981). Severe slugging characteristics; Part 1: Flow regime for severe slugging; Part 2: Point model simulation study. *Presented at Selected Topics in Two-Phase Flow*, Trondheim, Norway.

Bonnecaze, R. H. Erskine, W. and Greskovich, E. J. (1971). Holdup and pressure drop for two-phase slug flow in inclined pipelines. *AIChE Journal*, 17(5), p. 1109-1113.

Brill, J. P., Schmidt, Z., Coberly, W. A., Herring, J. D. and Moore, D. W. (1981). Analysis of two-phase tests in large-diameter flow lines in Prudhoe Bay field. *SPE Journal*, 21(3), p. 363-378.

Brown, L. D. (2002). Flow assurance: a π^3 discipline. In: *Offshore Technology Conference*, 6-9 May 2002, Houston, Texas USA, p. 183-189.

Burke, N. E. and Kashou, S. F. (1993). History matching of a North Sea flowline startup. *Journal of Petroleum Technology*, 45(5), p. 470-476.

Cao, Y., Yeung, H. and Lao, L. (2009). Inferential slug control system. *Report No. 09/YC/533*, Department of Offshore, Process and Energy Engineering, Cranfield University, UK.

CD-adapco (2010), STAR-CCM+ Version 5.04.006, *User Guide*.

Colligan, J. (1999). The economics of deep water. *Oil & Gas Executive*, 2(3), p. 36-42.

Cook, M. and Behnia, M. (2000). Slug length prediction in near horizontal gas liquid intermittent flow. *Chemical Engineering Science*, 55(11), p. 2009-2018.

Courbot, A. (1996). Prevention of severe slugging in the Dunbar 16" multiphase pipeline. In: *Offshore Technology Conference*, 6-9 May 1996, Houston, Texas USA, p. 445-452.

Department of Trade and Industry (2001). *An Overview of Offshore Oil and Gas Exploration and Production Activities*. Hartley Anderson Limited..

Dhulesia, H., Hustvedt, E. and Todal, O. (1993). Measurement and analysis of slug characteristics in multiphase pipelines. In: *6th International Conference on Multiphase Production*, 16-18 June 1993, Cannes, France, BHRG.

Drengstig, T. and Magndal, S. (2001). Slug control of production pipeline. *Technical report N-4091*, School of Science and Technology, Stavanger University College, Ullandhaug, Norway.

Dukler, A. E. and Hubbard, M. G. (1975). A model for gas-liquid slug flow in horizontal and near horizontal tubes. *Industrial & Engineering Chemistry Fundamentals*, 14(4), p. 337-347.

Durapipe, (2007). *ABS Technical Brochure*. Glynwed Pipe Systems Ltd..

Fabre, J. and Liné, A. (1992). Modelling of two-phase slug flow. *Annular Review of Fluid Mechanics*, 24(1), p. 21-46.

Fabre, J., Peresson, L. L., Corteville, J., Odello, R. and Bourgeois, T. (1987). Severe slugging in pipeline/riser systems. *SPE Annual Technical Conference and Exhibition*,

27-30 September 1987, Dallas, Texas USA, Society of Petroleum Engineers of AIME (SPE 16846).

Fagundes Netto, J. R., Fabre J., Grenier, P. and Peresson, L. (1998). An experimental study of an isolated long bubble in a horizontal liquid flow. In: *3rd International Conference on Multiphase Flow (ICMF)*, 8-12 June 1998, Lyon, France.

Fairhurst, C. P. (1983). Two-phase transient phenomena in oil production flowlines. BHRA the Fluid Engineering Centre.

Farghaly, M. A. (1987). Study of severe slugging in real offshore pipeline riser-pipe system. In: *5th Middle East oil show*, 7-10 March 1987, Manama, Bahrain, Society of Petroleum Engineers of AIME, p. 299-314 (SPE 15726).

FEESA (2004). Literature review for sub-project IX: active control of slug flows. *Joint Project on Transient Multiphase Flow (TMF3)*, December 2004.

Ghajar, A. J. (2004). Non-boiling heat transfer in gas-liquid flow in pipes – tutorial. In: *10th Brazilian Congress of Thermal Engineering and Science (ENCIT 2004)*, 29 November – 3 December, 2004, Rio de Janeiro, Brazil.

Goldzberg, V. and McKee, F. (1985). Model predictions liquid accumulation, severe terrain-induced slugging for two phase flow lines. *Oil and Gas Journal*, 19, p. 105-109.

Gregory, G. A., Nicholson, M. K. and Aziz, K. (1978). Correlation of the liquid fraction in the slug for horizontal gas-liquid slug flow. *International Journal of Multiphase Flow*, 4(1), p. 33-39.

Guo, B., Song, S., Ghalambor, A. and Chacko, J. (2005). *Offshore Pipelines*. Elsevier Science Ltd, p. 169-214.

Hale, C. P. (2000). *Slug Formation, Growth and Collapse*. PhD Thesis, Imperial College London, UK.

Hatton, S. A. and Howells, H. (1996). Catenary and hybrid risers for deepwater locations worldwide. In: *Advances in Riser Technologies Conference*, June 1996, Aberdeen, UK.

Havre, K. and Dalsmo, M. (2002). Active feedback control as a solution to severe slugging. *SPE Production and Facilities*, 17(3), p. 138-148.

Henriot, V., Courbot, A., Heintz, E. and Moyeux, L. (1999). Simulation of process to control severe slugging: application to the Dunbar pipeline. In: *SPE Annual Technical Conference and Exhibition*, 3-6 October 1999, Houston, Texas USA, Society of Petroleum Engineering, SPE 56461.

Hewitt, G. F. (1982). *Handbook of Multiphase Systems*. Hemisphere Publishing Corporation, New York.

Hewitt, G. F. and Robertson, D. N. (1969). Studies of two-phase flow patterns by Simultaneous X-ray and flash photography. *Report AERE-M2159*, The United Kingdom Atomic Energy Authority (UKAEA), Harwell, UK.

Hill, T. J. (1989). Riser-base gas injection into the S. E. Forties line. In: *4th International Conference on Multi-phase Flow*, Nice, France, BHRG, p. 133-148.

Hope, C. B. (1990). *The Development of a Water Soluble Photochromic Dye Tracking Technique and Its Application to Two-Phase Flow*. PhD Thesis, University of London, UK.

Hustvedt, E. (1993). Determination of slug length distributions by the use of the OLGA slug tracking model. In: *6th International Conference on Multi-phase Production*, 16-18 June 1993, Cannes, France, BHRG, p. 147-163.

Issa, R. I. and Kempf, M. H. W. (2003). Simulation of slug flow in horizontal and near horizontal pipes with the two-fluid model. *International Journal of Multiphase Flow*, 29(1), p. 69-95.

- Issa, R. I. and Woodburn, P. (1998). Numerical prediction of instabilities and slug formation in horizontal two-phase flows. In: *3rd International Conference on Multiphase Flow (ICMF'98)*, 8-12 June 1998, Lyon, France.
- Issa, R. I., Castagna, J. and Sheikh, A. (2011). Accurate simulation of intermittent/slug flow in oil and gas pipelines. In: *15th International Conference on Multiphase Production Technology*, 15-17 June 2011, Cannes, France, BHRG, p. 345-357.
- Jansen, F. E., Shoham, O. and Taitel, Y. (1996). The elimination of severe slugging - experiments and modeling. *International Journal of Multiphase Flow*, 22(6), p. 1055-1072.
- Johal, K.S., Teh, C. E. and Cousins, A. R. (1997). An alternative economic method to riser-base gas lift for deep water subsea oil/gas field developments. *Offshore Europe Conference*, 9-12 September 1997, Aberdeen, UK, Society of Petroleum Engineers, (SPE 38541).
- Jonnavithula, S., Lo, S. and Anderson, D. (2009). Simulation for energy engineering. *STAR Global Forum 2009*, June 2009, Houston, USA, CD-adapco.
- Kashou, S. F. (1996). Severe slugging in S-shaped or catenary risers: OLGA prediction and experimental verification. *Advances in Multiphase Technology Conference*, 24-25 June 1996, Houston, Texas USA.
- King, M. J. S. (1998). *Experimental and Modelling Studies of Transient Slug Flow*. PhD Thesis, Imperial College London, UK.
- Kordyban, E. S. (1961). A flow model for two-phase slug flow in horizontal tubes. *Journal of Basic Engineering*, December, p. 613-618.
- Kovalev, K., Cruickshank, A. and Purvis, J. (2003). The slug suppression system in operation. *Offshore Europe Conference*, 2-5 September 2003, Aberdeen, UK, Society of Petroleum Engineers, p. 352-356 (SPE 84947).

- Kovalev, K., Seelen, M. and Haandrikman, G. (2004). Vessel-less S3: advanced solution to slugging pipelines. In: *SPE Asia Pacific Oil and Gas Conference and Exhibition*, 18-20 October 2004, Perth, Australia, p. 983-987 (SPE 88569).
- Larsen, M., Hustvedt, E. and Straume, T. (1997). PeTra: a novel computer code for simulation of slug flow. In: *SPE Annular Technical Conference and Exhibition*, 5-8 October 1997, San Antonio, Texas USA, Society of Petroleum Engineers, p. 965-976, (SPE 38841).
- Lee, J. (2009). Introduction to offshore pipelines and risers, 2009C Revision. available at: http://www.jyplpipeline.com/Pipeline_2009C_Brief.pdf. (Last accessed on 20 August 2011).
- Linga, H. and Østvang, D. (1985). Tabulated data from transient experiments with naphtha. *Report No. 41*, SINTEF, Norway.
- Linga, H. (1987). Terrain slugging phenomena: some experimental results obtained at the SINTEF Two-Phase Flow Laboratory. In: *3rd International Conference on Multiphase Flow*, 18-20 May 1987, The Hague, Netherlands, BHRA, p. 37-53.
- Lockhart, R. W. and Martinelli, R. C. (1949). Proposed correlation of data for isothermal two-phase, two component flow in pipes. *Chemical Engineering Progress*, 45(1), p. 39-48.
- Makogan, T. Y. and Brook, G. J. (2007). Device for controlling slugging. *Patent*, WIPO: WO2007/034142.
- Makogan, T., Estanga, D. and Sarica, C. (2011). A new passive technique for severe slugging attenuation. In: *15th International Conference on Multiphase Production Technology*, 15-17 June 2011, Cannes, France, BHRG, p.385-396.
- Mandhane, J. M. (1974). A flow pattern map for gas-liquid flow in horizontal pipes. *International Journal of Multiphase Flow*, 1(4), p. 537-553.
- Manfield, P. D. (2000). *Experimental, Computational and Analytical Studies of Slug Flow*. PhD Thesis, Imperial College London, UK.

Mazzoni, A., Villa, M., Bonuccelli, M., Toma, G. D., Mazzei, D. and Crescenzi, T. (1993). Capability of the OLGA computer code to simulate measured data from AGIP oil field. In: *6th International Conference on Multiphase Production*, 16-18 June 1993, Cannes, France, BHRG, p. 51-79.

Milne-Thompson (1960). *Theoretical Hydrodynamics*. The Mac-Millan Company, New York, USA.

Moe, R. (1993). Transient simulation of 2-3D stratified and intermittent two-phase flows. Part II: applications. *International Journal for Numerical Methods in Fluids*, 16(11), p. 967-988.

Molyneux, P. D. and Kinvig, J. P. (2000). Method of eliminating severe slugging in a riser of a pipeline includes measuring pipeline pressure and operating a valve. *UK Patent*, No. 0013331.4.

Montgomery, J. A. (2002). *Severe Slugging and Unstable Flows in an S-Shaped Riser*. PhD Thesis, Cranfield University, UK.

Montgomery, J. A. and Yeung, H. C. (2002). The stability of fluid production from a flexible riser. *Journal of Energy Resources Technology, Transactions of the ASME*, 124(2), p. 83-89.

Nicklin, D. J., Wilkes, J. O. and Davidson, J. F. (1962). Two-phase flow in vertical tubes. *Transactions of the Institution of Chemical Engineers*, 40(2), p. 61-68.

Nordsveen, M., Andersson, P., Henriksen, S., Wangensteen, T. and Rasmussen, J. and Xu, Z. G. (2009). Void fronts in pipeline-riser slug flow. In: *14th International Conference on Multiphase Production Technology*, 17-19 June 2009, Cannes, France, BHRG, p. 449-461.

Nydal, O. J. and Banerjee, S. (1995). Object oriented dynamic simulation of slug flow. In: *2nd International Conference on Multiphase Flow (ICMF)*, 3-7 April 1995, Kyoto, Japan.

- Nydal, O. J. and Banerjee, S. (1996). Dynamic slug tracking simulations for gas-liquid flow in pipelines. *Chemical Engineering Communications*, 141-142, p. 13-39.
- Ogazi, A. I. (2011). *Multiphase Severe Slug Flow Control*. PhD Thesis, Cranfield University, UK.
- Pan, L. (1996). *High Pressure Three-Phase (Gas/Liquid/Liquid) Flow*. PhD Thesis, Imperial College London, UK.
- Pots, B. F. M., Bromilow, I. G. and Konijn, M. J. W. F. (1987). Severe slug flow in offshore flowline/riser systems. *SPE Production Engineering*, 2(4), p. 319-324.
- Sagatun, S. I. (2004). Riser slugging: a mathematical model and the practical consequences. *SPE Production and Facilities*, 19(3), p. 168-175.
- Sánchez, S. F., Toledo, V. M. and Hernández, G. A. (1998). Slug flow momentum transfer analysis to determine the forces acting on a 90° elbow in a horizontal pipe. In: *3rd International Conference on Multiphase Flow (ICMF)*, 8-12 June 1998, Lyon, France.
- Sarica, C. and Shoham, O. (1991). A simplified transient model for pipeline-riser systems. *Chemical Engineering Science*, 46(9), p. 2167-2179.
- Sarica, C. and Tengedal, J. Ø. (2000). A new technique to eliminate severe slugging in pipeline/riser systems. In: *SPE Annual Technical Conference and Exhibition*, 1-4 October 2000, Dallas, Texas USA, Society of Petroleum Engineers, (SPE 63185).
- Schmidt, Z., Brill, J. P. and Beggs, H. D. (1979). Choking can eliminate severe pipeline slugging. *Oil and Gas Journal*, 77(46), p. 230-238.
- Schmidt, Z., Brill, J. P. and Beggs, H. D. (1980). Experimental study of severe slugging in a two-phase-flow pipeline-riser pipe system. *SPE Journal*, 20(5), p. 407-414.
- Schmidt, Z., Doty, D. R. and Dutta-Roy, K. (1985). Severe slugging in offshore pipeline-riser pipe system. *SPE Journal*, 25(1), p. 27-38.

Scott, S. L., Shoham, O. and Brill, J. P. (1987). Modelling slug growth in large diameter pipes. In: *3rd International Conference on Multiphase Flow*, 18-20 May 1987, The Hague, Netherlands, BHRA, p. 55-63.

Shen, J. J. S. and Yeung, H. (2008). Apparatus for mitigating slugging in flowline systems. *Patent*, WO2008/134489.

Singh, G. and Griffith, P. (1970). Determination of the pressure drop optimum pipe size for a two-phase slug flow in an inclined pipe. *Journal of Engineering for Industry, Series B, Transaction of ASME*, 92, p. 717-726.

SPT Group (2006). Transient multiphase flow simulator. *User Manual*, Version 5.

Storkaas, E. (2005). *Stabilizing Control and Controllability: Control Solutions to Avoid Slug Flow in Pipeline-Riser Systems*. PhD Thesis, Norwegian University of Science and Technology, Norway.

Storkaas, E. and Skogestad, S. (2004). Cascade control of unstable systems with application to stabilization of slug flow. *Technical Report*, Department of Chemical Engineering, Norwegian University of Science and Technology, Norway.

Storkaas, E., Skogestad, S. and Godhavn, J. M. (2003). A low dimensional dynamic model of severe slugging for control design and analysis. In: *11th International Conference on Multiphase 03: Extending the Boundaries of Flow Assurance*, 11-13 June 2003, San Remo, Italy, BHRG, p. 117-133.

Straume, T., Nordsveen, M., and Bendikson, K. (1992). Numerical simulations of slugging in pipelines. *Winter Annual Meeting of the American Society of Mechanical Engineers*, 8-13 November 1992, Anaheim, California USA, American Society of Mechanical Engineers, p. 103-112.

Su, J. (2003). Flow Assurance of deepwater oil and gas production - a review. In: *22nd International Conference on Offshore Mechanics and Arctic Engineering; Safety and Reliability Pipeline Technology*, 8-13 June 2003, Cancun, Mexico, vol. 2, p. 601-620.

- Taha, T. and Cui, Z. F. (2006). CFD modelling of slug flow in vertical tubes. *Chemical Engineering Science*, 61(2), p. 676-687.
- Taitel, Y. (1986). Stability of severe slugging. *International Journal of Multiphase Flow*, 12(2), p. 203-217.
- Taitel, Y. (1994). Advances in two-phase flow modelling. *University of Tulsa Centennial Petroleum Engineering Symposium*, 29-31 August 1994, Tulsa, Oklahoma, USA.
- Taitel, Y. and Barnea, D. (1990). Two-phase slug flow. *Advances in Heat Transfer*, 20, p. 83-132.
- Taitel, Y. and Barnea, D. (1998). Effects of gas compressibility on a slug tracking model. *Chemical Engineering Science*, 53(11), p. 2089-2097.
- Taitel, Y. and Barnea, D. (2000). Slug-tracking model for hilly terrain pipelines. *SPE Journal*, 5(1), p. 102-109.
- Taitel, Y. and Dukler, A. E. (1976). A model for predicting flow regime transitions in horizontal and near horizontal gas-liquid flow. *AIChE Journal*, 22(1), p. 47-55.
- Taitel, Y., Vierkandt, S., Shoham, O. and Brill, J. P. (1990). Severe slugging in a riser system: experiments and modeling. *International Journal of Multiphase Flow*, 16(1), p. 57-68.
- Tay, B. L. (2002). *Forces on Pipe Bends due to Intermittent Gas-Liquid Flow*. PhD Thesis, University of Cambridge, UK.
- Tay, B. L. and Thorpe, R. B. (2002). Forces on pipe bends due to slug flow. In: *3rd North American Conference on Multiphase Flow Technology*, 6-7 June 2002, Banff, Canada, BHRG, p. 281-300.
- Tay, B. L. and Thorpe, R. B. (2004). Effects of liquid physical properties on the forces acting on a pipe bend in gas-liquid slug flow. *Chemical Engineering Research and Design*, 82(A3), p. 344-356.

Tengesdal, J. Ø., Thompson, L. and Sarica, C. (2003). A design approach for "self-lifting" method to eliminate severe slugging in offshore production systems. In: *SPE Annual Technical Conference and Exhibition*, 5-8 October 2003, Denver, Colorado USA, Society of Petroleum Engineers, p. 1549-1554 (SPE 84227).

Tin, V. (1991). Severe slugging in flexible risers. In: *5th International Conference on Multiphase Production*, 19-21 June 1991, Cannes, France, BHRG, p. 507-526.

Ujang, P. M. (2003). *Studies of Slug Initiation and Development in Two-Phase Gas-Liquid Pipeline Flow*. PhD Thesis, Imperial College London, UK.

Vázquez, E. G. and Fairuzov, Y. V. (2009). A study of normal slug flow in an offshore production facility with a large-diameter flowline. *SPE Production and Operations*, 24(1), p. 171-179.

Vermeulen, L. R. and Ryan, J. T. (1971). Two-phase slug flow in horizontal and inclined tubes. *The Canadian Journal of Chemical Engineering*, 49(2), p. 195-201.

Watson, M. J., Pickering, P. F. and Hawkes, N. J. (2003). The flow assurance dilemma: risks vs. costs. *Hart's E & P*, 76(5), p. 36-40.

Woods, B. D. and Hanratty, T. J. (1996). Relation of slug stability to shedding rate. *International Journal of Multiphase Flow*, 22(5), p. 809-828.

Xing, L. (2009). Passive slug mitigation. *Year 1 Progress Review Report*, Cranfield University, UK.

Yeung, H. and Cao, Y. (2007). Effects of geometry at the riser base on riser hydrodynamic behaviour. *Report No. 07/HY/502*, Cranfield University, Cranfield.

Yeung, H., Cao, Y. and Adedigba, G. (2006). The importance of downstream conditions on riser behaviour. In: *5th North American Conference on Multiphase Technology*, 31 May – 2 June 2006, Banff, Canada, BHRG, p. 311-319.

Yeung, H., Cao, Y. and Lao, L. (2008). Comparisons between severe slug mitigation methods by increasing backpressure and throttling riser outlet valve. In: *6th North*

American Conference on Multiphase Technology, 4–6 June 2008, Banff, Canada, BHRG, p. 385-394.

Yeung, H., Tchambak, E. and Montgomery, J. (2003). Simulating the behaviour of an S-shaped riser. In: *11th International Conference on Multiphase 03: Extending the Boundaries of Flow Assurance*, 11-13 June 2003, San Remo, Italy, BHRG, p. 617-626.

Yocum, B.T. (1973). Offshore riser slug flow avoidance, mathematical model for design and optimization. In: *SPE European Meeting*, 2-3 April 1973, London, UK, American Institute of Mining, Metallurgical and Petroleum Engineers (AIME), (SPE 4312).

Zheng, D., He, X. and Che, D. (2007). CFD simulations of hydrodynamic characteristics in a gas-liquid vertical upward slug flow. *International Journal of Heat and Mass Transfer*, 50(21-22), p. 4151-4165.

Zuber, N and Findlay, J. A. (1965). Average volumetric concentration in two-phase flow systems. *Journal of Heat Transfer*, 87, p. 453-468.

APPENDICES

Appendix A Test Facilities

A.1 Three-Phase Test Facility

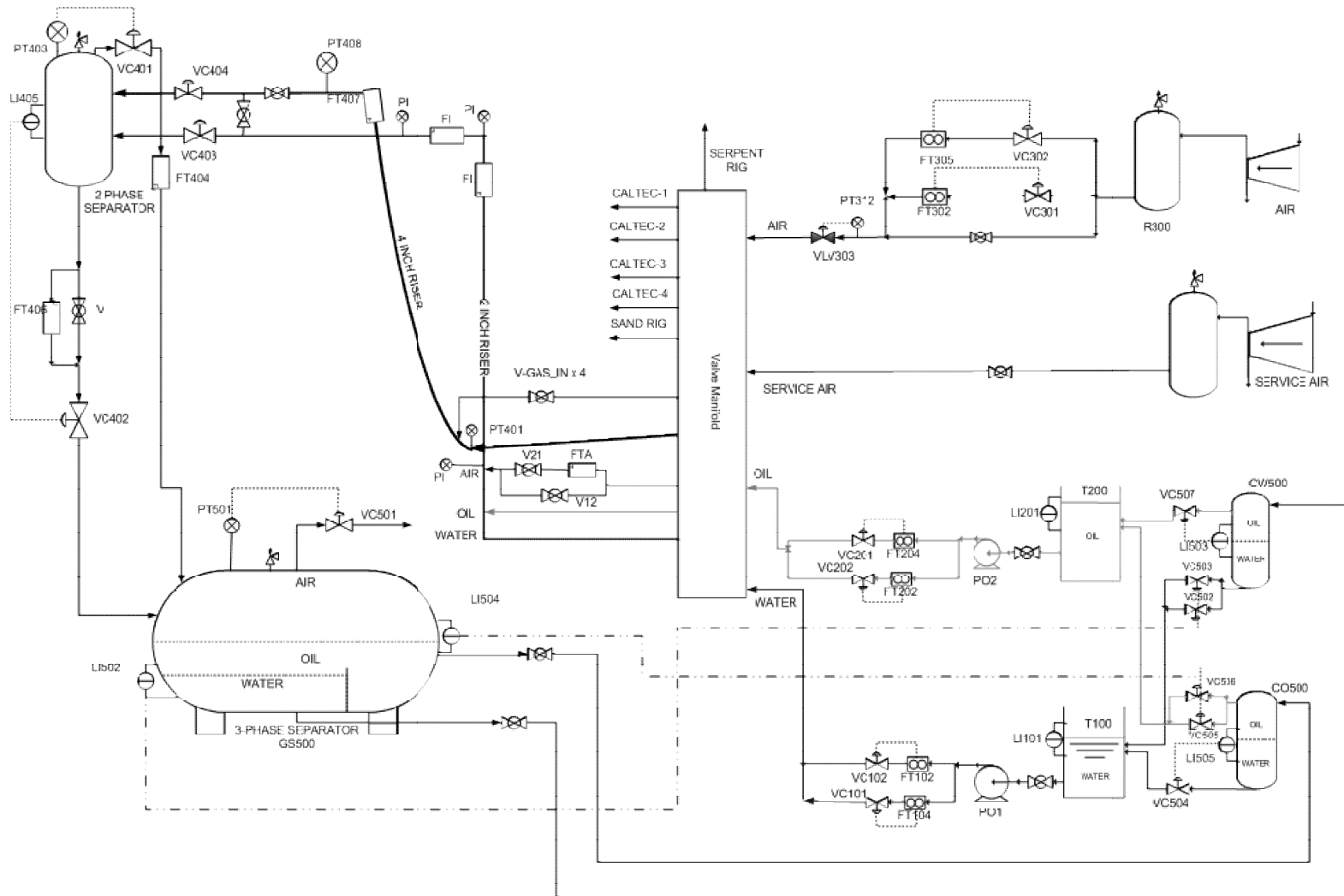


Figure A-1 Schematic of the Three-Phase Test Facility

A.2 Pipeline/Wavy-Pipe/Riser System

Figure A-2: Pipeline/wavy-pipe/riser system with a 7-bend wavy pipe located at the riser base (2" system)

Figure A-3: Pipeline/wavy-pipe/riser system with a 7-bend wavy pipe located at 1.5 m upstream of the riser base (2" system)

Figure A-4: Pipeline/wavy-pipe/riser system with a 11-bend wavy pipe located at the riser base (2" system)

Figure A-5: Pipeline/wavy-pipe/riser system with a 11-bend wavy pipe located at 1.5 m upstream of the riser base (2" system)

Figure A-6: Pipeline/wavy-pipe/riser system with a 7-bend wavy pipe located at 1.2 m upstream of the riser base (4" system)

Figure A-7: Pipeline/wavy-pipe/riser system with a 7-bend wavy pipe located at 4.2 m upstream of the riser base (4" system)

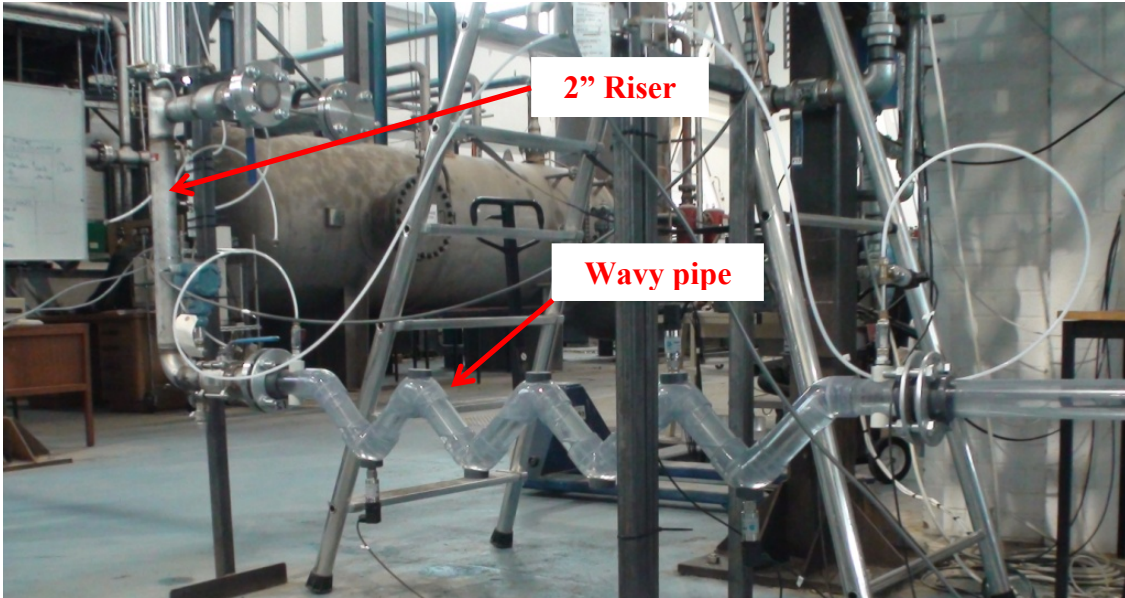


Figure A-2 Pipeline/wavy-pipe/riser system with a 7-bend wavy pipe located at the riser base (2 inch system)

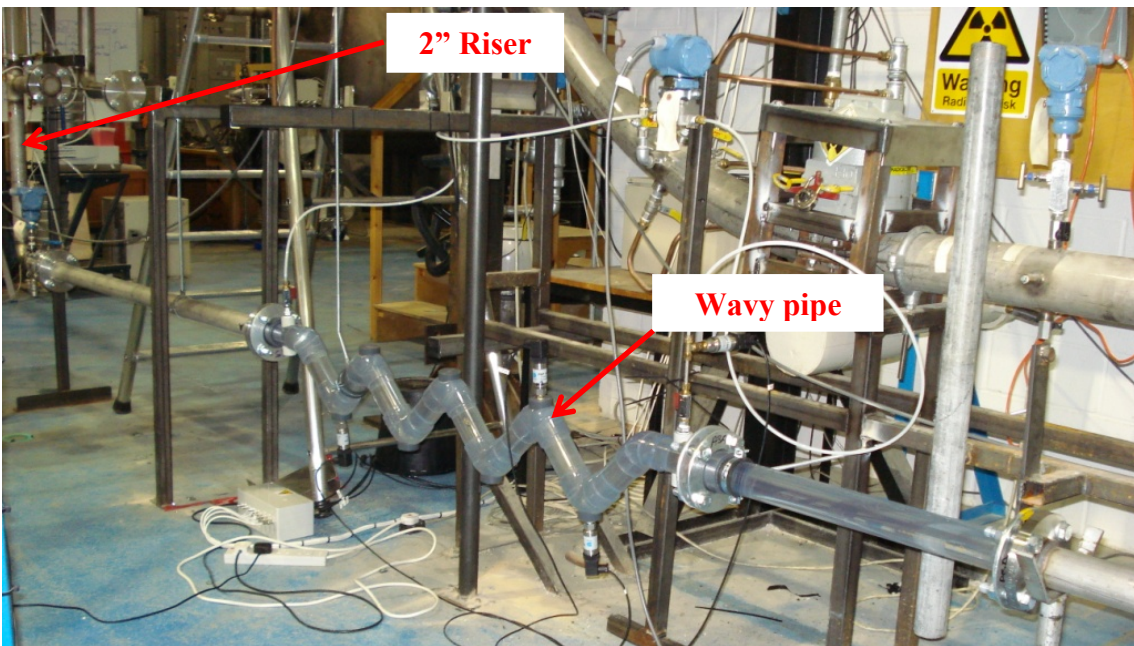


Figure A-3 Pipeline/wavy-pipe/riser system with a 7-bend wavy pipe located at 1.5 m upstream of the riser base (2 inch system)

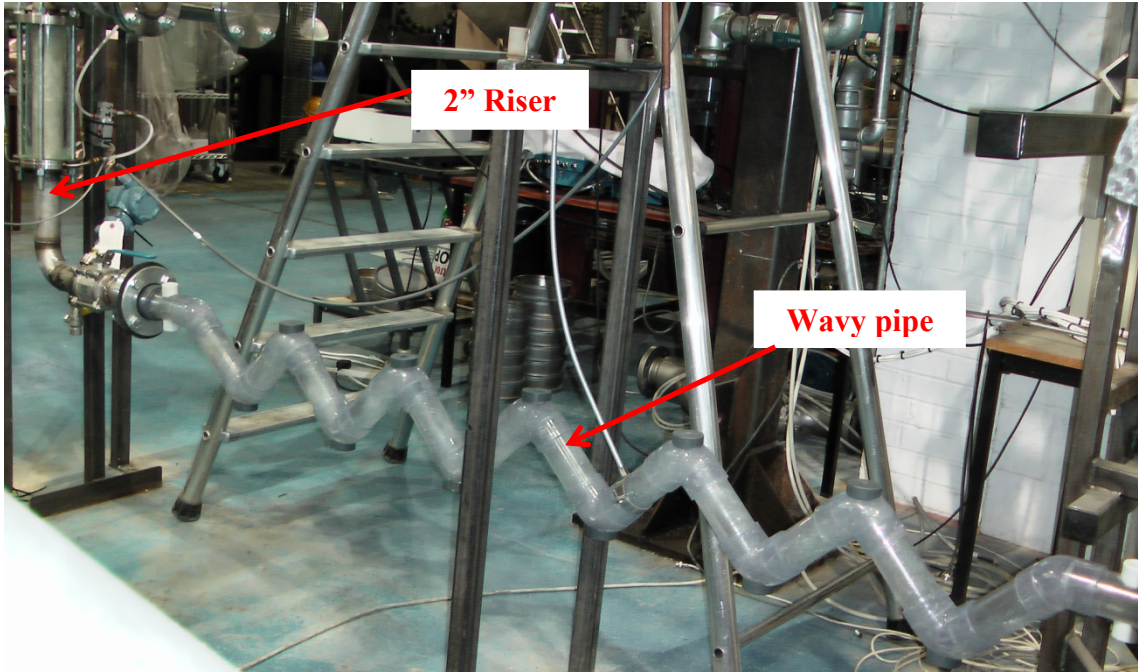


Figure A-4 Pipeline/wavy-pipe/riser system with a 11-bend wavy pipe located at the riser base (2" system)

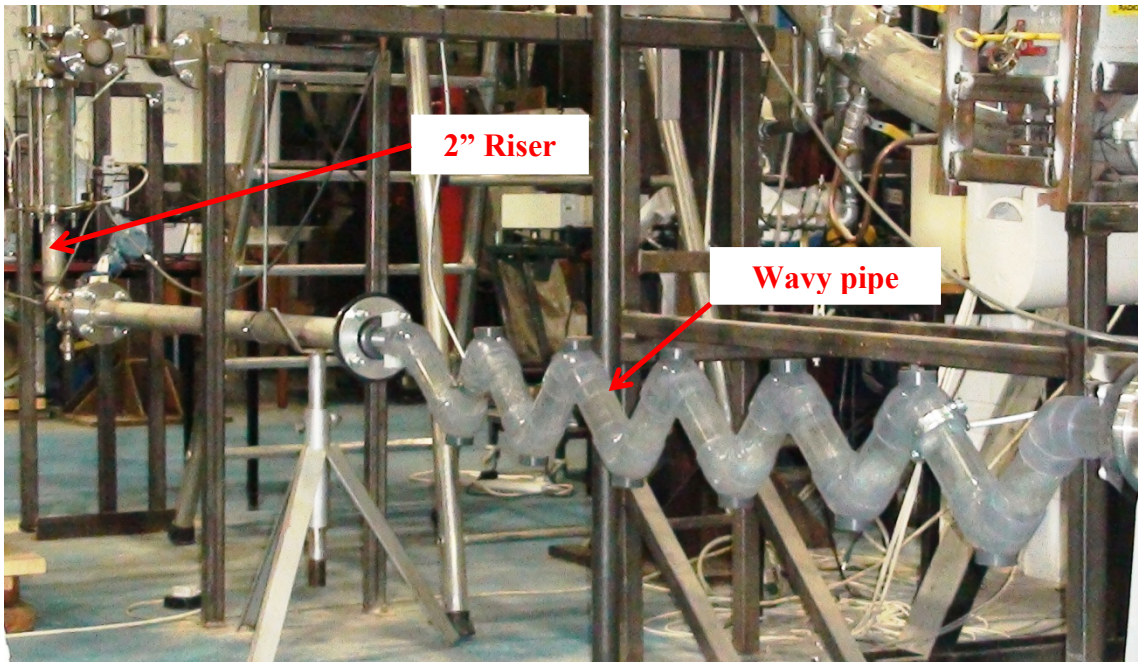


Figure A-5 Pipeline/wavy-pipe/riser system with a 11-bend wavy pipe located at 1.5 m upstream of the riser base (2" system)

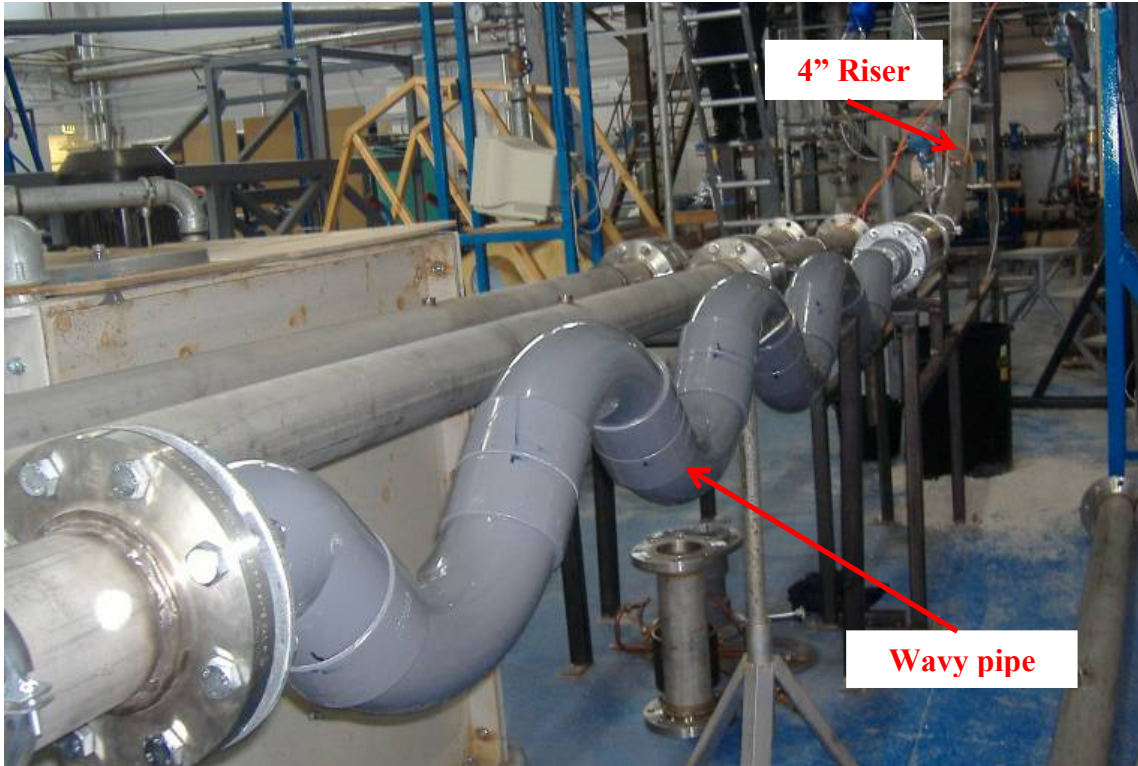


Figure A-6 Pipeline/wavy-pipe/riser system with a 7-bend wavy pipe located at 1.2 m upstream of the riser base (4 inch system)

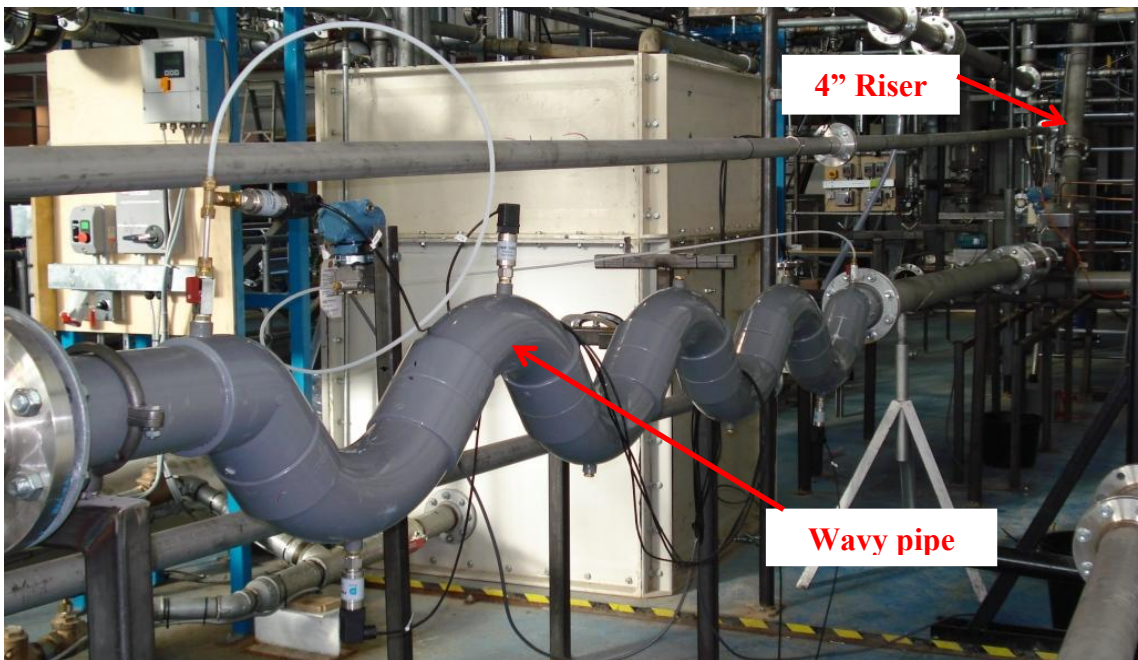


Figure A-7 Pipeline/wavy-pipe/riser system with a 7-bend wavy pipe located at 4.2 m upstream of the riser base (4 inch system)

A.3 Horizontal Two-Phase Test Facility



Figure A-8 Horizontal two-phase test facility

A.4 Horizontal Wavy-Pipe System



Figure A-9 Test section with a wavy pipe



Figure A-10 Upstream conductivity cells A and B

Appendix B Phase Distribution in Horizontal Wavy-Pipe Systems

The phase distribution in horizontal wavy-pipe systems has been discussed in Chapter 6. However, only some snapshots have been presented due to the space restriction in the main text. Therefore, to show the development of the flow, a series of snapshots are provided in this section.

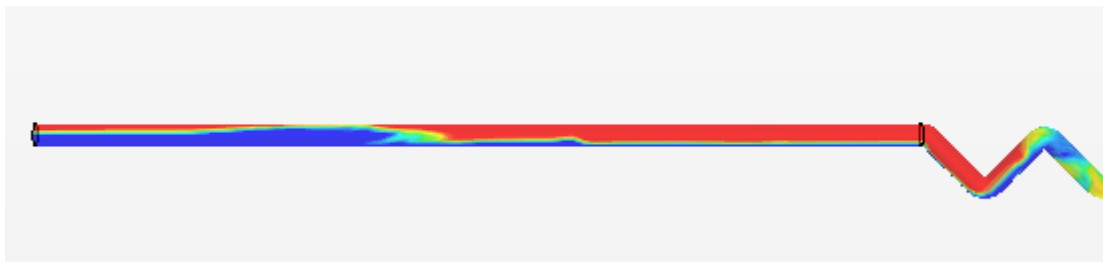
B.1 Upstream of the Wavy Pipe



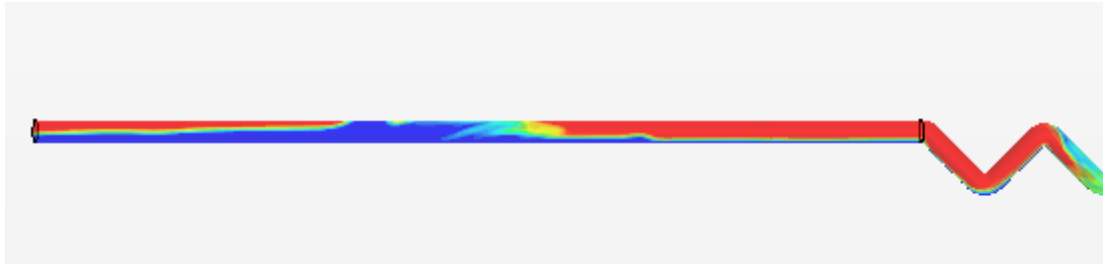
$t = 11.10$ s



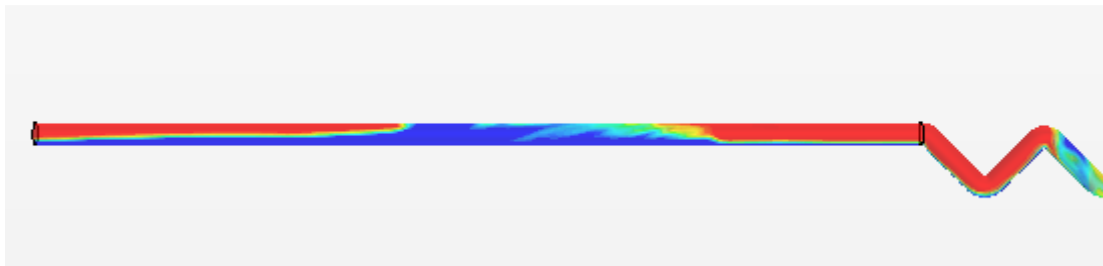
$t = 11.20$ s



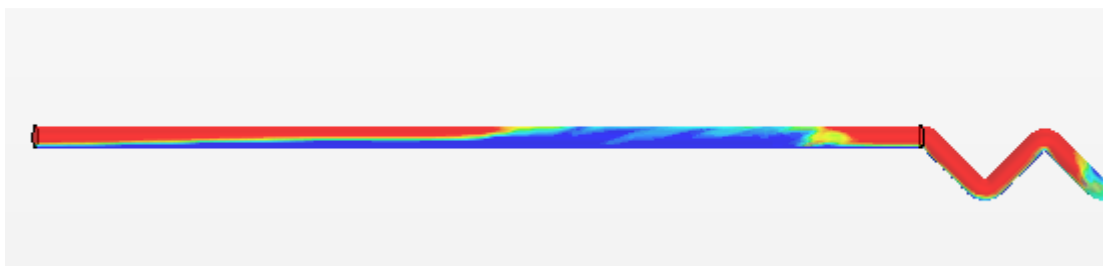
$t = 11.30$ s



$t = 11.40 \text{ s}$



$t = 11.50 \text{ s}$



$t = 11.60 \text{ s}$

→ Flow direction

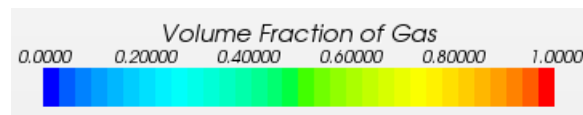
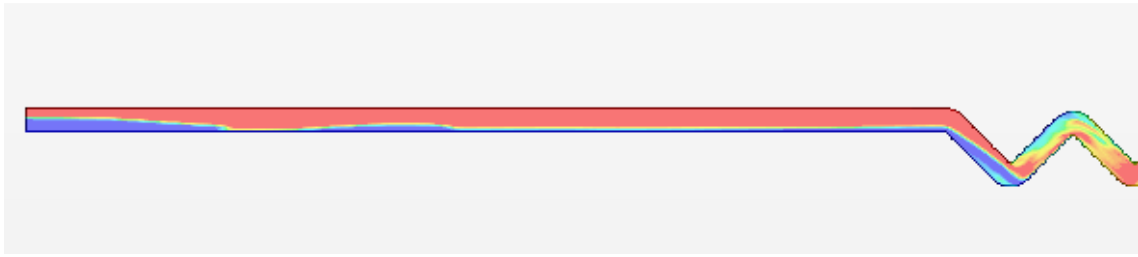


Figure B-1 Contour plots of gas volume fraction on the wall upstream of the wavy pipe ($U_{SL} = 0.47 \text{ m/s}$, $U_{SG} = 2.05 \text{ m/s}$)



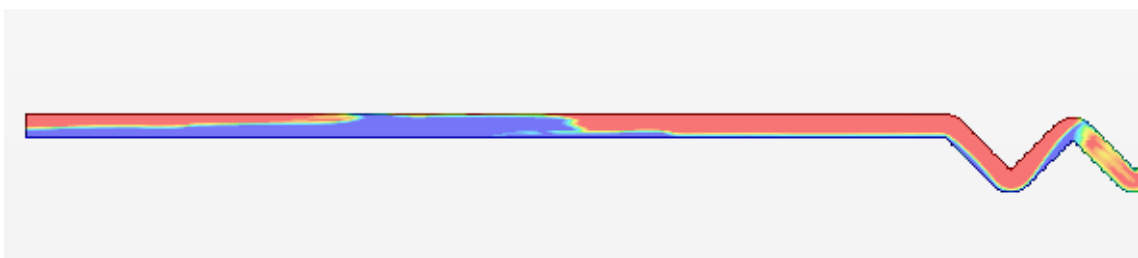
$t = 11.10$ s



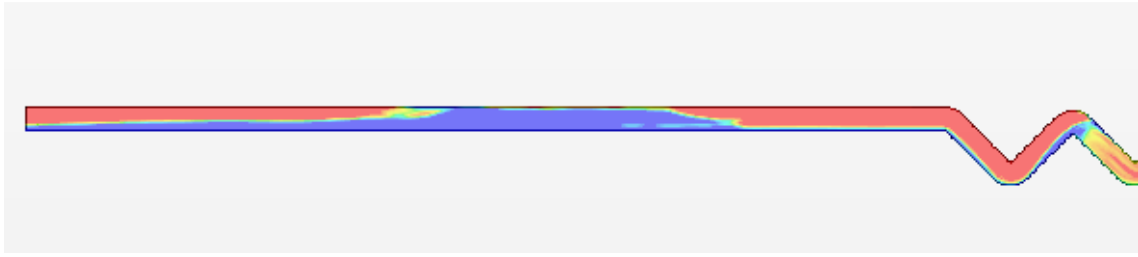
$t = 11.20$ s



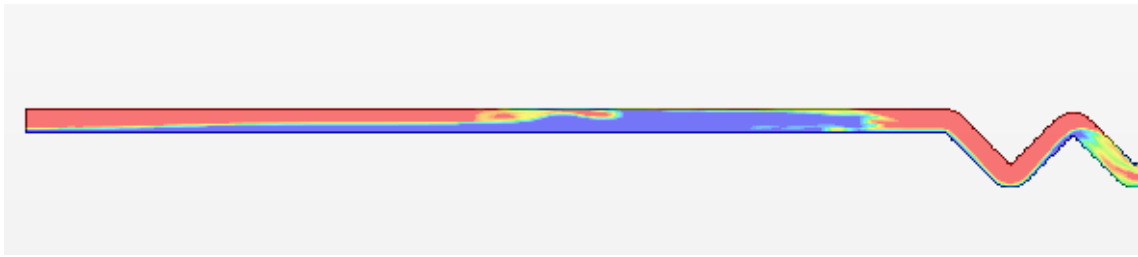
$t = 11.30$ s



$t = 11.40$ s



$t = 11.50$ s



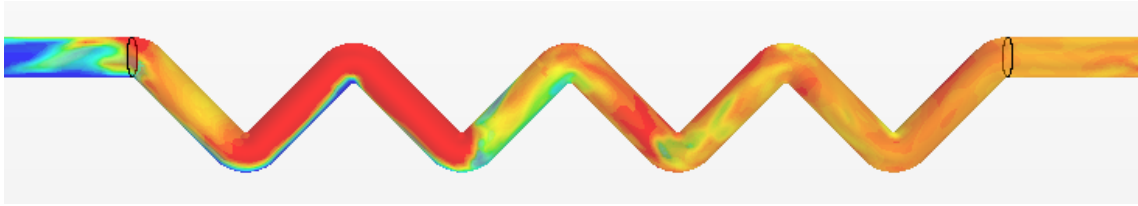
$t = 11.60$ s

→ Flow direction

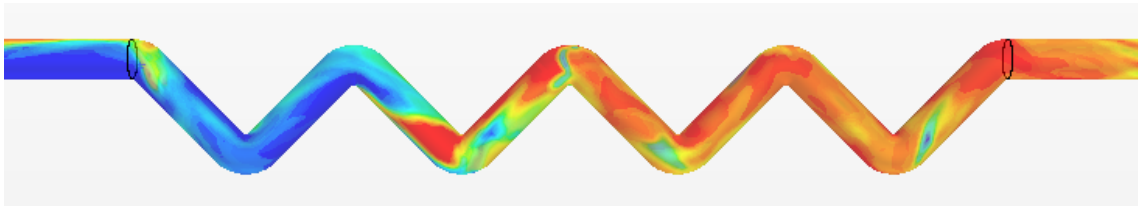


Figure B-2 Contour plots of gas volume fraction on the longitudinal section upstream of the wavy pipe ($U_{SL} = 0.47$ m/s, $U_{SG} = 2.05$ m/s)

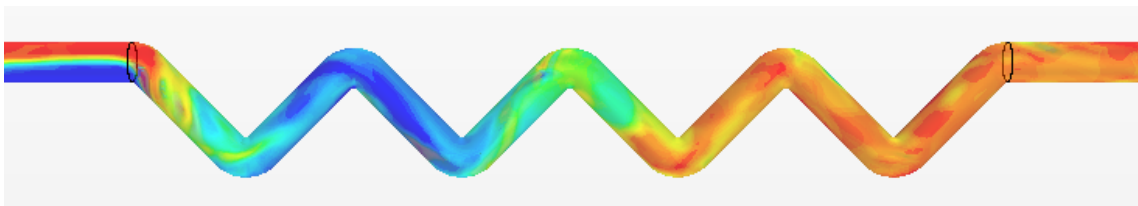
B.2 In the Wavy Pipe



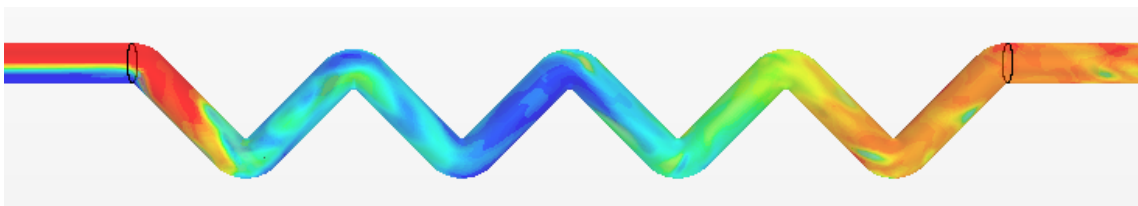
$t = 11.66 \text{ s}$



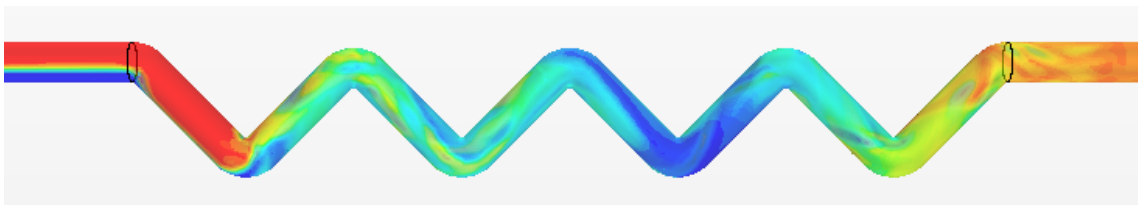
$t = 11.76 \text{ s}$



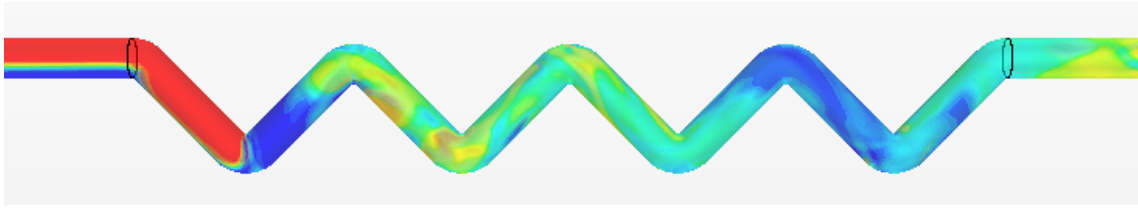
$t = 11.86 \text{ s}$



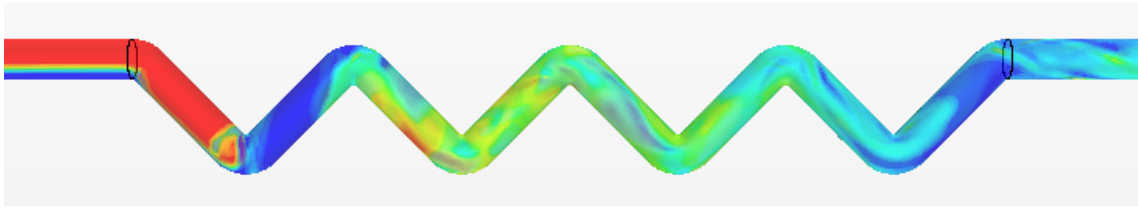
$t = 11.96 \text{ s}$



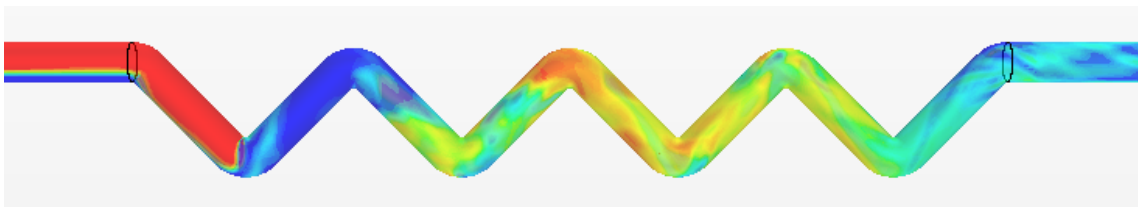
$t = 12.06 \text{ s}$



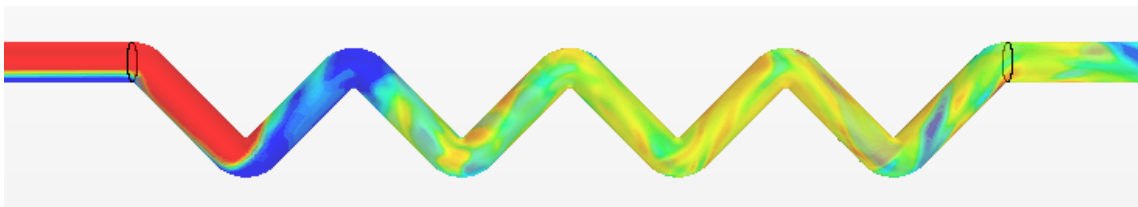
$t = 12.16$ s



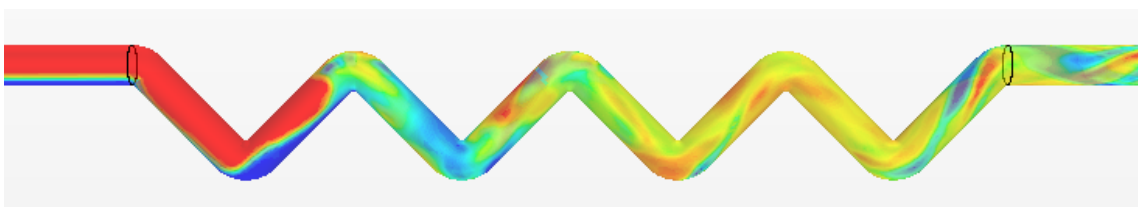
$t = 12.26$ s



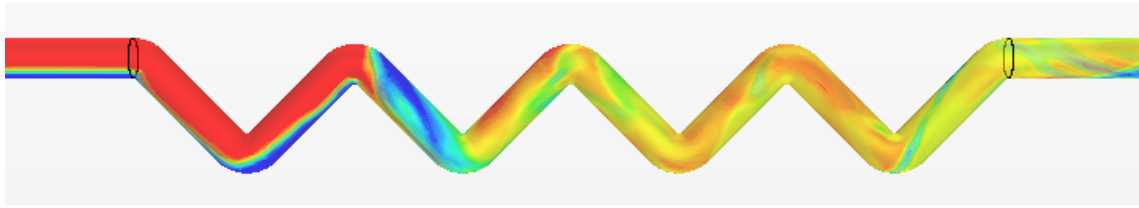
$t = 12.36$ s



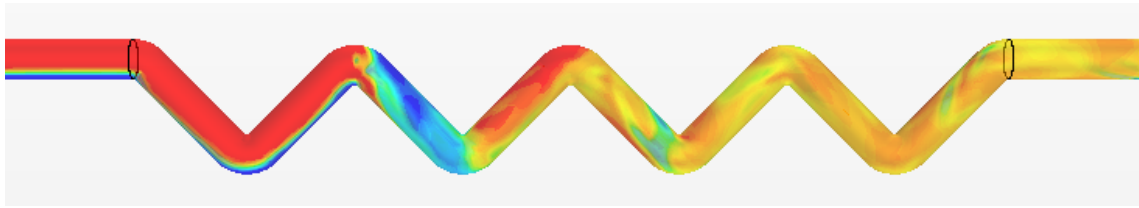
$t = 12.46$ s



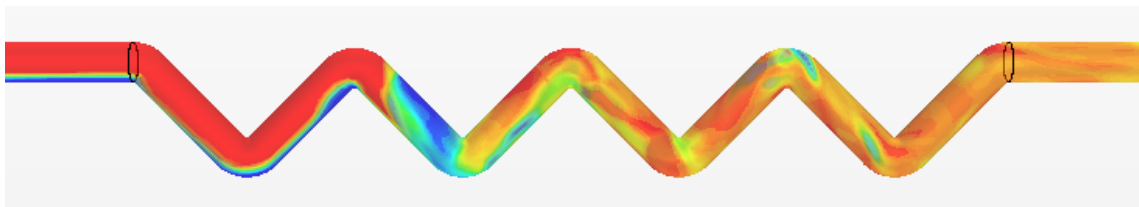
$t = 12.56$ s



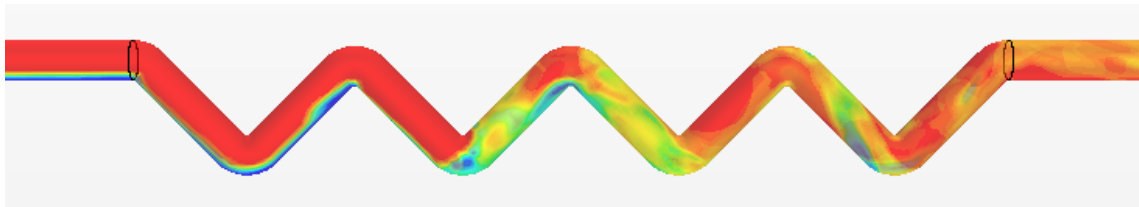
$t = 12.66$ s



$t = 12.76$ s



$t = 12.86$ s



$t = 12.96$ s

→ Flow direction

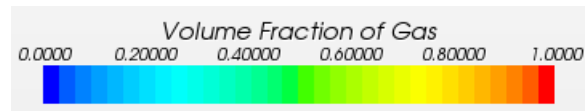
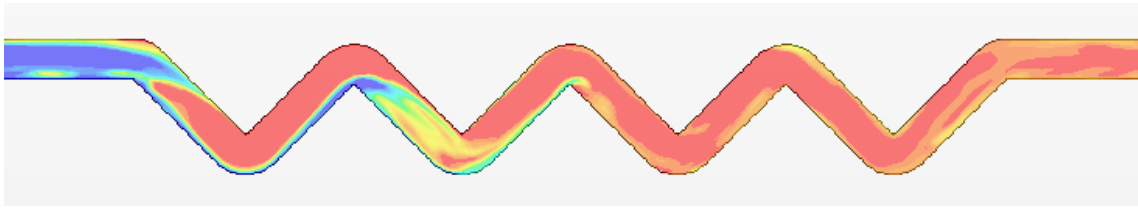
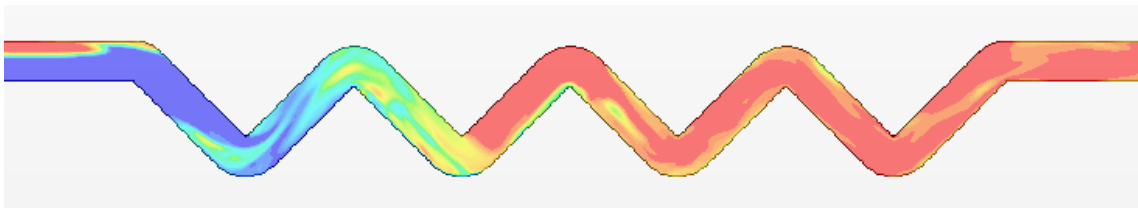


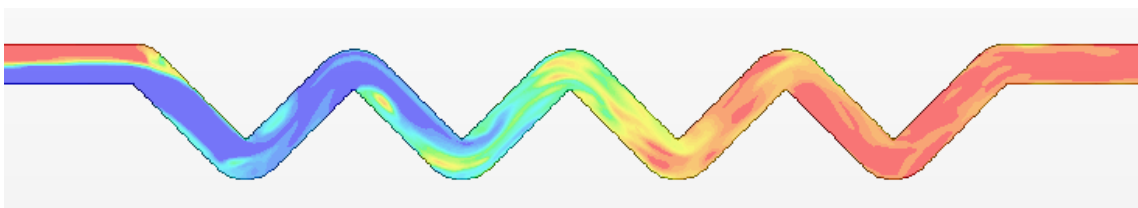
Figure B-3 Contour plots of gas volume fraction on the wall in the wavy pipe ($U_{SL} = 0.47$ m/s, $U_{SG} = 2.05$ m/s)



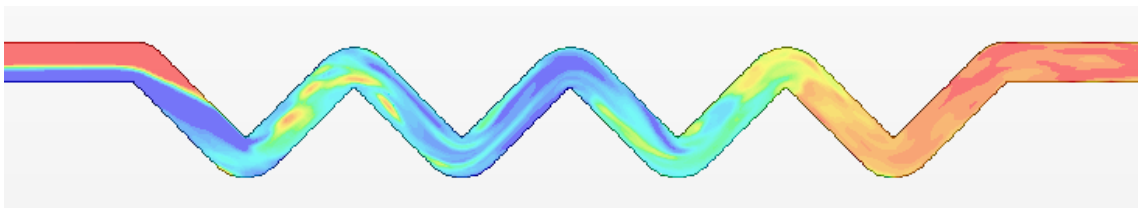
$t = 11.66$ s



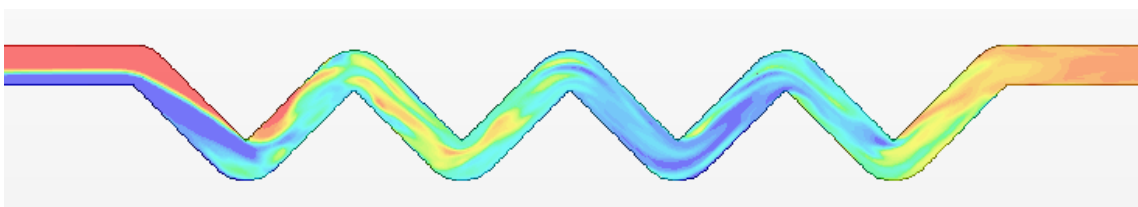
$t = 11.76$ s



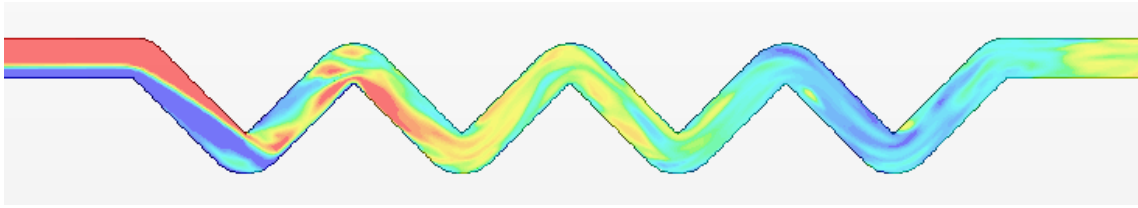
$t = 11.86$ s



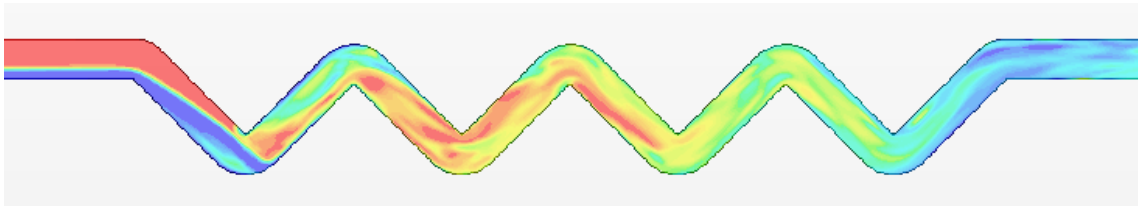
$t = 11.96$ s



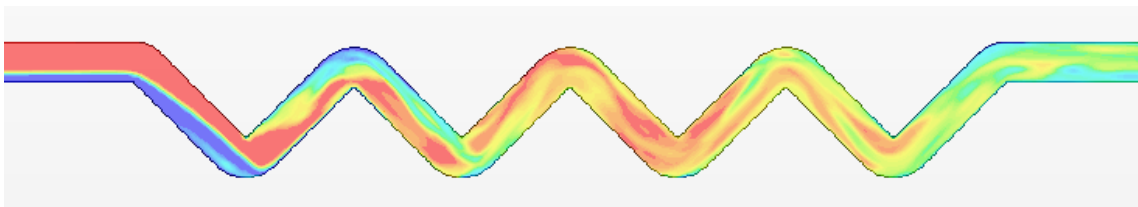
$t = 12.06$ s



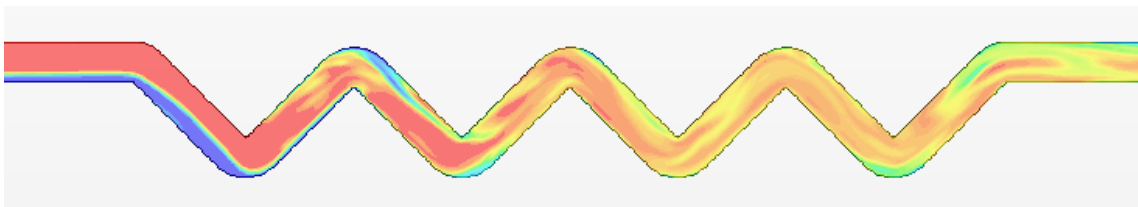
$t = 12.16$ s



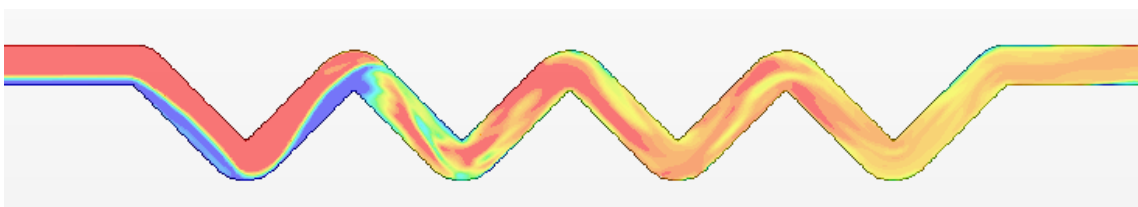
$t = 12.26$ s



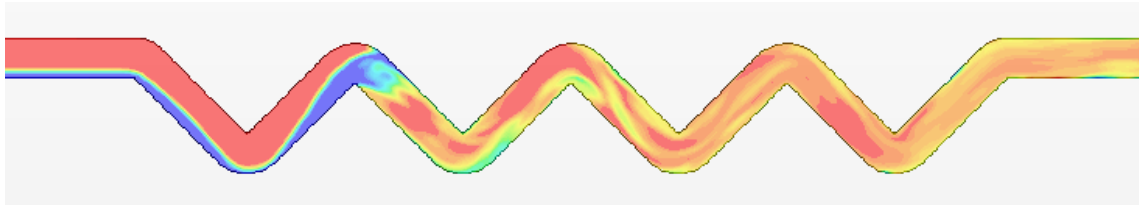
$t = 12.36$ s



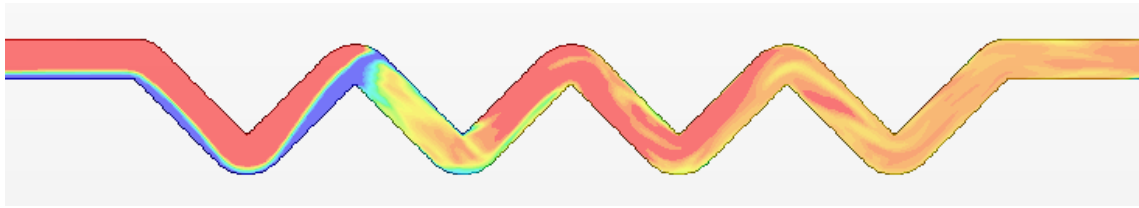
$t = 12.46$ s



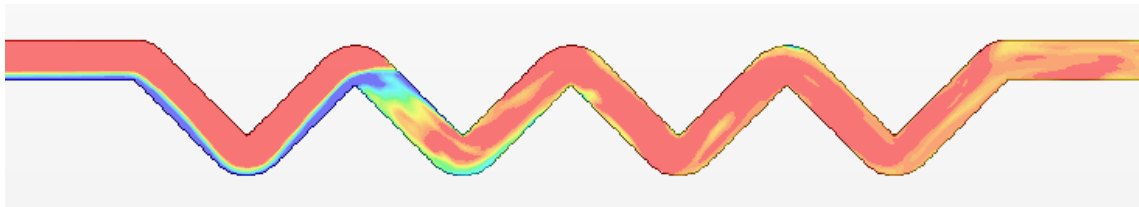
$t = 12.56$ s



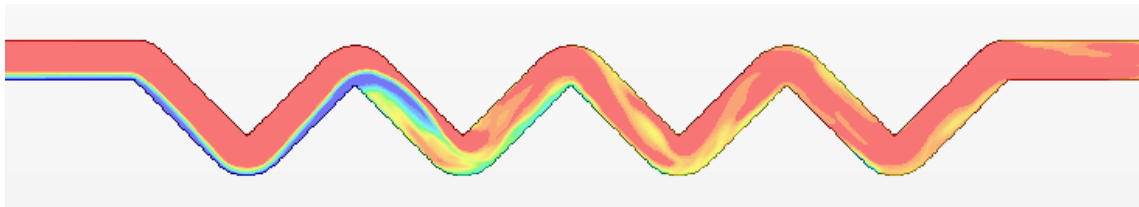
$t = 12.66$ s



$t = 12.76$ s



$t = 12.86$ s



$t = 12.96$ s

→ Flow direction



Figure B-4 Contour plots of gas volume fraction on the longitudinal section in the wavy pipe ($U_{SL} = 0.47$ m/s, $U_{SG} = 2.05$ m/s)

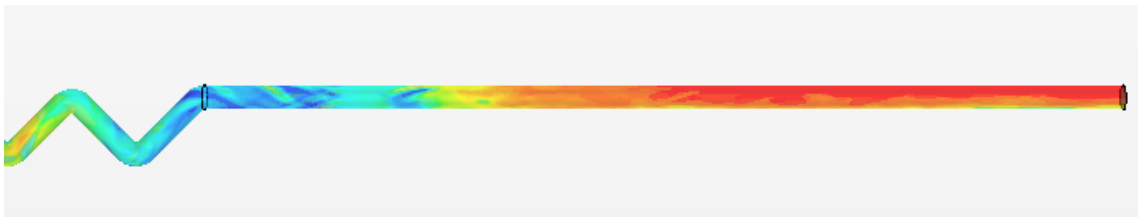
B.3 Downstream of the Wavy Pipe



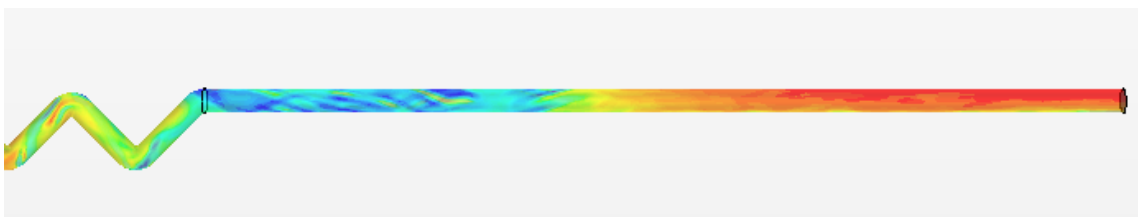
$t = 12.10$ s



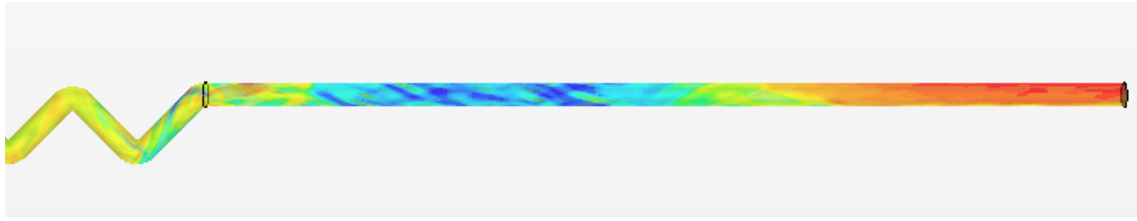
$t = 12.20$ s



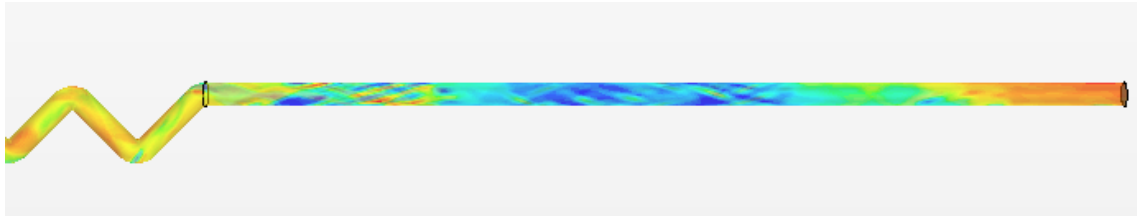
$t = 12.30$ s



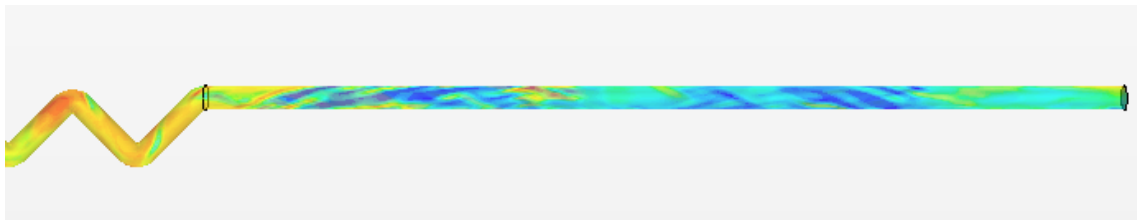
$t = 12.40$ s



$t = 12.50$ s



$t = 12.60$ s



$t = 12.70$ s

→ Flow direction

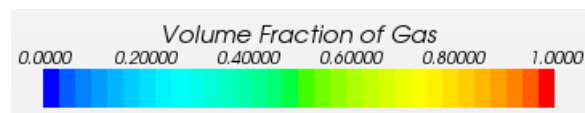
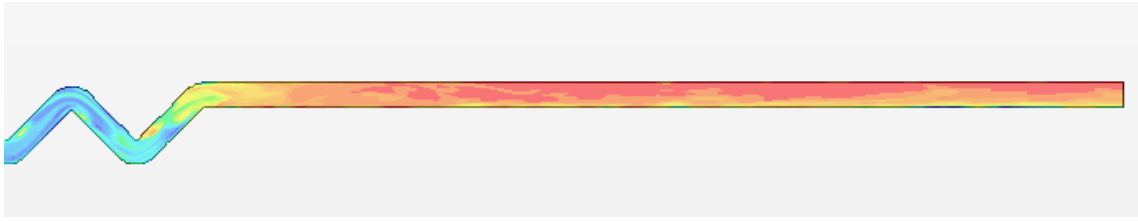


Figure B-5 Contour plots of gas volume fraction on the wall downstream of the wavy pipe ($U_{SL} = 0.47$ m/s, $U_{SG} = 2.05$ m/s)



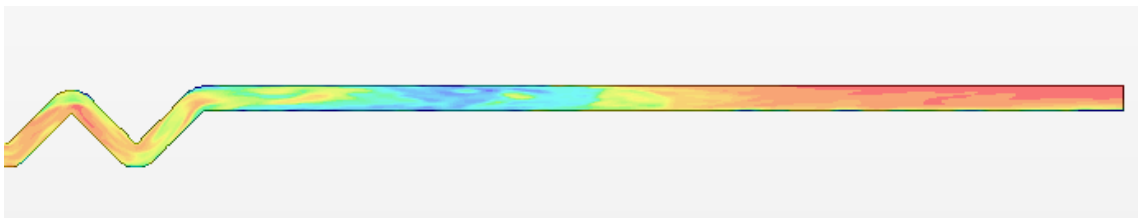
$t = 12.10$ s



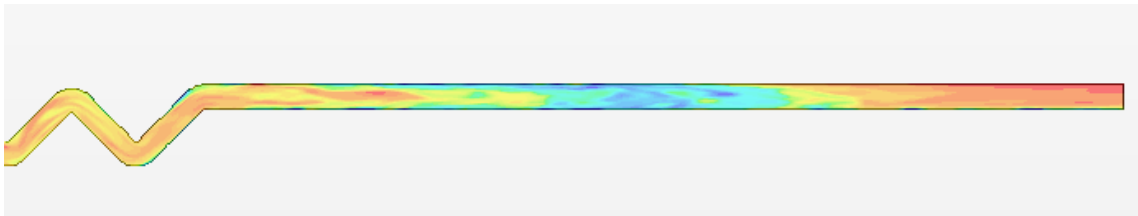
$t = 12.20$ s



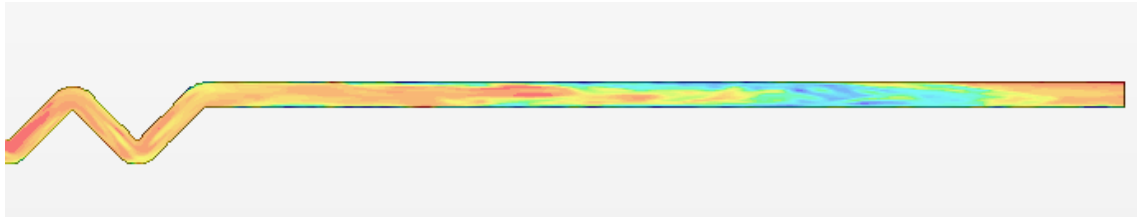
$t = 12.30$ s



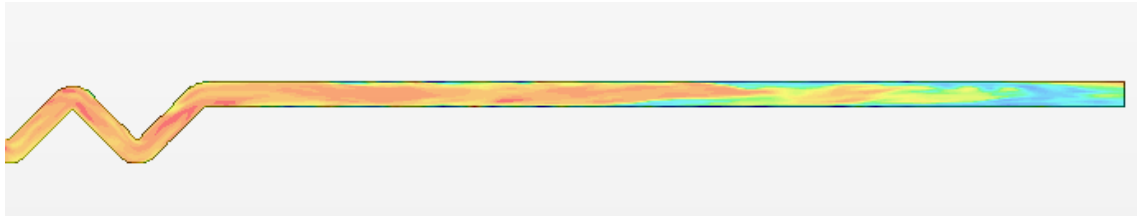
$t = 12.40$ s



$t = 12.50$ s



$t = 12.60$ s



$t = 12.70$ s

→ Flow direction

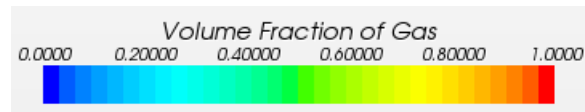


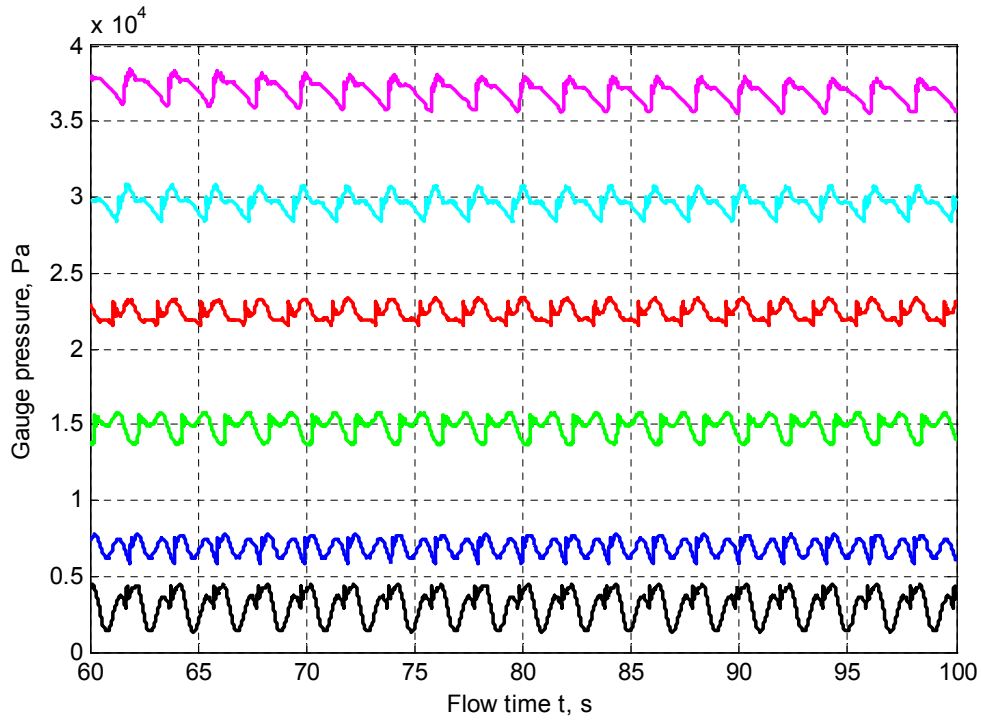
Figure B-6 Contour plots of gas volume fraction on the longitudinal section downstream of the wavy pipe ($U_{SL} = 0.47$ m/s, $U_{SG} = 2.05$ m/s)

Appendix C Effects of the Downstream Pipe length on the Forces on the Bend

It has been presented in Chapter 7 that a higher pressure-induced force on the pipe bend is induced by a longer downstream pipe. The pressure at the bend increases with the increasing length of the downstream pipe because the pressure increase is equal to the pressure drop along the downstream pipe. Significant force fluctuations induced by the pressure fluctuations have been observed. In this section the pressure fluctuations at the bend with downstream pipes of different lengths have been inspected.

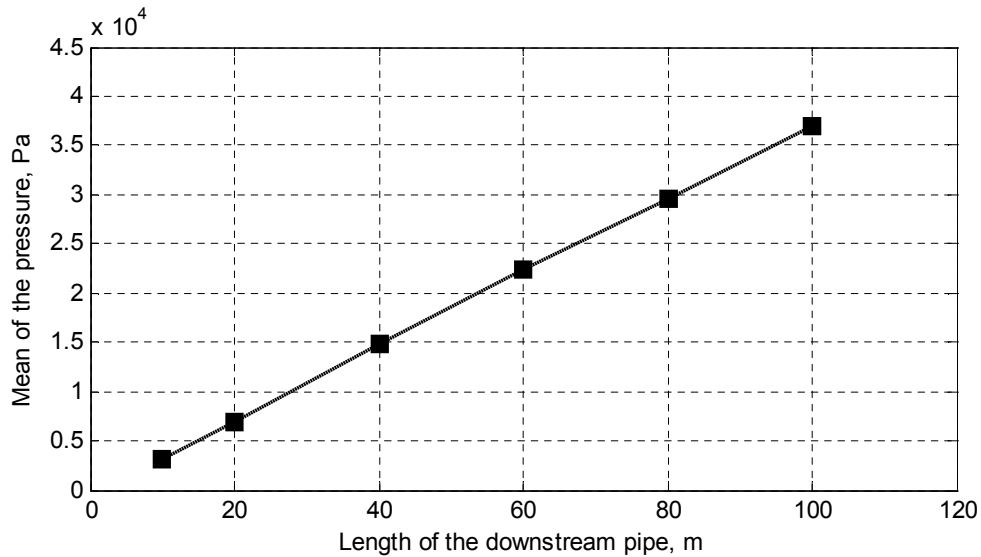
The same system with an upstream pipe of 20 m with that in Chapter 7 has been modelled. Differently the downstream pipes have various lengths, i.e. 10 m, 20 m, 40 m, 60 m, 80 m and 100 m, and the system has been modelled in OLGA only. The effects of the bend on the pressure in the system have been neglected because the horizontal bend cannot be modelled in the 1-D code OLGA.

The pressure where there used to be a bend is discussed below to demonstrate the effects of the downstream pipe length. Figure D-1 shows the time traces of the pressure with downstream pipes of different lengths. It can be seen that the mean of the pressure increases with the increase of the downstream pipe length and the pressure fluctuates with time. The pressure fluctuation mainly results from the passage of the slug units into or out of the downstream pipe. The pressure decreases with the reduction of the number of slugs in the downstream pipe.



— Downstream pipe: 10 m — Downstream pipe: 20 m — Downstream pipe: 40 m
 — Downstream pipe: 60 m — Downstream pipe: 80 m — Downstream pipe: 100 m

(a) Time traces of the pressure



(b) Mean of the pressure

Figure C-1 Time traces and mean of the pressure with downstream pipes of different lengths

The relation between the ratio of the fluctuation amplitude to the mean of the pressure and the length of the downstream pipe is shown in Figure D-2. As we can see the ratio decreases with the increase of the downstream pipe length. The fluctuation amplitude is even higher than the mean pressure with the 10 m long downstream pipe; however, with the 100 m long downstream pipe the fluctuation is only 8 % of the mean pressure. There are more slugs in a longer downstream pipe than those in a shorter pipe; consequently, the passage of a single slug into or out of the pipeline in a longer pipe has less impact on the mean of the system pressure.

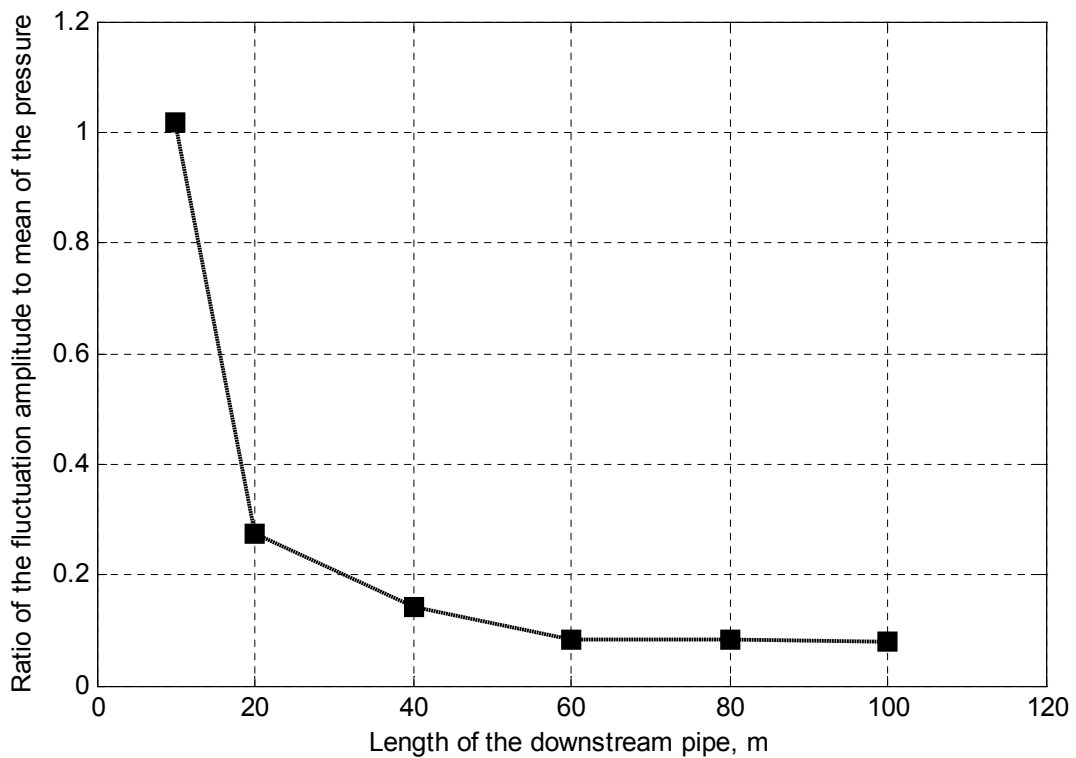


Figure C-2 Relation between the ratio of the fluctuation to average of the pressure and the length of the downstream pipe

To conclude, with the increase of the length of the downstream pipe, the mean force induced by pressure on the bend increases, however, the impact of the force fluctuation on the resultant force becomes less significant. It needs to be stressed that, when

designing a pipe bend and its supporting system, the force fluctuation has to be taken into account with a short downstream pipe.

Appendix D Modelling of the Pipeline/Wavy-pipe/Riser System Applying STAR-OLGA Coupling

The 4" pipeline/wavy-pipe/riser system has been modelled using STAR-OLGA coupling. The wavy pipe located upstream of the riser base was modelled in STAR-CCM+ while the upstream pipeline and downstream riser were modelled in OLGA. When severe slugging occurs the liquid slug grows in the pipeline and riser starting from the riser base. Thus there is a reverse flow from the downstream OLGA pipe to the wavy pipe in STAR-CCM+ and then to the upstream OLGA pipe (if the severe slug is long enough). However, in the current code of STAR-OLGA coupling the reverse flow has not been dealt with properly and thus the simulation cannot proceed successfully. Therefore, to identify the boundary between severe slugging and oscillation flow, the oscillation flow regime without a reverse flow involved has been considered instead of severe slugging.

As presented in the experimental study in Chapter 3 the severe slugging, transitional severe slugging, oscillation flow and continuous flow occurs in sequence with the increase of the gas flowrate at a fixed liquid flowrate. The cases discussed in this section have a fixed water flowrate 4 kg/s and different air flowrates. It needs to be noted that the boundary between severe slugging and oscillation flow in the experiment is located at 4 kg/s and 40 kg/h for water and air flowrates, respectively. The wavy pipe in the experiment was placed at 4.2 m upstream of the riser base.

Three of test cases have been designed as follows:

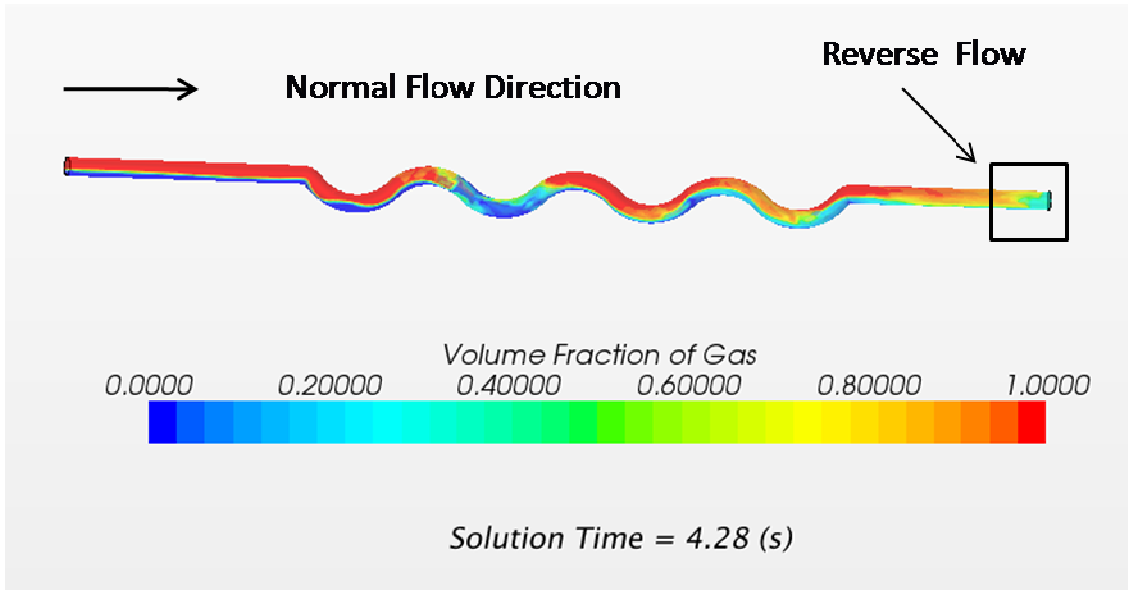
Case 1: the wavy pipe is located at 7.5 m upstream of the riser base; the inlet flowrates are 4 kg/s and 100 kg/h for water and air respectively;

Case 2: the wavy pipe is located at 15 m upstream of the riser base; the inlet flowrates are 4 kg/s and 50 kg/h for water and air respectively;

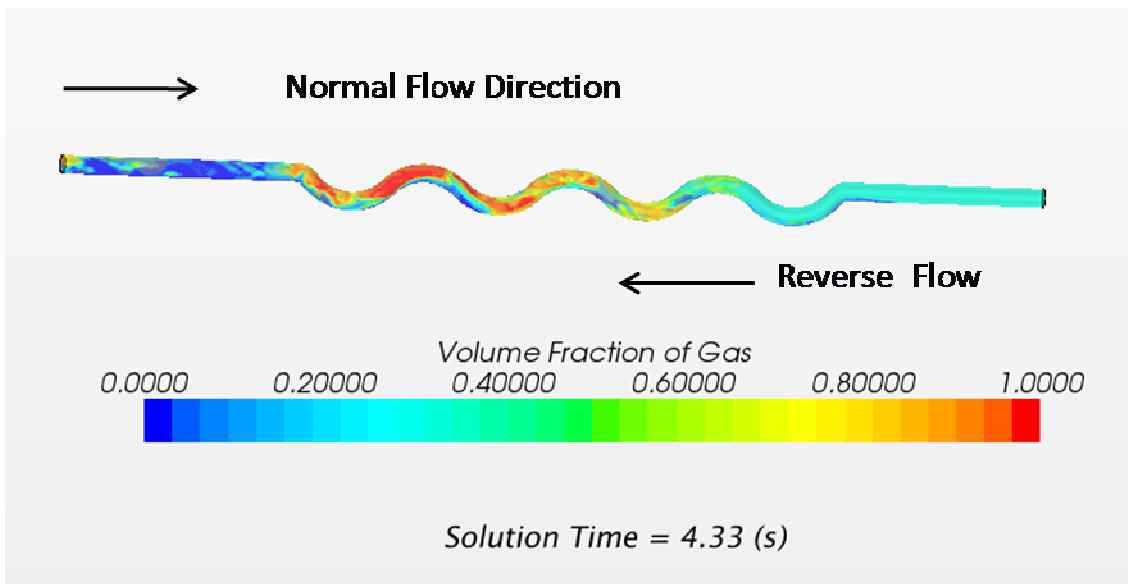
Case 3: the wavy pipe is located at 15 m upstream of the riser base; the inlet flowrates are 4 kg/s and 100 kg/h for water and air respectively.

Case 1 and Case 2 have stopped at the flow time $t = 4.28$ s and $t = 4.33$ s, respectively. It has been observed that Case 1 crashed once a reverse flow happens at the outlet of the wavy pipe; while Case 2 crashed when the reverse flow arrived at the inlet of the wavy pipe. Figure D-1 shows the phase distribution in the wavy pipe when the simulation crashed.

As mentioned above the crash of the simulation results from the improper treatment of the code on the reverse flow. The occurrence of the reverse flow predicted by the model indicates that the flow regime in the pipeline/riser system is still severe slugging rather than oscillation. Therefore, the air flowrates, i.e. 50 kg/h and 100 kg/h, are still not high enough for Case 1 and Case 2, although the critical air flowrate for oscillation flow to occur is 40 kg/h.



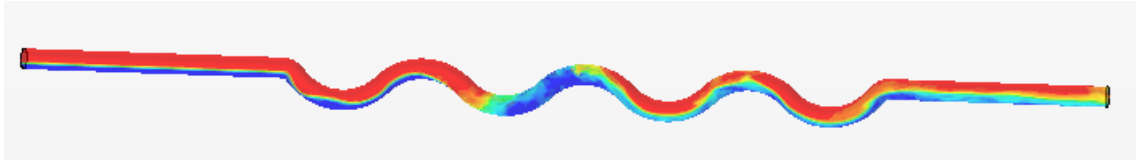
(a) Case 1



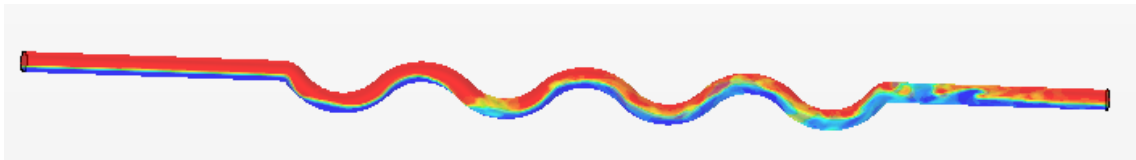
(b) Case 2

Figure D-1 Phase distribution in the wavy pipe with reverse flow

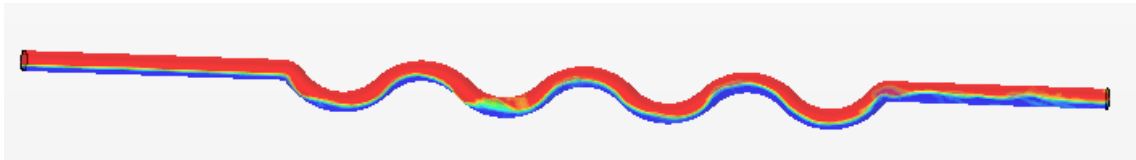
No reverse flow has been predicted by the model in Case 3. The flow has been simulated for $t = 10.0$ s. However, the air flowrate is 100 kg/h, much higher than the critical air flowrate for oscillation flow to occur, i.e. 40 kg/h. Figure D-2 presents a series of contour plots of gas volume fraction to show the phase distribution in the wavy pipe from $t = 4.0$ s to $t = 10.0$ s.



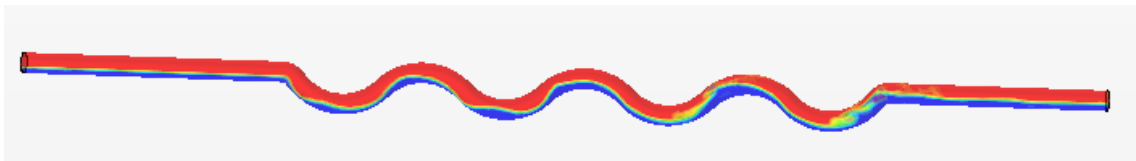
(a) $t = 4.0$ s



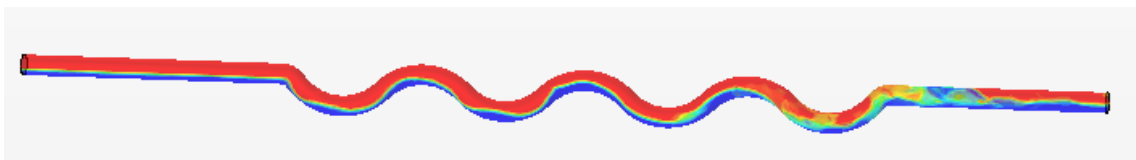
(b) $t = 5.0$ s



(c) $t = 6.0$ s



(d) $t = 7.0$ s



(e) $t = 8.0$ s

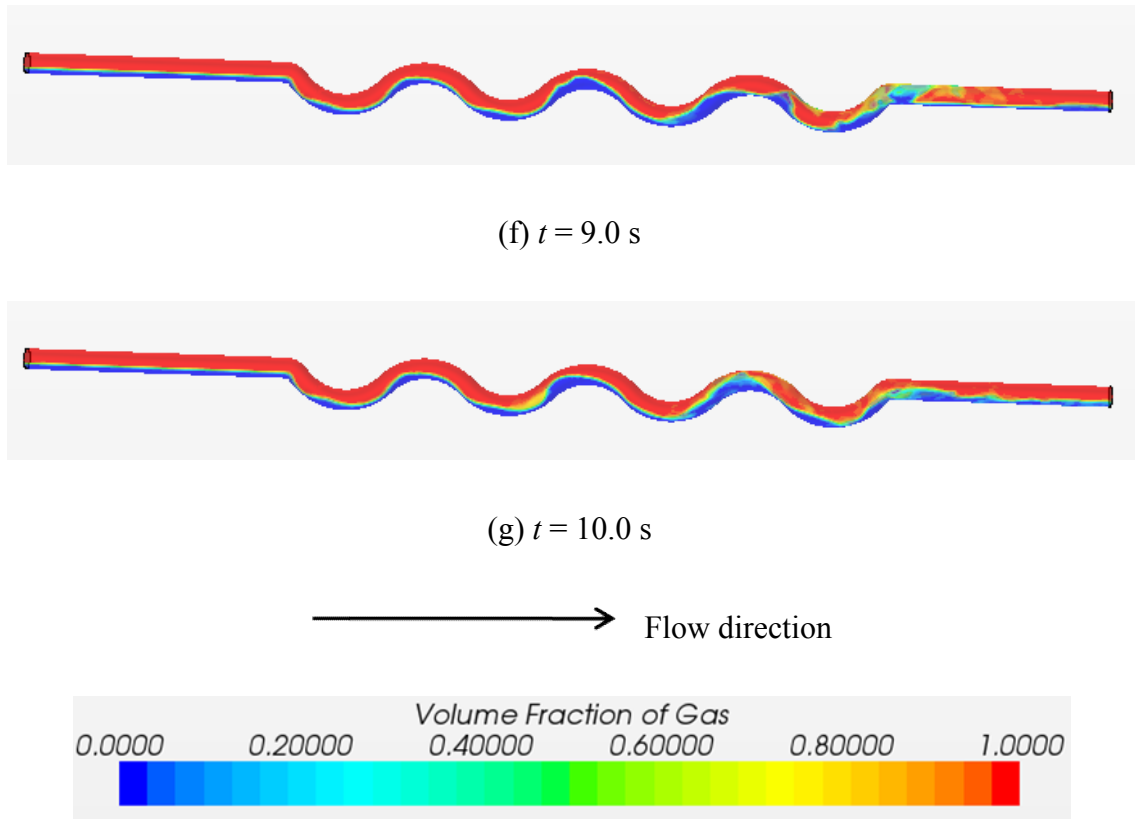


Figure D-2 Phase distribution in the wavy pipe without reverse flow

To summarise, it needs to be noted that there are some issues with these simulations:

- (1) the test configuration with the wavy pipe located close to the riser base cannot be simulated as shown by Case 1;
- (2) there is no experimental data to verify the model predictions because the wavy pipe in the experiment was only installed at 1.2 m and 4.2 m upstream of the riser base; in Case 3 the wavy pipe has to be installed at 15 m upstream;
- (3) the boundary between severe slugging and oscillation flow may not be obtained with reasonable accuracy as shown by Case 3.